ELECTROCHEMICAL SYNTHESIS OF POLY(METHYLSILYNE), AND THE EFFECT OF SILICON-BASED PRECERAMIC POLYMERS ON THE PROPERTIES OF POLYPROPYLENE BASED COMPOSITES

A THESIS SUBMITTED TO
THE GRADUATE SCHOOL OF NATURAL AND APPLIED SCIENCES
OF
MIDDLE EAST TECHNICAL UNIVERSITY

BY

DAMLA EROĞLU

IN PARTIAL FULFILLMENT OF THE REQUIREMENTS
FOR
THE DEGREE OF MASTER OF SCIENCE
IN
CHEMICAL ENGINEERING

SEPTEMBER 2008

Approval of the thesis:

ELECTROCHEMICAL SYNTHESIS OF POLY(METHYLSILYNE), AND THE EFFECT OF SILICON-BASED PRECERAMIC POLYMERS ON THE PROPERTIES OF POLYPROPYLENE BASED COMPOSITES

submitted by **DAMLA EROĞLU** in partial fulfillment of the requirements for the degree of **Master of Science in Chemical Engineering Department, Middle East Technical University** by,

Prof. Dr. Canan Özgen
Dean, Graduate School of **Natural and Applied Sciences**

Prof. Dr. Gürkan Karakaş
Head of Department, **Chemical Engineering**

Assoc. Prof. Dr. Göknur Bayram
Supervisor, **Chemical Engineering Dept., METU**

Examining Committee Members:

Prof. Dr. Ülkü Yılmazer
Chemical Engineering Dept., METU

Assoc. Prof. Dr. Göknur Bayram
Chemical Engineering Dept., METU

Prof. Dr. Sevil Savaşkan Yılmaz
Chemistry Dept., KTU

Prof. Dr. Levent Toppare
Chemistry Dept., METU

Assoc. Prof. Dr. Yusuf Uludağ
Chemical Engineering Dept., METU

Date: 02.09.2008

I hereby declare that all information in this document has been obtained and presented in accordance with academic rules and ethical conduct. I also declare that, as required by these rules and conduct, I have fully cited and referenced all material and results that are not original to this work.

Name, Last name: Damla EROĞLU
Signature:

ABSTRACT

ELECTROCHEMICAL SYNTHESIS OF POLY(METHYLSILYNE) AND THE EFFECT OF SILICON-BASED PRECERAMIC POLYMERS ON THE PROPERTIES OF POLYPROPYLENE BASED COMPOSITES

Eroğlu, Damla
M.S., Department of Chemical Engineering
Supervisor: Assoc. Prof. Dr. Göknur Bayram

September 2008, 209 pages

In the first part of this dissertation, poly(methylsilyne) was produced both in small and large-scales. In the small-scale, the aim was to synthesize the polymer by electrochemical polymerization of methyltrichlorosilane at a constant potential of -6 V supplied by batteries, using sodium dodecyl sulfate (SDS) as the supporting electrolyte. The polymer was characterized by ^{1}H-NMR, FTIR, UV-Visible Spectroscopy and GPC in addition to its distinctive yellow color. The yellow color and the ^{1}H-NMR, FTIR, UV-Visible and GPC results proved that poly(methylsilyne) was produced successfully in small-scale.

In the second part of the synthesis, the objective was to scale-up the electrochemical synthesis of poly(methylsilyne) while investigating the effects of the parameters like the electrode, solvent and supporting electrolyte types, monomer/solvent ratio and reaction time on the synthesis. Although successful results were obtained in large-scale synthesis with acetonitrile and SDS, the problems with the reproducibility of the synthesis were solved using a system containing 1.2-dimethoxyethane (DME) and tetrabutylammonium perchlorate (TBAP).

In the second part of the dissertation, the aim was to prepare polypropylene/silicon-based preceramic polymer blends and to characterize them in terms of flammability, thermal and mechanical properties and morphologies. In order to investigate the effect of the silicon-based preceramic polymers, two different polymers were used: poly(methylsilyne) (PMSy) and allylhydridopolycarbosilane (SMP-10) where the latter was a commercially available silicon carbide precursor. Triphenylphosphate (TPP) and a metal complex were also used in polypropylene based composites to gain a synergy with the silicon containing polymers. The polymer composites were prepared using a twin-screw extruder and molded in an injection molding machine.

As a result of the flammability tests, it was seen that in order to achieve a significant decrease in the flammability of polypropylene, at least 20 wt% additive was needed. Furthermore, it was observed that the most significant improvement in flame retardancy was obtained in PP/10SMP/5TPP/5M sample containing 10 wt% SMP-10, 5 wt% TPP and 5 wt% metal complex with a limiting oxygen index (LOI) value of 23.5%. This was explained by the synergy obtained by SMP-10, TPP and the metal complex. With the addition of these silicon containing polymers, thermal properties of the composites increased to a great extent. For the mechanical properties, it was seen that impact strength of the composites significantly increased with the addition of SMP-10, PMSy and TPP.

Keywords: Poly(methylsilyne), Silicon-Based Preceramic Polymers, Electrochemical Polymerization, Polypropylene

ÖZ

POLİ(METİLSİLİN) POLİMERİNİN ELEKTROKİMYASAL SENTEZİ VE SİLİKON BAZLI PRESERAMİK POLİMERLERİN POLİPROPİLEN BAZLI KOMPOZİTLERİN ÖZELLİKLERİNE ETKİLERİ

Eroğlu, Damla
Yüksek Lisans, Kimya Mühendisliği
Tez Yöneticisi: Doç. Dr. Güknur Bayram

Eylül 2008, 209 sayfa

Bu tez çalışmasının ilk kısmında poli(metilsilin) hem küçük hem de büyük ölçekte üretilmiştir. Küçük ölçekte amaç, poli(metilsilin)in metiltriklorosilanın elektrokimyasal polimerizasyonu ile pil kullanılarak sağlanan -6 V sabit potansiyelde destek elektrolit olarak sodium dodesil sülfat (SDS) kullanılarak sentezlenmesidir. Polimer kendine has sarı rengine ek olarak ^{1}H-NMR, FTIR, UV-Visible Spektroskopi ve GPC ile karakterize edilmiştir. Ürünün sarı rengi ve ^{1}H-NMR, FTIR, UV-Visible ve GPC sonuçları poli(metilsilin)in küçük ölçekte başarılı bir biçimde üretildiğini göstermiştir.

Sentez çalışmasının ikinci kısmında amaç, poli(metilsilin)in elektrokimyasal sentezinin ölçekçe büyütülmesi ve bu sırada elektrot, çözücü ve destek elektrolit tipleri, monomer/çözücü oranı ve reaksiyon süresi gibi parametrelerin sentez üzerindeki etkilerinin araştırılmasıdır. Büyük ölçekte, asetonitril ve SDS kullanılarak başarılı sonuçlar elde edilmesine rağmen, sentezin tekrarlanabilirliğindeki problemler ancak 1,2-dimetoksietan (DME) ve tetrabütilamonyum perklorat (TBAP) kullanılarak aşılabilmiştir.

Bu tez çalışmasının ikinci kısmında, polipropilen/silikon bazlı preseramik polimer karışımları hazırlanması ve bu karışımların yanıcılık, termal ve mekanik özelliklerine ve morfolojilerine bağlı olarak karakterize edilmeleri hedeflenmiştir. Silikon bazlı preseramik polimerlerin polipropilen bazlı kompozitlerdeki etkilerini araştırmak amacıyla iki farklı polimer kullanılmıştır: poli(metilsilin) (PMSy) ve silikon karbide dönüşen bir ticari preseramik polimer olan alilhidridopolikarbosilan (SMP-10). Trifenilfosfat (TPP) ve bir metal kompleksi de silikon bazlı polimerlerle sinerji kazanılması için polipropilene eklenmiştir. Polimer kompozitleri çift vidalı ekstruder ile hazırlanmış ve enjeksiyonlu kalıplama cihazı ile kalıplanmıştır.

Yanıcılık testlerinin sonucunda görülmüştür ki, polipropilende etkili bir alev geciktirme için en az %20 katkı malzemesine ihtiyaç vardır. Buna ek olarak, alev geciktirici özellikteki en önemli gelişme %10 SMP-10, %5 TPP ve %5 metal kompleksi içeren PP/10SMP/5TPP/5M kompozitinde görülmüş, bu karışımın sınırlayıcı oksijen indeksi (LOI) 23.5% bulunmuştur. Bu sonuç SMP-10, TPP ve metal kompleksinin yarattığı sinerjiden kaynaklanmıştır. Silikon bazlı polimerlerin polipropilene eklenmesi sonucunda kompozitlerin termal özellikleri önemli ölçüde gelişmiştir. Mekanik özellikler için, kompozitlerin darbe dayanımlarının SMP-10, PMSy ve TPP eklenmesiyle önemli ölçüde arttığı gözlemlenmiştir.

Anahtar Kelimeler: Poli(metilsilin), Silikon Bazlı Preseramik Polimerler, Elektrokimyasal Polimerizasyon, Polipropilen

To My Family

ACKNOWLEDGEMENTS

I would like to express my deepest gratitude to my thesis supervisor Assoc. Prof. Dr. Göknur Bayram for her guidance and support throughout my thesis. She always encouraged me with her valuable advice and enthusiasm. I would also like to thank her for her belief in me throughout my study.

I also wish to thank to Prof. Dr. Levent Toppare for his valuable advice and guidance during my study. In addition, I want to thank to Dr. Michael Pitcher for suggesting and introducing the topic of silicon-based preceramic polymers to me and his help during the first year of my study. Furthermore, I would like to thank to Prof. Dr. Ülkü Yılmazer for his help throughout my study.

In addition, I would like to thank to Prof. Dr. Levent Toppare's lab group for their help and kindness throughout my thesis. I also want to thank to Yusuf Nur, not only for his help and advice in my study but also for his friendship and support during my thesis.

I would like to thank to Mert Kılınç who taught me everything and helped me throughout my experiments. In addition, I would like to thank to my group members Sertan Yeşil and Dr. Özcan Köysüren for their help and friendship. I would also like to thank to Canan Yeniova, Canan Gücüyener and Filiz Cengiz who supported me throughout my thesis work by being my best friends. Without them, my graduate years in METU would not be this enjoyable and memorable. In addition, I would like to thank to Zeynep Tüzenli and Tijen Seyidoğlu for their friendship in the lab.

I also wish to thank to Mihrican Açıkgöz from Chemical Engineering Department for DSC, TGA and FTIR analysis, Cengiz Tan from Metallurgical and Materials

Engineering Department for SEM analysis and Central Laboratory and Chemistry Department for ^{1}H-NMR analysis.

Special thanks to TÜBİTAK for supporting me throughout my graduate study by the National Scholarship Program for MSc Students. In addition, this thesis work is supported by the 107M031 TÜBİTAK project.

My deepest gratitude also goes to Emre Aydınlık for his love, support, patience, understanding and encouragement in every step of my life, especially during my undergraduate and graduate studies.

Finally, I want to thank to my family, İnci, Mehmet and Çağla Eroğlu for their endless love and support in every step of my life. I could not achieve any of these without their support and belief in me.

TABLE OF CONTENTS

CHAPTER

APPENDICES

LIST OF TABLES

TABLES

LIST OF FIGURES

FIGURES

CHAPTER 1

INTRODUCTION

Ceramic materials are widely used in high-temperature applications due to their high thermal stabilities. They can be produced by different techniques: traditional powder technology, chemical vapor deposition (CVD), sol-gel technology and polymer pyrolysis [1]. Preceramic polymer is an oligomeric or polymeric material that is converted to ceramic materials upon heating above its decomposition temperature [2]. Preceramic polymers that are converted to silicon-based ceramics on pyrolysis are widely studied since ceramic materials like silicon carbide are used in many applications requiring hard, lightweight, temperature and wear resistant materials [1, 3].

Silicon-based preceramic polymers gained great importance for the last 30 years since production of silicon carbide by polymer pyrolysis is more efficient and successful than any other method [1]. Polysilanes, $[SiR_2]_n$, are high-yield precursors for silicon carbide and they are commonly studied due to their potential applications as conducting polymers, photo-resistant materials and nonlinear optical materials [4, 5]. Polysilynes, $[SiR]_n$, in other words network polysilanes, are a relatively new class of preceramic polymers. They were first synthesized in 1988 by Bianconi and Weidman [6]. They exhibit a broad UV band that tails into the visible region unlike the polysilanes, therefore they have also the visible absorption and emission characteristics [7, 8]. The polysilanes and related polysilynes are generally synthesized by the reductive coupling of dichlorosilanes and trichlorosilanes by the Wurtz method using alkali metal reducing agents in high-boiling solvents [5, 6, 9-12]. Poly(methylsilyne), $[SiCH_3]_n$, is a relatively new member of poly(alkylsilyne) family and it is a promising silicon carbide precursor with the optimum silicon to carbon ratio of 1:1 and solubility in common nonpolar organic solvents [3]. In the literature, poly(methylsilyne) is synthesized by a modified sono-chemical synthesis [3] and by electrochemical polymerization [7, 8]. In the electrochemical synthesis of poly(methylsilyne), the polymer is synthesized by the electrochemical reduction of methyltrichlorosilane at the constant potential of -6 V for 8 h at argon atmosphere by using tetrabutylammonium perchlorate or tetrahexylammonium perchlorate as the supporting electrolyte [7, 8].

The combustion of a polymer starts by the thermal decomposition of the polymer at relatively low temperatures producing volatile, combustible gases as a product which then ignite and combust in the presence of oxygen. The large amount of heat emitted from combustion is then thermally fed back to the polymer causing further decomposition. This cycle rapidly accelerates the fire [13]. Flame retardation is to decrease the flammability of a polymer by interrupting the combustion cycle of the polymer at thermal decomposition, ignition or combustion steps with the addition of certain chemicals [13].

Polypropylene is one of the most commonly used thermoplastic since it has important properties such as easy processing and good mechanical strength. Although it has good mechanical properties, polypropylene has a high flammability due to its wholly aliphatic hydrocarbon structure [14, 15]. In literature, many different flame retardants are added to polypropylene in order to decrease its flammability [2, 14-17].

Although there are some inherently flame retardant polymers, generally most of the thermoplastics need flame retardant additives to decrease their flammability [13]. However, there are some limitations in the use of flame retardant additives since some additives have undesirable results. For instance, antimony trioxide is toxic and when it is used as a flame retardant, smoke production is increased. In addition, phosphorus based compounds can increase the carbon monoxide yield and smoke production and hydrates must be added in very high amounts in order to achieve flame retardancy causing a significant decrease in mechanical properties of the matrix polymer [2, 13].

Environment-friendly flame retardants, meaning halogen-free flame retardants have received much attention since halogenated compounds release corrosive and toxic products and halogen gases as a result of decomposition. The degradation products of these environment-friendly flame retardants are less toxic, loss corrosive and they do not contain halogen gases. Therefore, although halogenated compounds are very effective in flame retardancy of polymers, they are limitedly used due to environmental reasons [13, 14, 17].

Silicon-based flame retardants are widely studied in literature since they provide effective flame retardancy without releasing harmful products to environment [13-18]. The main flame retardancy mechanism of silicon-based flame retardants are in condensed phase, by the formation of silicon dioxide which acts as a protective layer. This silica layer protects the polymer from the external heat and oxygen and also slows down the transfer of combustible gases to the combustion zone [14, 16, 19]. Silicon-based flame retardants are also effective in vapor phase by the trapping of active radicals [13, 19].

There are studies in literature in which silicon-based preceramic polymers are used as flame retardants in polypropylene [2, 20-23]. The addition of silicon-based flame retardants provides significant decrease in peak heat release rates, mean heat release rates, total heat release and total mass loss and significant increase in char formation. Preceramic polymers provide flame retardancy by the ceramic char formation which acts as a heat and diffusion barrier and protects the unburned polymer [2, 20-23].

Silicon-based flame retardants are also very effective in the improvement of the thermal properties of thermoplastic polymers due to their high thermal stabilities [14]. Addition of these silicon containing polymers provides a significant increase in the degradation temperatures of the composites. In addition, it is seen that addition of silicon-based compounds in small concentrations to polypropylene has positive effects on the mechanical properties of the composites [14].

This dissertation is composed of two main studies: electrochemical synthesis and characterization of poly(methylsilyne) and preparation and characterization of polypropylene/silicon-based preceramic polymer blends.

The objective of the first part of the study is to synthesize poly(methylsilyne) by the electrochemical polymerization of methyltrichlorosilane by using a simpler supporting electrolyte and power source with shorter reaction time and to characterize the polymer by ^{1}H-NMR, FTIR, UV-Visible Spectroscopy and GPC. After the polymer is synthesized and characterized in small-scale, it is aimed to scale-up the synthesis of poly(methylsilyne) while studying the effects of the parameters in the synthesis on the electrochemical polymerization.

In the second part, the objective of the study is to prepare PP/silicon-based preceramic polymer blends by the twin-screw extruder and to characterize these polypropylene based composites based on their flammability, thermal and mechanical properties and morphologies. In this part of the study, the effect of two different silicon-based preceramic polymers are studied: poly(methylsilyne), that is electrochemically synthesized, and a commercially available silicon carbide precursor, allylhydridopolycarbosilane. In addition, it is aimed to find synergistic materials with the silicon containing polymers in polypropylene based composites.

CHAPTER 2

BACKGROUND INFORMATION

2.1 Preceramic Polymers

Ceramic materials such as silicon carbide, silicon nitride, boron carbide and boron nitride are commonly used in industry due to their important properties. These ceramics have hardness, high oxidative and thermal stabilities, high resistance to corrosion, thermal shock and creep and low coefficient of thermal expansion. Because of these properties, ceramic materials are widely used in high-temperature applications [1]. Important application areas of these ceramics are given in Table 2.1.

Table 2.1 Advanced ceramics and their applications [1]

	Typical Applications
Silicon Carbide, SiC	Engines, Machinery, Cutting Tools, Metallurgy
Boron Carbide, B_4C	Wear, High-temperature Thermocouples (B_4C/C)
Boron Nitride, BN	High-temperature Lubricant (h-BN), Cutting Tools (c-BN)
Silicon Nitride, Si_3N_4	Parts in Heat Engines: Turbocharger Rotors, Glow Plugs, Swirl Chambers, Rocker Arm Pads; Valves and Piston Pins

These high-purity ceramic materials can be produced by traditional powder technology, chemical vapor deposition (CVD), sol-gel technology and polymer pyrolysis [1]. Preceramic polymers are the polymers which yield to ceramic materials on pyrolysis [1, 2]. Production of ceramic materials from preceramic polymers is commonly studied since Yajima et al. [24-26] first obtained non-oxide ceramics from the thermal decomposition of polymers. Preceramic polymer pyrolysis has important advantages such as ceramic materials can be produced in higher purity at relatively low temperatures than the materials produced by other methods. In addition, since the viscosity and other properties of the preceramic polymers can be tailored by the inherent properties of the polymer or the processing conditions, the production of ceramic films and fibers are easier [1]. Preceramic polymers are also used in the synthesis of multicomponent ceramic powders and bulk materials, in the formation of ceramic coatings for carbon fibers towards corrosion and in the synthesis of cellular porous ceramic foams. Furthermore, they are used as binders for ceramic powders and as flame retardant additives for thermoplastic polymers [1].

Polyborazines, polyboranes and polyborazylenes are some examples of preceramic polymers that are converted to boron-based ceramics, whereas polycarbosilanes, polysilazanes, polysilanes, polysiloxanes and polysilynes are some examples of preceramic polymers that are converted to silicon-based ceramics on pyrolysis [1].

2.1.1 Polysilynes

Polysilynes, $[SiR]_n$, which can also be called network polysilanes, are preceramic polymers that can be converted to silicon carbide on pyrolysis with a high yield without cross-linking because of their network structure [3]. The first poly(alkylsilynes), poly(n-hexylsilyne), poly(n-butylsilyne) and poly(n-propylsilyne), were synthesized by Bianconi et al. [6, 12] by the reductive condensation of alkyltrichlorosilanes using high-intensity ultrasound and liquid NaK alloy emulsions. Poly(alkylsilynes) are all yellow polymers. They are soluble in common nonpolar organic solvents like hexane or tetrahydrofuran therefore they can be cast or spun into smooth ceramic films [3, 6, 12]. Poly(alkylsilynes) oxidize in the presence of light in air to form polymeric siloxane networks. Although they are moderately sensitive to air and light, they are thermally stable up to 300^0C [6, 12].

The alkyl unit of the monomer significantly affects the properties of the resulting poly(alkylsilyne). As the chain length of the n-alkyl unit decreases, the solubility of the polymer decreases. For instance, poly(n-propylsilyne) is less soluble in organic solvents when compared with poly(n-hexylsilyne). In addition, it has seen that polysilynes with smaller alkyl groups have a portion with high molecular weight, whereas polysilynes with larger alkyl groups have lower polydispersity. This can be explained as the smaller alkyl groups allow the formation of an extensive polysilyne network while larger alkyl groups prevent this formation and prefer sheet like structure [12].

2.1.2 Poly(methylsilyne)

Poly(methylsilyne), $[SiCH_3]_n$, which is a relatively new member of polysilyne family, is a good candidate as a preceramic polymer for silicon carbide with its silicon to carbon ratio of 1:1 [3]. In poly(methylsilyne), each silicon is connected to a methyl and three other silicon atoms forming a silicon-silicon bonded network structure [27]. The chemical structure and graphic illustration of poly(methylsilyne) can be seen in Figures 2.1 and 2.2.

Pitcher et al. [3] synthesized poly(methylsilyne) with a modified sono-chemical synthesis, that can be converted to very smooth films of stoichiometric silicon carbide. The polymer synthesized is a yellow-orange powder which has the properties of other polysilynes like the solubility in organic solvents. Poly(methylsilyne) is also synthesized by electrochemical methods in the literature which will be discussed in the following section in detail.

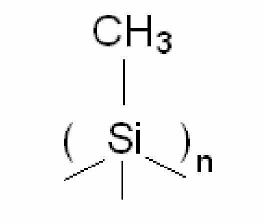

Figure 2.1 Chemical structure of poly(methylsilyne)

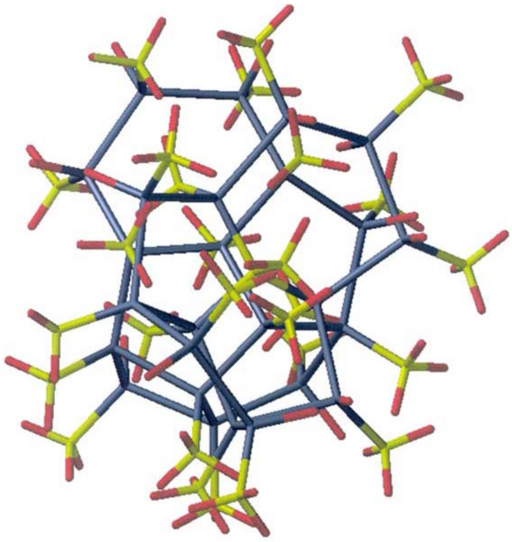

Figure 2.2 Graphic illustration of poly(methylsilyne) [27]

2.1.3 Electrochemical Synthesis of Poly(methylsilyne)

In the literature, poly(methylsilyne) is synthesized by the electrochemical polymerization of methyltrichlorosilane [7, 8]. Electrochemical synthesis of poly(methylsilyne) provides products with lower polydispersity and more sensitive functionality. In addition, in the electrochemical synthesis of the polymer, high-boiling solvents or alkali metal reducing agents are not required [7, 8]. Vermeulen and Huang [7], synthesized poly(methylsilyne) and a series of poly(cyclohexylsilyne-co-methylsilyne) network polymers by electrochemical reduction of methyltrichlorosilane and methyltrichlorosilane/ cyclohexyltrichlorosilane mixture, respectively. The electrochemical reduction of the monomer or the mixture of the monomers is carried out in an undivided cell, using 1,2-Dimethoxyethane (DME) as the solvent, coiled copper electrodes as the electrodes and tetrabutylammonium perchlorate (TBAP) as the supporting electrolyte. A constant potential of -6 V is applied under argon atmosphere and the electrolysis is continued at room temperature within an ultrasonic bath, until no progress is observed by GPC. After the reaction is finished, the solution is quenched by stirring it with methanol for 2 hours. After purification, the yellow polymers are precipitated by methanol addition. The reaction route for poly(methylsilyne) synthesis can be seen in Figure 2.3 [7].

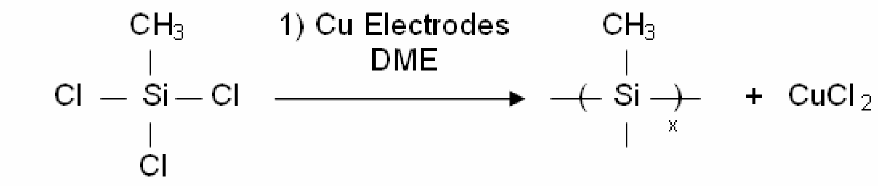

Figure 2.3 Electrochemical synthesis of poly(methylsilyne) [7]

In another study, the electrochemical polymerization of trichlorosilane monomers, methyltrichlorosilane, butyltrichlorosilane and cyclohexyltrichlorosilane are done [8]. The electrochemical polymerizations are carried out in an undivided cell with copper electrodes for both the cathode and the anode. During the electrochemical polymerization, DME is used as the solvent and tetrahexylammonium perchlorate is used as the supporting electrolyte. The reaction is carried out under the constant potential of -6 V under argon atmosphere at room temperature for 8 h. After the reaction has finished, the solution is stirred with lithium aluminum hydride for 3 h in order to convert all the remaining Si-Cl bonds. After filtering the solution and evaporating the solvent, the remaining residue is dissolved in fresh toluene and filtered. When the toluene is evaporated, the polymer is obtained as yellow oil. In Figure 2.4, the reaction route can be seen [8].

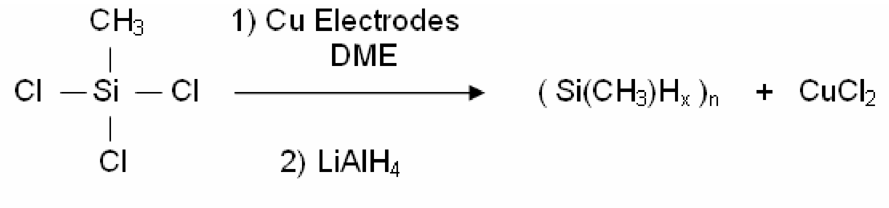

$$\mathrm{Cl-Si(CH_3)(Cl)-Cl} \xrightarrow[\text{2) LiAlH}_4]{\text{1) Cu Electrodes, DME}} (\mathrm{Si(CH_3)H_x})_n + \mathrm{CuCl_2}$$

Figure 2.4 Electrochemical synthesis of poly(methylsilyne) [8]

2.1.4 Experimental Techniques for the Characterization of Poly(methylsilyne)

In the previous studies in literature, poly(methylsilyne) is characterized by ^{1}H-NMR (Nuclear Magnetic Resonance), FTIR (Fourier Transform Infrared Spectroscopy), UV-Visible Spectroscopy and GPC (Gel Permeation Chromatography) in addition to its distinctive yellow color [3, 7, 8].

2.1.4.1 Nuclear Magnetic Resonance, NMR

NMR spectroscopy is widely used for determining the structure of a material. By NMR spectroscopy, certain atoms or groups in a material can be identified. In addition to that, the positions of the atoms relative to each other can be determined [28]. NMR is based on the quantum mechanical magnetic properties of an atom's nucleus. All nuclei containing odd numbers of protons and neutrons have an intrinsic magnetic moment or angular momentum [29]. The angular momentum of the spinning charge of the nuclei is described by the spin quantum number, I, which can have values of 0, 1/2, 1, 3/2, 2 etc. Nuclei containing even numbers of protons and neutrons have an I value of zero therefore no NMR signal is obtained. Therefore nuclei with I values of 1/2 such as ^{1}H, ^{13}C, ^{31}P, ^{19}F, ^{119}Sn, ^{29}Si, ^{15}N are used in material characterization [28, 29].

Proton NMR is one of the most commonly used characterization methods to obtain physical, chemical, electronic and structural information about the material. In ^{1}H-NMR, information with respect to hydrogen nuclei within the molecules of a substance is obtained. In ^{1}H-NMR spectroscopy, the material is dissolved in a deuterated solvent that has deuterium in order to prevent the interference of the solvent's protons with the material's protons. ^{1}H-NMR spectra is generally recorded against tetramethylsilane as the standard, to set zero. In ^{1}H-NMR, the chemical shifts are between +12 and -4 ppm. The groups in a material and their positions relative to each other can be identified from the chemical shifts in the ^{1}H-NMR spectra [30].

In ^{1}H-NMR spectrum of poly(methylsilyne), a broad intense peak between 0-0.4 ppm is expected indicating the $Si\text{-}CH_3$ bond in the polymer. In addition, weaker resonances at 3.45 ppm, 4.2 ppm and 5.5 ppm are expected due to Si-H and $Si\text{-}H_2$ bonds in the polymer as a result of stirring with $LiAlH_4$ [3, 8]. For the polymers that are quenched with methanol, a peak at 3.7 ppm is observed showing $Si\text{-}OCH_3$ bond [7]. The NMR results of the polymer also shows some peaks due to the remaining electrolyte [8].

2.1.4.2 Fourier Transform Infrared Spectroscopy, FTIR

Infrared spectroscopy is one of the most common characterization methods used for the identification of the structure of the polymer and the functional groups. In addition, FTIR is one of the most useful methods for determination of the structure of an unknown material [28]. Fourier transform infrared spectroscopy is a technique for collecting infrared spectra [31]. Infrared is the wide region between the visible and microwave regions in the electromagnetic spectrum. The infrared region is divided into three regions as near-infrared, mid-infrared and far-infrared regions. The mid-infrared region (4000 – 666 cm^{-1}) is divided into two as the group frequency region between 4000-1300 cm^{-1} and the fingerprint region between 1300-650 cm^{-1}. In the group frequency region in IR, the absorption bands are assigned to the vibration units of only two atoms of a molecule, therefore these units only depend on the functional group giving the absorption, they are independent of the molecular structure of the complete material. However in the fingerprint region of the IR, they depend on the complete molecular structure. The molecular vibrations in low frequency are sensitive to changes in overall structure of the molecule [28].

In FTIR spectrum of poly(methylsilyne), peaks corresponding to C-H bonds in Si-CH_3 are observed at 2957, 2855, 1464, 1377 and 1272 cm^{-1}. In addition, Si-H and Si-H_2 bonds are observed at 2163 cm^{-1} and 917 cm^{-1}, respectively. Furthermore, peaks at 722 cm^{-1} (C-H), 856 cm^{-1} (-CH_3) and 770, 667 cm^{-1} (Si-C) are expected for the polymer. Si-O-Si peaks are present in the results at 1093 cm^{-1} due to the reactivity of the polymer towards oxygen [3, 7, 8].

2.1.4.3 UV-Visible Spectroscopy

UV-Visible spectroscopy is used in the identification of the types of bonds and the functional groups in a given molecule. It works by the principle that many molecules absorb the ultraviolet or visible light and undergo electronic transitions in which valence electrons in a molecule are excited from one energy level to a higher energy level. By determining these electronic transitions in UV or visible regions, information about the structure of a molecule can be collected. In the UV-Visible spectra, the light absorbance is plotted versus wavelength of the light. Although it gives information about the structure of a molecule, this spectrum is not specific for any compound and can be affected from many other parameters [32].

The UV-Visible spectrum of poly(methylsilyne) is similar to other poly(alkylsilyne)s, showing a broad UV band tailing down into the visible region at 450 nm which is characteristic of the network Si polymers [3, 7, 8].

2.1.4.4 Gel Permeation Chromatography, GPC

Gel permeation chromatography is a type of size exclusion chromatography (SEC) in which large molecules like polymers or proteins are separated based on their sizes [33]. GPC provides information about the relative molecular weight of the polymer and the molecular weight distribution [28]. GPC is a very important characterization test since molecular weight and molecular weight distribution of a polymer have significant effects on the polymer’s properties. GPC consists of a column in which extremely small porous polymers beads with different pore sizes are present. In GPC, the separation of the polymer molecules based on their sizes is accomplished by the ability to penetrate through the pores of the stationary phase at different times. The polymer moves through the column with the mobile phase, which is an organic-solvent in GPC, and the particles of the same size filter through the column together. Since the larger particles can not enter many pores, they are collected at first [28, 33]. In Figure 2.5, the principle of separation in GPC columns can be seen.

The molecular weight of poly(methylsilyne) is generally determined by GPC with polystyrene standards [3, 7, 8]. It is seen that for the polymers synthesized by the modified sono-chemical synthesis, the M_w is determined as 7000-29000 Da with polydispersities of 4-7 [3]. For poly(methylsilyne) that is produced by electrochemical synthesis, M_w is determined as 5608 [7] and 6457 [8] with polydispersities of 1.70 and 3.0, respectively.

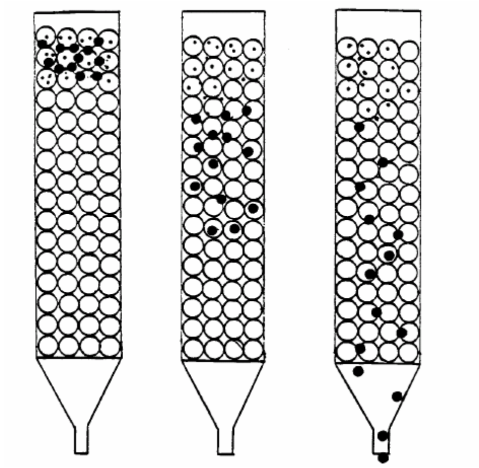

Figure 2.5 GPC column separation of a polymer [28]

2.2 Polypropylene

Polypropylene, PP, was first synthesized in the mid-1950's by the usage of Ziegler-type catalysts by Natta. By using different forms of the catalysts, Natta produced different types of high molecular weight polypropylene [34]. Since the raw material cost is very low and the catalysts have very high efficiencies, polypropylene is a very low-cost polymer [15]. Due to these reasons, the commercial exploitation of polypropylene was very rapid. In 1998 the global capacity of polypropylene was estimated as 26.3 x 10^6 tones [34].

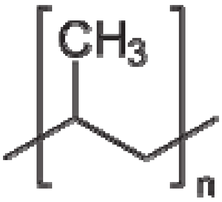

Figure 2.6 Chemical structure of polypropylene [35]

Polypropylene is a polyolefin, a linear hydrocarbon polymer like polyethylene. There is a methyl group attached to alternate carbon atoms on the chain backbone [34]. The chemical structure of polypropylene can be seen in Figure 2.6.

Although polypropylene has similar properties with polyethylene, due to the presence of methyl group it shows some important differences. This group can cause a slight stiffening of the chain which results in an increase in the softening and melting points of the polymer. Due to these increases, polypropylene has higher working temperatures than polyethylene. The only important disadvantage of polypropylene is that it oxidizes more easily than polyethylene due to the presence of the methyl group [34].

The most important effect of the methyl group is that different polypropylene types with different tacticities can be obtained. Therefore, three different types of polypropylene are present; atactic, syndiotactic and isotactic. In isotactic polypropylene, all the methyl groups are on one side of the molecule resulting in crystallization in a helix, not in a planar zigzag like polyethylene [34]. The structure of isotactic polypropylene can be seen in Figure 2.7. Isotactic polypropylene has higher stiffness, crystallinity, melting point, tensile strength, modulus and hardness than the other types of polypropylene. The commercial polypropylene polymers are 90-95% isotactic [34].

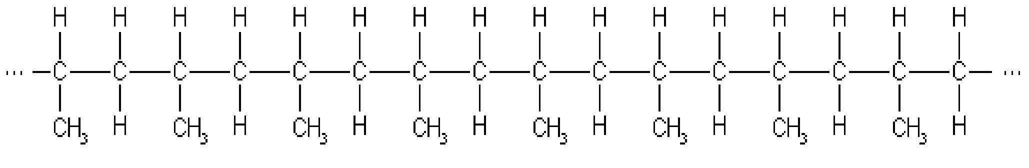

Figure 2.7 Isotactic polypropylene [35]

Table 2.2 Properties of isotactic PP [36]

	Value
Melting Point (^{0}C)	160-175
Softening Point (^{0}C)	140-160
T_g (^{0}C)	-19
Density (g/cm^3)	0.90
M_n	> 10^6
Polydispersibility (M_w/M_n)	9-11
Heat of Combustion (kJ/g)	44
Heat of Fusion (J/g)	21
Limiting Oxygen Index, LOI (%)	17.4
Decomposition Range (^{0}C)	328-410

Polypropylene has good chemical, heat, crack and fatigue resistances. It has excellent stress resistance and dielectric properties. It is resistant to most alkalis, acids and organic solvents [34, 35]. It has high mechanical properties. One of the most important properties of polypropylene is that isotactic and syndiotactic polypropylene have fiber-forming properties due to the order in the polymer structure [15, 34, 35]. Therefore, isotactic polypropylene is commercially used both as a fiber and a thermoplastic [15]. Some important properties of isotactic polypropylene can be seen in Table 2.2.

Polypropylene is commonly used in packaging, textiles, stationery, plastic parts and reusable containers of various types, laboratory equipments, loudspeakers and polymer banknotes [35]. It is used in many automotive parts like automobile accelerator pedals, dome lights, kick panels, door frame parts and car battery cases. In addition, it is used in hospital sterilisable equipments, luggage, stacking chairs, washing machine parts and toilet cisterns. It is also taking the place of polystyrene in thin-wall packaging like margarine tubs. Non-oriented polypropylene films, that are glass clear, are used in textile packaging, confectionery wrap and fast food packaging. Oriented film, on the other hand, has greater clarity, impact strength and barrier properties and used in bread, biscuit and potato crisps's packaging and as a capacitor dielectric. Since PP has fiber properties, it is commonly used in carpeting and in blankets [34].

2.3 Thermal Decomposition of Polymers

In the thermal decomposition of polymers, chemical and physical processes are interacting. The chemical processes like the formation of combustible gases also affect the physical processes such as melting and charring [17, 37].

In the thermal decomposition of polymers, they generally decompose into five different products [37]:

- Combustible gases like methane, ethane and carbon monoxide;
- Noncombustible gases like carbon dioxide, hydrogen chloride and hydrogen bromide;
- Liquids;
- Fine solid particles or soot in gaseous products;
- Carbonaceous char or inorganic residues originating from heteroatoms.

Organic polymers undergo four different types of thermal decomposition mechanisms [38]:

- Random-chain scission;
- End-chain scission (unzipping);
- Chain stripping;
- Cross-linking.

The decomposition mechanism of a polymer depends significantly on the chemical structure of the polymer. Polyethylene undergoes random-chain scission, whereas PMMA undergoes unzipping reactions. PVC is an example for chain stripping and high-charring polymers are examples of cross-linking polymers. Some polymers decompose in a mixed behavior [37].

2.4 Combustion of Polymers

In polymer combustion, there are four main steps [38]:

- Heating of the polymer;
- Decomposition;
- Ignition;
- Combustion.

The combustion of a polymer is a cycle starting by the heating of the polymer to its decomposition temperature. The volatile combustible decomposition products then ignite and undergo combustion in the presence of oxygen. Since combustion is an exothermic process, a large amount of heat is emitted which is then partially fed back to the polymer causing further decomposition therefore more fuel for the combustion [13, 37]. This combustion cycle can be seen in Figure 2.8.

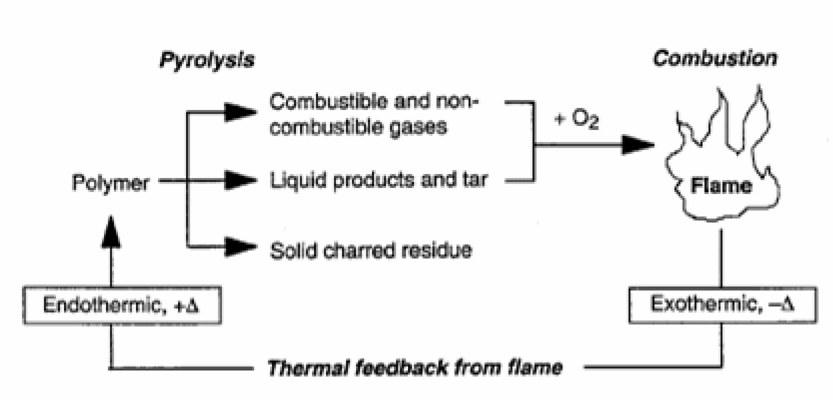

Figure 2.8 Polymer combustion cycle [39]

In the flames, self-propagation combustion reactions are present. The principal reactions in the flames are free-radical reactions. The flames of the polymers are generally hydrocarbon flames due to the structures of the polymers. In the hydrocarbon flames, $H^{\cdot}$, $O^{\cdot}$, and $OH^{\cdot}$ radicals are the most important radicals whereas small amount of $HO_2^{\cdot}$, $HCO^{\cdot}$ and $CH_3^{\cdot}$radicals are also present. Chain-branching reactions during combustion accelerate the burning process since more radicals are formed as a result of these reactions [37]. The chain propagating reaction and chain branching reactions can be seen in Figure 2.9 [40].

$$CH_4 + O_2 \longrightarrow CH_3\cdot + H\cdot + O_2$$
$$H\cdot + O_2 \longrightarrow OH\cdot + O\cdot$$
$$CH_4 + OH\cdot \longrightarrow CH_3\cdot + H_2O$$
$$CH_3\cdot + O\cdot \longrightarrow CH_2O\cdot + H\cdot$$
$$CH_2O\cdot + OH\cdot \longrightarrow HCO\cdot + H_2O$$
$$HCO\cdot + O_2 \longrightarrow H\cdot + CO + O_2$$
$$CO + OH\cdot \longrightarrow CO_2 + H\cdot$$

Figure 2.9 Chain propagating and branching reactions [40]

2.5 Flame Retardancy in Polymers

Flame retardation is to decrease the flammability of a polymer by altering or retarding the degradation or combustion processes of the polymer with the addition of certain chemicals [13]. These chemicals act through a chemical or physical mechanism and interrupt the combustion cycle in heating, thermal decomposition, ignition or combustion steps [17]. In flame retardancy in polymers, the main aim is to decrease the flammability of a polymer by decreasing the amount and rate of combustible gaseous decomposition product formation [37]. In addition, flame retardancy in polymers aim to decrease the ease of ignition, the flame spread, the fire endurance meaning the speed of fire penetrating through a wall or barrier, the rate of heat release, the smoke evolution and to increase the ease of extinction [37].

There are two types of flame retardant approaches in polymer flame retardancy [17, 37]: (1) reactive type flame retardants and (2) additive type flame retardants. In the reactive type flame retardation, flame retardant unit containing heteroatoms is chemically incorporated into the polymer either in the chain or as a pendant group. This approach involves designing of a new polymer or modification of the existing polymer. Reactive flame retardation approach is the most effective way since it provides efficient flame retardancy without destroying the original physical and mechanical properties of the polymer. However additive type flame retardants are more common due to economical reasons. In the additive type flame retardants, the flame retardant is mixed with the polymer physically. This approach is widely used since it is very economical and it provides an easy method for the flame retardancy of commercial polymers. However there are some limitations in the additive type flame retardants such as poor compatibility, reduction in mechanical properties and increase in the smoke and CO production [17, 37].

2.5.1 Mechanisms of Flame Retardancy

There are two mechanisms of flame retardancy in polymers: (1) condensed-phase mechanism and (2) vapor-phase mechanism.

2.5.1.1 Condensed-Phase Mechanism

In condensed phase mechanism, the additive changes the nature of the products of degradation and combustion before volatilization [41]. In other words, flame retardancy is provided by the changes in the polymer substrates [37]. There are two main mechanisms in condensed-phase by which flame retardancy is achieved: (1) char-formation and (2) dehydration. Char-formation is a very important way of flame retardation since it forms a protective layer on the polymer surface which prevents the contact of the polymer with oxygen and heat therefore from further decomposition into fuels for combustion [17, 37]. In addition, char helps the polymer to preserve its structural integrity [37]. Another important flame retardancy mechanism in condensed phase is dehydration. As mentioned before, combustion of a polymer starts by the endothermic heating of the polymer to its decomposition temperature. Another way to decrease the flammability of a polymer is to increase the endothermic heat demand for the thermal decomposition of the polymer [37]. This can be achieved if the system evolves water which will decompose endothermically and cool the pyrolysis zone or other noncombustible gases which will dilute the combustible gases [17, 37].

2.5.1.2 Vapor-Phase Mechanism

In the vapor phase, the flame retardancy is achieved by the trapping of radicals interrupting the exothermic combustion process. In the radical trap theory of flame retardation, radical species from flame retardants compete with the $H^{\cdot}$, $O^{\cdot}$, and $OH^{\cdot}$ radicals those are essential for the propagation of the flame [13, 17, 37, 40]. The most important example of radical trapping is in halogenated flame retardants. In halogen-based flame retardants, the bromine or chlorine molecules that are built into the polymer diffuse into the flame zone and create free-radical inhibitors. In the reactions, $H^{\cdot}$, $O^{\cdot}$, and $OH^{\cdot}$ radicals are replaced with less reactive $Br^{\cdot}$ and $Cl^{\cdot}$ radicals [37, 40]. The radical scavenge reactions can be seen in Figure 2.10 [40].

The combustion process in the vapor phase can also be prevented by the physical effects like the suppressant characteristic of an inert gas such as carbon dioxide or nitrogen [17, 40].

Some flame retardants act both in condensed and vapor phases for flame retardancy whereas some flame retardants act only in one phase [37].

$$CH_4 + Br\cdot \longrightarrow HBr + CH_3$$
$$H\cdot + HBr \longrightarrow H_2 + Br\cdot$$
$$OH\cdot + HBr \longrightarrow H_2O + Br\cdot$$
$$O\cdot + HBr \longrightarrow Br\cdot + OH\cdot$$

Figure 2.10 Radical scavenge reactions [40]

2.5.2 Types of Flame Retardants

As mentioned before, flame retardancy can be achieved either by designing new inherently flame-retardant polymers or by addition of flame retardant chemicals.

2.5.2.1 Inherently Flame Retardant Polymers

Inherently flame retardant polymers are polymers with high thermal stabilities due to high chain interactions. These polymers have high decomposition temperatures therefore the combustion process is retarded. Chain interactions can be improved by increasing crystallinity and introducing polar groups, hydrogen bonding and aromatic or heteroatoms to the polymer backbone [37]. In addition, the polymers containing aromatic groups in the backbone can provide flame retardancy by char-formation [37]. Polyimide, polybenzoxazole, polybenzimidazole and polybenzthiazoles are some examples of inherently flame retardant polymers [37].

2.5.2.2 Flame Retardant Additives

There are seven types of flame retardant additives that are commonly used in the flame retardation of organic polymers [37]:

- Halogenated flame retardants
- Inorganic hydroxide flame retardants
- Phosphorus-based flame retardants
- Nitrogen-based flame retardants
- Silicon-based flame retardants
- Boron-based flame retardants
- Polymeric flame retardants

Halogenated compounds are very effective in flame retardation since they interrupt the combustion process by the trapping of radicals, as mentioned before. However, although they are very effective flame retardants, they are limitedly used since their products are highly toxic and corrosive [13, 14, 17]. Since the use of halogenated flame retardants are restricted due to environmental reasons, the recent studies in literature about flame retardancy are centered on environment-friendly flame retardants that are inorganic hydroxides and phosphorus, nitrogen, silicon and boron containing compounds. The degradation products of these flame retardants are less toxic, loss corrosive and they do not contain halogen gases [14].

Inorganic hydroxides decrease the amount and concentration of the combustible gases and cool the pyrolysis zone by decomposing endothermically [37]. However, since they have to be used in large amounts for effective flame retardation [37], they significantly decrease the mechanical properties of the matrix polymer [13]. Phosphorus based flame retardants act in both condensed and vapor phases by a glassy surface layer formation, char promotion, pyrolysis zone cooling, dilution of combustible gases and free-radical inhibition [42]. Nitrogen-based flame retardants are generally used as reactive flame retardants or with phosphorus based flame retardants to achieve synergistic effect [37]. Boron containing compounds generally act in condensed phase by the formation of a protective char layer [37]. They are also commonly used with halogenated compounds to achieve synergy [17]. Polymeric materials such as polydibromostyrene and polyphosphazanes are effective in flame retardation since the flammability can be adjusted by composition without affecting the physical and mechanical properties of the polymer significantly like other flame retardants [37].

2.5.2.3 Intumescent Flame Retardants

Intumescent flame retardants (IFRs) are commonly used in order to provide flame retardancy. IFRs are composed of three constituents: acid source, char source and gas source. IFRs act in condensed phase to provide flame retardancy mainly by changing the mode of decomposition. The acid source degrades before the matrix polymer in order to dehydrate the char source. As a result of this, a thermally stable char is formed on the polymer surface preventing the polymer from oxygen and heat therefore from further degradation [14]. The gas source on the other hand, produces incombustible gases which provide the swelling of the char. In an IFR system, generally phosphorus-based compounds are used as the acid source, a polyol like pentaerythritol (PER) is used as the char source and nitrogen-based compounds are used as the gas source [14].

2.5.3 Silicon-Based Flame Retardants

Silicon-based flame retardants are commonly studied since they provide effective flame retardancy without emitting toxic and corrosive products [13-23]. In the literature, many silicon containing compounds such as silicones, silicas, organosilanes, silsesquioxanes and silicates are studied as flame retardants [37, 43]. Among the silicon-based flame retardants, the most commonly studied one is polydimethylsiloxane, PDMS (silicone) [37]. The silicon-based flame retardants are used in blends, coatings, copolymers or as the matrix polymers [43].

2.5.3.1 Mechanisms of Flame Retardancy in Silicon-Based Flame Retardants

Silicon-based flame retardants act both in condensed and vapor phases [15, 17]. The main mechanism of flame retardancy in silicon-based flame retardants are in condensed phase, due to the formation of a silicon dioxide layer which acts as a protective silica layer. This thermal degradation product, silicon dioxide, prevents the contact of the polymer with oxygen and heat therefore prevents further degradation of the polymer [14, 37]. In other words, the silica layer that is deposited on the surface of the polymer has heat and diffusion shielding effects [16]. It protects the polymer and reduces the external heat fluxes by reradiating the heat and insulating the polymer with its low thermal conductivity [16]. Due to the diffusion-barrier effect of silica ash layer, the formation and transport of the combustible decomposition products are slowed significantly [16]. Silicon-based flame retardants also provide flame retardancy by char promotion and dilution of combustible gases in the condensed phase and trapping of radicals in the vapor phase [15, 17].

2.5.3.2 Silicon-Based Preceramic Polymer Flame Retardants

Silicon-based preceramic polymers such as polycarbosilane (PCS), polysilastyrene (PSS) and silsesquioxane are used as flame retardants in blends with organic polymers [23]. The structures of these preceramic polymers can be seen in Figure 2.11.

Preceramic polymers do not produce toxic and corrosive materials like halogenated compounds and they do not cause an increase in CO or smoke production. By blending preceramic polymers with the thermoplastics, the properties of the polymer such as modulus and char yield can be controlled with the amount of preceramic added. They provide a significant decrease in the overall mass loss rate. Furthermore, addition of these preceramic polymers to thermoplastics cause an increase in the melt viscosity of the polymer blends and when this increase in melt viscosity is combined with the ceramic char, dripping during burning can be decreased significantly. In addition, the increase in the melt viscosity increases the thickness and therefore the performance of the ceramic char layer [2].

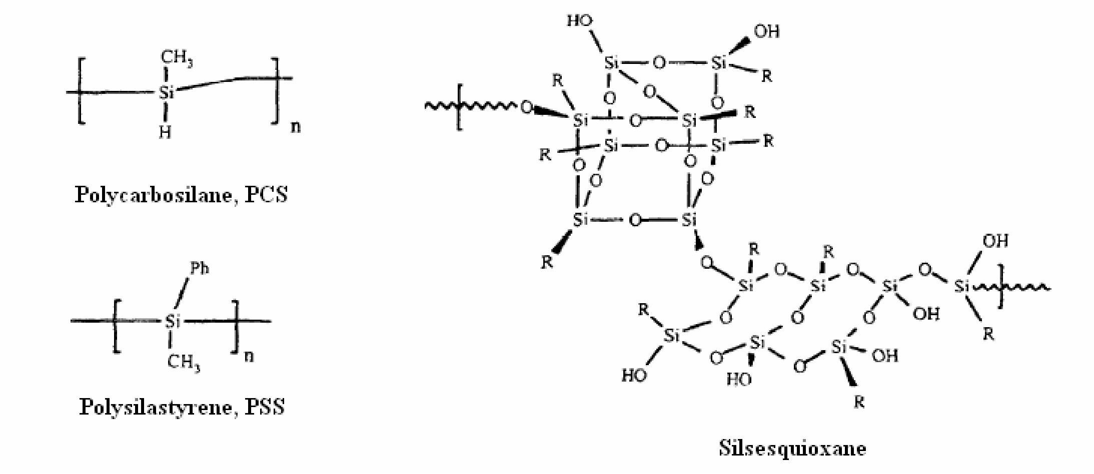

Figure 2.11 Chemical structures of silicon-based preceramic polymers [43]

Preceramic polymers provide flame retardancy due to their char-forming and thermal properties. The main flame retardancy mechanism of these preceramic polymers is the char formation. The char layer protects the virgin polymer from the external heat while it prevents the transport of the volatile decomposition products to the combustion zone. The char layer can also reradiate the external heat from the polymer. Therefore the char layer reduces the amount of volatile, combustible gaseous product formation which decreases the fuel for the combustion and hence the heat emitted and fed back to the polymer. Foamy chars are generally more effective in flame retardancy than the brittle, thin char layer. The char should be formed above the processing temperature but below the decomposition temperature of the thermoplastic polymer [2].

In a patent [2], thermoplastic/preceramic polymer blends of PP, Pebax and Kraton with PCS, PSS and silsesquioxane are prepared by solution mixing in THF. It has seen that with the addition of the preceramic polymer, there is a significant increase in the char yield percentage and a significant decrease in peak (PHRR) and mean heat release rates.

Bolf and Lichtenhan [23] also studied the flame retardancy of PCS, PSS and silsesquioxane by preparing preceramic polymer/thermoplastic polymer blends via solution blending in tetrahydrofuran. SBS, PTME-PA (polytetramethyleneylether-glycol-b-polyamide-12, 1% polyamide-12) and polypropylene are blended with PCS, PSS and silsesquioxane. With the increase in preceramic percentages in the blends, the ceramic or char yield also increases. The addition of preceramic polymers even in low amounts results in a significant decrease in the peak and average heat release rates. However, although PHRR and average HRR are reduced, there is no significant change in the total heat release rate. The decrease in the heat release rates of the blends can be explained by the significant decrease in the mass loss with the addition of preceramic polymers. The ceramic char formed on the polymer surface slows the release rate of the fuel to the gas phase therefore mass loss rate is decreased. Finally, it is concluded that preceramic polymers are only effective in condensed phase not in the vapor phase since the addition of these polymers do not affect the heat of combustion, carbon monoxide yield and specific extinction area. Therefore the main flame retardancy mechanism of silicon containing preceramic polymers is the ceramic char formation on the surface of the polymer which acts as heat and mass barriers.

In order to provide flame retardancy both in vapor and condensed phases, a substituent group can be incorporated to the preceramic polymer. This substituent can also increase the compatibility of the preceramic polymer with the thermoplastic or it can increase the char-formation or decrease the heat release [2].

These preceramic polymer flame retardants can be used in many polymers in applications such as carpeting, adhesives, wire and cable insulation and jacketing, fabrics, furniture, structural plastics, chassis and housing [2].

2.6 Flame Retardancy of Polypropylene

Polypropylene is a highly flammable polymer due to its wholly aliphatic hydrocarbon structure. Its pyrolysis is dominated by the initial chain scission and the main volatile pyrolysis compounds are C9 compounds. It burns completely with a smoke-free flame and it does not leave a char residue [15]. Flame retardation of PP is commonly studied since it is used in many different applications in the industry [14, 15, 17, 20-23, 37, 43].

2.6.1 Mechanisms in the Flame Retardancy of Polypropylene

The flammability of polypropylene can be decreased both in condensed and vapor phases by the following mechanisms [44]:

- By changing the decomposition process to favor char-forming which will decrease the heat and fuel transport;
- By the trapping of active radicals in the vapor phase;
- By the addition of hydrated inorganic additives which will cool the pyrolysis zone and dilute the combustible decomposition products by decomposing endothermically and releasing water;
- By changing the decomposition process of the polymer with changing its chemical structure;
- By the addition of additives which will promote char-formation and have intumescent property.

2.6.2 Flame Retardants for Polypropylene

Many different types of flame retardants are used in polypropylene in order to reduce its flammability. As mentioned in the previous section, flame retardants added to polypropylene improve the flame retardancy of the polymer with different mechanisms. In addition, the flame retardants used in polypropylene should have the following characteristics [15]:

- The flame retardant should be thermally stable at the processing temperatures of polypropylene, at temperatures lower than 260^0C;
- The flame retardant should be compatible with polypropylene;
- The flame retardant should also be effective in a polypropylene fiber;
- The flame retardant should decrease the smoke and carbon monoxide production;
- The flame retardant should be effective in small concentrations such as less than 10wt% not to affect the fiber properties of polypropylene.

Since polypropylene has a very high flammability and very poor char-forming ability, generally high charring flame retardants are used in the flame retardation of the polymer. In addition, because of these reasons, generally 20 wt% or higher amounts of flame retardants are needed for effective flame retardancy of the polymer [15].

2.6.3 Silicon-Phosphorus Synergism in Flame Retardants for Polypropylene

The silicon-phosphorus synergism is commonly studied in literature for the flame retardancy of polypropylene [20-22]. The phosphorus-based flame retardants are effective in polypropylene through the following mechanisms [45-47]:

- Polyphosphoric acid formation on the surface of the polymer as a protective layer;
- The cooling action of the vaporizing phosphorus compounds;

- Dilution of combustible decomposition products by noncombustible products;
- Decrease in the melt viscosity of the polymer in order to favor dripping for the removal of heat from the polymer and extinction.

Ammonium polyphosphate (APP) is a very commonly used compound for the flame retardancy of polypropylene [48]. In the literature, silicon-based preceramic polymers are used with APP in order to improve the flame retardancy of polypropylene [20-22]. For instance, Marosi et al. [21] used APP (21 wt%), pentaerythritol (PER) (7 wt%) and a borosiloxane polymer (1-5 wt%) to improve the flame retardancy of polypropylene. As a result, peak heat release rate and onset of heat release decreased with the addition of these flame retardants. This is explained by the formation of a ceramic protective layer and the binding of APP and PER particles by the silicon-based polymer prior to ceramic char formation [20]. In another study, when the total composition of APP, PER and borosiloxane is 34 wt%, including 9.7 wt% borosiloxane, the limiting oxygen index (LOI) value is increased up to 33.5 for polypropylene [22]. Although there are significant improvements in the flame retardancy of polypropylene in these studies, since the amounts of flame retardants are too high, the mechanical properties are significantly affected.

Li et al. [14], studied the effect of a silicon-containing intumescent flame retardant, PSiN2, on the flammability, thermal and mechanical properties and morphologies of polypropylene. With the addition of the silicon-containing intumescent flame retardant, LOI values are increased therefore flame retardancy is improved. For instance, with the addition of 20 wt% PSiN2, the LOI value is increased to 29.5 from 17.4. In addition, char yields and average decomposition temperatures are increased with the addition of PSiN2 although the initial degradation temperatures are decreased. For instance, with the addition of 20 wt% PSiN2, the char yield is increased to 7.4% from 0%. These improvements in the flammability and thermal properties of polypropylene can be explained as follows. During the heating of the polymers in air or N_2 atmospheres, the silicon-based flame retardants migrate to the surface due to their lower surface energies. The phosphorus-based groups in the IFR dehydrate the char source before polypropylene starts to degrade. The char source then forms the continuous, protective carbon layer on the surface of the polymer. This protective layer slows down the contact of the polymer with heat and the contact of the combustible decomposition products with the oxygen. The nitrogen-based compounds of the IFR foam this carbon layer and this expanded char protects the polymer from further decomposition. The silicon-based groups decompose to silicon dioxide which reacts with phosphate to form silicophosphate which stabilizes phosphorus species. From the TGA curves of the PP/PSiN2 samples in air, no mass loss is observed for the temperatures above 500^{0}C. In the literature however, mass loss is observed at these temperatures for silicon-free polymers. This result indicates that the addition of a silicon-containing compound improves the thermal and flammability properties of PP in air [14].

2.7 Flammability of Polysilynes

The flammability and thermal properties of poly(methylsilyne) and poly(phenylsilyne) are studied in literature [37]. The TGA curves of the polymers can be seen in Figure 2.12.

From the TGA curves of poly(methylsilyne) and poly(phenylsilyne), it can be seen that after 600^{0}C, there is no further mass loss. These polymers leave more than 60% char as a result of their thermal decomposition. It can be seen that poly(phenylsilyne) has a higher thermal stability when compared with poly(methylsilyne) since it decomposes slower and produces more char. The thermal decomposition products of poly(methylsilyne) are siloxanes which can be because of the oxidation of the polymer [37].

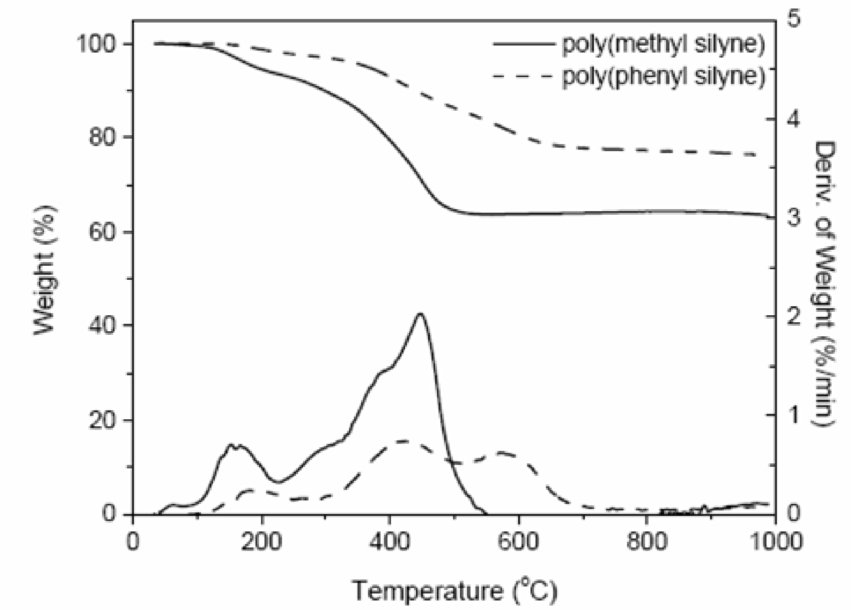

Figure 2.12 TGA and DTG curves of polysilynes [37]

Poly(methylsilyne) and poly(phenylsilyne) have both low flammability. The flammability of polysilynes only comes from the methyl or phenyl group. The flammability and thermal decomposition properties of polysilynes can be seen in Table 2.3.

Table 2.3 Flammability properties of polysilynes [37]

	H.R. Capacity (J/g-K)	Total Heat (kJ/g)	Char Yield (%)	Max. Mass Loss Rate ($x10^3$/s)	T_{max} (^{0}C)	T_{onset} (^{0}C)
Poly(methylsilyne)	92	15	64	0.34	447	126
Poly(phenylsilyne)	32	13	77	0.12	425	140

2.8 Mechanical Properties of Polypropylene with Silicon-Based Additives

Although silicon-based additives are generally added to polypropylene in order to improve the flammability and thermal properties, it is also aimed to minimize the loss of mechanical properties [49]. In a previous study in literature, Ryan et al. [50] concluded that the addition of siloxane powder to polypropylene provides an improvement both in the processability and mechanical properties of polypropylene. In this study, it is seen that the addition of 1 wt% of siloxane powder increased the impact strength of the polypropylene based composite containing other flame retardant additives by approximately 100%. In addition, it is proposed that the siloxane powders can break into smaller pieces when mixed with the polymer and improve the mechanical properties [51].

Li et. al [14] studied the effect of a silicon-containing intumescent flame retardant, PSiN2, on the mechanical properties of polypropylene based composites. It is seen that the addition of PSiN2 provides an increase in the tensile strength at first and reaches to a maximum at 10%. With further increase in the amount of silicon-based compound, decrease at tensile strength values are observed. In addition, it is seen that after 25% addition of PSiN2, there is a significant decrease in the tensile strength. Although a maximum is observed for tensile strength values at first, elongation at break values decrease with the addition of the silicon material. From the SEM pictures of the composites it is seen that in low amounts of the additive, it is well dispersed in the system and since polypropylene is the continuous phase, its high mechanical properties are kept. However as the composition of the silicon-based compound increases the continuity of the polypropylene phase decreases therefore mechanical properties are reduced.

2.9 Polymer Blends and Composites

Polymer blends are homogeneous mixtures of two or more polymers that are mixed at macro levels. Homogeneous polymer blends are miscible, they are mixed at molecular level to form a single phase whereas heterogeneous polymer blends are immiscible, they exhibit multiphase. Polymer composites are multicomponent mixtures of polymeric materials with organic and inorganic materials. Polymer composites are composed of two or more phases [52]. Polymer blends and composites are prepared in order to enhance the polymer's properties like physical, mechanical, thermal and flammability properties.

2.9.1 Polymer Processing Techniques

Polymer processing can be defined as the converting process of the raw polymer to the final products of desired shape [53]. Polymer processing includes the mixing of the polymer with the additives and the molding of the mixture to the final shape [53]. The polymer blends and composites can be prepared by different methods. The most common method is the melt blending of polymers by extrusion [34].

2.9.1.1 Extrusion

Extrusion is a process by which thermoplastics with uniform cross section are formed [53]. During extrusion process, the additives are mixed with the molten polymer and the melt is forced through the die giving it its final shape [53].

There are two types of extruders: (1) single-screw extruder and (2) twin-screw extruder [53]. Single-screw extruders generally do not provide good mixing. Twin-screw extruders can be divided into two: (1) counter-rotating twin-screw extruders and (2) co-rotating twin-screw extruders. Counter-rotating extruders can generate high pressures which are essential for some extrusion applications. Co-rotating extruders can provide excellent mixing and a narrow residence time therefore they are commonly used in many polymer processing applications [53]. A schematic view of a twin-screw extruder can be seen in Figure 2.13.

The screw of the extruder contains three sections: melting, compression and metering. In the melting section, the solid polymer particles are transported from the hopper and melted. In the compression section, the depth of the screw flight decreases in order to compact and mix the molten polymer and additives for obtaining a homogeneous mixture. Finally, in the metering section of the screw, the molten polymer is pumped through the die [53].

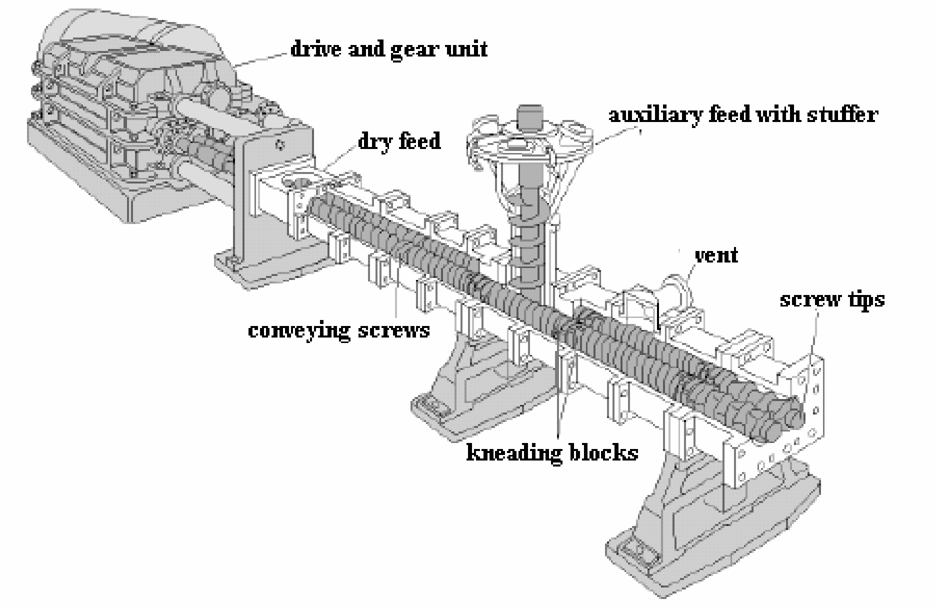

Figure 2.13 Schematic view of a twin-screw extruder [54]

2.9.1.2 Injection Molding

Molding is to give the final shape of the polymer blends or composites after they are mixed in the extruder and pelletized in the pelletizer. Injection molding is one of the most common molding techniques used for polymer processing. In injection molding process, the polymer pellets are melted and the molten polymers are forced into the cold mold where they solidify, taking the shape of the mold cavity [53].

2.9.2 Characterization Techniques for Polymer Blends and Composites

There are different characterization techniques for polymer blends based on their flammability, mechanical and thermal properties and morphologies.

2.9.2.1 Flammability Tests

There are 5 different standard flammability tests which measure different flammability properties of polymeric materials. These tests are [17, 37]:

- Ignitability tests
- Flame spread tests
- Limiting oxygen index (LOI)
- Heat release tests (cone calorimeter)
- Smoke tests

Limiting oxygen index is a commonly used flammability test which measures the minimum concentration of oxygen in a oxygen/nitrogen mixture required for continuing burning after ignition [17, 37]. The materials having a LOI value of greater than 26 are classified as self-extinguishing materials [17]. By this test, the ease of extinction of the materials can be investigated [17].

In UL 94 flame tests, the flammability is usually measured by a vertical burn test. The flammability of a material is classified from V0 to V2. The classification V0 is the best flame retardancy in which the material should stop burning within 10 s without dripping after two applications [17]. In addition to vertical burning test, horizontal burning test can be applied to polymers in order to measure the ignitability of the materials. Horizontal burning test can be applied both by UL 94 standard or ASTM D635 standard.

The heat release rate (HRR) is one of the most important flammability parameter of a material [16]. Addition to heat release rate, time to ignition, peak heat release rate (PHRR), average heat release rate, total heat released (THR), mass loss rate, effective heat of combustion, smoke density and CO and CO_2 production can be measured in a cone calorimeter [16].

In addition to these flammability tests, char yield calculated from thermogravimetric analysis (TGA) is also an indication of flame retardancy since as mentioned before, char promotion is an effective way to decrease the flammability of a material [17].

2.9.2.2 Mechanical Tests

The characterization of the polymers based on their mechanical properties is very important. The mechanical properties of polymers can be described based on the tensile and impact test results.

2.9.2.2.1 Tensile Test

In the tensile test, the load that is required for a specific elongation is measured while the specimen is pulled in tension at a constant rate. As a result of tensile test, the load versus elongation data is obtained and converted to stress versus strain data [55]. The engineering stress, σ is defined as:

$$\sigma = P / A_0 \tag{2.1}$$

where P is the load on the sample and A_0 is the original cross-sectional area of the specimen.

The engineering strain, ε, is defined as:

$$\varepsilon = (l - l_0) / l_0 = \Delta l / l_0 \tag{2.2}$$

where l is the gauge length at the given load and l_0 is the original length.

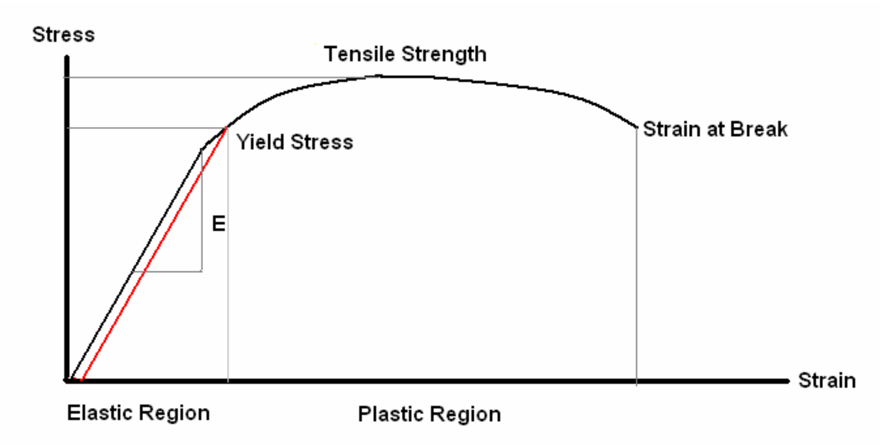

Figure 2.14 Stress-strain curve for a typical polymeric material

A stress-strain curve for a typical polymer can be seen in Figure 2.14. There are two different regions in a strain-stress curve: (1) elastic deformation and (2) plastic deformation regions. In elastic deformation, the deformation is not permanent, it is recovered. However, in plastic deformation the deformation is permanent.

In elastic region the stress-strain curve is linear. The slope of the curve in this region gives the modulus of elasticity, Young's modulus, E. The mathematical representation of Hooke's law:

$$\sigma = E \, . \, \varepsilon \tag{2.3}$$

The modulus indicates the stiffness of the material, in other words its resistance to deformation. The elastic region finishes at the yield point which is the intersection point of the stress-strain curve with a straight-line that is parallel to the linear portion of the curve from 0.2% on strain axis. The tensile strength of the polymer is the maximum stress value. Therefore, many important mechanical properties can be obtained from the stress-strain curve by tensile testing.

2.9.2.2.2 Impact Test

Impact energy of a material is the energy needed to fracture a specimen under an impact load [55]. The impact strength of a polymer is analogous to the toughness of the material. Therefore tough materials, which are both ductile and strong, have also high impact strengths.

There are two types of impact tests: (1) Charpy impact strength test and (2) Izod impact strength test. Charpy impact test is the most commonly used method to determine the amount of energy absorbed by a material during fracture [56]. The Charpy test is illustrated in Figure 2.15. In this test, the energy absorbed during fracture is directly calculated from the difference in initial and final heights of the swinging pendulum [55].

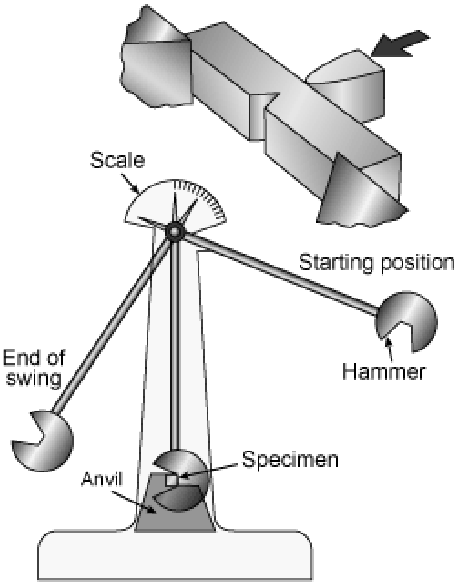

Figure 2.15 The Charpy impact strength test [55]

2.9.2.3 Thermal Tests

2.9.2.3.1 Thermogravimetric Analysis (TGA)

Thermogravimetric analysis (TGA) is commonly used in the characterization of polymers based on their thermal properties. In TGA, the change in the mass of the material with time and temperature is obtained [28]. The TGA curve is recorded either weight loss of the sample versus temperature or the change of sample weight with time versus temperature. In addition to mass loss data, decomposition temperature of the material can be obtained from TGA curve [28]. TGA is also important in the determination of flame retardancy of a material since char yield can be determined from TGA. Another important characteristic of TGA is that since each polymer has a different decomposition profile, the material can be distinguished from TGA curves [28].

2.9.2.3.2 Differential Scanning Calorimetry (DSC)

Differential scanning calorimetry is an important analysis in polymer characterization since it determines the energy changes in a system resulted from either chemical or physical reasons. Its working principle is to measure the heat necessary to maintain the same temperature in the sample versus a reference material with a known specific heat. It also measures the enthalpy changes in the system due to a change of state of the sample.

DSC analysis is very commonly used to determine important physical changes in the samples such as the glass transition temperature (T_g), the crystallization temperature (T_c), the melt temperature (T_m) and the decomposition temperature (T_D). In addition to the physical changes in the system, chemical changes as a result of polymerization and degradation reactions can also be determined by using DSC analysis [28]. A typical DSC curve showing the determination of T_g, T_c, T_m and T_D can be seen in Figure 2.16.

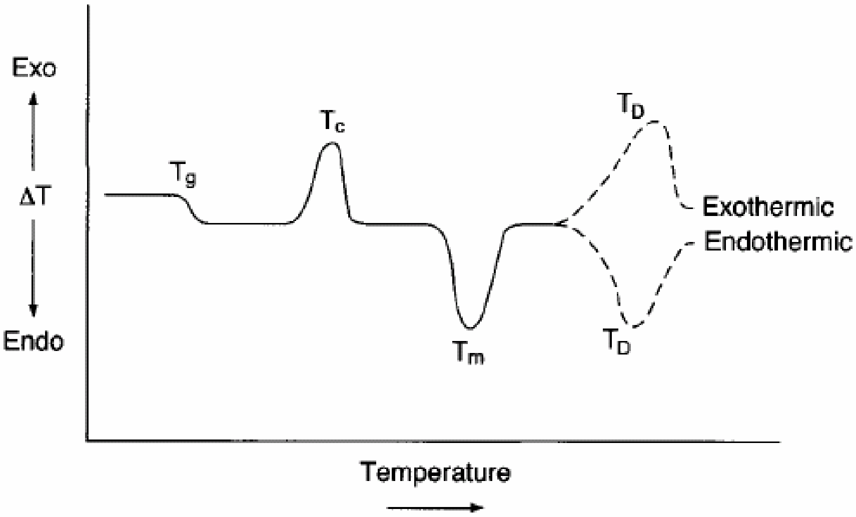

Figure 2.16 A typical DSC curve showing the transitions in a system [28]

2.9.2.4 Morphological Tests

2.9.2.4.1 Scanning Electron Microscopy (SEM)

The morphology of polymers is commonly studied since the mechanical properties are directly related with the microstructure of the materials [14]. The most common morphological test is the scanning electron microscopy (SEM). SEM gives information about the topography and composition of the surface of the sample by scanning it with high-energy beam of electrons [57].

In SEM, the material is coated with a layer of materials such as gold, gold/palladium alloy, platinum, tungsten or graphite in order to make it conductive. The material must be conductive during imaging for electron beam to scan the surface [57].

CHAPTER 3

EXPERIMENTAL

The experimental chapter is divided into two parts in the dissertation. In the first part, the materials and methods for the electrochemical synthesis of poly(methylsilyne) and the characterization of the synthesized polymer are described for both small and large scale synthesis. In the second part, the materials, methods and the characterization techniques used in the preparation of polypropylene / preceramic polymer blends are given.

3.1 Electrochemical Synthesis of Poly(methylsilyne)

Poly(methylsilyne) was synthesized by the electrochemical polymerization of methyltrichlorosilane both in small and large scales.

3.1.1 Electrochemical Synthesis of Poly(methylsilyne) in Small Scale

3.1.1.1 Materials

The materials used in the synthesis of poly(methylsilyne) can be seen in Table 3.1. Methyltrichlorosilane, the monomer in the synthesis, and sodium dodecyl sulfate (SDS), the supporting electrolyte in the synthesis, were used as they received. However acetonitrile, the solvent in the synthesis, was distilled before the experiments. The chemical structures of the materials used in the synthesis can be seen in Figure 3.1.

Table 3.1 The materials used in the synthesis of poly(methylsilyne)

Material Type	Material	Supplier
Monomer	Methyltrichlorosilane (≥ 97%)	Aldrich
Solvent	Acetonitrile (ACS reagent, ≥ 99.5%)	Aldrich
Supporting Electrolyte	Sodium Dodecyl Sulfate (ACS reagent, ≥ 99.0%)	Aldrich

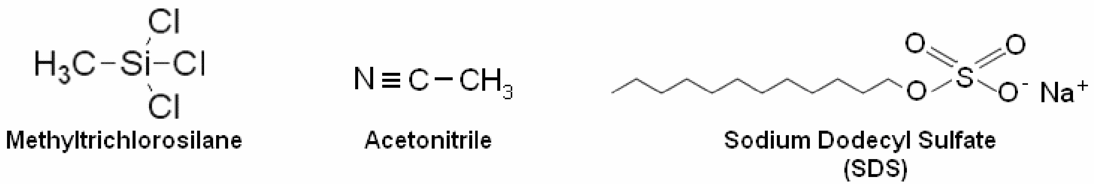

Figure 3.1 The chemical structures of the materials used in the synthesis

After the electrochemical synthesis was completed, the solution was stirred with lithium aluminum hydride (powder for synthesis) purchased from Merck. In addition, the solvents used in the purification of the polymer, tetrahydrofuran (extra pure) and n-pentane were purchased from Merck.

3.1.1.2 Experimental Parameters and Procedure

Poly(methylsilyne) was synthesized by the electrochemical polymerization of methyltrichlorosilane. In the electrochemical synthesis of poly(methylsilyne), there are different synthesis parameters such as electrode type and dimensions, supporting electrolyte type and amount, solvent type, power source, monomer to solvent ratio and reaction time. In addition, lithium aluminum hydride ($LiAlH_4$) amount and refluxing time are important parameters in the synthesis. The values of the experimental parameters used in the small-scale synthesis can be seen in Table 3.2.

Table 3.2 Experimental parameters in small-scale polymerization

Parameters	Values
Electrodes	413. No Stainless steel electrodes
Electrode Dimensions	1.5 cm x 2 cm
Supporting Electrolyte Type	SDS
Supporting Electrolyte Amount	0.025 g
Solvent	Acetonitrile (freshly distilled)
Power Source	Batteries (4x1.5V batteries in series)
Monomer to Solvent Ratio	1 ml monomer / 5 ml solvent
Reaction Time	30 min
$LiAlH_4$ Amount	27.5 mg
Refluxing Time	40 min

In the poly(methylsilyne) synthesis, the electrochemical polymerization was carried out in an undivided cell of 25 ml. Stainless steel plates were used for both the anode and the cathode. The electrodes were cleaned with acetone before they were used. In the synthesis, first 0.025 g of SDS was placed into the electrolysis cell. After the cell was filled with 5 ml of freshly distilled acetonitrile, the electrodes were placed and the cell was purged with argon. 1 ml of methyltrichlorosilane was then injected to the cell and the electrodes were connected to the batteries. The reaction was carried out at room temperature under constant potential of -6 V for 30 min. After the reaction has finished, the solution was stirred with 27.5 mg of $LiAlH_4$ at 50^0C for 40 min under argon atmosphere in order to convert all the remaining Si-Cl bonds [8]. The solution was then filtered and evaporated. For purification, the residue was dissolved in tetrahydrofuran (THF). Then pentane and distilled water were added to the solution, respectively. The organic layer containing the polymer, THF and pentane were separated from the water layer and the solvents were evaporated. Finally, the yellow solid residue was characterized by ^1H-NMR, FTIR, UV-Visible Spectroscopy and GPC. The experimental set-up of the small-scale poly(methylsilyne) synthesis can be seen in Figure 3.2.

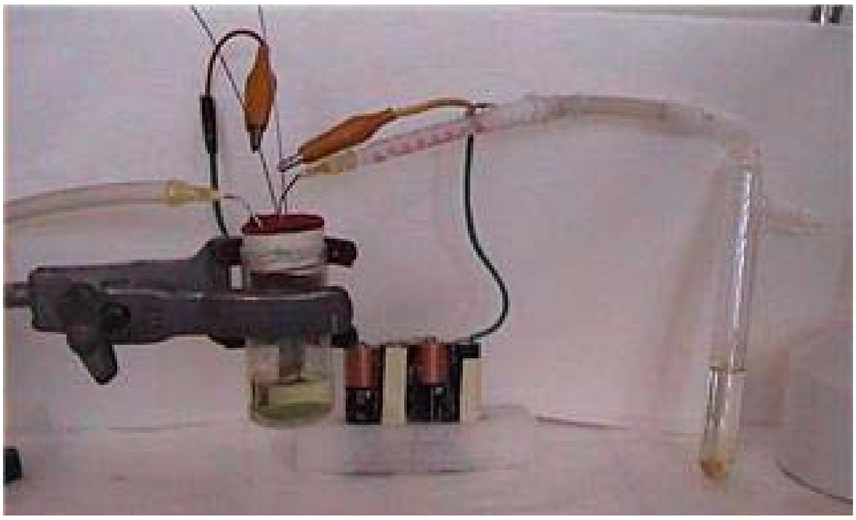

Figure 3.2 The experimental set-up of small scale synthesis

3.1.2 Electrochemical Synthesis of Poly(methylsilyne) in Large-Scale and Investigation of Effects of Parameters on the Synthesis

3.1.2.1 Materials

The materials used in the electrochemical synthesis of poly(methylsilyne) in large-scale are given in Table 3.3. The chemical structures of the additional solvent and supporting electrolyte can also be seen in Figure 3.3.

Table 3.3 The materials used in the synthesis of poly(methylsilyne)

Material Type	Material	Supplier
Monomer	Methyltrichlorosilane (≥ 97%)	Aldrich
Solvent	Acetonitrile (Dried)	Merck
	1,2-Dimethoxyethane (Anhydrous, 99.5%)	Aldrich
Supporting Electrolyte	Sodium Dodecyl Sulfate (ACS reagent, ≥ 99.0%)	Aldrich
	Tetrabutylammonium perchlorate (≥ 98.0%)	Fluka

The solution was stirred with lithium aluminum hydride and methanol (extra pure) that were purchased from Merck after the electrochemical synthesis was completed. In addition, toluene (extra pure) and THF (extra pure) that were used in the purification of the polymer were obtained from Merck.

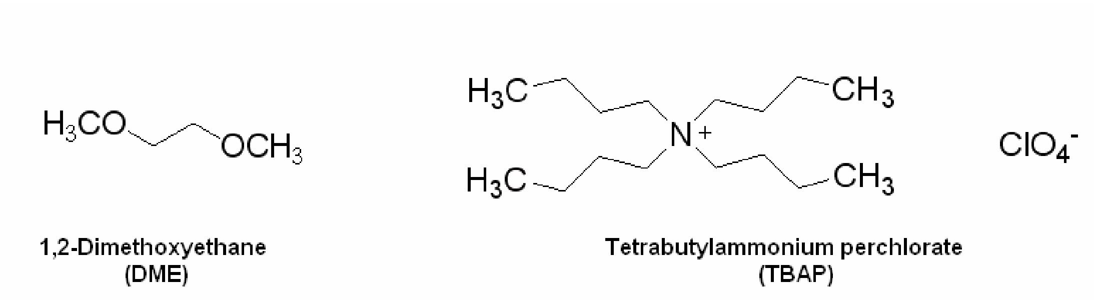

Figure 3.3 The chemical structures of the materials used in the synthesis

3.1.2.2 Experimental Parameters and Procedure

In the scaling-up of poly(methylsilyne) synthesis, the effects of the parameters such as electrolysis cell dimensions, electrode type and dimensions, supporting electrolyte type and amount, solvent type, monomer to solvent ratio and reaction time on the electrochemical polymerization was investigated. During large scale synthesis, the electrolysis cell and electrode dimensions were changed by using a thinner and a larger cell. Stainless steel and copper plates were used as the electrodes and SDS and TBAP were used as the supporting electrolyte. Two different solvents were used throughout the experiments, acetonitrile and DME. In addition, the monomer to solvent ratio was changed as 1:4, 1:5, 1:6, 1:10 and 1:20. Finally, the effect of the reaction time was investigated by keeping the electrolysis 30 min, 1 h and 4 h. During each large-scale synthesis, a DC power supply was used as the power source and methyltrichlorosilane was used as the monomer. Although the reaction was normally carried out at room temperature, in order to minimize the effect of temperature change, some of the experiments were carried out in a constant temperature bath at 25^0C. The experimental parameters used in each experiment are summarized in Tables 3.4-3.8.

The experimental procedure of large-scale synthesis is same with the small-scale electrochemical production of poly(methylsilyne). The copper electrodes were cleaned firstly with 5% aqueous solution of HCl, and then washed with distilled water and acetone. Then, the supporting electrolyte was added to the cell and the cell was closed after the electrodes were placed in it. The solvent and the monomer were injected to the cell that was purged with argon. Finally, the electrodes were connected to the power source and the reaction was carried out at the constant potential of -6 V under argon atmosphere. After the reaction has finished, the solution was stirred with $LiAlH_4$ or methanol under argon atmosphere. The experimental set-up of large scale synthesis can be seen in Figure 3.4.

In large-scale synthesis, the products synthesized by using SDS as the supporting electrolyte were not purified, whereas the products synthesized by TBAP were purified by different methods. In order to find the best purification method, PMS0204 sample was divided into two, the first portion was purified by dissolving in toluene, filtering and evaporating the solvent (PMS0204TS). The other portion was purified by dissolving in toluene, then washing with water and evaporating the toluene (PMS0204TW). Likewise, PMS1405 sample was divided into three. The first portion was dissolved in toluene, filtered and the toluene was evaporated (PMS1405TS). The second portion was dissolved in THF and added to cold methanol for precipitation (PMS1405M) and the third portion was dissolved in THF, filtered and THF was evaporated (PMS1405THF). PMS1104, PMS1505, PMS1605, PMS1905, PMS0506 and PMS0606 samples were purified by dissolving in toluene, filtering and evaporating the solvent.

Table 3.4 Parameters in poly(methylsilyne) synthesis with acetonitrile, stainless steel electrodes and SDS

Sample Name	PMS2211	PMS2311	PMS2411	PMS2611	PMS2711
Electrolytic Cell Dimensions	80 ml	80 ml	80 ml	80 ml	80 ml
Electrode Type	Stainless steel	Stainless steel	Stainless steel	Stainless steel	Stainless steel
Electrode Dimensions	1.5cm x 10cm	1.5cm x 10cm	1.5cm x 10cm	1.5cm x 10cm	1.5cm x 10cm
Supporting Electrolyte Type	SDS	SDS	SDS	SDS	SDS
Supporting Electrolyte Amount	0.200 g	0.200 g	0.200 g	0.200 g	0.200 g
Solvent Type	Acetonitrile	Acetonitrile	Acetonitrile	Acetonitrile	Acetonitrile
Monomer Amount	5 ml	7 ml	5 ml	5 ml	5 ml
Solvent Amount	25 ml	28 ml	30 ml	25 ml	25 ml
Monomer to Solvent Ratio	1:5	1:4	1:6	1:5	1:5
Reaction Time	30 min	30 min	30 min	1 h	4 h
Temperature	Room temp.	Room temp.	Room temp.	Room temp.	Room temp.
$LiAlH_4$ Amount	100 mg	100 mg	100 mg	100 mg	100 mg
Refluxing Time	3 h	3 h	3 h	3 h	3 h

Table 3.5 Parameters in poly(methylsilyne) synthesis with acetonitrile, copper electrodes and SDS

Sample Name	PMS0512	PMS0712	PMS1112	PMS1312	PMS1712
Electrolytic Cell Dimensions	200 ml	200 ml	200 ml	200 ml	200 ml
Electrode Type	Cu	Cu	Cu	Cu	Cu
Electrode Dimensions	2.5cm x 7.5cm	2.5cm x 7.5cm	2.5cm x 7.5cm	2.5cm x 7.5cm	2.5cm x 7.5cm
Supporting Electrolyte Type	SDS	SDS	SDS	SDS	SDS
Supporting Electrolyte Amount	0.400 g	0.400 g	0.400 g	0.400 g	0.400 g
Solvent Type	Acetonitrile	Acetonitrile	Acetonitrile	Acetonitrile	Acetonitrile
Monomer Amount	10 ml	5 ml	10 ml	5 ml	5 ml
Solvent Amount	50 ml	50 ml	50 ml	50 ml	50 ml
Monomer to Solvent Ratio	1:5	1:10	1:5	1:10	1:10
Reaction Time	30 min	30 min	4 h	1 h	30 min
Temperature	Room temp.	Room temp.	Room temp.	Room temp.	Room temp.
$LiAlH_4$ Amount	100 mg	100 mg	100 mg	100 mg	100 mg
Refluxing Time	3 h	3 h	3 h	3 h	3 h

Table 3.6 Parameters in poly(methylsilyne) synthesis with acetonitrile, copper electrodes and temperature control

Sample Name	PMS1601	PMS1701	PMS2101	PMS2501
Electrolytic Cell Dimensions	200 ml	200 ml	200 ml	200 ml
Electrode Type	Cu	Cu	Cu	Cu
Electrode Dimensions	2.5cm x 7.5cm	2.5cm x 7.5cm	2.5cm x 7.5cm	2.5cm x 7.5cm
Supporting Electrolyte Type	SDS	SDS	SDS	TBAP
Supporting Electrolyte Amount	0.400 g	0.400 g	0.400 g	1.375 g
Solvent Type	Acetonitrile	Acetonitrile	Acetonitrile	Acetonitrile
Monomer Amount	5 ml	5 ml	5 ml	5 ml
Solvent Amount	50 ml	50 ml	50 ml	50 ml
Monomer to Solvent Ratio	1:10	1:10	1:10	1:10
Reaction Time	30 min	4 h	1 h	30 min
Temperature	25^0C	25^0C	25^0C	25^0C
$LiAlH_4$ Amount	100 mg	100 mg	100 mg	100 mg
Refluxing Time	3 h	3 h	3 h	3 h

Table 3.7 Parameters in poly(methylsilyne) synthesis with DME, copper electrodes and temperature control

Sample Name	PMS1405	PMS1505	PMS1605	PMS1905	PMS0506	PMS0606
Electrolytic Cell Dimensions	200 ml	200 ml	200 ml	200 ml	200 ml	200 ml
Electrode Type	Cu	Stainless steel	Cu	Cu	Cu	Cu
Electrode Dimensions	2.5 x 7.5cm	2.5 x 7.5cm	2.5 x 7.5cm	2.5 x 7.5cm	2.5 x 7.5cm	2.5 x 7.5cm
Supporting Electrolyte Type	TBAP	TBAP	TBAP	TBAP	TBAP	TBAP
Supporting Electrolyte Amount	0.1 M	0.1 M	0.1 M	0.1 M	0.1 M	0.1 M
Solvent Type	DME	DME	DME	DME	DME	DME
Monomer Amount	5 ml	5 ml	10 ml	5 ml	5 ml	5 ml
Solvent Amount	50 ml	50 ml	50 ml	50 ml	100 ml	50 ml
Monomer to Solvent Ratio	1:10	1:10	1:5	1:10	1:20	1:10
Reaction Time	30 min	30 min	30 min	1 h	30 min	4 h
Temperature	25^0C	25^0C	25^0C	25^0C	25^0C	25^0C
$LiAlH_4$ Amount	100 mg	100 mg	200 mg	100 mg	100 mg	100 mg
Refluxing Time	3 h	3 h	3 h	3 h	3 h	3 h

Table 3.8 Parameters of the experiments with different methods to convert the remaining Si-Cl bonds

Sample Name	PMS0204	PMS1104
Electrolytic Cell Dimensions	200 ml	200 ml
Electrode Type	Cu	Cu (cathode) / Stainless Steel (anode)
Electrode Dimensions	2.5 x 7.5cm	2.5 x 7.5cm
Supporting Electrolyte Type	TBAP	TBAP
Supporting Electrolyte Amount	0.1 M	0.1 M
Solvent Type	Acetonitrile	Acetonitrile
Monomer Amount	5 ml	5 ml
Solvent Amount	50 ml	50 ml
Monomer to Solvent Ratio	1:10	1:10
Reaction Time	30 min	30 min
Method to Convert Remaining Si-Cl Bonds	30 ml methanol	100 mg $LiAlH_4$ in 50 ml dried THF
Refluxing Time	2 h	3 h

Figure 3.4 Large-scale experimental set-ups (a) 80 ml cell, (b) 200 ml cell

3.1.3 Characterization of Poly(methylsilyne)

The primary characterization of the synthesized polymer was its yellow color which is distinctive for polysilynes. Besides the color, the products were characterized by ^{1}H-NMR and FTIR methods, since those tests directly gave information about the chemical structure of the synthesized product. UV-Visible Spectroscopy and GPC were used for further characterization and they were applied only to products with successful ^{1}H-NMR and FTIR results.

^{1}H-NMR spectra were obtained using a Bruker-Spectrospin Avance DPX 400 Ultra-Shield (400 MHz) and deuterated chloroform as the solvent. FTIR spectra were collected by IR Prestige-21 SHIMADZU FTIR spectrometer (THF solution on KBr film). UV-Visible spectra were obtained using a HP8453A UV-Visible spectrometer using cyclohexane as the solvent. Finally, GPC was carried out using a Agilent (HP) GPC with THF solvent and polystyrene standards.

3.2 Preparation of Polypropylene/Preceramic Polymer Blends

Polypropylene/preceramic polymer blends were prepared with two different preceramic polymers: poly(methylsilyne) (PMSy) synthesized electrochemically and allylhydridopolycarbosilane (SMP-10) which was a commercially available silicon-based preceramic polymer similar to poly(methylsilyne).

3.2.1 Preparation of PP / Allylhydridopolycarbosilane (SMP-10) and PP / Poly(methylsilyne) (PMSy) Blends

3.2.1.1 Materials

Polypropylene (PETOPLEN MH 418) was purchased from PETKIM. The properties of PETOPLEN MH 418 can be seen in Table 3.9.

Table 3.9 Properties of polypropylene (PETOPLEN MH 418)

Properties	Value	Method
Melt Flow Rate	4.0 – 6.0 g/10min	ASTM D-1238
Impurities, 100 g	Max. 10 piece	TM-113
Tensile Stress at Yield Point	34.3 MPa	ASTM-638
Tensile Strength at Break Point	42.2 MPa	ASTM-638

The commercially available silicon-based preceramic polymer, allylhydridopolycarbosilane (SMP-10) was purchased from Starfire Systems. SMP-10 is a clear, amber liquid with a density of 0.998 g/ml, viscosity of 40 to 100 cps at 25^{0}C and surface tension of 30 dynes/cm^2. SMP-10 is a precursor for silicon carbide like poly(methylsilyne). It also has similar properties with poly(methylsilyne) such as solubility in THF, hexane and toluene. The chemical structure of SMP-10 can be seen in Figure 3.5.

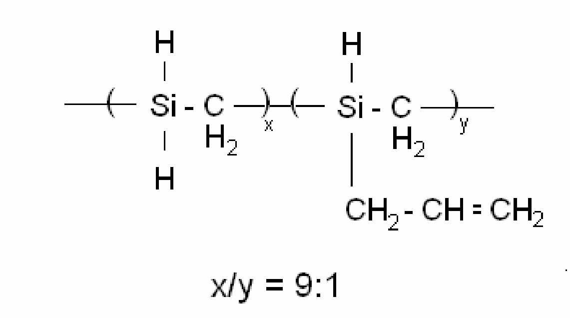

Figure 3.5 Chemical structure of allylhydridopolycarbosilane (SMP-10)

Poly(methylsilyne) that was synthesized with PMS1405 parameters and characterized was used in blend preparation with PP without purification.

Triphenylphosphate (TPP) which was purchased from ACROS Organics (98%, Mw=326.28) was also used in the preparation of flame retardant polypropylene blends in order to obtain synergism with SMP-10 and poly(methylsilyne). The chemical structure of TPP can be seen in Figure 3.6.

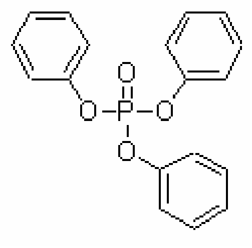

Figure 3.6 Chemical structure of TPP

Finally, a metal complex with the trade name of Smokebloc AZ-12/BFR-4 was supplied by Great Lakes Chemical Corporation to accomplish synergetic effect with silicon-based preceramic polymers and TPP in polypropylene. It was a blend of antimony trioxide, zinc/magnesium oxide complex and a proprietary mineral silicate.

3.2.1.2 Blend and Composite Preparation

Polypropylene was ground to powder form by Wiley mill intermediate model grinder before blend preparation in order to achieve better mixing with the preceramic polymers. Silicon-based preceramic polymers, poly(methylsilyne) and SMP-10 were dry mixed with polypropylene before they were fed and melt blended with polypropylene in a co-rotating twin-screw extruder (Thermoprism TSE 16 TC). The blends were prepared with a screw speed of 100 rpm and a temperature profile of 180 - 185 - 195 - 205 - 215^{0}C from hopper to die. The polymer blends were pelletized in the pelletizer after extrusion. Then they were dried at 100^{0}C for 4 h before they were molded in injection molding (DSM Xplore Micro 10 cc Injection Molding Machine). During injection molding, the barrel temperature was adjusted to 210^{0}C. The polymers were preheated for 3 min and then molded at 13.0 bars for the characterization tests. Photographs of the extruder and injection molding machine can be seen in Figures 3.7 and 3.8, respectively. The flowchart of the blend preparation procedure can be seen in Figure 3.9.

Figure 3.7 The co-rotating twin-screw extruder used in this study

Figure 3.8 The laboratory scale injection molding machine used in this study

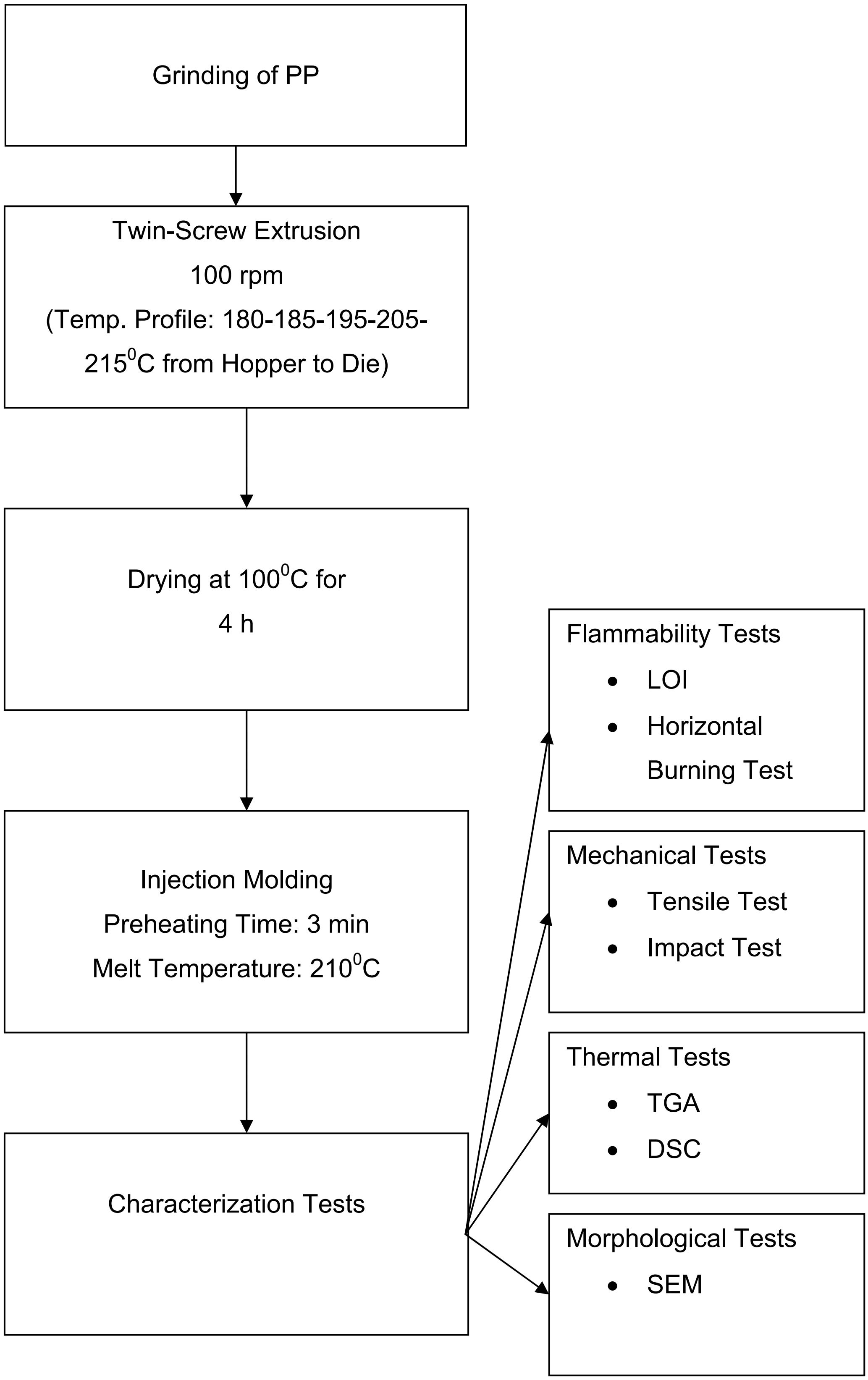

Figure 3.9 Flowchart of the experimental procedure

Table 3.10 The compositions of PP/SMP-10 blends prepared in the extruder

Components	PP%	SMP-10%	TPP%	Metal Complex %
PP/1SMP	99	1	-	-
PP/2SMP	98	2	-	-
PP/3SMP	97	3	-	-
PP/5SMP	95	5	-	-
PP10SMP	90	10	-	-
PP/5SMP/5TPP	90	5	5	-
PP/10SMP/10TPP	80	10	10	-
PP/10SMP/5TPP/5M	80	10	5	5

Table 3.11 The compositions of PP/PMSy blends prepared in the extruder

Components	PP%	PMSy%	SMP-10%	TPP%	Metal Complex %
PP/1PMS	99	1	-	-	-
PP/10PMS/10TPP	80	10	-	10	-
PP/10PMS/5TPP/5M	80	10	-	5	5
PP/5PMS/7.5TPP/7.5M	80	5	-	7.5	7.5
PP/5PMS/5SMP/5TPP/5M	80	5	5	5	5

The compositions of SMP-10, TPP and the metal complex and the compositions of PMSy, TPP and the metal complex in each set prepared by the twin-screw extruder can be seen in Table 3.10 and 3.11, respectively. In addition to PP/preceramic polymer blends, pure polypropylene was also ground and extruded in order to compare its properties with the blends. Furthermore, PP/10TPP/10M blend containing 10% TPP and 10% metal complex was prepared in the twin-screw extruder in order to see the effect of TPP and the metal complex alone in polypropylene.

3.2.2 Characterization of PP/Allylhydridopolycarbosilane (SMP-10) and PP/Poly(methylsilyne) (PMSy) Blends

3.2.2.1 Flammability Tests

3.2.2.1.1 Limiting Oxygen Index (LOI) Test

As mentioned in the previous sections, LOI is the minimum oxygen concentration (volume percent of oxygen in an oxygen/nitrogen mixture) that will sustain burning. LOI test was performed according to the ASTM D2863 standards in the Dynisco Polymer Test LOI machine which can be seen in Figure 3.10. The specimen used in LOI test had a length of 8 cm, width of 1 cm and thickness of 4 mm.

Figure 3.10 Dynisco polymer test LOI machine

During LOI test, the specimen was positioned in the vertical position in the transparent column. The concentration of oxygen in the column was set by adjusting the flow rates of oxygen and nitrogen gases that were moving upward through the column. The polymer was ignited from the top [58]. The schematic drawing of LOI can be seen in Figure 3.11.

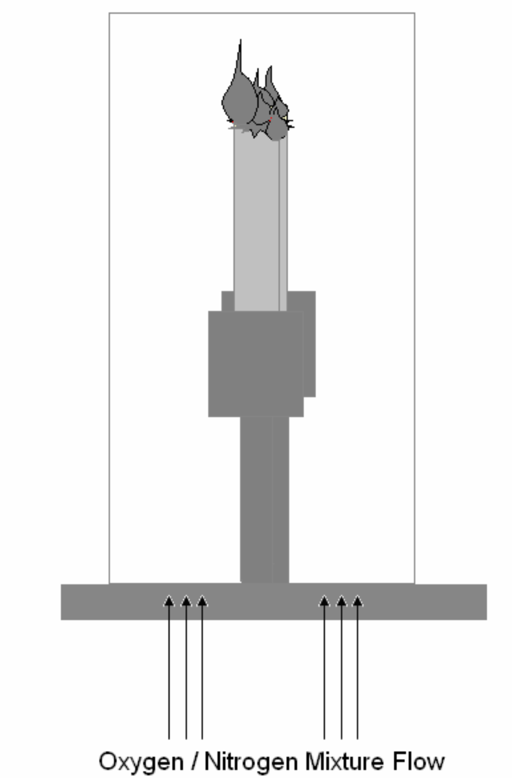

Figure 3.11 LOI test

3.2.2.1.2 Horizontal Burning Test

The horizontal burning test was performed according to the ASTM D635 standard which is the standard test method for determining the rate of burning and/or extent and time of burning of plastics in a horizontal position. In horizontal burning test, specimens with a length of 8 cm, width of 1 cm and thickness of 4 mm were used. In the test, 5 specimens were used for each set.

In horizontal burning test, firstly the specimen was marked at 25 mm from one end. Then, it was positioned horizontally from the other end. During the test, a flame was directly applied to the free end for 30 seconds or until the flame reached to the mark at 25 mm, then the flame was removed. The burning rate was calculated for the samples that were burned completely and average burning time and average burned length were calculated for the samples that were extinguished. The test was repeated for five samples in each set and average values were reported. A schematic drawing of horizontal burning test can be seen in Figure 3.12.

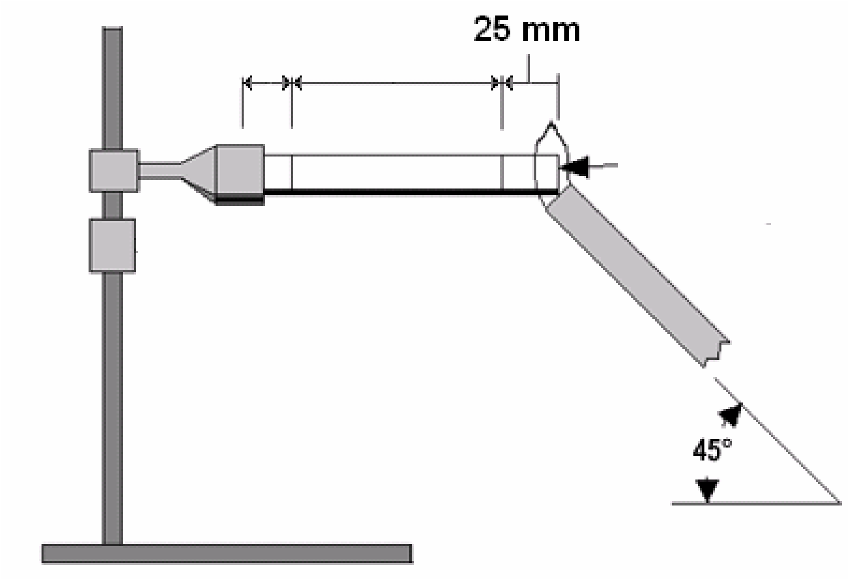

Figure 3.12 Horizontal burning test [59]

3.2.2.2 Mechanical Tests

3.2.2.2.1 Tensile Test

Tensile test of the polymers were performed according to the ASTM D638 standard by using Shimadzu Autograph AG-100 KNIS MS tensile testing machine. The injection molded specimen used in the tensile test had a gauge length, L_0, of 20 mm, width of 4 mm and thickness of 2 mm. The specimen can be seen in Figure 3.13. During the test, the crosshead speed of the testing instrument was set to 20 mm/min. As a result of the test, tensile stress at yield and at break, Young's modulus and elongation at break values were calculated. Each set was repeated for 5 specimens and the average values and standard deviations were reported.

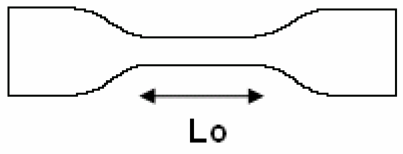

Figure 3.13 Tensile test specimen

3.2.2.2.2 Impact Test

Charpy impact test was applied to the unnotched specimen according to the ASTM D256 standards by using a Pendulum Ceast Resil Impactor with a pendulum of 7.5 J. For impact tests, specimens with a length of 8 cm, width of 1 cm and thickness of 4 mm were used. Impact strengths were calculated by dividing the impact energy to the area of 40×10^{-6} m^2 shown in Figure 3.14 and expressed in kJ/m^2. The test was repeated for five samples and the average values were reported.

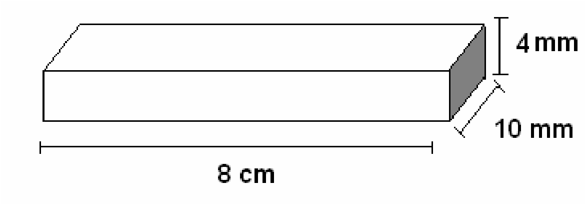

Figure 3.14 Impact test specimen and the area used in calculations

3.2.2.3 Thermal Tests

3.2.2.3.1 Thermogravimetric Analysis (TGA)

TGA was performed by using a SHIMADZU 60H-DTG machine. It was performed at nitrogen atmosphere, in the temperature range of room temperature to 800^{0}C by the heating rate of 20^{0}C/min. As a result of TGA analysis, the average decomposition temperature, the mass loss and char yield at 800^{0}C were reported for the polymer blends.

3.2.2.3.2 Differential Scanning Calorimetry Analysis (DSC)

DSC was performed by using a SHIMADZU DSC-60 Machine. It was performed from room temperature to 260^{0}C with a heating rate of 20^{0}C/min. As a result of DSC analysis, the melting temperatures were determined from the DSC curves of the blends.

3.2.2.4 Morphological Tests

3.2.2.4.1 Scanning Electron Microscopy (SEM) Analysis

For the SEM analysis, a low voltage JEOL JSM-6400 scanning electron microscope was used. For obtaining SEM photographs, the impact fractured surfaces were used. These surfaces were coated with a thin layer of gold in order to provide conductivity on the surfaces. In this study, SEM analysis was used to observe the distribution of the flame retardant additives and their effects on the morphology of PP. The SEM photographs were taken at x250, x500 and x1500 magnifications for each set.

CHAPTER 4

RESULTS AND DISCUSSION

The results and discussion part of this dissertation is divided into two: (1) electrochemical synthesis and characterization of poly(methylsilyne) and (2) preparation and characterization of polypropylene/silicon-based preceramic polymer blends. In the first part, the ^{1}H-NMR, FTIR, UV-Visible Spectroscopy and GPC results of small-scale and large-scale synthesis are discussed. In the second part, the flammability, mechanical, thermal and morphological results are given for polypropylene/preceramic polymer blends.

4.1 Electrochemical Synthesis of Poly(methylsilyne)

4.1.1 Electrochemical Synthesis of Poly(methylsilyne) in Small-Scale

The yellow solid product synthesized by the electrochemical polymerization of methyltrichlorosilane at constant potential of -6 V under argon atmosphere is characterized by ^{1}H-NMR, FTIR, UV-Visible Spectroscopy and GPC methods.

The ^{1}H-NMR result of the polymer can be seen in Figure 4.1. The presence of poly(methylsilyne) is determined by the broad peak between 0 and 0.5 ppm indicating the Si-CH_3 bond in the polymer [3, 7, 8]. This characteristic poly(methylsilyne) peak can be seen in the ^{1}H-NMR result of the small-scale product. In addition to the peak between 0 and 0.5 ppm, a peak corresponding to Si-H bond can be seen at 4.2 ppm [8]. The presence of Si-

CH_3 and Si-H bonds in the ^{1}H-NMR result proves the formation of a silicon backbone polymer with $-CH_3$ and –H side groups. Si-H group formation is obtained because of the stirring of the solution with $LiAlH_4$ after electrolysis in order to convert all the remaining Si-Cl bonds [8]. Therefore the ^{1}H-NMR result indicates that poly(methylsilyne) is synthesized successfully in small-scale. In the ^{1}H-NMR result, peaks corresponding to the solvents used in purification, THF and pentane are also present at 1.7, 3.6 and 1.3 ppm. SiHCl or SiOH peaks are not observed in the result [3].

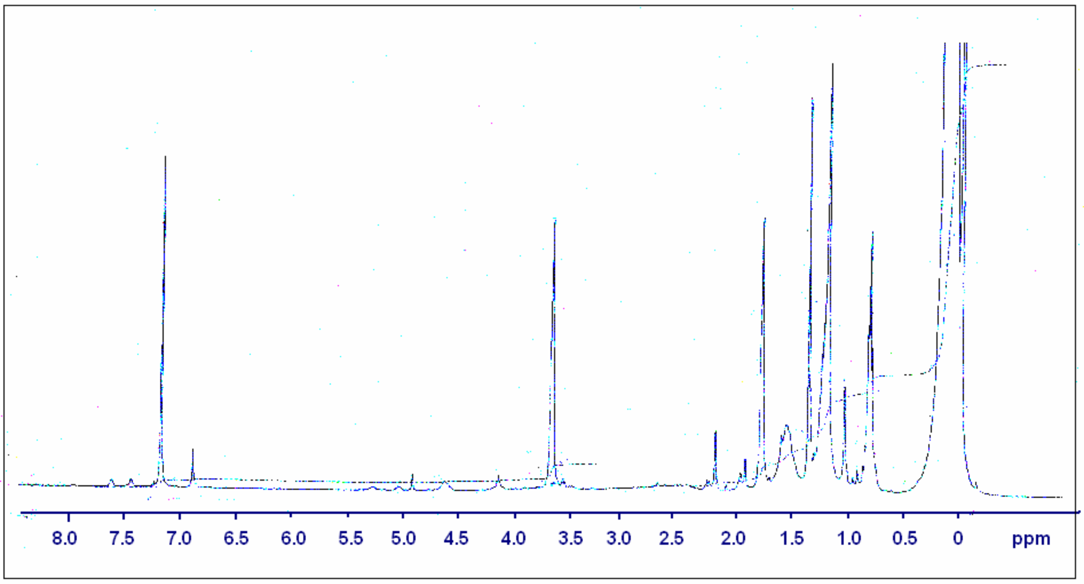

Figure 4.1 ^{1}H-NMR result of poly(methylsilyne) synthesized in small-scale

The polymer is also characterized by FTIR after ^{1}H-NMR since it is an important method in polymer characterization. The FTIR result of the polymer can be seen in Figure 4.2. The FTIR spectrum obtained for the polymer is consistent with the previous results in literature [3, 7, 8]. The peaks at 2980, 2866, 1463 and 1268 cm^{-1} corresponding to C-H bonds in Si-CH_3 and peaks at 919 and 778 cm^{-1}

corresponding to SiH_2 and Si-C bonds, respectively, are the peaks expected for poly(methylsilyne) [3, 7, 8]. A peak at 1083 cm^{-1} is also observed in the FTIR spectrum indicating the presence of Si-O-Si bond which can be explained by the reactivity of the polymer towards oxygen [8]. In the FTIR spectrum, no peak corresponding to Si-Cl bond is observed proving that all the remaining Si-Cl bonds are converted.

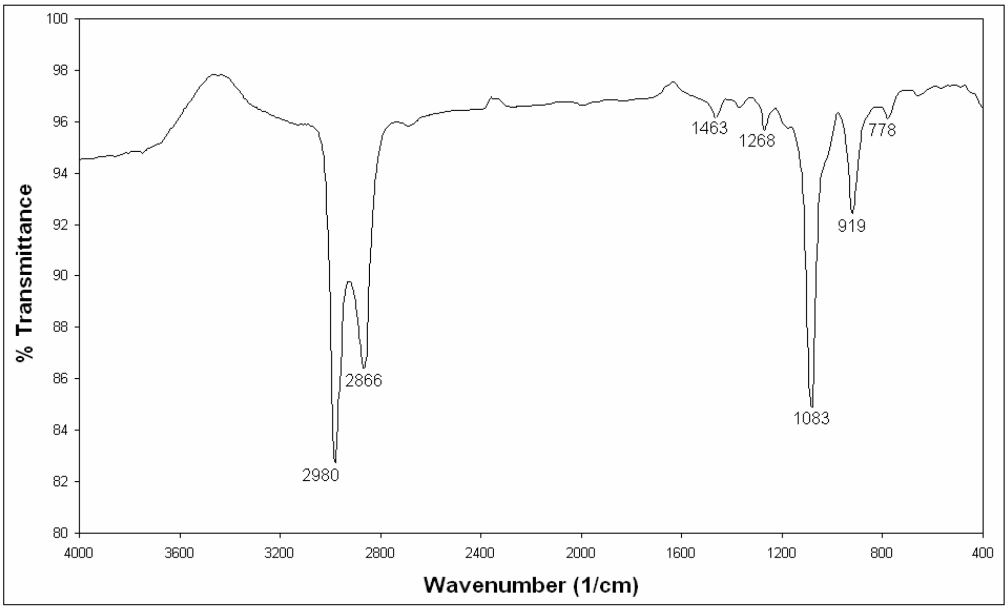

Figure 4.2 FTIR spectrum of poly(methylsilyne) synthesized in small-scale

The polymer that is synthesized in small-scale is then characterized by UV-Visible Spectroscopy. The UV-Visible spectrum of the polymer can be seen in Figure 4.3. The UV-Visible spectrum of the polymer exhibits a broad UV band that tails into the visible region at approximately 400 nm. This broad UV band is characteristic for polysilynes [3, 6-8, 11, 12]. In addition, this spectrum indicates the branched structure of the polymer, since linear polysilanes have a significantly different UV-Visible spectrum which has two sharp absorption peaks [9, 11].

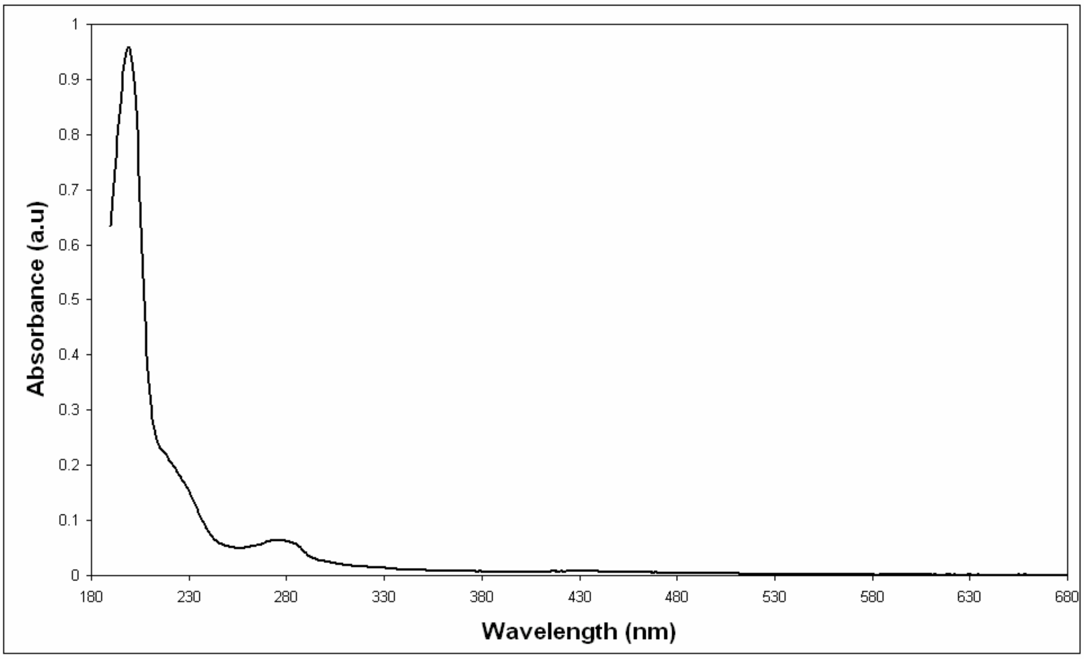

Figure 4.3 UV-Visible spectrum of poly(methylsilyne) synthesized in small-scale

Finally, the polymer's molecular weight is determined by GPC with polystyrene standards. The molecular weight, M_w, and polydispersity index are determined as 5900 and 1.15, respectively. This molecular weight is reasonable when compared with the values in literature. For instance, Vermeulen et al. [8] determined M_w as 6457.

As a conclusion, the yellow color of the polymer and the results of ^{1}H-NMR, FTIR, UV-Visible Spectroscopy and GPC tests prove that the synthesis of poly(methylsilyne) is successful in small-scale with SDS and batteries.

4.1.2 Electrochemical Synthesis of Poly(methylsilyne) in Large-Scale and Investigation of Effects of Parameters on the Synthesis

After poly(methylsilyne) is successfully synthesized in small-scale with SDS and batteries and characterized by ^{1}H-NMR, FTIR, UV-Visible Spectroscopy and GPC methods, the synthesis is scaled-up for 5 times and the important parameters and their effects on the synthesis are investigated. The ^{1}H-NMR and FTIR spectra of each experiment are given in Appendix A.

4.1.2.1 Poly(methylsilyne) Synthesis with Acetonitrile, SDS and Stainless Steel Electrodes

Since the polymer is successfully synthesized in small-scale with stainless steel electrodes, SDS and acetonitrile, the first scale-up experiments are done with these parameters. The values of the experimental parameters of the synthesis with acetonitrile, SDS and stainless steel electrodes, PMS2211, PMS2311, PMS2411, PMS2611 and PMS2711, are given in Table 3.4 in Chapter 3. In these large-scale syntheses, the effects of monomer to solvent ratio and reaction time on the physical properties and ^{1}H-NMR and FTIR results of the products are discussed.

4.1.2.1.1 The Effect of Monomer/Solvent Ratio

The effect of monomer to solvent ratio on the synthesis is investigated by PMS2311, PMS2211 and PMS2411 samples with the monomer/solvent ratios of 1/4, 1/5 and 1/6 , respectively. Poly(methylsilyne) is obtained as a yellow oil or solid in the studies in literature [3, 7, 8]. Therefore, the products can be primarily characterized by their physical properties. In order to investigate the effect of this ratio on the synthesis, first the physical properties of the products are compared in Table 4.1.

Table 4.1 Physical properties of PMS2311, PMS2211 and PMS2411

Sample Name	Physical Properties
PMS2311	Brown oil
PMS2211	Yellow solid
PMS2411	White solid

It can be seen that the monomer/solvent ratio in the synthesis has a significant effect on the physical properties of the products. For instance, PMS2311, which has the highest ratio, is a brownish oil unlike the polymer obtained in small-scale. The only product with successful physical properties is PMS2211 with a monomer/solvent ratio of 1/5 as seen in small-scale synthesis.

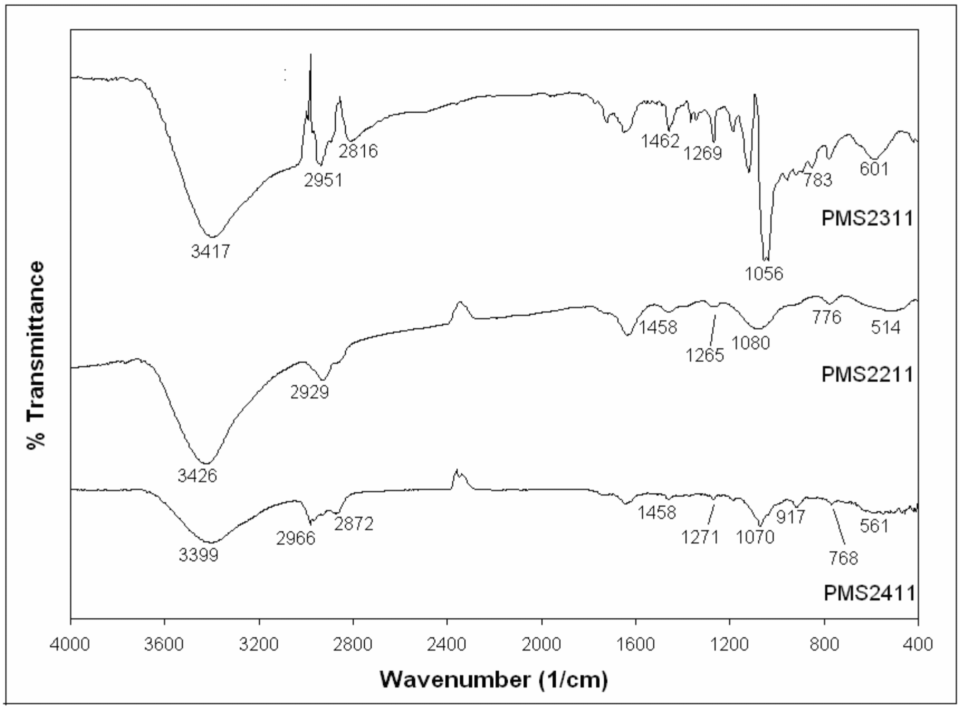

Figure 4.4 FTIR spectra of PMS2311, PMS2211 and PMS2411

The FTIR spectra of PMS2311, PMS2211 and PMS2411 samples can be seen in Figure 4.4. From these results, it can be seen that FTIR results of PMS2211 and PMS2411 are very similar to the small-scale FTIR spectrum, exhibiting all the expected peaks for poly(methylsilyne), whereas the FTIR result of PMS2311 is not. In addition, it has seen that Si-Cl peak is present in all of the results unlike the small-scale result, showing that there are still some unconverted Si-Cl bonds during refluxing. From the physical properties and FTIR results, it is clear that increasing the monomer/solvent ratio has negative effects on the synthesis.

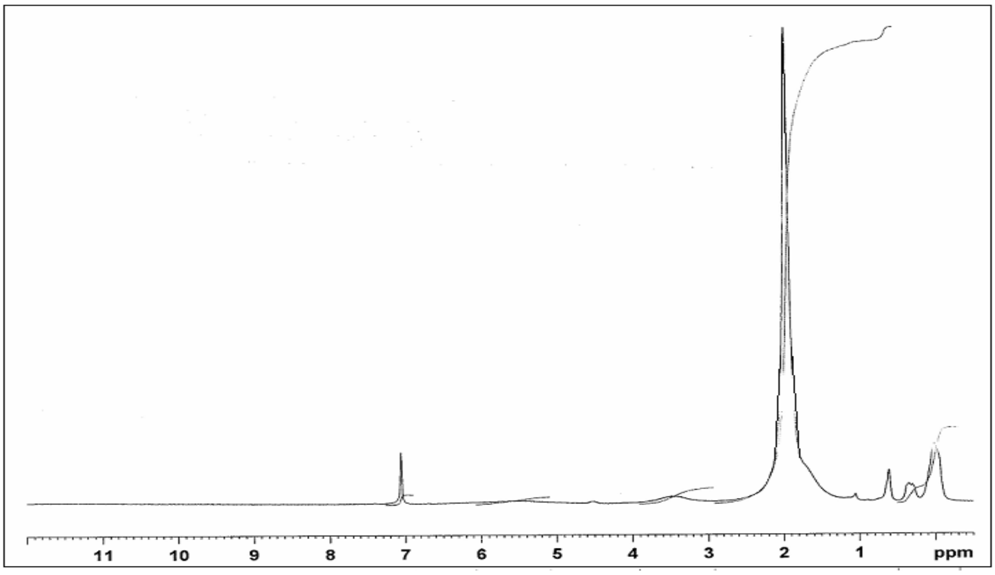

Figure 4.5 ^{1}H-NMR spectrum of PMS2211

Since only PMS2211 has both successful physical properties and FTIR result, only its ^{1}H-NMR result is given in Figure 4.5. From the NMR result it can be seen that there is a small broad peak observed at 0.1 ppm corresponding to Si-CH$_3$ bond. However this peak is relatively small when compared with small-scale NMR results. In addition, broad peak at 3.48 ppm indicates the presence of Si-H bond [8]. Furthermore, peaks corresponding to acetonitrile and chloroform are observed in the result at 1.94 and 7.05 ppm, respectively.

4.1.2.1.2 The Effect of Reaction Time

The effect of reaction time on the syntheses with acetonitrile, SDS and stainless steel electrodes is investigated by PMS2211, PMS2611 and PMS2711 samples with the reaction times of 30 min, 1 h and 4 h, respectively.

The physical properties of the products can be seen in Table 4.2. It is observed that only PMS2211 has the expected physical properties. PMS2611 and PMS2711, on the other hand, have darker colors. It can be concluded that increasing the reaction time in a system with acetonitrile, SDS and stainless steel electrodes has a negative effect on the physical properties of the products.

Table 4.2 Physical properties of PMS2211, PMS2611 and PMS2711

Sample Name	Physical Properties
PMS2211	Yellow solid
PMS2611	Black oil
PMS2711	Green oil & solid

The FTIR spectra of PMS2211, PMS2611 and PMS2711 can be seen in Figure 4.6. It can be seen that in the FTIR spectra of PMS2211 and PMS2611, the characteristic peaks for poly(methylsilyne) corresponding to C-H, SiH_2 and Si-C bonds are observed. Therefore, these results are successful. However, in the FTIR spectrum of PMS2711, the C-H peaks at 2970 and 2890 cm^{-1} can not be observed. In addition, the siloxane bond at 1032 cm^{-1} is much broader than the other two results indicating that the product contains significant amount of siloxanes due to oxidation. Furthermore, the Si-Cl bond at 586 cm^{-1} in PMS2711 result is more significant when compared with the other two results. As a conclusion of the physical properties and FTIR results of the products, it can be seen that for the electrochemical synthesis of poly(methylsilyne) using acetonitrile, SDS and stainless steel electrodes, increasing the reaction time affects the synthesis in a negative manner.

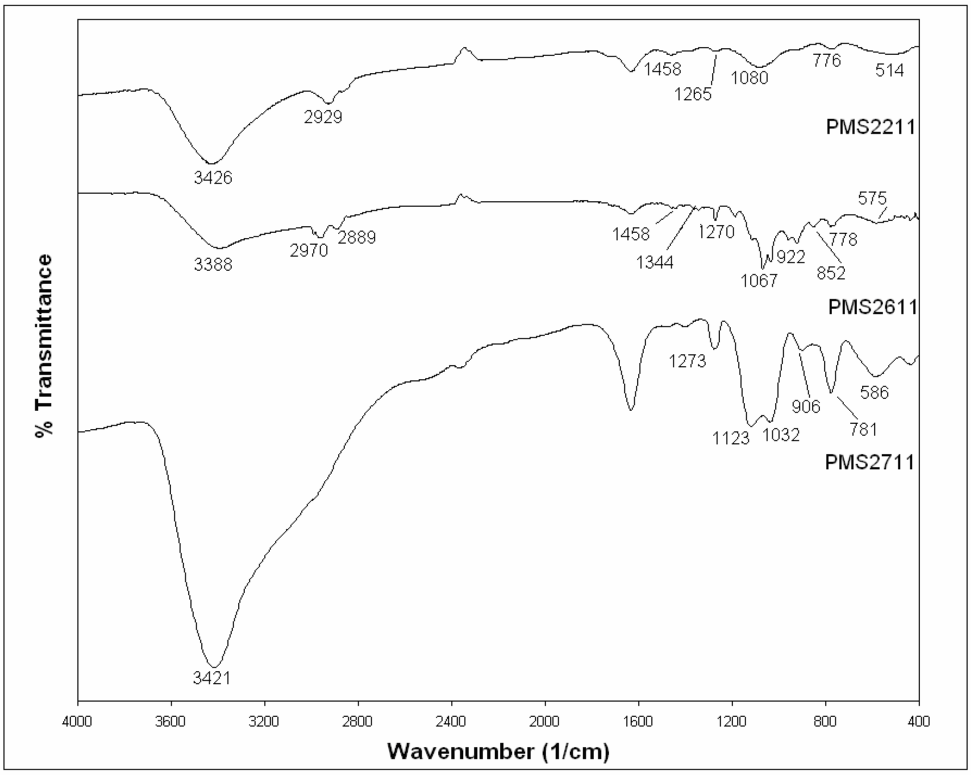

Figure 4.6 FTIR spectra of PMS2211, PMS2611 and PMS2711

For the large-scale electrochemical production of poly(methylsilyne) with acetonitrile, SDS and stainless steel electrodes, it has seen that the small scale parameters, monomer to solvent ratio of 1/5 and reaction time of 30 min give the best result. However, the ^{1}H-NMR result of PMS2211 still shows some differences with the small-scale result.

4.1.2.2 Poly(methylsilyne) Synthesis with Acetonitrile, SDS and Copper Electrodes

Although stainless steel electrodes give successful results in small-scale synthesis, the use of these electrodes cause some problems in large-scale. It has seen that in large-scale synthesis, the deformation of the stainless steel electrodes with increasing reaction time causes impurities in the product. Therefore, products with darker colors are obtained. In order to minimize the impurities coming from the electrodes, the synthesis is done with copper electrodes. The values of the experimental parameters of the synthesis with acetonitrile, SDS and copper electrodes, PMS0512, PMS0712, PMS1112, PMS1312 and PMS1712 are given in Table 3.5 in Chapter 3. The effects of monomer to solvent ratio and reaction time on the physical properties and FTIR and ^{1}H-NMR results of the products are investigated in the syntheses with acetonitrile, SDS and copper electrodes.

4.1.2.2.1 The Effect of Monomer/Solvent Ratio

The effect of monomer/solvent ratio is investigated in PMS0512 and PMS0712 samples with the ratios of 1/5 and 1/10, respectively. Since increasing the monomer/solvent ratio affects the system negatively, in the syntheses with copper electrodes, smaller monomer/solvent ratios are taken.

The physical properties of the products can be seen in Table 4.3. It can be seen that both of the products have yellow color as expected. Therefore, it can be concluded that by replacing stainless steel electrodes with the copper electrodes, the effect of monomer/solvent ratio on the color of the product is eliminated. However, it can be seen that the decrease in monomer/solvent ratio still creates a difference in the physical properties since PMS0512 is an oil and PMS0712 is a solid. As mentioned before, poly(methylsilyne) is synthesized both as an oil and a solid in literature. Yellow oil products were obtained for polymers with lower molecular weights [8] and yellow solid products were obtained for polymers with higher molecular weights [3, 7].

Table 4.3 Physical properties of PMS0512 and PMS0712

Sample Name	Physical Properties
PMS0512	Yellow oil
PMS0712	Yellow solid

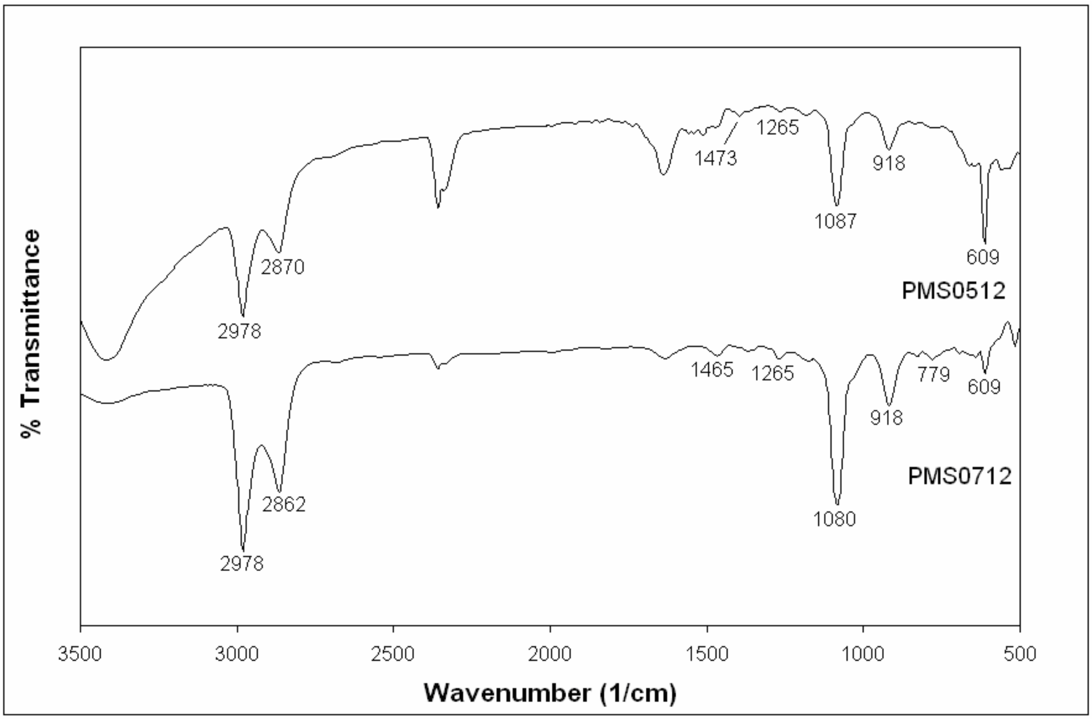

Figure 4.7 FTIR spectra of PMS0512 and PMS0712

The FTIR spectra of PMS0512 and PMS0712 can be seen in Figure 4.7. The FTIR results of both of the samples are very successful exhibiting all the characteristic poly(methylsilyne) peaks.

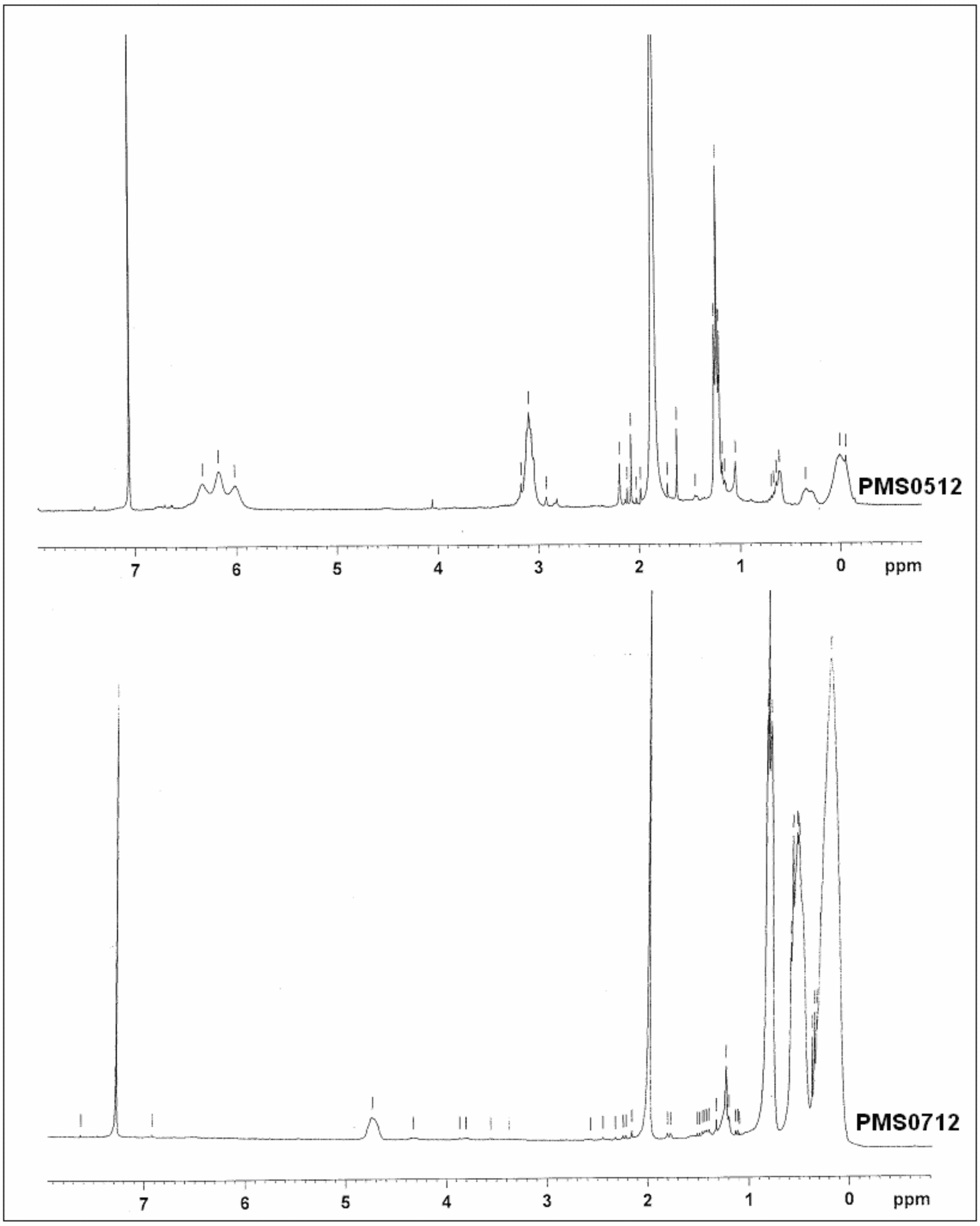

Figure 4.8 ^{1}H-NMR spectra of PMS0512 and PMS0712

The ^{1}H-NMR results of the two samples can be seen in Figure 4.8. In the NMR result of PMS0712, the broad peak between 0 and 0.5 ppm which is the characteristic peak of poly(methylsilyne) can be observed. In PMS0512, a broad peak is also observed between 0 and 0.4 ppm however it is relatively small when compared with the peak in small-scale or PMS0712 results. In the results, appart from Si-CH_3 bond, peaks corresponding to acetonitrile, SDS and chloroform are also seen.

As a conclusion, it is observed that in large-scale synthesis with acetonitrile, SDS and copper electrodes, decreasing the monomer to solvent ratio affects the synthesis in a positive manner. PMS0712 sample with a monomer/solvent ratio of 1/10 is a yellow solid with successful FTIR and ^{1}H-NMR results.

4.1.2.2.2 The Effect of Reaction Time

The effect of reaction time on the large-scale synthesis of poly(methylsilyne) is investigated both in the samples with monomer/solvent ratios of 1/5 and 1/10. In monomer/solvent ratio of 1/5, the effect of reaction time is investigated by PMS0512 and PMS1112 samples with reaction times of 30 min and 4 h, respectively, whereas in monomer/solvent ratio of 1/10, it is studied by PMS0712 and PMS1312 samples with reaction times of 30 min and 1 h, respectively.

Table 4.4 Physical properties of PMS0512, PMS1112, PMS0712 and PMS1312

Sample Name	Physical Properties
PMS0512	Yellow oil
PMS0712	Yellow solid
PMS1112	Yellow solid
PMS1312	Yellow wax

The physical properties of the samples can be seen in Table 4.4. It can be seen that all of the products have yellow colors. The reaction time only affects the physical state of the product.

The FTIR spectra of PMS0512 and PMS0712 can be seen in Figure 4.9. The results are very similar to each other and to the FTIR result of the small-scale synthesis exhibiting all the characteristic peaks for poly(methylsilyne). However, in the FTIR spectrum of PMS0512, the peak at 609 cm^{-1} indicating Si-Cl bond is more significant than the peak in PMS1112 result. Since in PMS1112 sample the reaction time is much longer than PMS0512, it is reasonable to obtain less amount of unconverted Si-Cl bond.

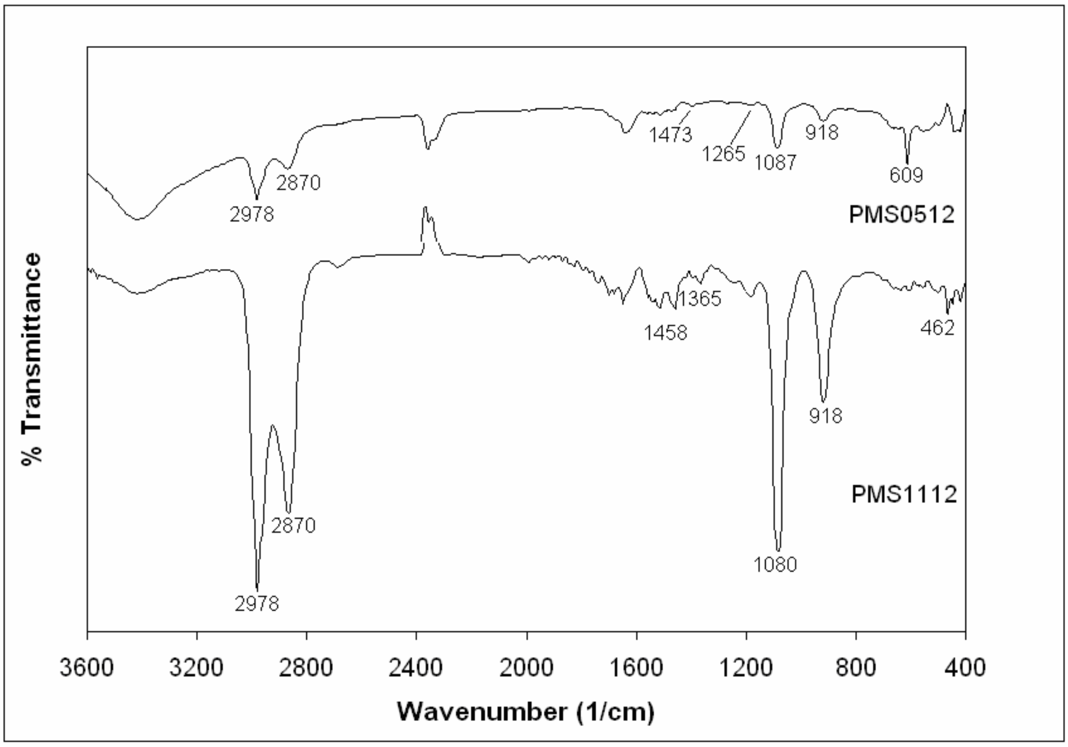

Figure 4.9 FTIR spectra of PMS0512 and PMS1112

The FTIR spectra of PMS0712 and PMS1312 can be seen in Figure 4.10. The FTIR results of the samples are both very similar to the small-scale result showing all the expected peaks.

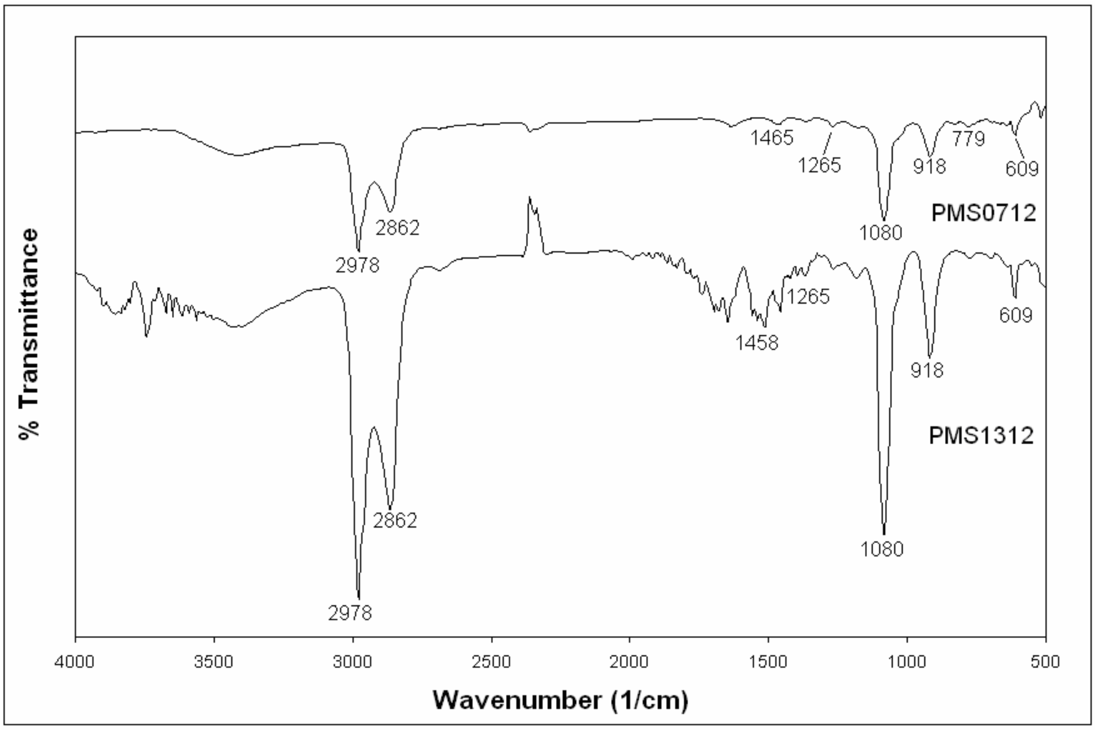

Figure 4.10 FTIR spectra of PMS0712 and PMS1312

The ^{1}H-NMR spectra of PMS0512 and PMS1112 samples which are represented in Figure 4.11, are very similar to each other showing the same peaks. The peak at 0.1 ppm is relatively small in both of the results. As a conclusion, it is observed that in the samples with monomer/solvent ratios of 1/5, the reaction time does not affect the FTIR and ^{1}H-NMR results of the products. The only difference of the two samples is the physical state of the polymers which can be explained by the differences in the molecular weights of the products due to different reaction times.

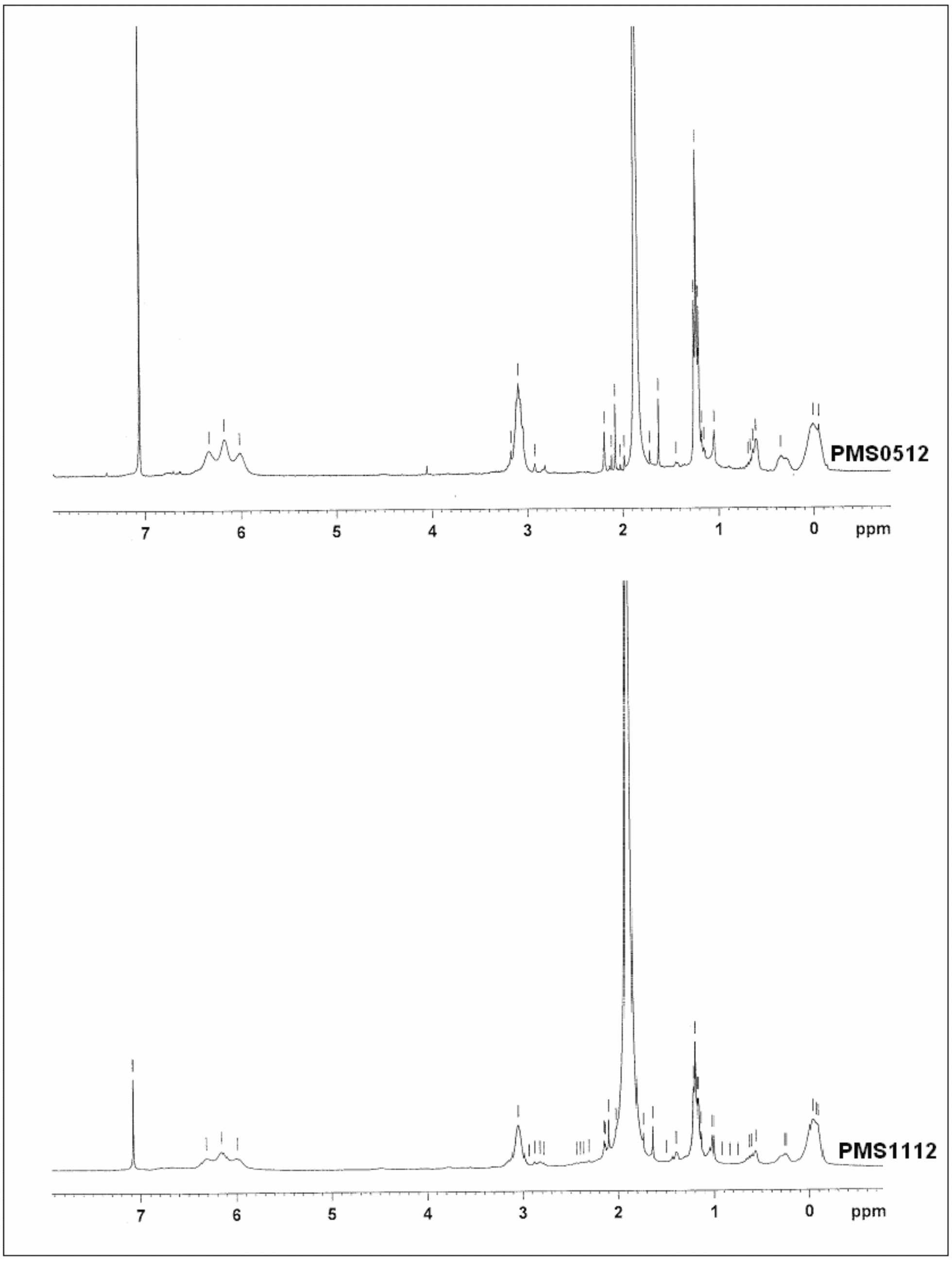

Figure 4.11 ^{1}H-NMR spectra of PMS0512 and PMS1112

The ^{1}H-NMR spectra of PMS0712 and PMS1312 can be seen in Figure 4.12. Similar to PMS0512 and PMS1112 samples, the ^{1}H-NMR spectra of PMS0712 and PMS1312 samples are very similar to each other showing the same peaks.

In both of the results, a broad peak between 0 and 0.5 ppm is observed showing the presence of poly(methylsilyne). This result indicates that poly(methylsilyne) is synthesized in both samples with a monomer/solvent ratio of 1/10 both at 30 min and 1 h.

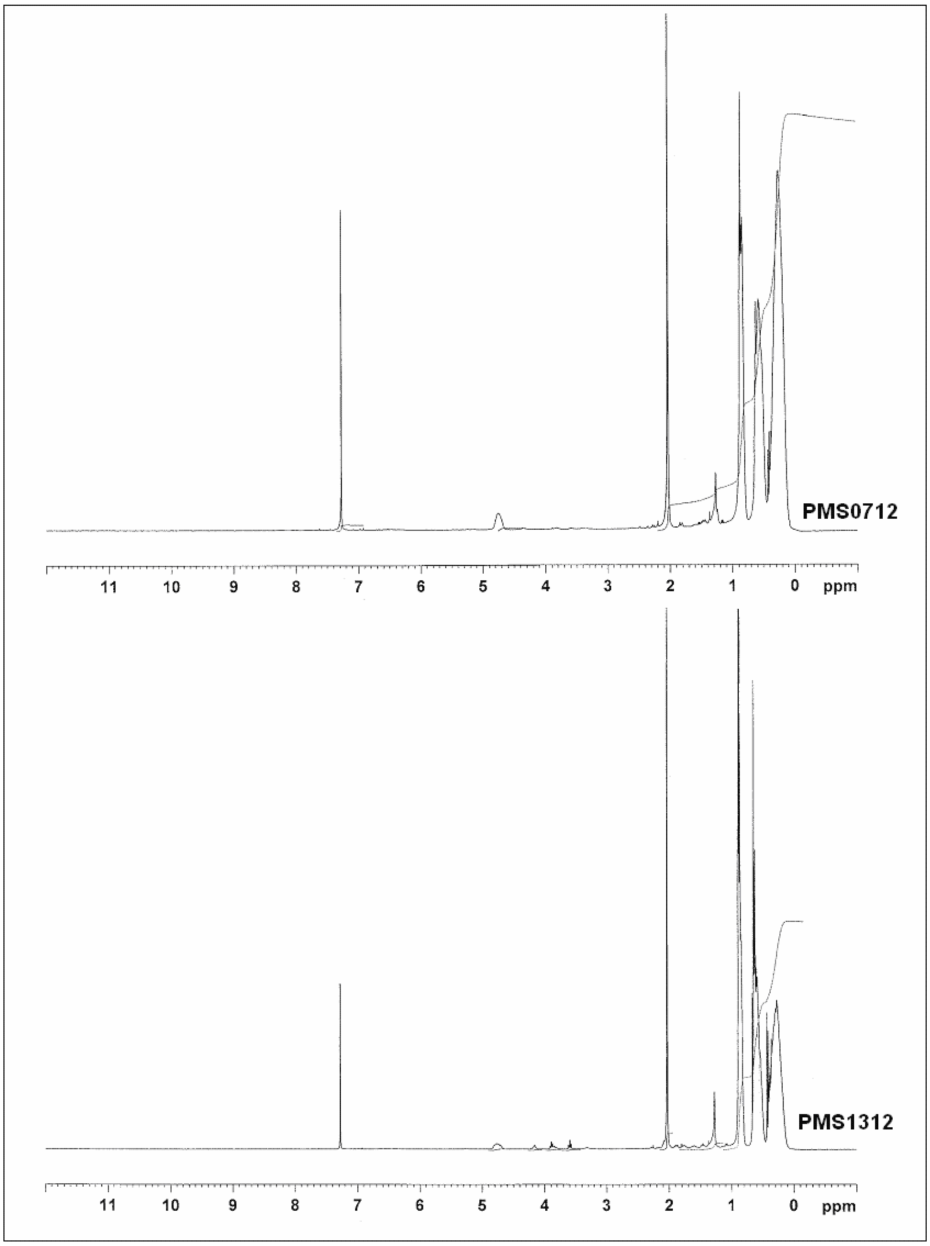

Figure 4.12 ^{1}H-NMR spectra of PMS0712 and PMS1312

These results show that the reaction time does not affect the FTIR and ^{1}H-NMR results of the polymer significantly. Therefore it can be concluded that the success of the product depends significantly on the monomer/solvent ratio rather than the reaction time. This can be explained by the fact that reaction time only affects the molecular weight of the product not the chemical structure. However, this conclusion is only valid for the large-scale synthesis with copper electrodes. In the synthesis by using stainless steel electrodes it is observed that increasing the reaction time results in increase in the impurities in the system due to the deformation of the electrodes and therefore affects the product in a negative manner.

4.1.2.2.3 Reproducibility of the System

The physical properties and FTIR and ^{1}H-NMR spectra of PMS0712 and PMS1312 prove that successful products are obtained in large-scale synthesis of poly(methylsilyne) with acetonitrile, SDS and copper electrodes. Although successful products are obtained with acetonitrile, SDS and copper electrodes, the main problem is the reproducibility of the synthesis. In order to investigate the reproducibility of the large-scale synthesis, the results of PMS0712 and PMS1712 having the exactly same parameters are compared.

The physical properties of the products can be seen in Table 4.5. It can be seen that although all the parameters of the two samples are the same, the products are different.

Table 4.5 Physical properties of PMS0712 and PMS1712

Sample Name	Physical Properties
PMS0712	Yellow solid
PMS1712	Dark yellow wax

The FTIR spectra of PMS0712 and PMS1712 can be seen in Figure 4.13. The FTIR spectra of the two samples are very similar to each other although the physical properties of the products are different.

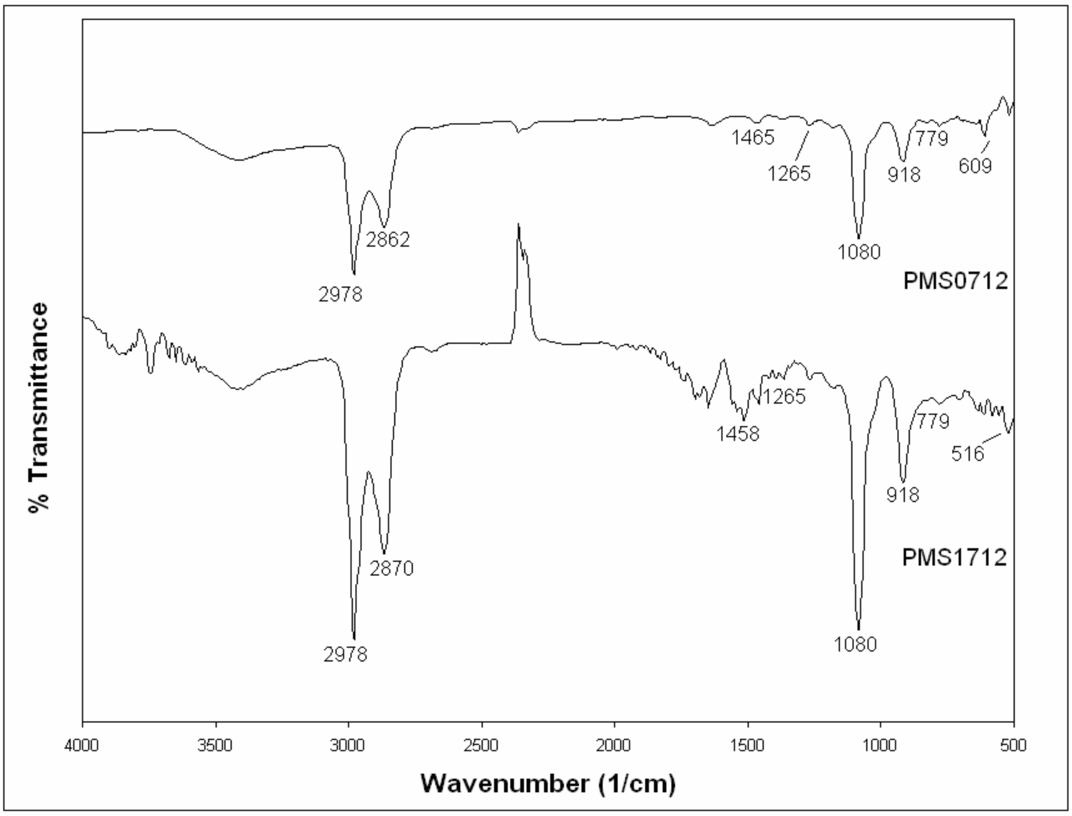

Figure 4.13 FTIR spectra of PMS0712 and PMS1712

The ^{1}H-NMR spectra of PMS0712 and PMS1712 are represented in Figure 4.14. The differences in the NMR results of the two samples indicate the problems in the reproducibility of the synthesis. Although the samples are synthesized with the same parameters, the Si-CH_3 peak in PMS1701 is smaller compared with the peak in PMS0712 result.

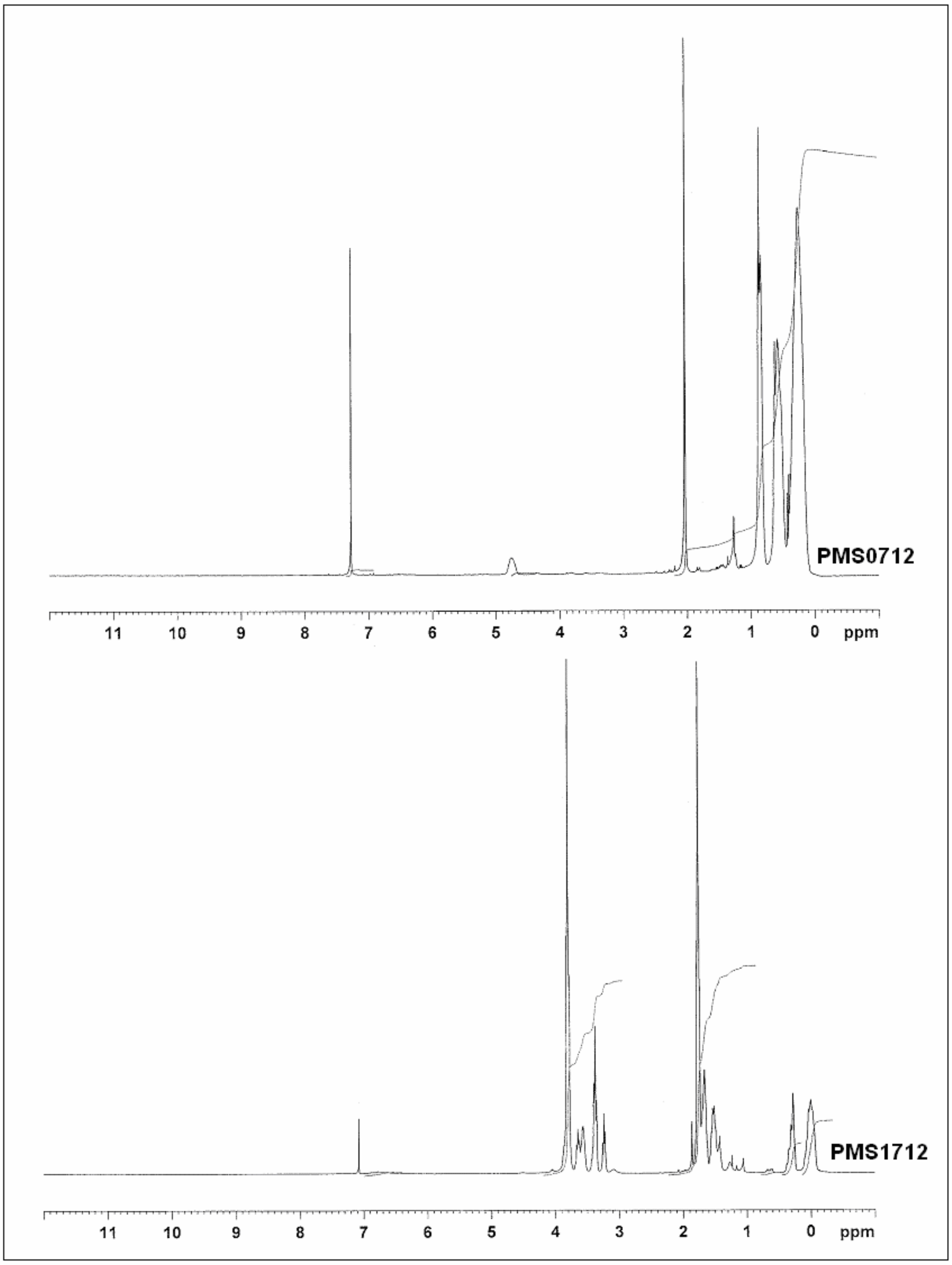

Figure 4.14 ^{1}H-NMR spectra of PMS0712 and PMS1712

As a conclusion, although very successful products are obtained in large-scale synthesis such as PMS0712 and PMS1312, the reproducibility can not be provided. The results of PMS0712 and PMS1712 show that although all the parameters are the same in those samples, PMS0712 is a successful product whereas PMS1712 is not.

In the small-scale and large-scale synthesis, SDS is used as the supporting electrolyte because it is a simple anionic surfactant which does not create a significant amount of impurity in the product due to its low solubility. Purification is not needed at the end of the electrolysis because of this reason. However, the main disadvantage of SDS is also due to its low solubility. Since it is not very soluble in acetonitrile, the solution is not conductive enough, therefore the current is very low. The problems in the reproducibility of the system can be explained by the low current caused by SDS.

4.1.2.3 Poly(methylsilyne) Synthesis with Acetonitrile, Copper Electrodes and Temperature Control

The electrochemical synthesis of poly(methylsilyne) is normally carried out at room temperature. However, since the main problem is the reproducibility of the system in large-scale synthesis, the temperature is also controlled in PMS1601, PMS1701, PMS2101, PMS2401 and PMS2501 samples in order to minimize the effect of temperature change on the synthesis. The temperature is controlled by carrying out the experiments in a constant temperature bath at 25^0C. In this set of experiments, the effect of reaction time and effect of supporting electrolyte type is investigated. The monomer/solvent ratio in each trial is kept constant at 1/10 since the best results are obtained at this ratio in the previous experiments.

4.1.2.3.1 The Effect of Reaction Time

The effect of reaction time is investigated in PMS1601, PMS2101 and PMS1701 samples with reaction times of 30 min, 1 h and 4 h, respectively. In all of these samples, acetonitrile, SDS, copper electrodes and monomer/solvent ratio of 1/10 is used. The physical properties of the products can be seen in Table 4.6. It can be seen that all the products have yellow color as expected for polysilynes.

Table 4.6 Physical properties of PMS1601, PMS2101 and PMS1701

Sample Name	Physical Properties
PMS1601	Pale yellow solid
PMS2101	Yellow wax
PMS1701	Yellow solid

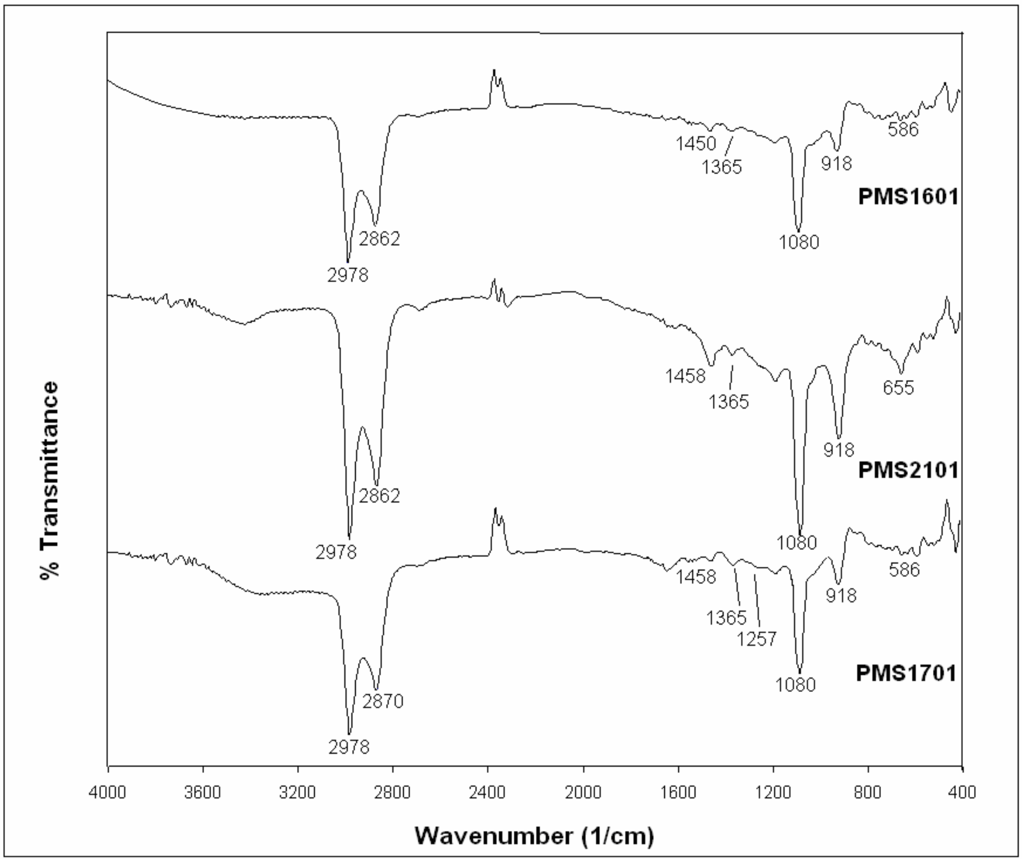

Figure 4.15 FTIR spectra of PMS1601, PMS2101 and PMS1701

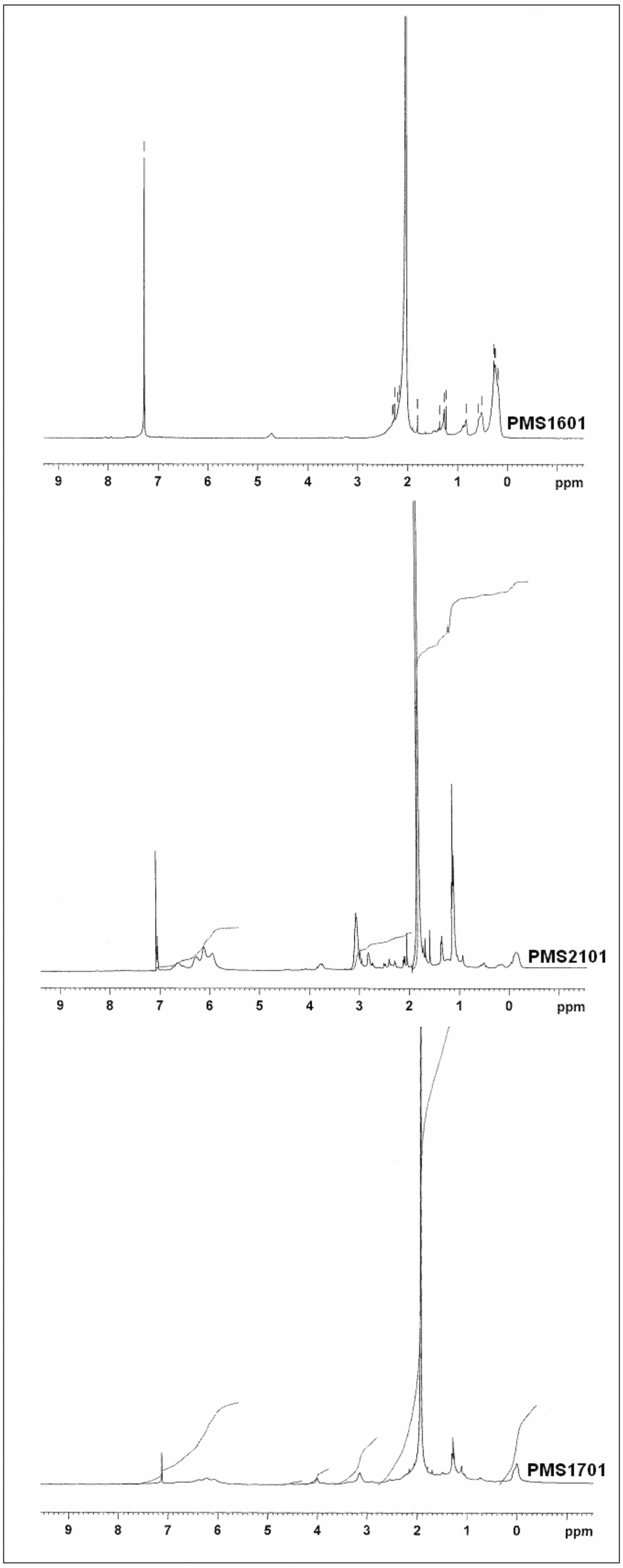

Figure 4.16 ^{1}H-NMR spectra of PMS1601, PMS2101 and PMS1701

FTIR spectra of the samples can be seen in Figure 4.15. There is not a significant difference between the three results. All of the results are successful showing all the expected peaks.

In the ^{1}H-NMR results of PMS1601, PMS2101 and PMS1701 samples which can be seen in Figure 4.16, broad peaks around 0.1 ppm are observed for all of the three results however they are relatively small when compared with the other successful results. It can be seen from the NMR results that the characteristic poly(methylsilyne) peak gets smaller with increasing reaction time. Therefore, it can be concluded that for the systems with acetonitrile, SDS and copper electrodes, increasing the reaction time affects the synthesis negatively. This negative effect can be explained by the increase in the impurities in the product due to deformation of the electrodes with the increasing reaction time.

Another conclusion that can be obtained from the NMR spectra of these samples is that PMS1601 does not give the same ^{1}H-NMR result with PMS0712 although their parameters are exactly the same. This shows that controlling temperature is not enough to solve the problem with reproducibility.

4.1.2.3.2 The Effect of Supporting Electrolyte Type

Since the current is very low with SDS due to its low solubility, another supporting electrolyte, tetrabutylammonium perchlorate (TBAP) is used in PMS2501 sample. The effect of supporting electrolyte type is studied by comparing PMS1601 and PMS2501 samples that have both monomer/solvent ratio of 1/10 and reaction time of 30 min.

It is observed that by using TBAP instead of SDS, the current is increased nearly 10 times. In PMS2501, the current that is smaller than 0.01 A in PMS1601 is increased up to 0.09 A with the change of the supporting electrolyte.

The physical properties of the samples are compared in Table 4.7. In literature, orange solid products are obtained in the synthesis of poly(methylsilyne) with higher molecular weights [3].

Table 4.7 Physical properties of PMS1601 and PMS2501

Sample Name	Physical Properties
PMS1601	Pale yellow solid
PMS2501	Orange solid

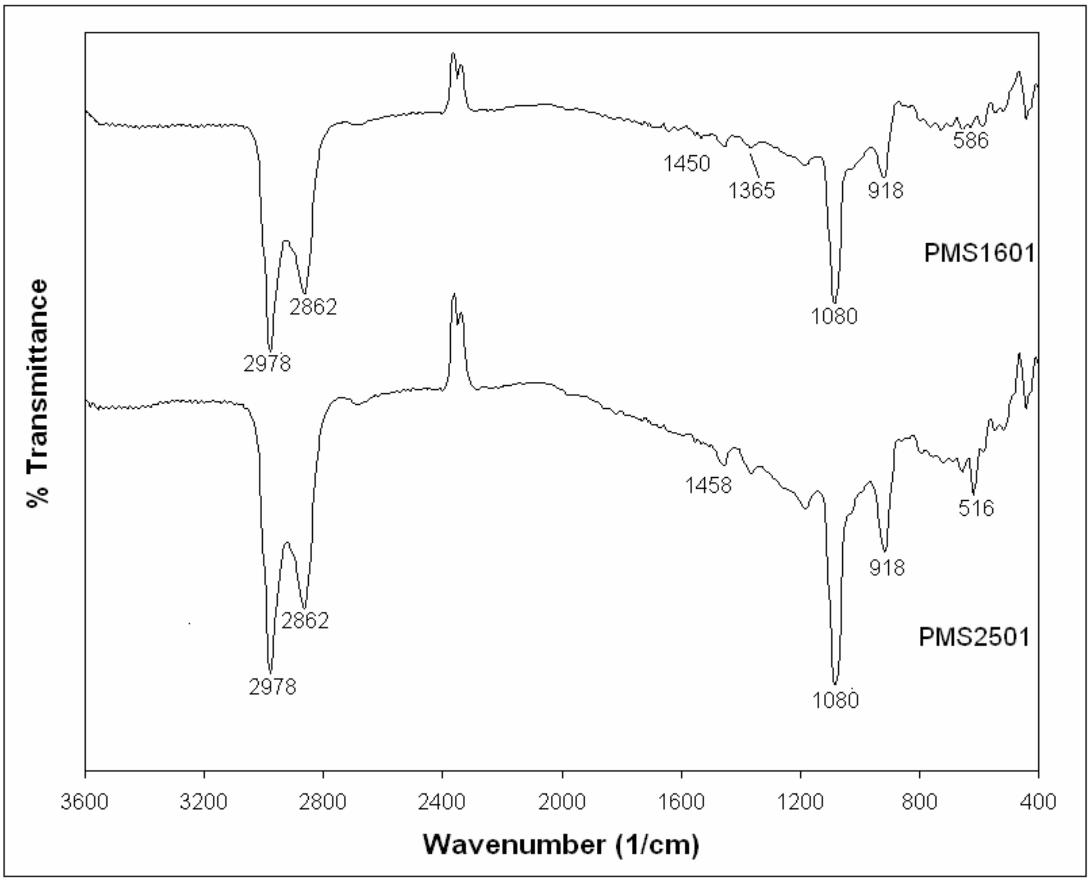

Figure 4.17 FTIR spectra of PMS1601 and PMS2501

The FTIR spectra of PMS1601 and PMS2501 can be seen in Figure 4.17. The FTIR results of the samples are very similar two each other showing all the characteristic peaks.

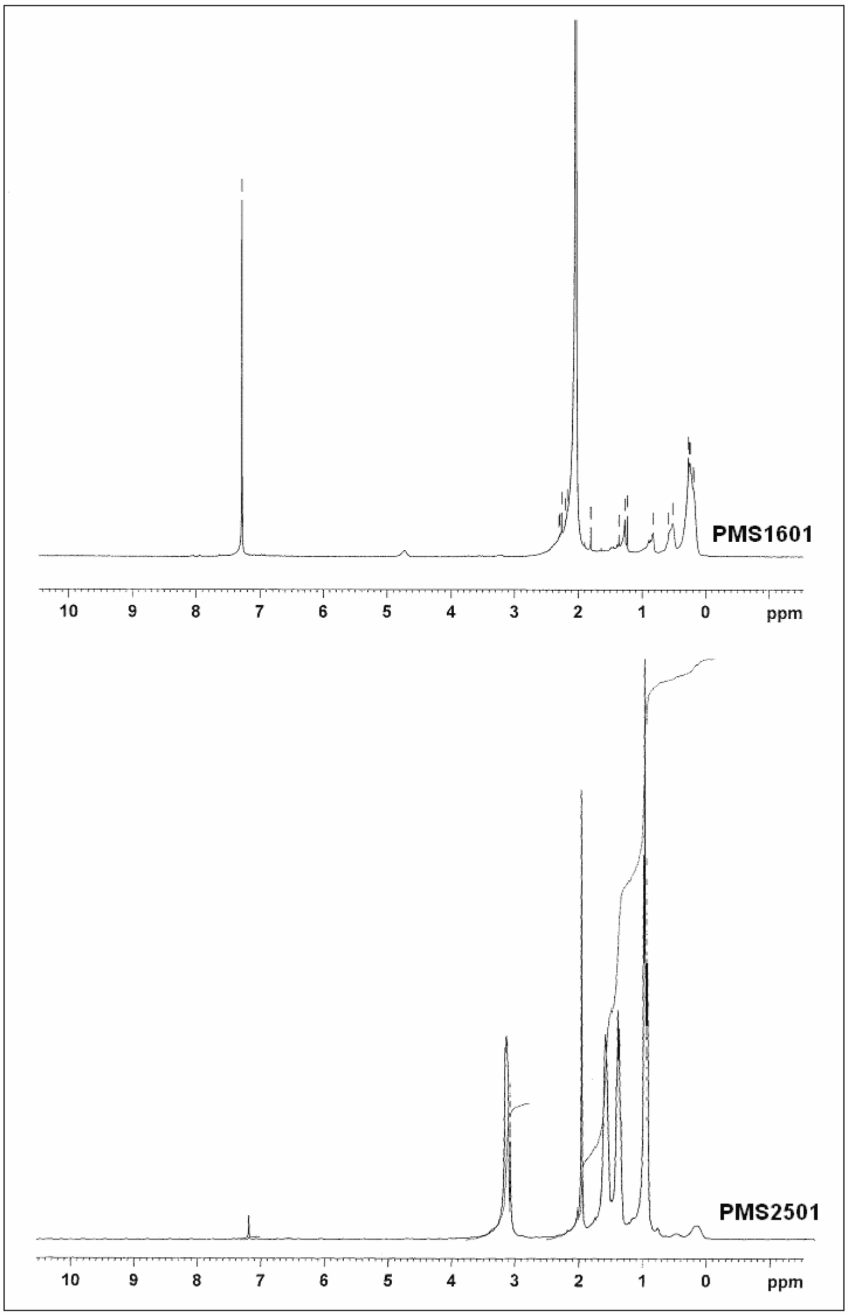

Figure 4.18 ^{1}H-NMR spectra of PMS1601 and PMS2501

The ^{1}H-NMR results of the two samples are shown in Figure 4.18. The two results show some significant differences. Firstly, the Si-CH_3 peak observed for PMS2501 is smaller than the one observed for PMS1601. In addition, in PMS2501 there are additional peaks due to TBAP. The NMR result of PMS1601 looks more successful than the result of PMS2501 although the low current problem is solved by using TBAP. However, the smallness of Si-CH_3 peak in the NMR result of PMS2501 can be explained by the significant amount of TBAP present in the product. Since TBAP is very soluble in acetonitrile, the product contains significant amount of TBAP and the peaks corresponding to the supporting electrolyte repress the characteristic poly(methylsilyne) peak. This problem does not occur in the samples with SDS, since the amount of SDS in the product is very limited. Therefore it can be concluded that the products obtained by using TBAP as the supporting electrolyte should be purified at first.

4.1.2.4 Poly(methylsilyne) Synthesis with Acetonitrile, TBAP, Copper Electrodes and Different Methods to Remove Remaining Si-Cl Bonds

In the large-scale synthesis of poly(methylsilyne) in PMS2211-PMS2501 samples, each time the solution is stirred with $LiAlH_4$ for 3 h. As mentioned before, refluxing with $LiAlH_4$ is required for the conversion of the remaining Si-Cl bonds [8]. In PMS0204 and PMS1104 samples (see Table 3.8), different methods are applied to the solution at the end of the electrolysis to convert the remaining Si-Cl bonds.

In the previous section, the importance of purification in large-scale synthesis with TBAP is mentioned. Therefore, before discussing the effect of different methods to remove Si-Cl bonds on the synthesis, the effect of purification method is investigated in PMS0204 sample.

4.1.2.4.1 The Effect of the Purification Method

The effect of method of purification is investigated in PMS0204 sample, which is a dark yellow solid, by dividing it into two for different purification methods. The first half, PMS0204TS, is dissolved in fresh toluene. After filtration and evaporation of toluene, a dark yellow oil is obtained. The second half, PMS0204TW, on the other hand, is dissolved in toluene and then washed with water. After separating the toluene layer and drying it with Na_2SO_4, toluene is evaporated and a yellow oil product is obtained.

The FTIR spectra of PMS0204TS and PMS0204TW can be seen in Figure 4.19. When the FTIR results of the samples are compared, no significant difference is observed. Both of the spectra show the important peaks that are expected for the polymer.

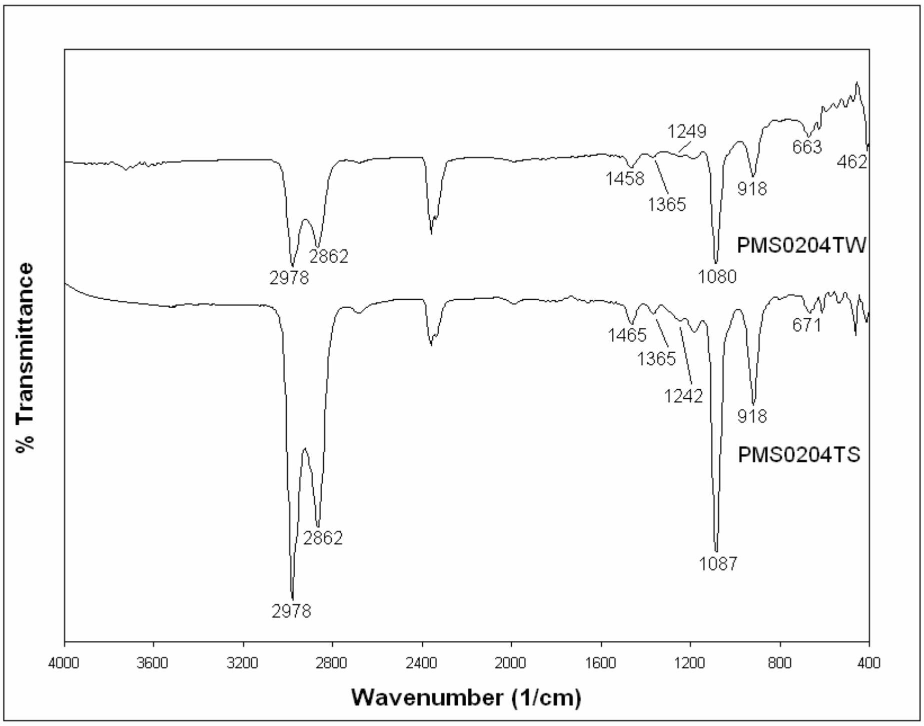

Figure 4.19 FTIR spectra of PMS0204TW and PMS0204TS

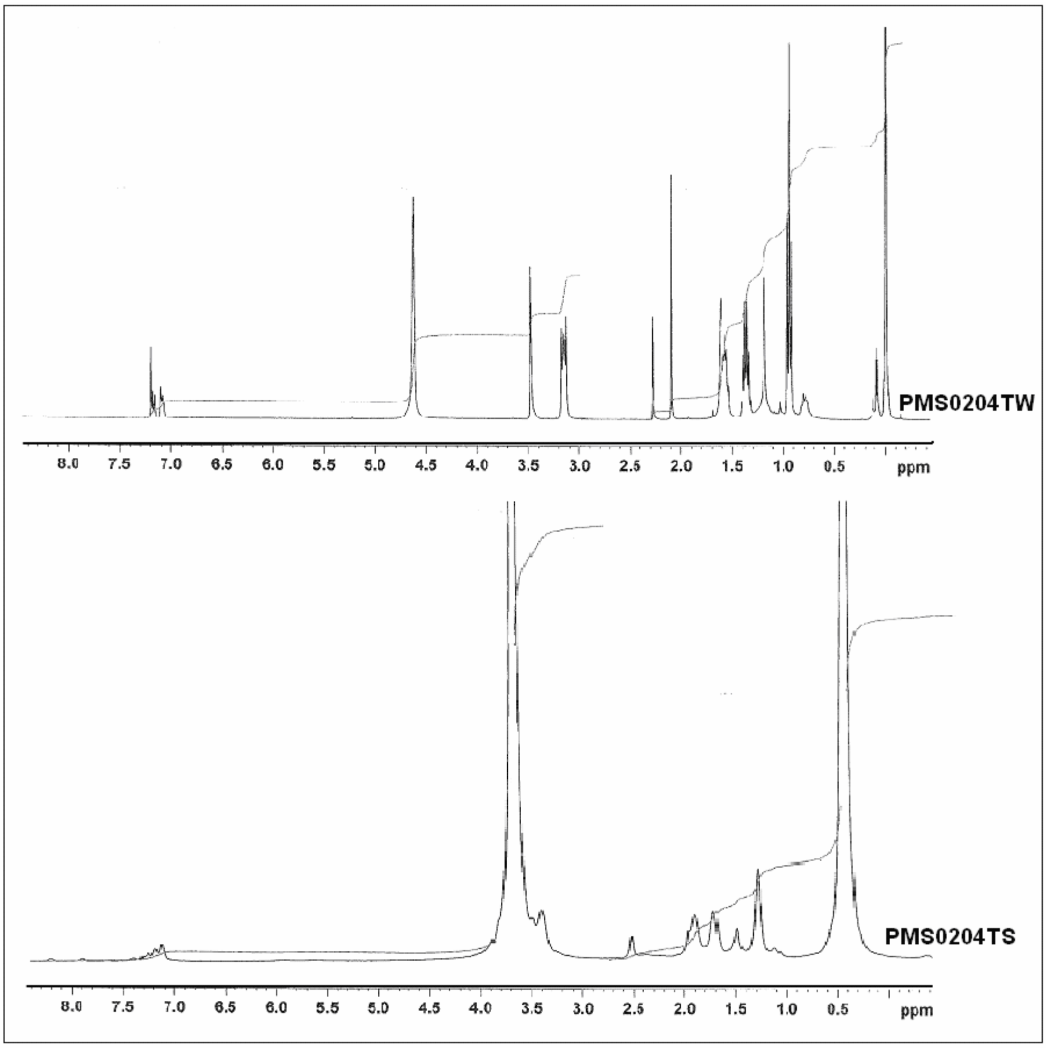

Figure 4.20 ^{1}H-NMR result of PMS0204TW and PMS0205TS

The effect of the purification method can be seen from the ^{1}H-NMR spectra of the samples shown in Figure 4.20 which represent some important differences. It can be seen that PMS0204TS exhibits the desired broad Si-CH_3 peak. In addition, this peak is much more significant than the other peaks corresponding to TBAP showing that the polymer is purified successfully. However, in PMS0204TW sample, the Si-CH_3 peak is not that significant. Furthermore, in the NMR spectrum of PMS0204TW, there are many other peaks indicating the impurities in the system. Therefore, it can be concluded that for the purification of the product, dissolving in toluene and filtering is a better purification method.

4.1.2.4.2 The Effect of Different Methods to Remove Remaining Si-Cl Bonds

In order to see the effect of different methods, PMS0204 and PMS1104 are treated differently after electrolysis. In PMS0204, the solution is quenched with methanol instead of $LiAlH_4$ and stirred for 2 h. At the end of the stirring with methanol, a white powder is precipitated. After filtration of this white powder and evaporation of acetonitrile and methanol, a dark yellow solid residue is obtained. In PMS1104, on the other hand, the solution is refluxed with $LiAlH_4$ like in previous experiments however this time $LiAlH_4$ is not added directly to the acetonitrile solution. After the electrolysis is finished, acetonitrile is evaporated and the residue is dissolved in THF. Then $LiAlH_4$ is added to the THF solution. It is suspected that acetonitrile and $LiAlH_4$ react when $LiAlH_4$ is added directly to the acetonitrile solution and cause impurities in the system. Therefore $LiAlH_4$ is added to the THF solution in this sample.

The effect of the method for Si-Cl removal is investigated for the toluene soluble parts of PMS1104 and PMS0204 samples since purification is needed for TBAP containing products. The physical properties of PMS1104TS and PMS0204TS samples can be seen in Table 4.8. Both of the samples do not have very successful physical properties.

Table 4.8 The physical properties of PMS0204TS and PMS1104TS

Sample Name	Physical Properties
PMS1104TS	Yellow-gray solid
PMS0204TS	Dark yellow oil

The FTIR spectra of PMS1104TS and PMS0204TS can be seen in Figure 4.21. Both of the products have successful FTIR results showing no significant differences.

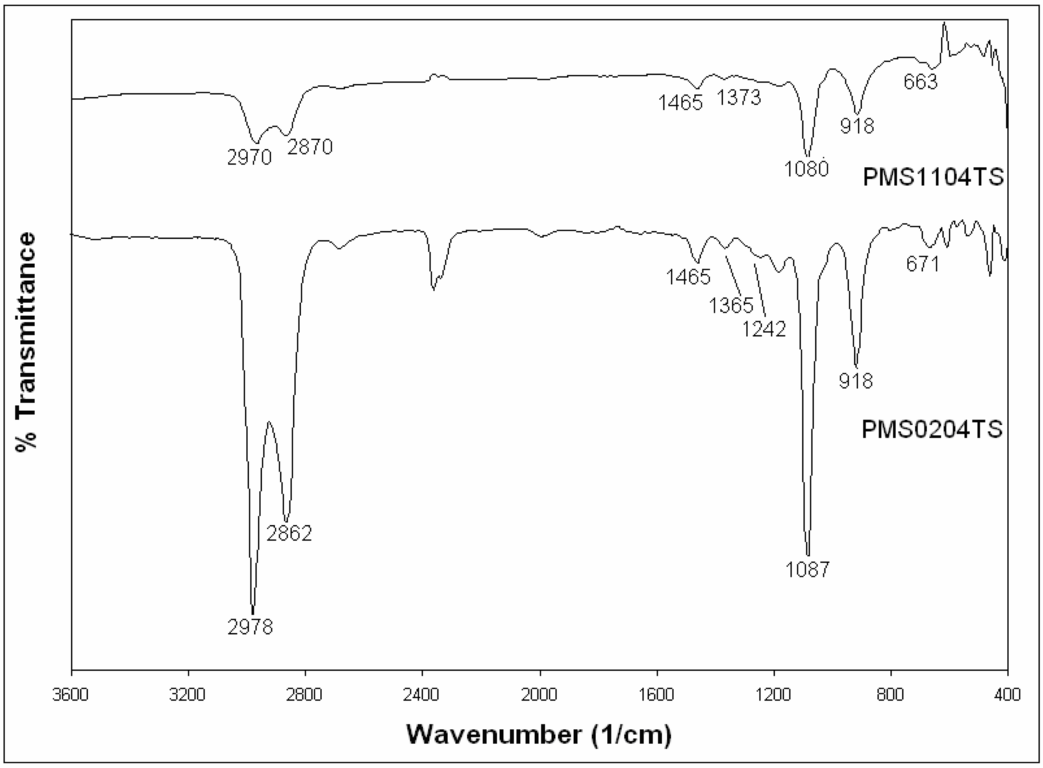

Figure 4.21 FTIR spectra of PMS1104TS and PMS0204TS

On the other hand, the ^{1}H-NMR results shown in Figure 4.22 exhibit some differences. The NMR result of PMS0204TS exhibits a significant peak at 3.5 ppm corresponding to the methoxy bond ($SiOCH_3$) in the polymer. The presence of the methoxy side group is due to quenching the reaction with methanol to convert the remaining Si-Cl bonds [7]. The NMR result of PMS1104 does not exhibit the desired broad $Si-CH_3$ bond and exhibits significant peaks corresponding to TBAP although the polymer is purified with toluene. This result is rather unexpected since in PMS1104TS, it is aimed to decrease the impurities in the system by eliminating the possible reaction of acetonitrile and $LiAlH_4$.

As a conclusion, it is seen that the only effect of the quenching method on the product is the formation of the different side groups of the polymer as a result of the conversion of the remaining Si-Cl bonds.

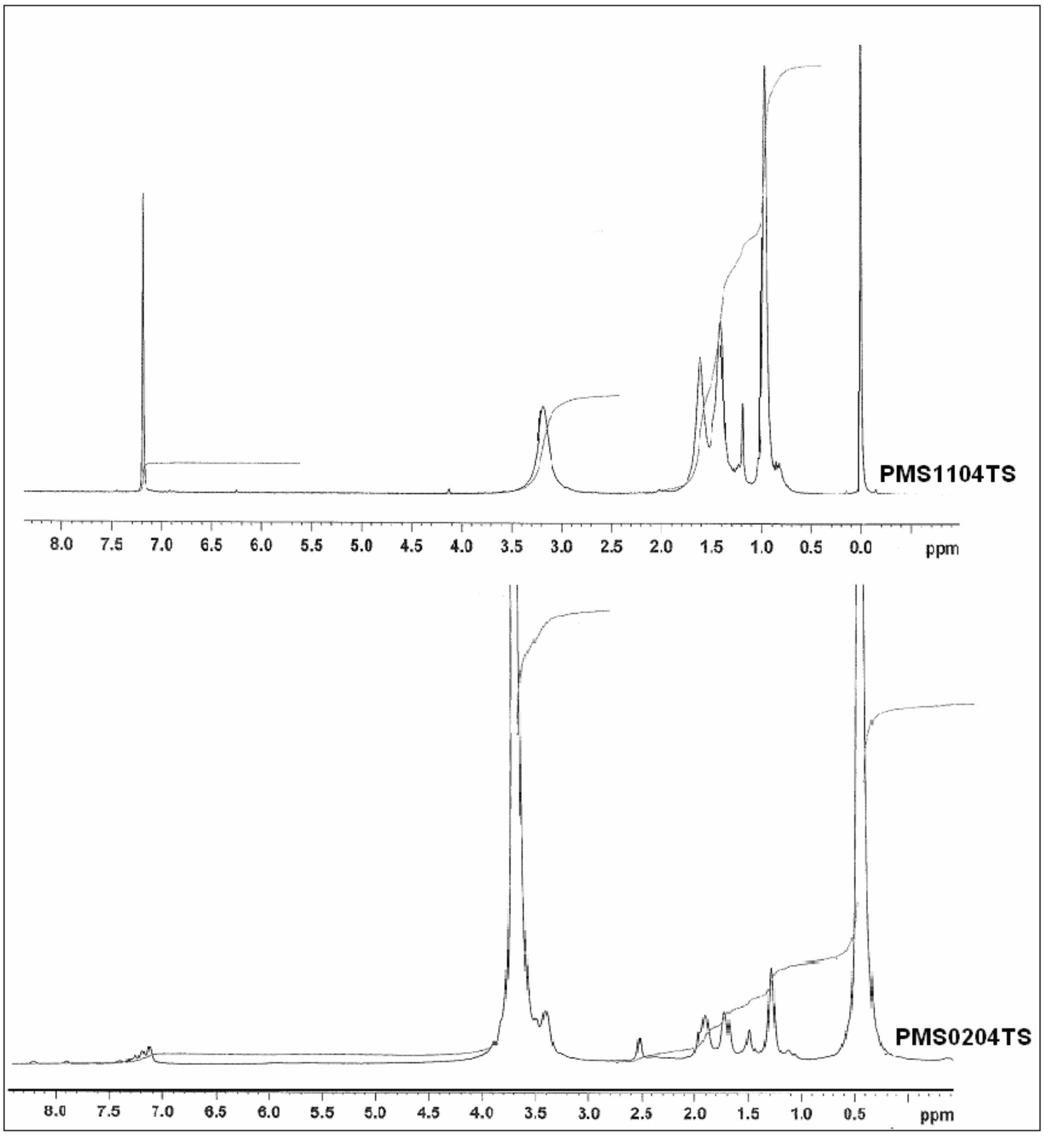

Figure 4.22 H-NMR spectra of PMS1104TS and PMS0204TS

4.1.2.5 Poly(methylsilyne) Synthesis with DME and TBAP

In the large-scale synthesis with acetonitrile and SDS, reproducibility problems occurred due to the low solubility of SDS in acetonitrile and impurities coming from the possible reaction of acetonitrile and $LiAlH_4$, as mentioned in the previous sections. In the PMS1405, PMS1505, PMS1605, PMS1905, PMS0506 and PMS0606 samples, 1,2-dimethoxy ethane is used as the solvent. DME is chosen as the solvent since it is resistant to -6 V and also it is more stable than acetonitrile against $LiAlH_4$. The use of DME as the solvent in the production of poly(methylsilyne) by the electrochemical reduction of methyltrichlorosilane is also observed in the literature [7, 8]. In the samples with DME and TBAP, the effects of electrode type, monomer/solvent ratio and reaction time are investigated. Before the investigation of these effects, the method of purification is examined in PMS1405 sample and the other effects are studied with purified products with the selected method. Although certain conclusions are derived according to the effect of these parameters for other large-scale systems in previous sections, the effects of all of the parameters are investigated and summarized for DME systems.

4.1.2.5.1 The Effect of Purification Method

The effect of purification is studied in PMS1405 sample. In order to compare different purification methods, PMS1405 is divided into three parts. The first part, PMS1405M, is dissolved in THF and then precipitated by adding methanol. The second part, PMS1405TS, on the other hand, is dissolved in fresh toluene, then filtered and obtained after evaporation of toluene. The third part, PMS1405THF, is dissolved in THF, filtered and obtained after evaporation of THF.

The physical properties of PMS1405, PMS1405M, PMS1405THF and PMS1405TS are given in Table 4.9. It can be seen that although the polymer synthesized is a yellow solid, after precipitation with methanol a white solid product is obtained. This indicates that this purification method does not give the desired purified product. PMS1405TS, on the other hand, is a yellow solid as expected for poly(methylsilyne).

Table 4.9 The physical properties of PMS1405, PMS1405THF, PMS1405M and PMS1405TS

Sample Name	Physical Properties
PMS1405	Yellow solid
PMS1405THF	Pale yellow solid
PMS1405M	White solid
PMS1405TS	Yellow solid

The ^{1}H-NMR results of PMS1405, PMS1405THF, PMS1405M and PMS1405TS can be seen in Figure 4.23. In the NMR result of the yellow solid product of the electrolysis, PMS1405, the broad characteristic poly(methylsilyne) peak can not be observed. As explained before, the reason of this is the suppression of this peak by the TBAP peaks since it is present significantly in the product. The white solid product obtained by the precipitation with methanol in THF, PMS1405M, does not have a successful NMR result either. The color and the ^{1}H-NMR spectrum of PMS1405M proves that the solid obtained by precipitation is not poly(methylsilyne). The NMR result of PMS1405THF is very similar to the result of PMS1405 proving that no purification is obtained by this method. The reason of this is the high solubility of both the polymer and the supporting electrolyte in THF.

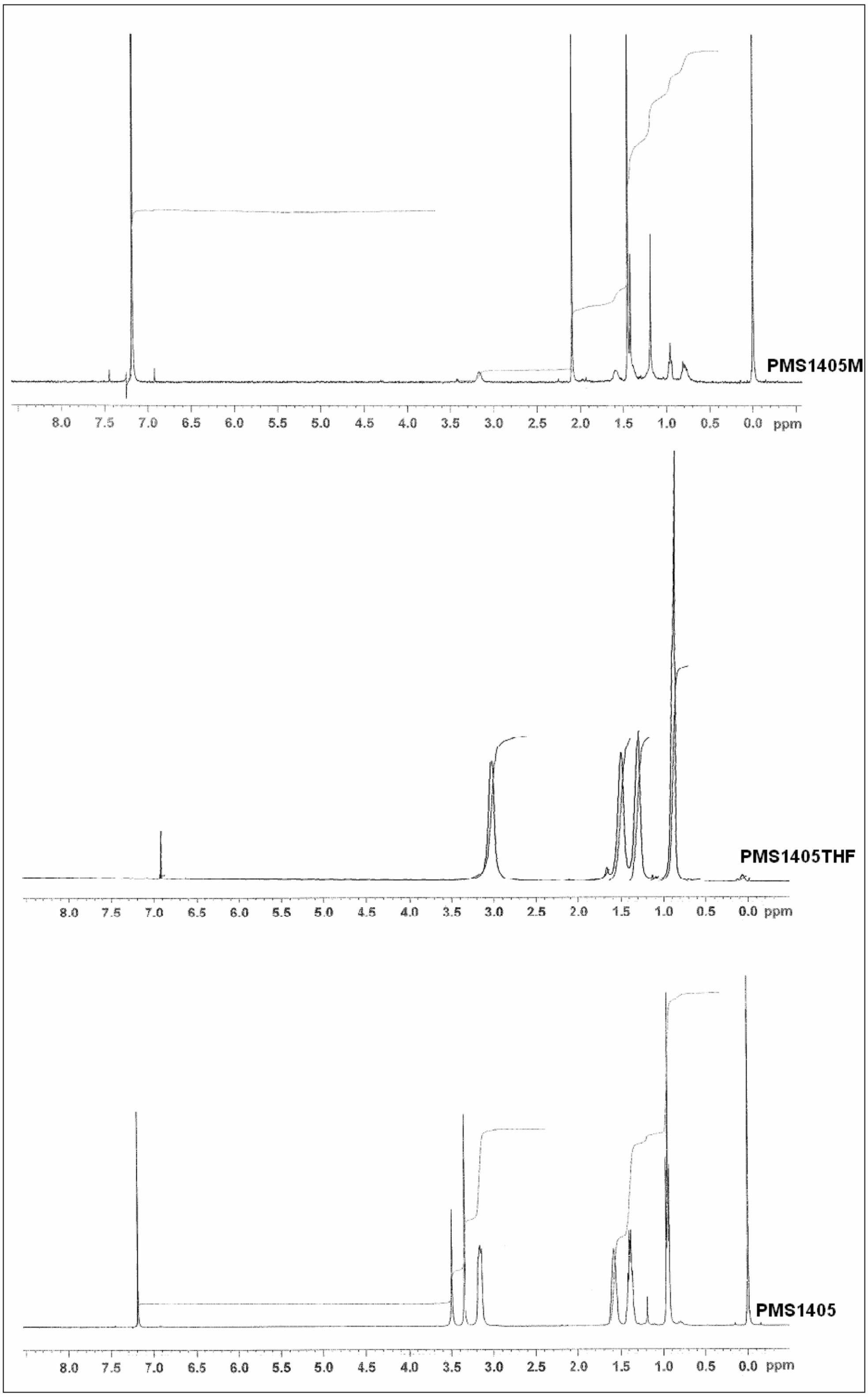

Figure 4.23 ^{1}H-NMR spectra of PMS1405, PMS1405THF, PMS1405M and PMS1405TS

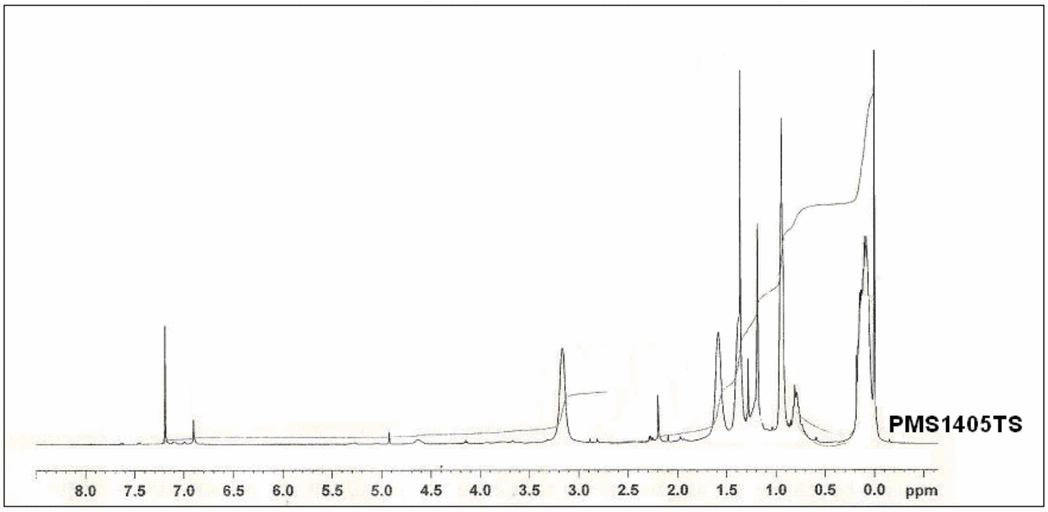

Figure 4.23 (cont'd) ^{1}H-NMR spectra of PMS1405, PMS1405THF, PMS1405M and PMS1405TS

When the H-NMR results of PMS1405 and PMS1405TS are compared, it is observed that the broad Si-CH_3 peak between 0 and 0.5 ppm that is characteristic for poly(methylsilyne) is observed in PMS0204TS although it can not be seen in PMS0204. This proves that the toluene soluble part of PMS1405 is the purified polymer. Therefore, in order to understand the effect of parameters such as electrode time, monomer/solvent ratio and reaction time, the toluene soluble parts of the samples are compared in the following sections.

It can be concluded that dissolving the product in toluene and filtering is required for the purification of the polymer from TBAP. Although this method is quite effective, the main disadvantage is the low solubility of poly(methylsilyne) in toluene. Due to this low solubility, only a small percent of the polymer produced can be obtained as a purified product and the rest is lost with the insoluble part.

4.1.2.5.2 The Effect of Electrode Type

The effect of electrode type is investigated in PMS1405 and PMS1505 samples with copper and stainless steel electrodes, respectively. PMS1405 is a yellow solid whereas PMS1505 is a grayish yellow solid. It can be seen that the sample with stainless steel electrodes do not have dark color like PMS2311-PMS2711 samples since the reaction time is not very long. However, the color of the product is still different than expected. When the samples are purified with toluene, yellow solids are obtained for both of the products.

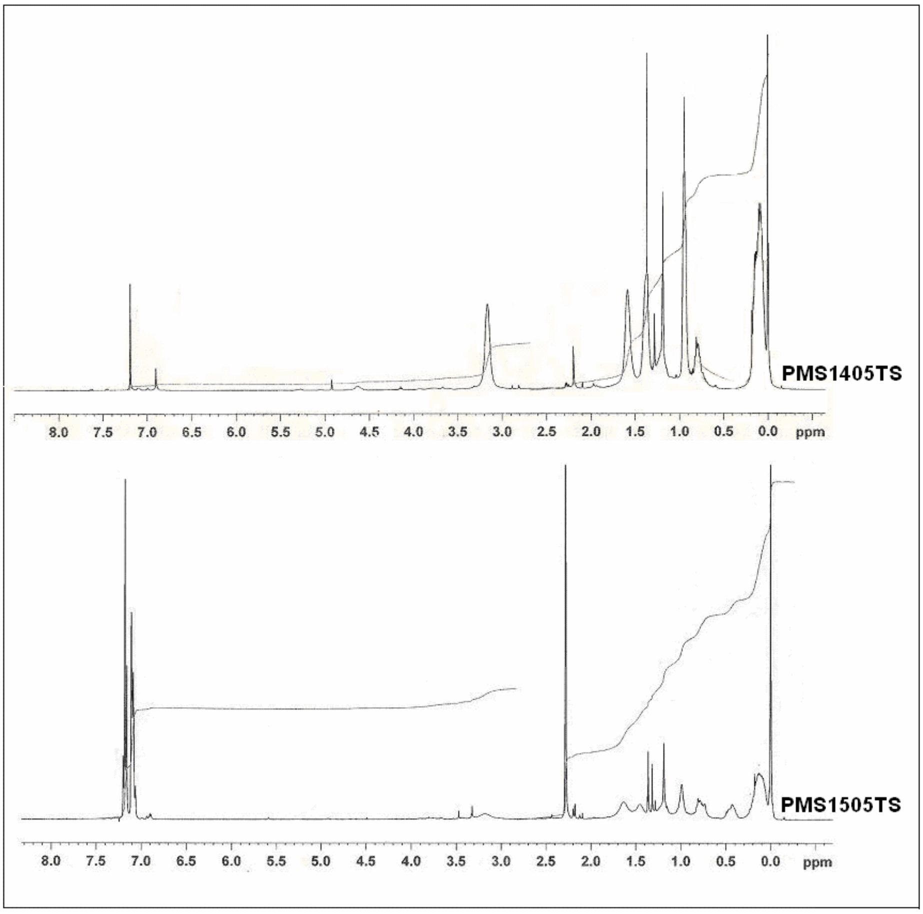

Figure 4.24 H-NMR result of PMS1405TS and PMS1505TS

The ^{1}H-NMR results of PMS1405TS and PMS1505TS are compared in Figure 4.24. In the NMR spectra of both of the samples, the broad Si-CH_3 peak can be seen. This shows that poly(methylsilyne) is produced in both syntheses and purified by dissolving in toluene. Although both of the results are successful, the peak in the NMR result of PMS1405TS is more significant. As a conclusion, it is seen that since the reaction time is only 30 min, stainless steel electrodes do not cause a significant problem in the product.

4.1.2.5.3 The Effect of Monomer/Solvent Ratio

The effect of monomer/solvent ratio is investigated in PMS1605, PMS1405 and PMS0506 samples with the ratios of 1/5, 1/10 and 1/20, respectively. During the investigation of the effect of monomer/solvent ratio, each trial is done with copper electrodes and TBAP for 30 min. The physical properties of the products are compared in Table 4.10. From the previous trials it is known that increasing the monomer/solvent ratio does not affect the system in a positive manner. However from the physical properties of the products it can be seen that PMS0506 sample with a monomer/solvent ratio of 1/20 also have unexpected physical properties. PMS1405 with a monomer/solvent ratio of 1/10 has the best physical properties. However when they are purified by dissolving in toluene, yellow solid products are obtained for all of the samples.

Table 4.10 Physical properties of PMS1605, PMS1405 and PMS0506

Sample Name	Physical Properties
PMS1605	Dark yellow solid
PMS1405	Yellow solid
PMS0506	Brown solid

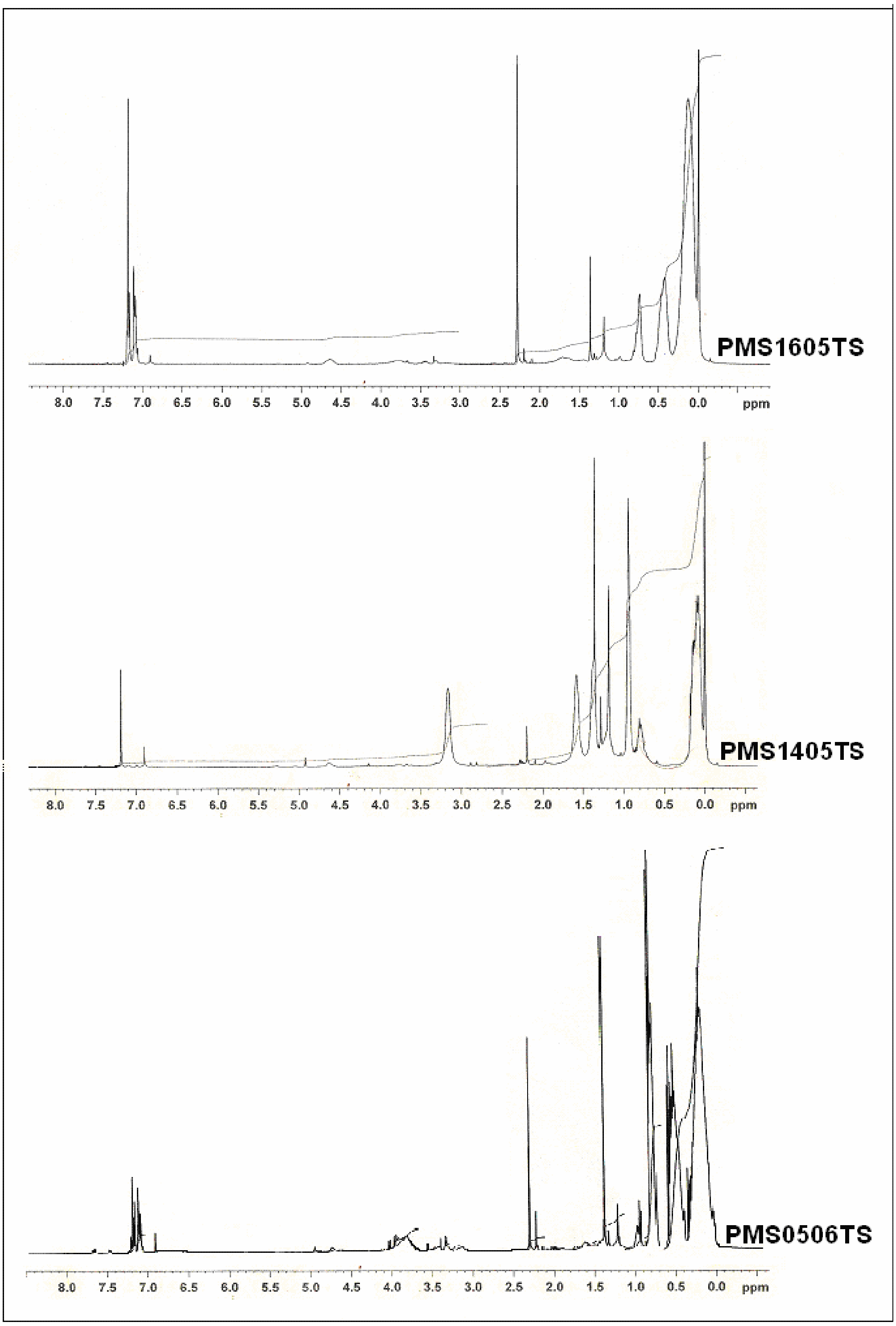

Figure 4.25 ^{1}H-NMR result of PMS1605TS, PMS1405TS and PMS0506TS

The ^{1}H-NMR results of PMS1605TS, PMS1405TS and PMS0506TS are shown in Figure 4.25. It can be seen that the NMR results of the all three samples are very successful showing a broad significant peak between 0 and 0.5 ppm. This proves that poly(methylsilyne) is synthesized in each monomer/solvent ratio and purified successfully. An important effect of monomer/solvent ratio can not be observed from these NMR results since the Si-CH_3 peak is very significant in all of the results.

4.1.2.5.4 The Effect of Reaction Time

The effect of reaction time is studied in PMS1405, PMS1905 and PMS0606 samples with reaction times of 30 min, 1 h and 4 h. In each trial, the synthesis is done with copper electrodes, TBAP and monomer/solvent ratio of 1/10.

The physical properties of the products can be seen in Table 4.11. It can be seen that although the sample with 30 min is a yellow solid, the samples with higher reaction times have orange colors. This result is expected since as mentioned before orange solid products are obtained for poly(methylsilyne) with higher molecular weights [3]. Increasing the reaction time most probably cause higher molecular weight products. The physical properties of the purified polymers are the same with the unpurified products.

Table 4.11 Physical properties of PMS1405, PMS1905 and PMS0606

Sample Name	Physical Properties
PMS1405	Yellow solid
PMS1905	Orange solid
PMS0606	Orange solid

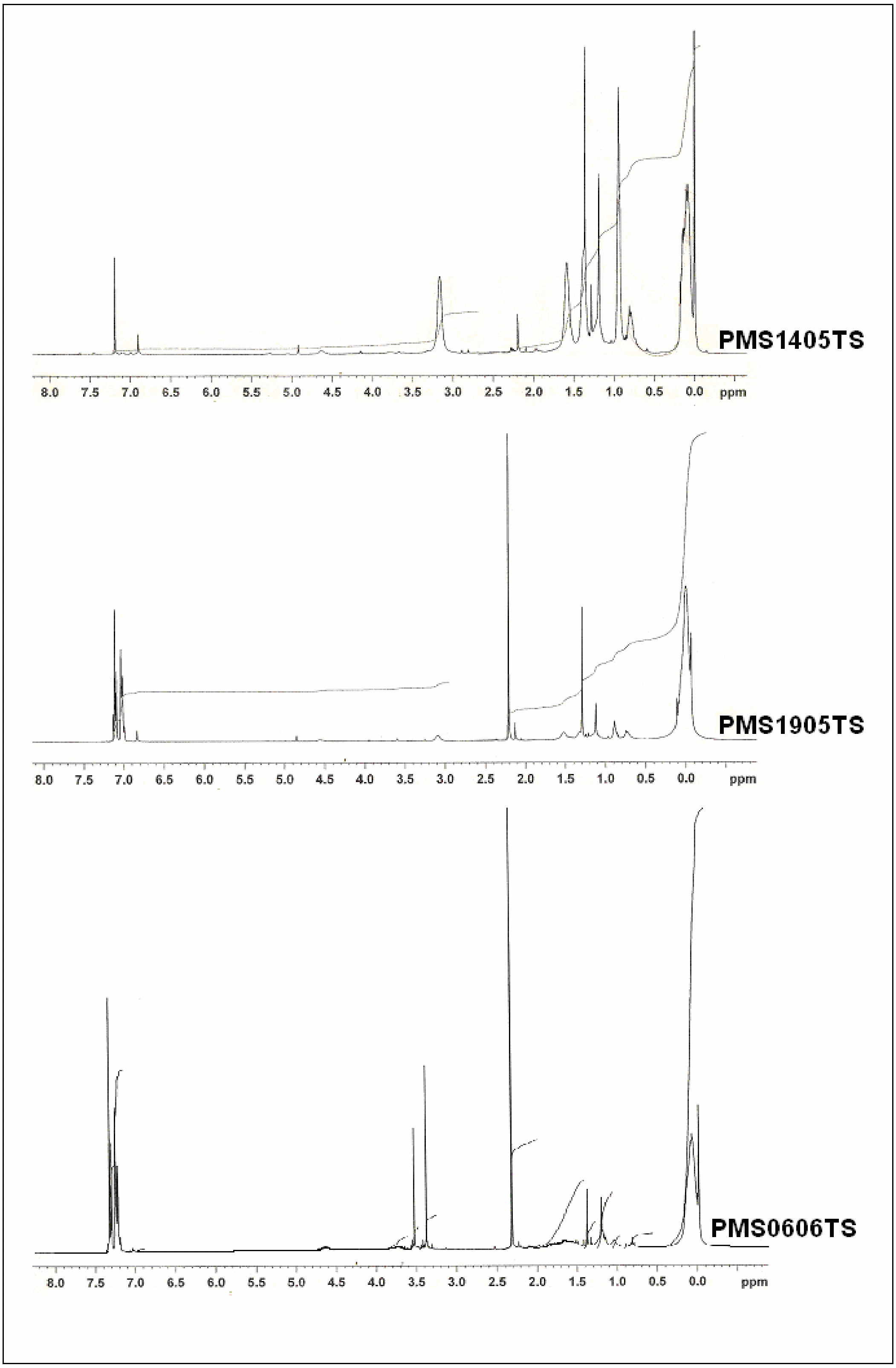

Figure 4.26 ^{1}H-NMR spectra of PMS1405TS, PMS1905TS and PMS0606TS

The ^{1}H-NMR spectra of PMS1405TS, PMS1905TS and PMS0606TS can be seen in Figure 4.26. In the previous large-scale syntheses with different systems, it is observed that increasing the reaction time affects the synthesis negatively. However it can be seen that when the NMR results of the three samples are compared in the figure, a significant effect of increasing reaction time can not be observed. All of the three results exhibit the expected poly(methylsilyne) peak. In the previous sections, it is suspected that the synthesis is affected negatively due to the increase of impurities in the system with increasing reaction time however since the results in this section are all for purified samples, the effect of impurities on the system can not be observed. This may be the main reason why a significant effect of reaction time can not be seen in the NMR results.

4.1.2.6 Poly(methylsilyne) Synthesis in Large-Scale with the Selected Parameters and Purification Method

Throughout the large-scale synthesis of poly(methysilyne), the effect of many different parameters such as electrode type, supporting electrolyte type, monomer to solvent ratio, solvent type, reaction time and quenching method are investigated and the effects of these parameters on the physical properties and FTIR and NMR results are discussed. Successful products are produced with different synthesis parameters by making improvements in the system according to the problems faced during each trial. As a conclusion, the large-scale production of poly(methylsilyne) is decided to be done with PMS1405 parameters using DME, copper electrodes, TBAP with monomer/solvent ratio of 1/10 and reaction time of 30 min.

The polymer produced is a yellow solid which is then extracted with toluene in order to be purified. The ^{1}H-NMR spectrum of the purified polymer (PMS1405TS) is given in Figure 4.22. Addition to the ^{1}H-NMR result, FTIR and UV-Visible Spectroscopy results are presented for the large-scale synthesis with selected parameters.

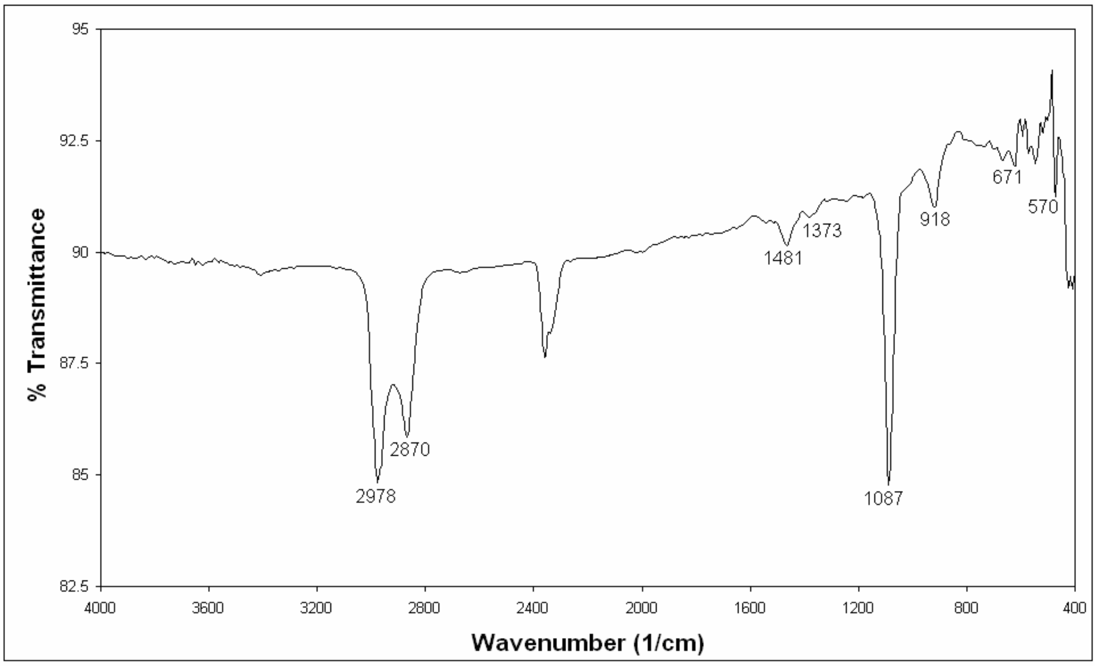

Figure 4.27 FTIR spectrum of poly(methylsilyne) produced in large-scale

The FTIR spectrum of the polymer can be seen in Figure 4.27. The FTIR result of the polymer synthesized is very similar to the small-scale result showing the expected C-H (Si-CH_3) peaks in 2978, 2870, 1481 and 1373 cm^{-1}, SiH_2 peak at 918 cm^{-1} and Si-C peak at 671 cm^{-1}. The peak at 1087 ppm corresponding to Si-O-Si bond in the polymer is not desired however it is expected due to the reactivity of the polymer towards oxygen. The only difference is the presence of Si-Cl bonds in the FTIR at 570 ppm indicating that all the remaining Si-Cl bonds are not converted as in small-scale synthesis of poly(methylsilyne).

The UV-Visible spectrum of the polymer synthesized in large-scale is shown in Figure 4.28. As observed in small-scale result, the UV-Visible spectrum shows a broad UV band tailing down into the visible region around 400 nm exhibiting the characteristic behavior of polysilynes. As mentioned before, the UV-Visible spectrum of the polymer proves the branched structure of the polymer since linear polysilanes have a completely different UV-Visible spectra showing two sharp absorption peaks [9, 11].

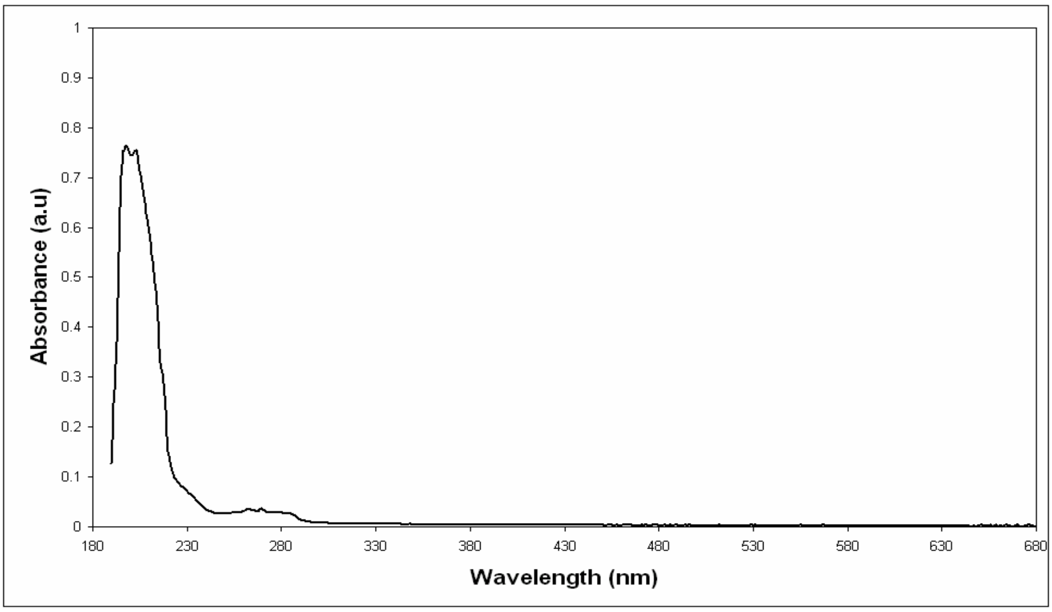

Figure 4.28 UV-Visible spectrum of poly(methylsilyne) produced in large-scale

Poly(methylsilyne) produced by PMS1405 parameters are used in blend preparation without purification since the polymer is obtained in very low amount after dissolving in toluene due to its low solubility. Therefore, in order to minimize the loss of the polymer, unpurified product containing TBAP is used in the blends.

4.2 Flammability, Thermal and Mechanical Properties and Morphologies of Polypropylene/Preceramic Polymer Blends

In the second part of this dissertation, silicon-based preceramic polymers are blended with polypropylene in order to improve the flame retardancy of the polymer. Polypropylene/preceramic polymer blends are prepared with two different silicon carbide precursors, allylhydridopolycarbosilane (SMP-10) which is a commercial polymer and poly(methylsilyne) (PMSy) synthesized electrochemically with PMS1405 parameters. The blends are characterized based on their flammability, thermal and mechanical properties and morphologies. The results of the blends are compared with pure polypropylene that is ground and extruded and PP/10TPP/10M blend that contains only TPP and the metal complex.

4.2.1 Flammability Properties

4.2.1.1 LOI Results

The polymer blends prepared in the twin-screw extruder are firstly characterized by LOI test in order to evaluate the flame retardancy of the polymers by determining the limiting amount of oxygen that is required for sustaining burning.

Polypropylene is a very flammable polymer due to its wholly hydrocarbon structure. Its high flammability can also be understood from its low LOI value of 17.5%. The aim in blending silicon-based preceramic polymers with polypropylene is to improve the flame retardancy of the blends that can be determined by an increase in the LOI value. The LOI values of the polymer blends containing SMP-10 and PMSy can be seen in Tables 4.12 and 4.13, respectively. In both of the tables, the LOI values are compared with pure polypropylene and PP/10TPP/10M containing only TPP and the metal complex in polypropylene.

Table 4.12 LOI values of PP/SMP-10 blends

Composite Name	LOI (%)
PP	17.5
PP/1SMP	17.5
PP/2SMP	18.0
PP/3SMP	18.5
PP/5SMP	18.5
PP/10SMP	19.0
PP/5SMP/5TPP	19.0
PP/10SMP/10TPP	20.5
PP/10SMP/5TPP/5M	23.5
PP/10TPP/10M	19.5

SMP-10 polymer is blended with polypropylene in different compositions of 1-10 wt% in the first 5 blends. It can be seen that when the composition of SMP-10 is very low in polypropylene, no improvement can be obtained in the LOI values. For instance, with addition of 3 wt% and 5 wt% SMP-10, the LOI value is only increased to 18.5% from 17.5%. This shows that SMP-10 is not an effective flame retardant in polypropylene in low amounts.

Since flame retardants are generally added to polypropylene in 10-20 wt% for effective flame retardation [15], SMP-10 is added in 10 wt% to polypropylene. As a result, it is seen that the sample containing 10 wt% SMP-10 has a LOI value of 19.0% which is only 0.5% higher than the LOI value of the sample containing 5 wt% SMP-10. This result shows that increasing the amount of SMP-10 in polypropylene is not enough to obtain effective flame retardancy, therefore synergistic material should be found to be used together with the silicon-based polymer in polypropylene. For this purpose, TPP and SMP-10 are used together in polypropylene for synergistic effect in PP/5SMP/5TPP and PP/10SMP/10TPP blends. It can be seen that using these two flame retardants in polypropylene does not provide a synergism since it can be seen that PP/10SMP and PP/5SMP/5TPP blends both containing 10 wt% of total flame retardant have the same LOI values of 19.0. Therefore, it can be concluded that for more significant increases in LOI values, the total flame retardant amount should be increased and other synergistic materials should be searched.

In the LOI results, it can be seen that when the total flame retardant composition is 20 wt%, a significant increase can be seen in the results. For instance, in PP/10SMP/10TPP set where 10% SMP-10 and 10% TPP are used together in polypropylene, LOI value of 20.5 is obtained. The most significant improvement in the flame retardancy is obtained in PP/10SMP/5TPP/5M set where SMP-10, TPP and the metal complex are used together in polypropylene since the LOI value is increased to 23.5% from 17.5%. When this result is compared with the LOI value of PP/10TPP/10M blend containing only TPP and the metal complex, it can be concluded that SMP-10, TPP and the metal complex provide a synergy when used together in polypropylene. This can be concluded since although both blends contain totally 20 wt% of flame retardant, PP/10TPP/10M has a LOI value of 19.5% whereas PP/10SMP/5TPP/5M has 23.5%.

Table 4.13 LOI values of PP/PMSy blends

Composite Name	LOI (%)
PP	17.5
PP/1PMS	18.0
PP/10PMS/10TPP	21.0
PP/10PMS/5TPP/5M	21.0
PP/5PMS/7.5TPP/7.5M	21.5
PP/5PMS/5SMP/5TPP/5M	20.0
PP/10TPP/10M	19.5

Polypropylene/poly(methylsilyne) blends also show a little improvement in flame retardancy when the flame retardant is added in low amounts (see Table 4.13). For instance, the blend containing 1% PMSy has a LOI value of 18.0. It can be seen that PMSy is more effective than SMP-10 in low amounts in polypropylene since 1% addition of PMSy provides a LOI value of 18.0 whereas 1% addition of SMP-10 does not cause any change in the LOI value.

Since in the blends with SMP-10, the significant increases in LOI values are only obtained with 20 wt% flame retardant addition, the flame retardants are added to polypropylene in PP/10PMS/10TPP – PP/5PMS/5SMP/5TPP/5M blends in this composition. When PP/10PMS/10TPP and PP/10SMP/10TPP results are compared, it can be seen that the blend with PMSy has a LOI value that is 0.5% higher than the one with SMP-10. This result again shows that PMSy is more effective in polypropylene than SMP-10. Since SMP-10, TPP and the metal complex provide a synergy in PP/10SMP/5TPP/5M blend and increase the LOI up to 23.5%, PMSy is also tried with the same composition. However it can be seen that PMSy, TPP and the metal complex do not provide a synergy in polypropylene like SMP-10. This can be concluded since although PMSy is more effective than SMP-10 in polypropylene, PP/10PMS/5TPP/5M blend has a LOI value of 21.0%, whereas PP/10SMP/5TPP/5M blend has a value of 23.5%. In PP/5PMS/7.5TPP/7.5M sample, the amounts of TPP and metal complex are increased without changing the total flame retardant composition of 20 wt%. It is seen that increasing the amount of TPP and metal complex in PMSy, TPP and metal complex blend in polypropylene results in an increase in the LOI value. However, it can be observed that all the blends containing PMSy (PP/10PMS/10TPP – PP/5PMS/7.5TPP/7.5M) have higher LOI values than PP/10TPP/10M containing only TPP and the metal complex. This proves that PMSy is the main reason of the increases in the LOI values.

Finally, in PP/5PMS/5SMP/5TPP/5M blend, PMSy and SMP-10 are used together with TPP and the metal complex in polypropylene. It is seen that both the blends of SMP-10, TPP and metal complex and PMSy, TPP and metal complex have higher LOI values than PP/5PMS/5SMP/5TPP/5M sample showing that using PMSy and SMP-10 together has a negative effect in the flame retardancy of polypropylene. This negative effect is also observed by a significant increase in dripping during the LOI test.

4.2.1.2 Horizontal Burning Test Results

Horizontal burning test is applied for the polymer blends after LOI test in order to evaluate the flammability of the blends. The results of the horizontal burning test can be seen in Tables 4.14 and 4.15 for SMP-10 and PMSy, respectively. In the tables, the burning rate of pure PP is also given in order to make comparisons with the results of the blends.

Table 4.14 Horizontal burning test results of PP/SMP-10 blends

Composite Name	Burning Rate (mm/min)	Average Burning Time (s)	Average Burned Length (mm)
PP	30.66 +/- 4.12	-	-
PP/1SMP	23.39 +/- 0.74	-	-
PP/2SMP	23.82 +/- 2.19	-	-
PP/3SMP	22.47 +/- 0.27	-	-
PP/5SMP	20.66 +/- 0.14	-	-
PP/10SMP	20.57 +/- 0.13	-	-
PP/5SMP/5TPP	21.19 +/- 0.61	-	-
PP/10SMP/10TPP	19.05 +/- 0.42	-	-
PP/10SMP/5TPP/5M	-	115 +/- 7.23	14.67 +/- 2.89

The results show that even with the addition of SMP-10 in low amounts, the burning rate is reduced significantly. For instance, with the addition of 5% SMP-

10 to polypropylene in PP/5SMP sample, there is nearly a 33% decrease in the burning rate. These significant decreases in the burning rates show that SMP-10 acts as a flame retardant. However, although there are significant decreases in the burning rates, all the polymer blends except PP/10SMP/5TPP/5M burn completely like polypropylene. Therefore average burning time and average burned length could not be calculated for them. The blend containing SMP-10, TPP and the metal complex, PP/10SMP/5TPP/5M, extinguished during horizontal burning test and average burning time and average burned length could be determined for it. In addition, during the burning of PP/10SMP/5TPP/5M set, it is seen that the polymer surface is coated by a char residue which slows down the transfer of heat and mass, and reduces dripping of the polymer by conserving the structural integrity [2, 13-17, 37].

Table 4.15 Horizontal burning test results of PP/PMSy blends

Composite Name	Burning Rate (mm/min)	Average Burning Time (s)	Average Burned Length (mm)
PP	30.66 +/- 4.12	-	-
PP/1PMS	30.39 +/- 3.51	-	-
PP/10PMS/10TPP	27.36 +/- 6.47	-	-
PP/10PMS/5TPP/5M	30.24 +/- 3.23	-	-
PP/5PMS/7.5TPP/7.5M	25.87 +/- 0.70	-	-
PP/5PMS/5SMP/5TPP/5M	24.23 +/- 0.98	-	-

In the horizontal burning test results of the blends with PMSy, it is seen that addition of PMSy in small amount does not cause a significant decrease in the burning rates. In addition, it is seen that although addition of PMSy provides a change in LOI values, there are no important changes in the horizontal burning results. Furthermore it can be observed that all the blends burned completely like pure polypropylene. Therefore it can be concluded that although addition of PMSy provides an increase in the LOI values, the decrease in the horizontal burning rates are not significant as in the blends with SMP-10.

When both the LOI and horizontal burning test results are evaluated, since there is not a significant increase in the LOI values and the polymers burn completely although having lower burning rates, it can be concluded that SMP-10 and PMSy are not effective flame retardants in low compositions. When the flammability results of PP/10SMP and PP/5SMP/5TPP are compared, since there is not a significant difference in their results, it can be concluded that SMP-10 and TPP alone do not provide a synergy. An increase in the flame retardancy can only be seen when they are used together in 20 wt%. Therefore, it is seen that at least 20 wt% of flame retardant is needed for a significant change in the flammability of polypropylene as in PP/10SMP/10TPP and PP/10SMP/5TPP/5M sets. In addition, it is seen that SMP-10, TPP and the metal complex provide a synergy in polypropylene and improve the flame retardancy significantly.

For the blends with PMSy, it can be seen that it is more effective in PP than SMP-10 when used alone or with TPP in polypropylene. However, the synergy obtained by SMP-10, TPP and the metal complex can not be obtained with PMSy. Therefore the highest LOI value obtained is 21.5% in PP/5PMS/7.5TPP/7.5M blend. Although this result is lower than PP/10SMP/5TPP/5M blend, still the LOI value of polypropylene is increased to 21.5% from 17.5% with a total flame retardant composition of 20 wt%.

The main reason of this decrease in the flammability with addition of silicon-based preceramic polymers is the ceramic char formation which acts as a heat and mass barrier. This ceramic char layer insulates the virgin polymer from the external heat and prevents the formation of combustible gaseous decomposition products. In addition, it prevents the transport of these combustible products to the pyrolysis zone, thus reducing the amount of fuel for combustion. This results in a decrease in the heat released and fed back to the polymer [2, 20-23]. The synergy obtained in silicon and phosphorus-based compounds are mainly due to the increase in the amount and thermal stability of the char formed during burning. Both silicon and phosphorus containing flame retardants act in condensed phase by char promotion. However, when they are used together, a synergistic effect is seen due to the thermal stability of the char coming from the silicon-based compounds and increase in the char formation due to the phosphorus-based compounds. Therefore, the main mechanism of the synergy is the improvement of the thermal stability of the char by the incorporation of silicon-based compounds which results in a decrease in the mass loss rates [14, 60]. The addition of the metal complex clearly provides a synergy with silicon and phosphorus-containing compounds most probably by increasing the thermal stability of the polymer by char promotion [19, 61].

4.2.2 Thermal Properties

4.2.2.1 Thermogravimetric Analysis Results

In order to investigate the thermal stability of the polymers, TGA is applied to the polymer blends under N_2 atmosphere. TGA analysis is also necessary for the complete evaluation of flame retardancy, since char yield calculated by TGA gives important information about the flame retardancy mechanisms.

The TGA curves of pure polypropylene and the blends with SMP-10 and PMSy are shown in Figures 4.29 and 4.30, respectively. The char yield % at 800^0C and the average decomposition temperature of the blends determined by the TGA curves are also represented in Tables 4.16 and 4.17. The TGA curves, the average decomposition temperatures and overall mass loss percentages are shown in Appendix B.1 for each blend. Char yield for a blend is calculated by subtracting the overall mass loss percentage at 800^0C from 100%.

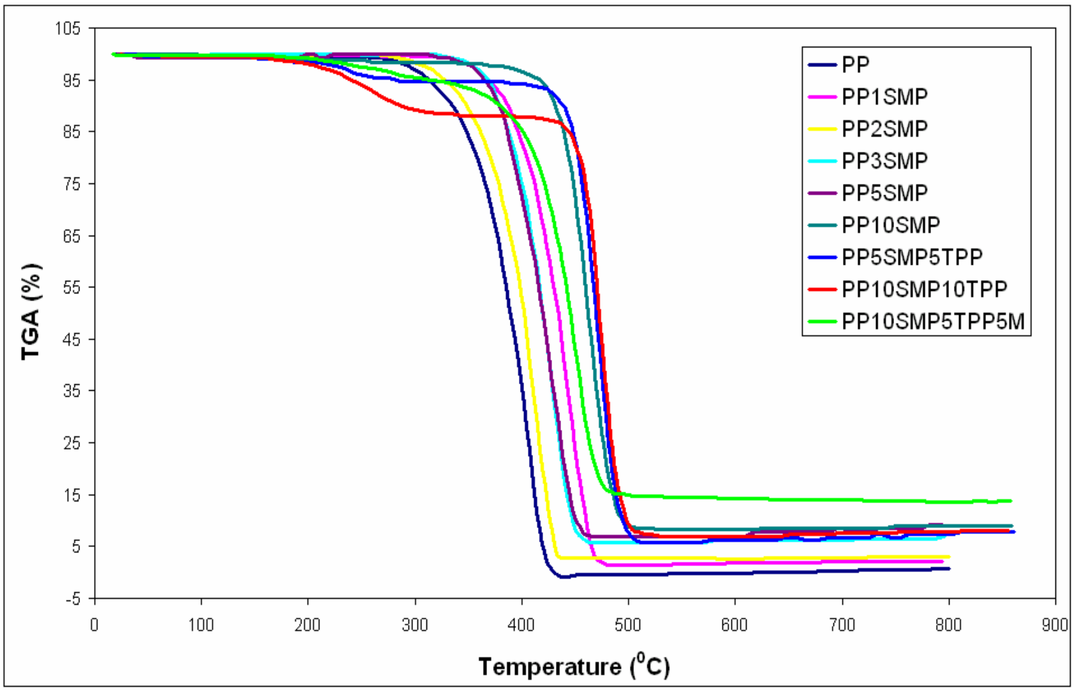

Figure 4.29 TGA curves of PP/SMP-10 blends in N_2 atmosphere

Table 4.16 Char yield % at 800^{0}C and average decomposition temperature of PP/SMP-10 blends

Composite Name	Char Yield (%)	Average Decomposition Temperature (^{0}C)
PP	0.83	406
PP/1SMP	2.21	448
PP/2SMP	3.14	417
PP/3SMP	6.89	429
PP/5SMP	9.22	434
PP/10SMP	8.82	467
PP/5SMP/5TPP	7.60	473
PP/10SMP/10TPP	7.92	478
PP/10SMP/5TPP/5M	13.74	453

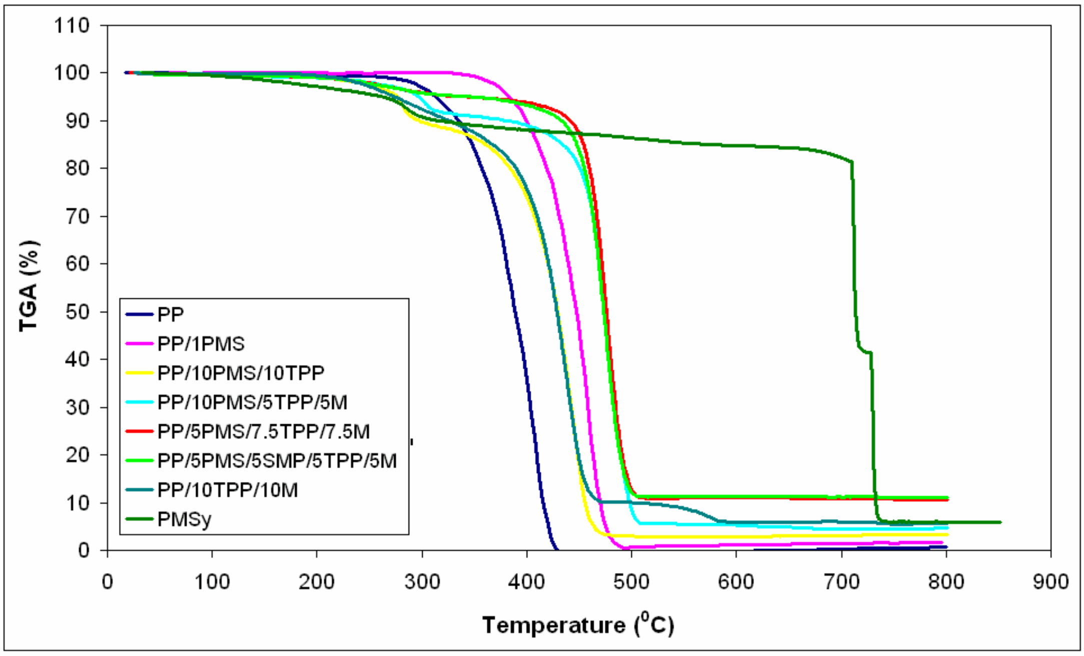

Figure 4.30 TGA curves of PP/PMS blends in N_2 atmosphere

Table 4.17 Char yield % at 800^{0}C and average decomposition temperature of PP/PMSy blends

Composite Name	Char Yield (%)	Average Decomposition Temperature (^{0}C)
PP	0.83	406
PP/1PMS	1.62	457
PP/10PMS/10TPP	3.40	446
PP/10PMS/5TPP/5M	4.69	480
PP/5PMS/7.5TPP/7.5M	10.64	480
PP/5PMS/5SMP/5TPP/5M	11.16	478
PP/10TPP/10M	5.63	440
PMSy	5.86	730

The improvement in the thermal stability of polypropylene can be observed from the TGA curves of the blends. In the TGA curves of the blends containing only SMP-10 as a flame retardant (PP/1SMP – PP/10SMP), it can be seen that the TGA curves are shifted to the right, to higher decomposition temperatures. In addition, it is obvious that addition of SMP-10 provides a significant decrease in the mass loss. These results can also be seen from Table 4.16. For instance, with addition of 5% SMP-10 to polypropylene (PP/5SMP), the char yield % is increased up to 9.22% from 0.83%. When the average decomposition temperatures are compared for the polymer blends, it is observed that for the blends with SMP-10, the average decomposition temperatures are increased to a great extent. For instance, with addition of 10% SMP-10 in polypropylene in PP/10SMP set, the average decomposition temperature is increased up to 467 from 406^0C. These results prove that addition of a silicon-based preceramic polymer, SMP-10, significantly improves the thermal stability of polypropylene. Therefore, the mechanism proposed for the flame retardancy of the polymer blends in the previous section is proved. The flame retardancy of SMP-10 comes from the improvement in the amount and thermal stability of the ceramic char formed during burning.

It can also be observed that the TGA curves of the samples containing TPP are different than the others. In the TGA curves of these samples (PP/5SMP/5TPP – PP/10SMP/5TPP/5M), two different decomposition stages are seen. This may be explained by the earlier decomposition of TPP than polypropylene and SMP-10. Although the decomposition starts earlier with the addition of TPP, it provides a significant increase in the average decomposition temperatures of the polymer blends. For instance, the maximum average decomposition temperature is obtained in the sample containing 10% TPP in PP/10SMP/10TPP set. The average decomposition temperature is increased to 478^0C from 406^0C in this set. When the char yields are compared, it is seen that SMP-10 itself promotes char formation more than the sets containing both TPP and SMP-10. This can be also seen from the char yield results of PP/10SMP and PP/5SMP/5TPP. Although both sets have the same total flame retardant composition of 10%, PP/10SMP has higher char yield. However, although the samples containing

TPP has lower char yields, they have still higher thermal stabilities due to higher decomposition temperatures. It can be seen that PP/10SMP and PP/10SMP/10TPP sets have very similar char yields and thermal stabilities. However, PP/10SMP/10TPP set has a LOI value of 20.5% whereas PP/10SMP sample has a LOI value of 19.0%. This result shows that the improvement in the flame retardancy is not only due to the increase in char yield % and thermal stability of the blend. Therefore, most probably addition of TPP also provides flame retardancy by the gas phase mechanism.

PP/10SMP/5TPP/5M set containing both SMP-10, TPP and a metal complex as flame retardants have the highest char yield % as shown in Table 4.16. This set has a char yield of 13.74% which is increased significantly when compared with the char yield of pure polypropylene which is 0.83%. Although the average decomposition temperature of this set is lower than the samples containing only SMP-10 and TPP, still when compared with polypropylene, the average decomposition temperature is increased to 453 from 406^{0}C. This proves that SMP-10, TPP and the metal complex provides a synergy and promotes char formation. This superiority in the ceramic char formation is most probably the main reason of the significant increase in flame retardancy.

For the blends with PMSy as a flame retardant, the same trend is observed. Addition of the flame retardants provides a significant increase in the thermal stabilities. This effect can be clearly seen from the increase in the average decomposition temperatures of the blends. For instance, addition of PMSy, TPP and the metal complex in polypropylene results average decomposition temperatures as high as 480 for PP/10PMS/5TPP/5M and PP/5PMS/7.5TPP/7.5M. It can be seen that although PP/10TPP/10M blend containing only TPP and metal complex has 20 wt% flame retardant like PP/10PMS/5TPP/5M and PP/5PMS/7.5TPP/7.5M blends, its decomposition temperature is nearly 40^{0}C lower than these samples. This shows that the presence of the silicon-based polymer is essential for high thermal stabilities. The reason of this can be seen from the TGA curve of PMSy. PMSy itself has a decomposition temperature of 730^{0}C.

Although decomposition temperatures of the composites with PMSy are higher than SMP-10, for the char yield percentages, an opposite effect is seen. The samples with PMSy have significantly lower char yields when compared with the samples with SMP-10. For instance, it can be seen that although PP/10SMP/5TPP/5M blends has a char yield of 13.74%, PP/10PMS/5TPP/5M blend has a value of 4.69%. This also explains the reason of the differences in the LOI values of these two blends. The only significant increases in the char yield are observed for the blends with 5% PMSy, PP/5PMS/7.5TPP/7.5 and PP/5PMS/5SMP/5TPP/5M.

As a conclusion, the reason of PMSy to be more effective than SMP-10 when used alone or with TPP in polypropylene is most probably its higher thermal stability due to higher decomposition temperatures. However, SMP-10 is more effective when used together with TPP and metal complex, since they provide a synergy and promote char formation.

4.2.2.2 Differential Scanning Calorimeter Results

The DSC analysis is done in order to assess the effect of the additives on the thermal properties of the blends. The DSC curves of the polymer blends containing SMP-10 and PMSy can be seen in Figures 4.31 and 4.32, respectively. In addition, the melting points of the blends are presented in Tables 4.18 and 4.19, respectively. The DSC curves for all composites are present in Appendix B.2.

It can be seen from Figure 4.31 and Table 4.18 that the DSC results of the blends with SMP-10 are very similar to each other having nearly the same melting temperatures. The melting points of the blends with SMP-10 and TPP together are lower compared with the blends with SMP-10 alone, however this decrease in the melting points of the blends is not that significant. For the blends with PMSy, again no significant change is observed for the DSC curves and the melting points of the blends.

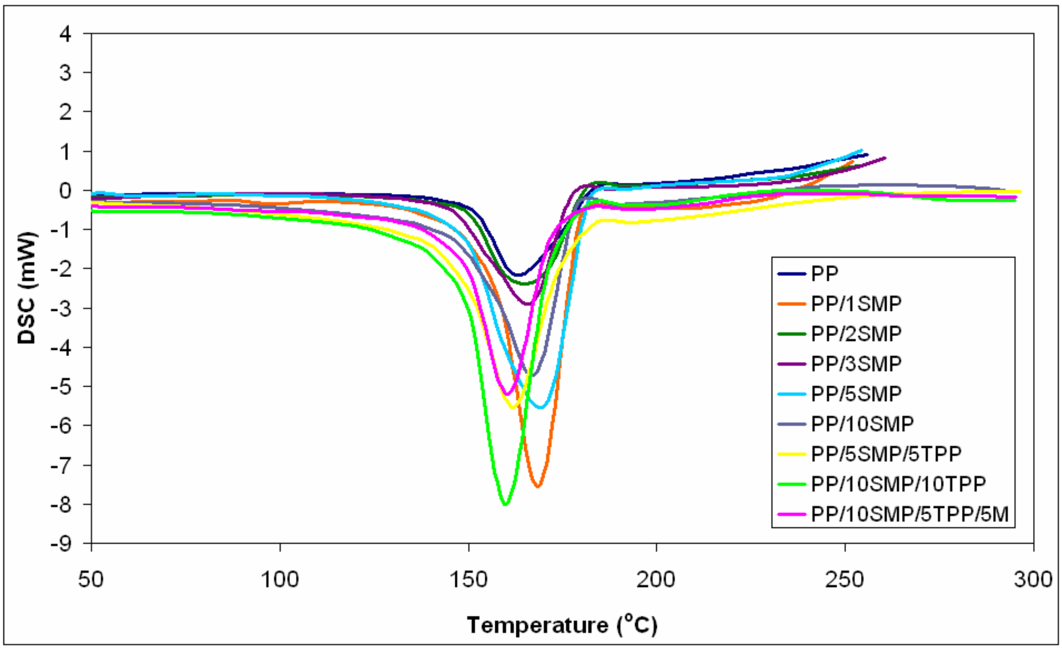

Figure 4.31 DSC curves of PP/SMP-10 blends

Table 4.18 Melting points of PP/SMP-10 blends

Composite Name	T_m (^{0}C)
PP	168
PP/1SMP	168
PP/2SMP	166
PP/3SMP	164
PP/5SMP	167
PP/10SMP	166
PP/5SMP/5TPP	162
PP/10SMP/10TPP	164
PP/10SMP/5TPP/5M	163

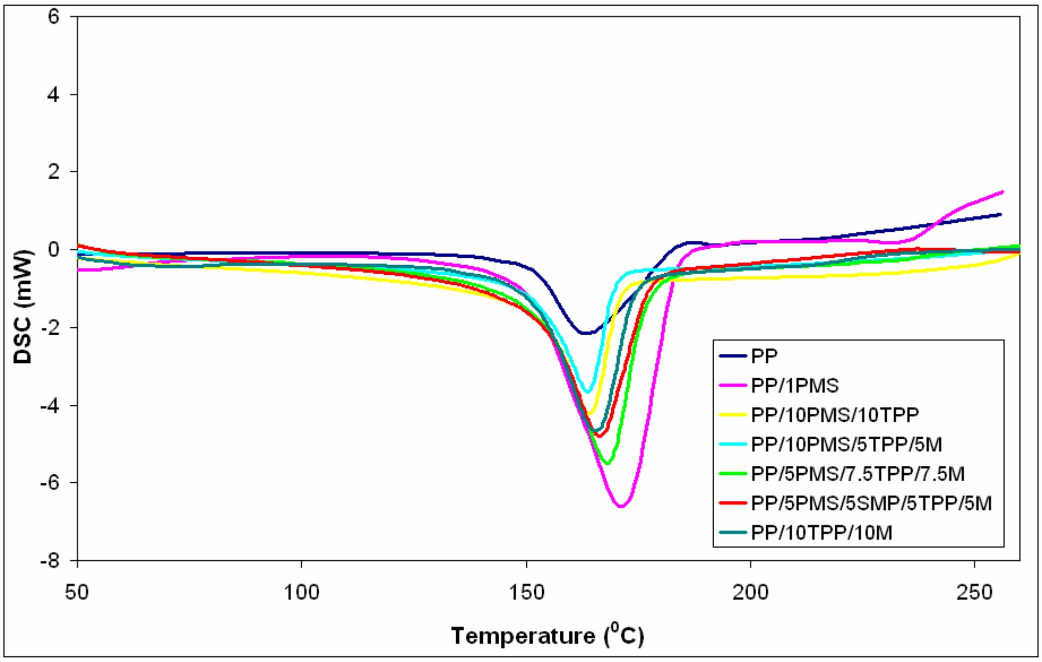

Figure 4.32 DSC curves of PP/PMSy blends

Table 4.19 Melting points of PP/PMSy blends

Composite Name	T_m (^{0}C)
PP	168
PP/1PMS	170
PP/10PMS/10TPP	164
PP/10PMS/5TPP/5M	164
PP/5PMS/7.5TPP/7.5M	168
PP/5PMS/5SMP/5TPP/5M	167
PP/10TPP/10M	166

4.2.3 Morphological Results

After flammability and thermal tests, SEM analysis is done in order to examine the morphological structures of the polymer blends. Morphological properties are important in order to evaluate the mechanical properties in a complete picture.

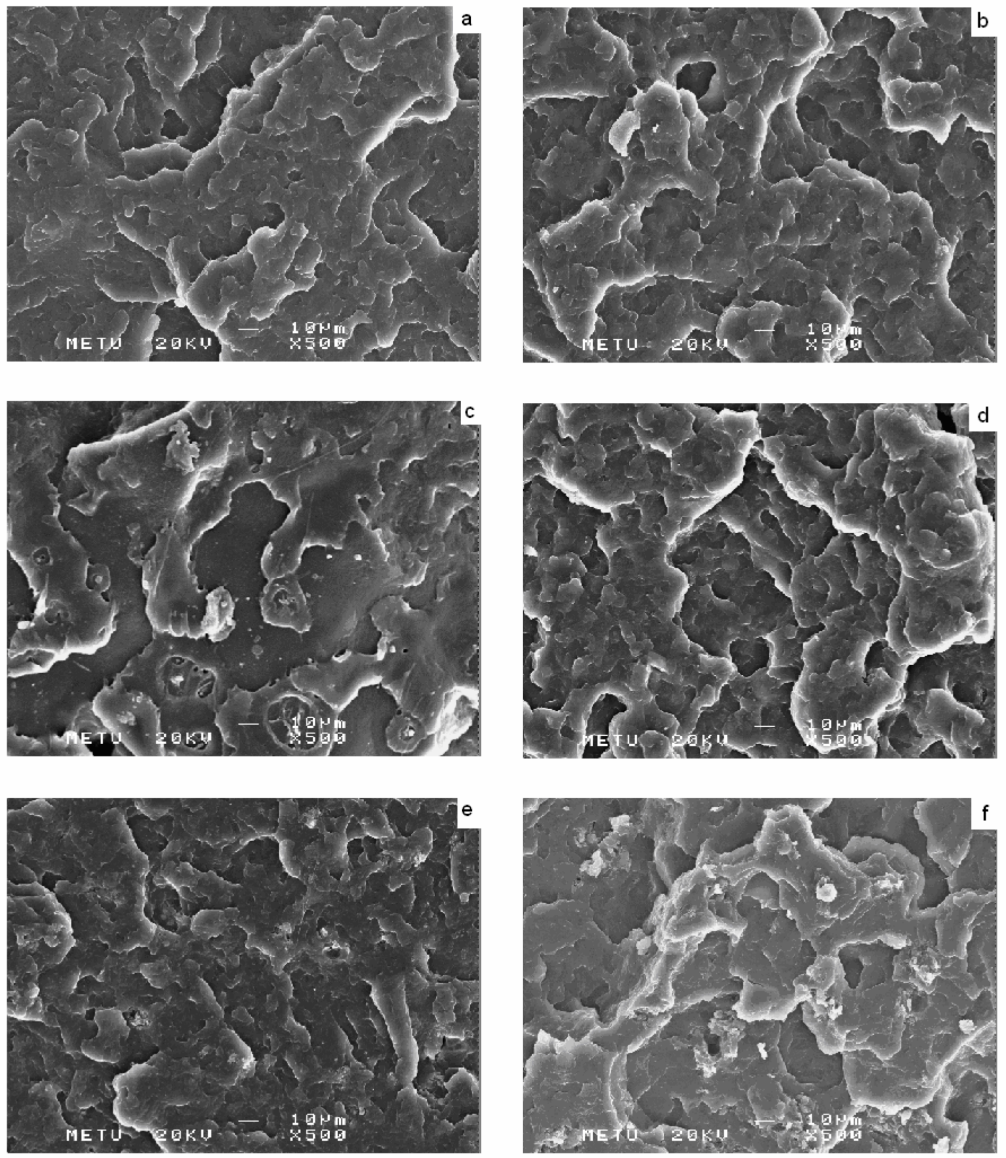

Figure 4.33 SEM micrographs of (a) PP (b) PP/1SMP (c) PP/2SMP (d) PP/3SMP (e) PP/5SMP (f) PP/10SMP sets at x500 magnification

The SEM pictures of all the composites in different magnifications and the EDX analysis done for the SEM pictures can be seen in Appendices C and D, respectively.

The SEM micrographs of pure polypropylene and the blends containing only SMP-10 can be seen in Figure 4.33. It is observed that addition of SMP-10 to PP in 1-5% does not cause a significant change in the morphology of the polymer (Figures 4.33a - e). SMP-10 can be noticed in the matrix polymer as white spots and it can be seen that it is dispersed well in the matrix therefore there is no important change in the morphology of the polymers. However when SMP-10 addition is 10% (Figure 4.33f), the agglomerates of SMP-10 can be observed distinctively from SEM micrographs.

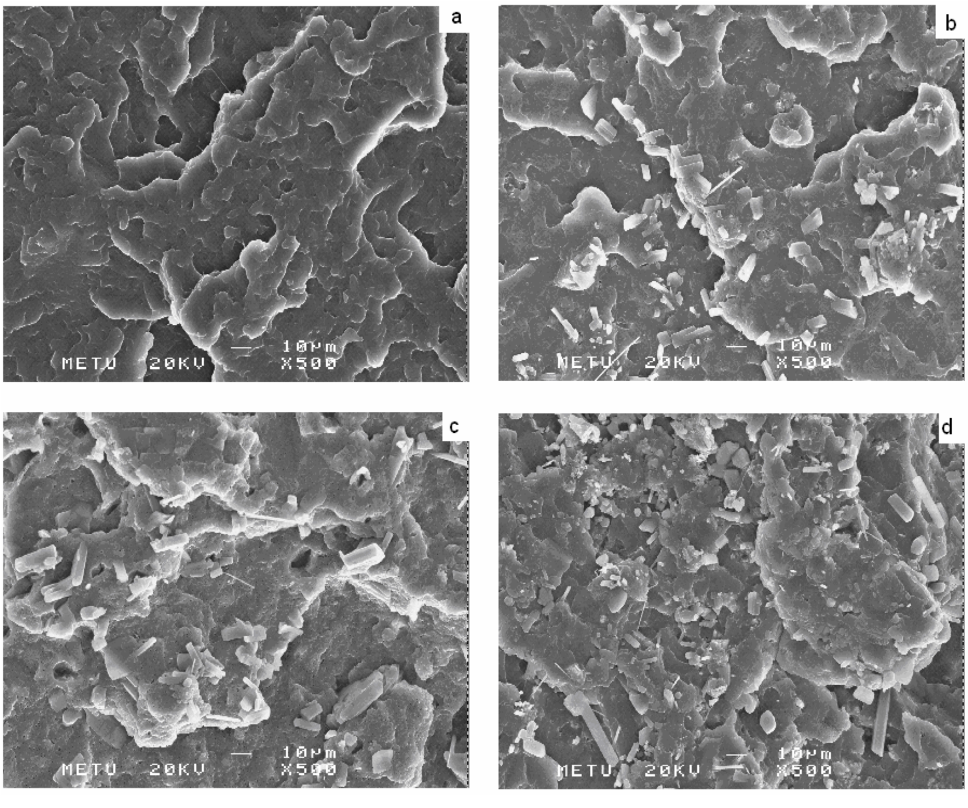

Figure 4.34 SEM micrographs of (a) PP (b) PP/5SMP/5TPP (c) PP/10SMP/10TPP (d) PP/10SMP/5TPP/5M sets at x500 magnification

The SEM micrographs of the blends with SMP-10, TPP and the metal complex can be seen in Figure 4.34. It is obvious that addition of TPP to the blends cause significant changes in the morphologies of the polymers. First of all, with the addition of TPP, inorganic crystalline structures emerge in the system. There are three different kinds of structures identified in the SEM pictures of the samples with both SMP-10 and TPP. These are cubical structures, irregular shaped structures and rectangular prisms. When EDX analysis is done for these structures, it is seen that cubical structures are most probably agglomerates of SMP-10 since only Si and C elements are detected for these structures. For the irregular shaped structures and rectangular prisms, both Si, C, P and O elements are detected showing that these structures contain both TPP and SMP-10. These different structures can be seen from Figure 4.35.

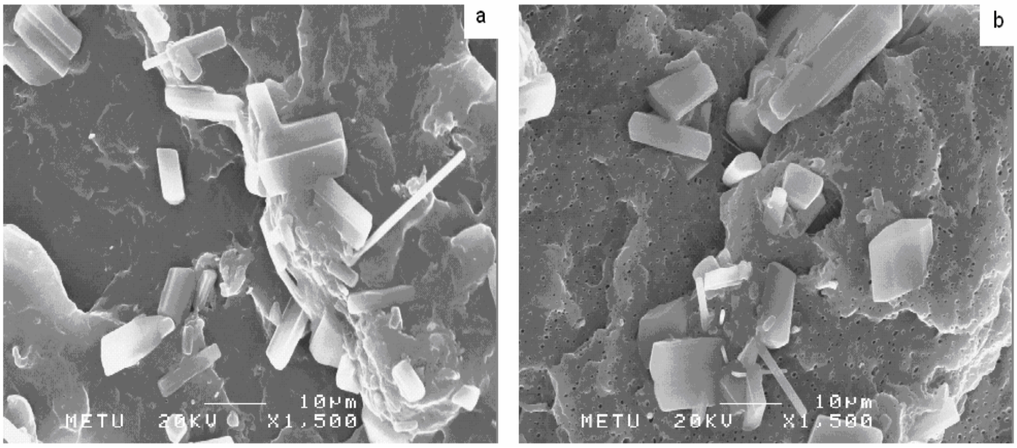

Figure 4.35 SEM micrographs of (a) PP/5SMP/5TPP (b) PP/10SMP/10TPP sets at x1500 magnification

Another interesting difference in the morphologies of the samples containing both SMP-10 and TPP is that very tiny holes are observed in the matrix in PP/5SMP/5TPP and PP/10SMP/10TPP sets. In PP/5SMP/5TPP set, these holes are only present in some distinct areas and are not that significant. However, in PP/10SMP/10TPP set, the whole matrix contains these holes (Figure 4.35b). Since these holes are too small to be air bubbles, it is suspected that they can be formed as a result of a gaseous product of a reaction between SMP-10 and TPP. The irregular structures obtained in SEM micrographs may also be formed as a result of this reaction.

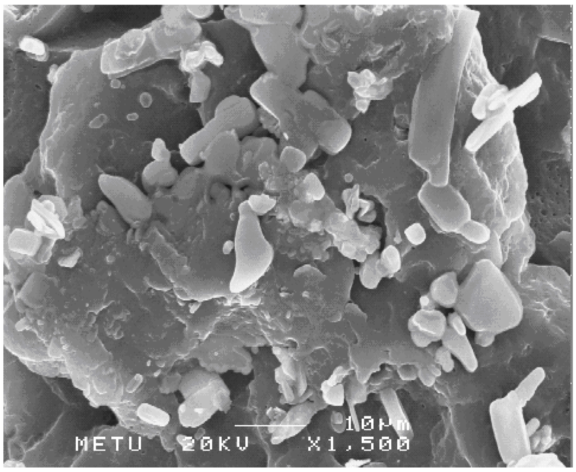

Figure 4.36 SEM micrograph of PP/10SMP/5TPP/5M at x1500 magnification

In PP/10SMP/5TPP/5M set containing both SMP-10, TPP and the metal complex, the irregular structures are present as in the case of previous results (Figure 4.36). When EDX analysis is done for these irregular structures, Si, C, P, O and Sb elements are detected proving that these structures contain SMP-10, TPP and the metal complex. From the SEM micrographs, it can be observed that the tiny holes are not significant in this set.

In order to get more information about the formation of these small holes and the crystalline structures, a blend containing only TPP and the metal complex is prepared and the SEM micrograph of PP/10TPP/10M is shown in Figure 4.37.

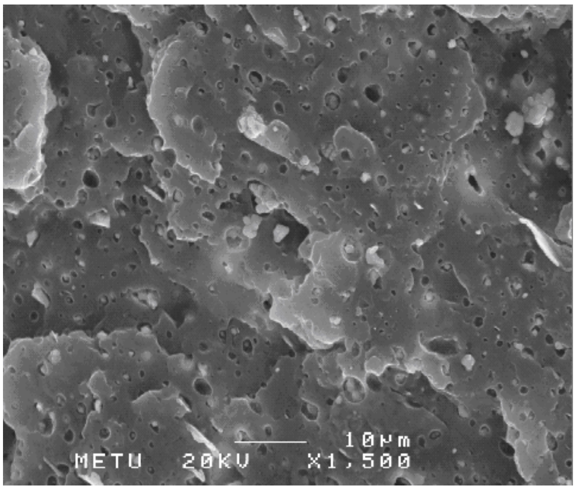

Figure 4.37 SEM micrograph of PP/10TPP/10M at x1500 magnification

When SEM micrograph of PP/10TPP/10M is compared with PP/10SMP/5TPP/5M blend, it can be seen that the blend without SMP-10 does not contain crystalline structures as in the case of the previous results. This SEM micrograph supports the formation of these structures as a result of a reaction between SMP-10 and TPP. The holes in the matrix are still present in Figure 4.37. Therefore, these holes are most probably formed as a result of TPP in the system.

Before the SEM analysis of the polypropylene based composites with PMSy are done, the SEM morphology of poly(methylsilyne) is investigated. The SEM micrographs of the polymer can be seen in Figure 4.38. From the SEM micrographs of the polymer, the highly branched structure of the polymer can be distinguished.

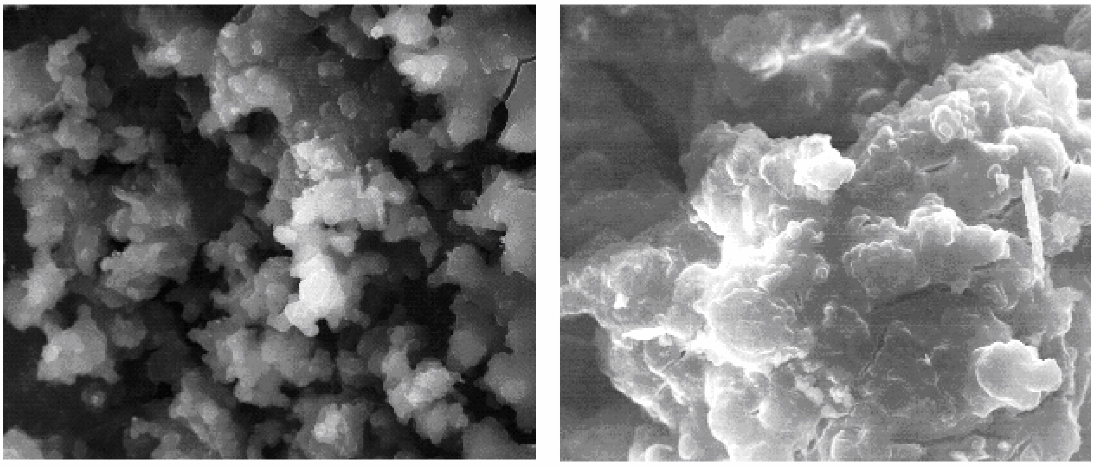

Figure 4.38 SEM micrographs of PMSy at x5000 magnification

The SEM pictures of the blends containing PMSy can be seen in Figure 4.39. It can be seen that when PMSy is in 1 wt% in polypropylene (Figure 4.39b), there is no difference in the morphologies of the blend with pure polypropylene. This is due to the good dispersion of the polymer in polypropylene since it is in very low amount. In addition, it can be observed that although PP/10PMS/10TPP blend has total flame retardant amount of 20 wt%, its morphology is also similar to polypropylene (Figure 4.39c). The inorganic crystalline structures are not observed for the blends with PMSy and TPP unlike the results with SMP-10. This shows that most probably PMSy and TPP do not give any interaction which creates a change in the polymer's morphology.

In the SEM micrographs of the blends with PMSy, TPP and the metal complex (Figures 4.39d and e), the crystalline structures are again not present. The particles observed in the SEM micrographs of these blends are most probably TPP and metal salts. PMSy is most probably well dispersed in the matrix and can not be seen in the SEM results. Finally, in the last SEM micrograph, a slightly different morphology is observed. As mentioned before, in this blend since four different flame retardants are used together in polypropylene, the properties of the polymer are affected in a negative manner. This can also be seen from the deformation of the polymer matrix in PP/5PMS/5SMP/5TPP/5M blend in Figure 4.40. This deformation is most probably the reason of the increase in the dripping.

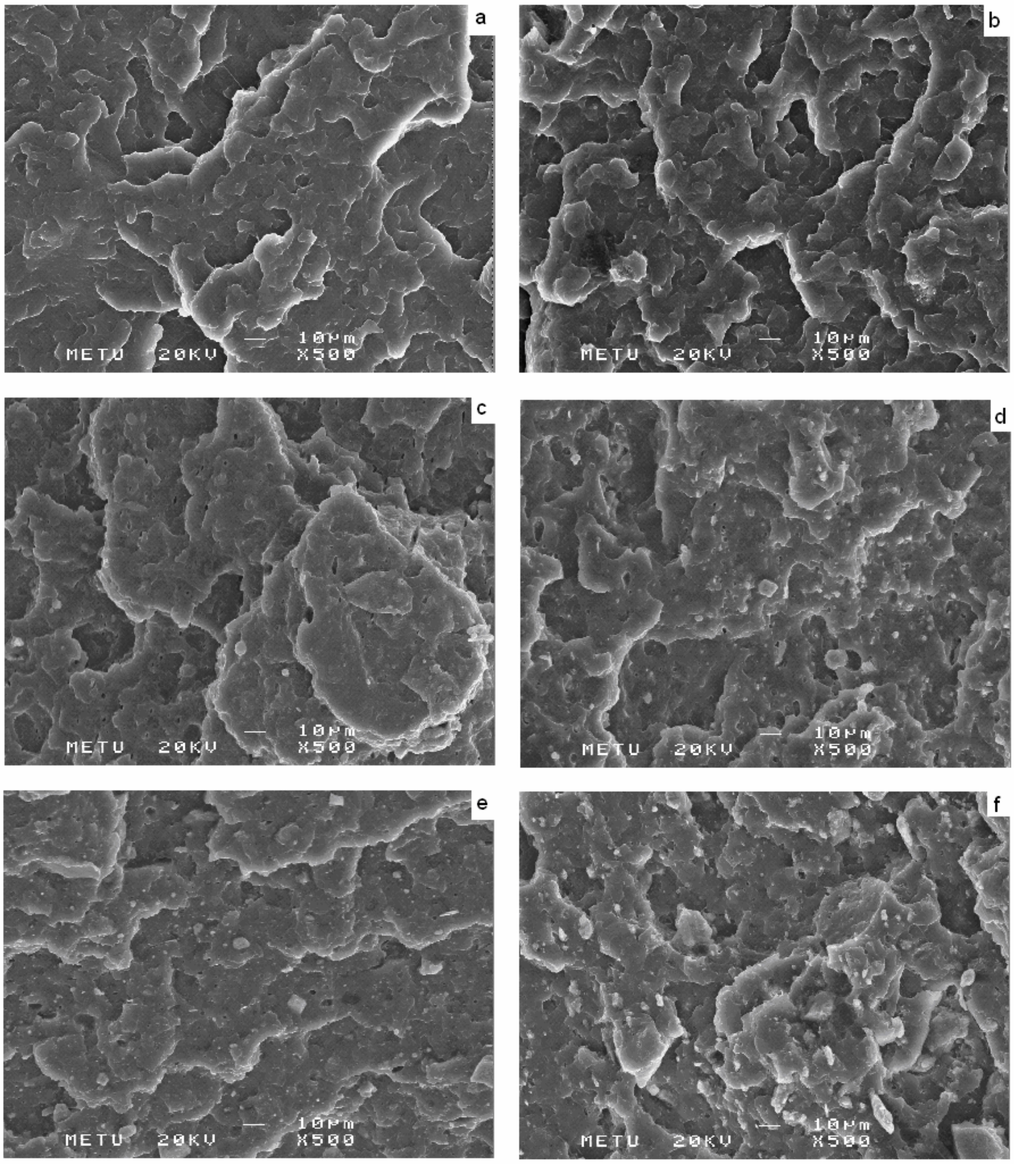

Figure 4.39 SEM pictures of (a) PP (b) PP/1PMS (c) PP/10PMS/10TPP (d) PP/10PMS/5TPP/5M (e) PP/5PMS/7.5TPP/7.5M and (f) PP/5PMS/5SMP/5TPP/5M sets at x 500 magnification

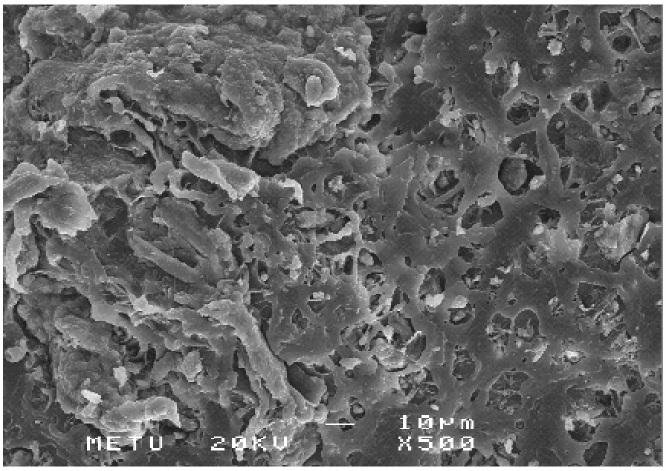

Figure 4.40 SEM picture of PP/5PMS/5SMP/5TPP/5M set at x 500 magnification

4.2.4 Mechanical Properties

4.2.4.1 Tensile Properties

After the flammability and thermal properties of the blends are completed, mechanical tests are applied to the polymer blends in order to see the effect of flame retardant addition to the mechanical properties of polypropylene. The tensile properties of the blends are investigated by evaluating the tensile strength, Young's modulus and elongation at break results. It is seen that for all the PP/silicon-based preceramic blends, the typical stress-strain curve for pure polypropylene is obtained with stress whitening followed by necking and drawing. Therefore, yield point is observed for all blends. The tensile properties of the blends with SMP-10 and PMSy are shown in Figures 4.41-4.44 and Figures 4.45-4.48, respectively.

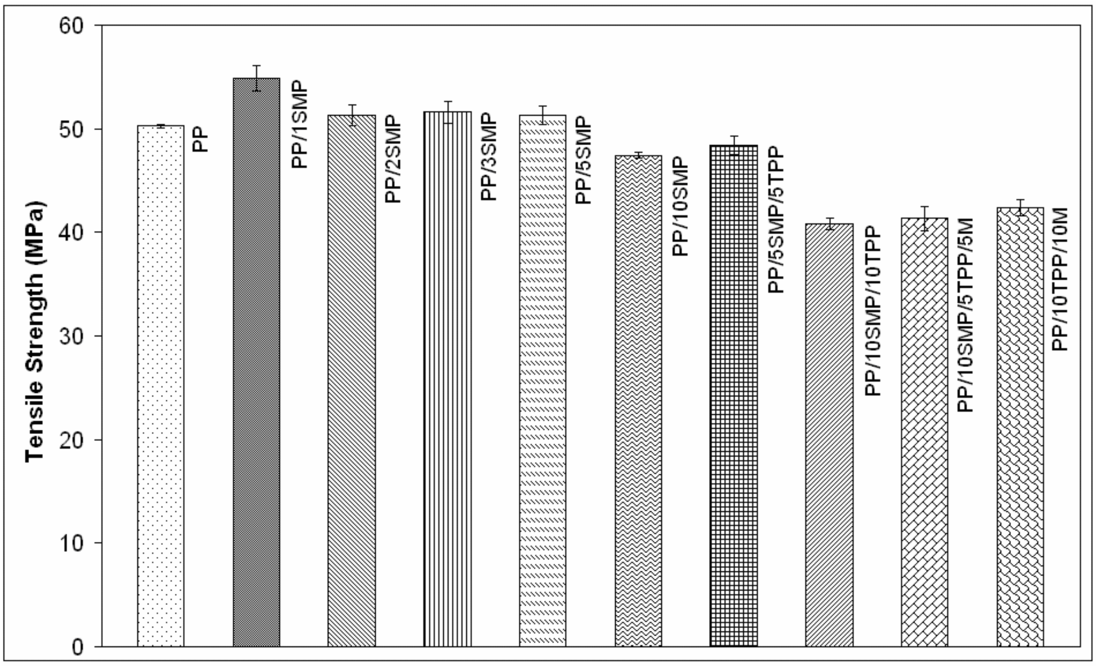

Figure 4.41 Tensile strength of PP/SMP-10 blends at break

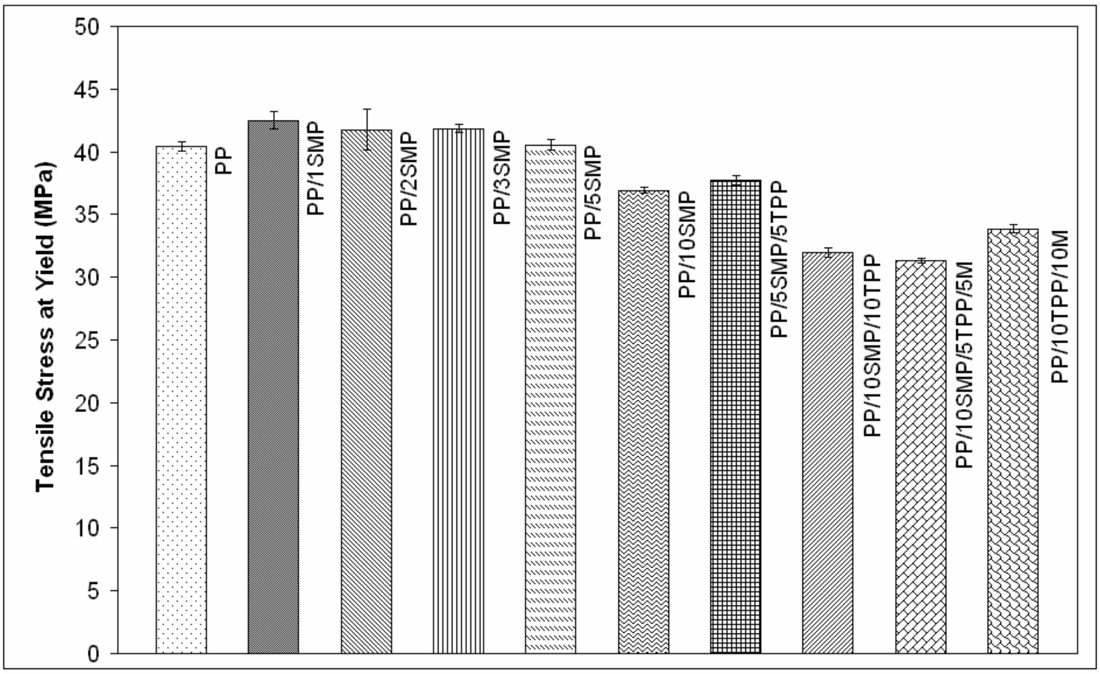

Figure 4.42 Tensile stress of PP/SMP-10 blends at yield

The tensile stresses at break and at yield of the polymer blends with SMP-10 are shown in Figures 4.41 and 4.42, respectively. It can be seen from Figure 4.41 that there is an increase in the tensile strength for PP/1SMP containing 1% SMP-10. This shows that addition of SMP-10 in small amounts results in an increase in the tensile strength of the polymer blend. In addition, it can be observed that when the composition of SMP-10 is 5% or lower, there is a slight increase in the tensile strength values. For the blends with total flame retardant composition of 10 wt%, there is not a significant change in the values. However, when the total flame retardant composition is 20 wt%, a significant decrease in tensile strength values can be observed due to the stress concentrate effect of the components. In these sets, flame retardant compositions are very high, therefore these decreases in the mechanical properties of the matrix polymer are not suprising.

Tensile stress values at yield for PP/SMP-10 blends also show the same trend. There is a slight increase in the values when the total flame retardant composition is 5% or lower. On the other hand, in the sets with 10% or 20%, a significant decrease is observed. However, this decrease is endurable, since the high yield stress values are still kept.

The elastic modulus of the polymer blends can be seen in Figure 4.43 for PP/SMP-10 blends. SMP-10 addition to polypropylene in 5% or lower compositions results in a significant increase in the elastic modulus of the polymer due to the adhesion between PP and SMP-10 and the interaction between the similar groups in the structure. Similar to the tensile strength results, the highest elastic modulus is obtained when SMP-10 composition is 1% in polypropylene. Further increase in SMP-10 concentration results in a decrease in the modulus. After 10% of flame retardant addition, the modulus values decrease below the modulus of pure polypropylene because the adhesion between PP and SMP-10 is destroyed with the existence of TPP, the metal complex and the excess amount of SMP-10. However, still the decreases in the modulus values with 10% and 20% flame retardant addition are not that significant.

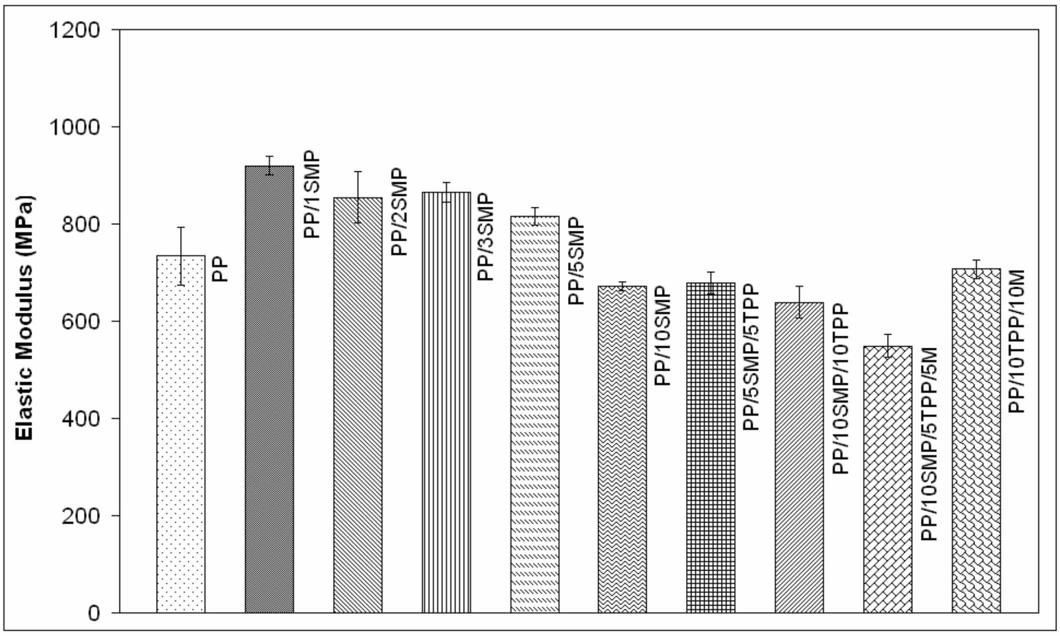

Figure 4.43 Elastic modulus results of PP/SMP-10 blends

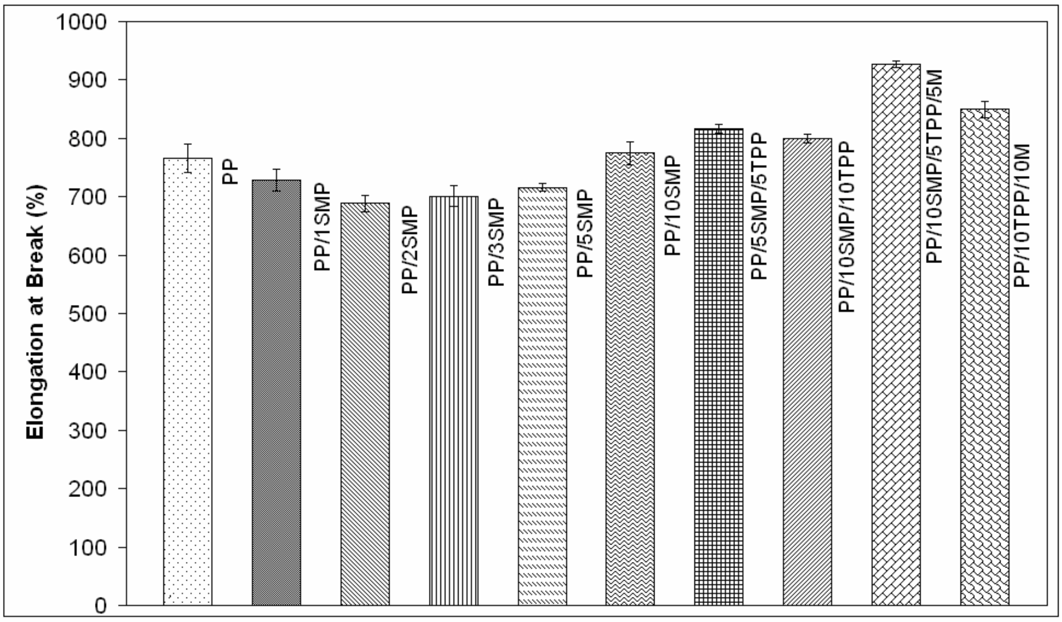

Figure 4.44 Elongation at break values of PP/SMP-10 blends

Finally, the elongation at break values are calculated and compared for PP/SMP-10 blends in Figure 4.44. It can be seen that with the addition of SMP-10 in low amounts in the first four sets, there is a slight decrease in the elongation at break values. However, for the last four sets that contain 10% or higher flame retardant, elongation at break values increase significantly. These results are expected since the tensile strength and elastic modulus values of these blends are lower. Furthermore, it can be seen that the addition of the metal complex to SMP-10 and TPP resulted in a significant increase in the elongation at break value. This is most probably due to the plasticizing effect of SMP-10, TPP and the metal complex when used together in polypropylene.

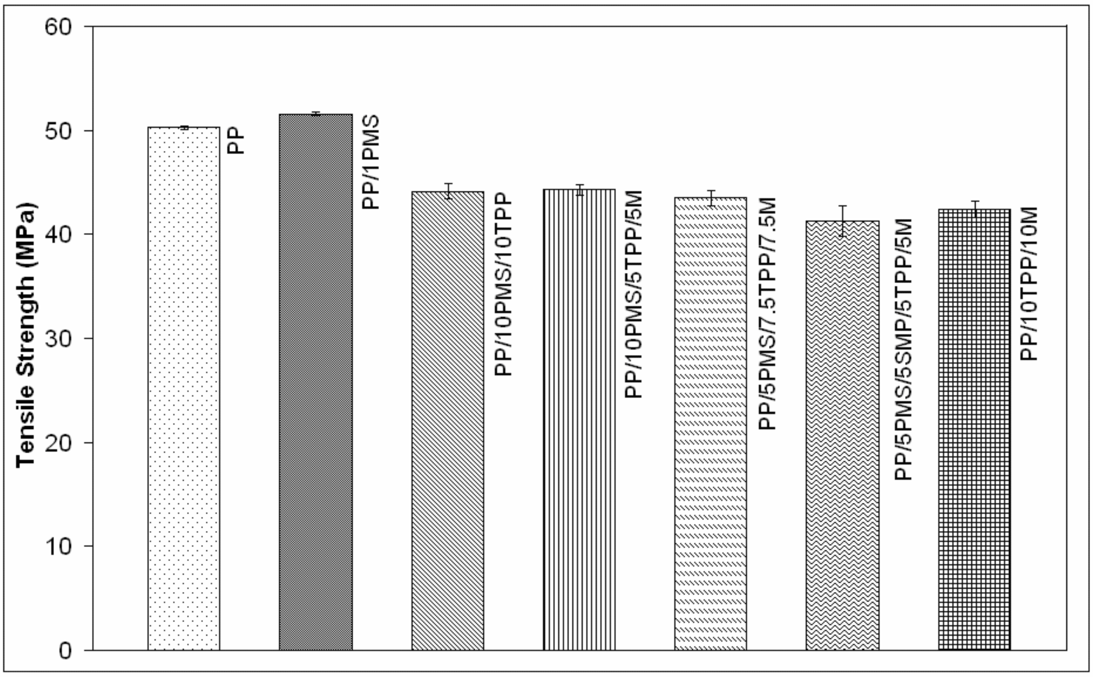

Figure 4.45 Tensile strength of PP/PMSy blends at break

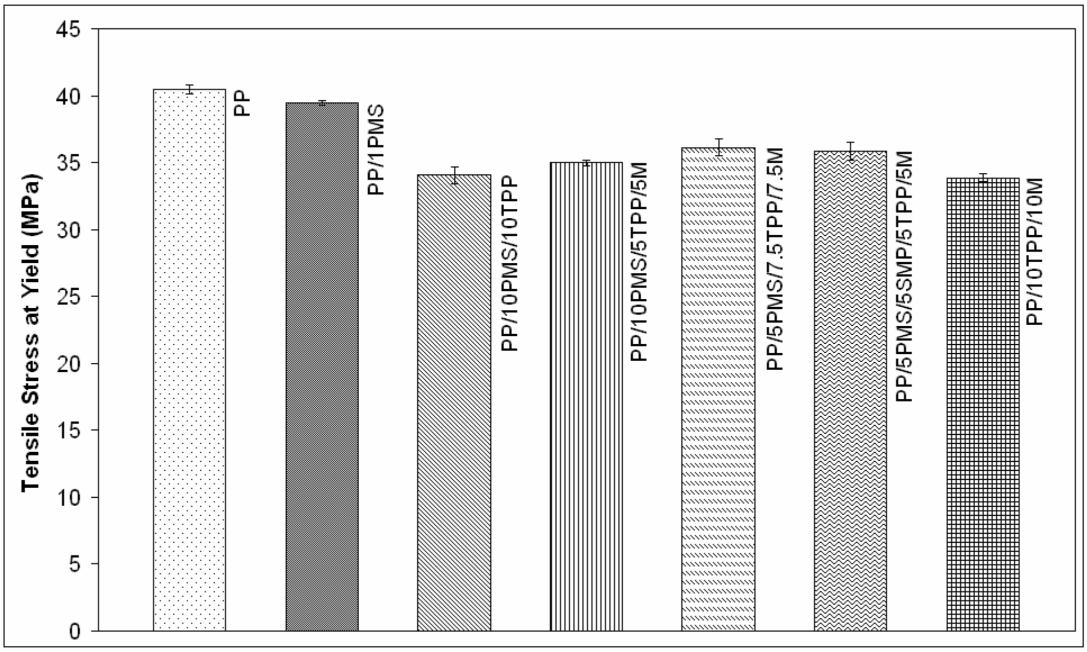

Figure 4.46 Tensile stress of PP/PMSy blends at yield

The tensile stress values of PP/PMSy blends at break and at yield can be seen in Figures 4.45 and 4.46, respectively. It can be seen that similar to the blends with SMP-10, addition of PMSy in low amount results in an increase in the tensile strength at break. However, for the other blends containing 20 wt% flame retardant, there are significant decreases in the tensile strengths. This can be attributed to the insufficient dispersion of the components which act as stress concentrators. However, these decreases are not very important since the tensile strength values are still very high.

The elastic modulus results for PP/PMSy blends are shown in Figure 4.47. It can be seen that again the best result is obtained for PP/1PMS blend containing 1% PMSy. There is no significant change in the elastic modulus results of the other blends containing total flame retardant amount of 20 wt%.

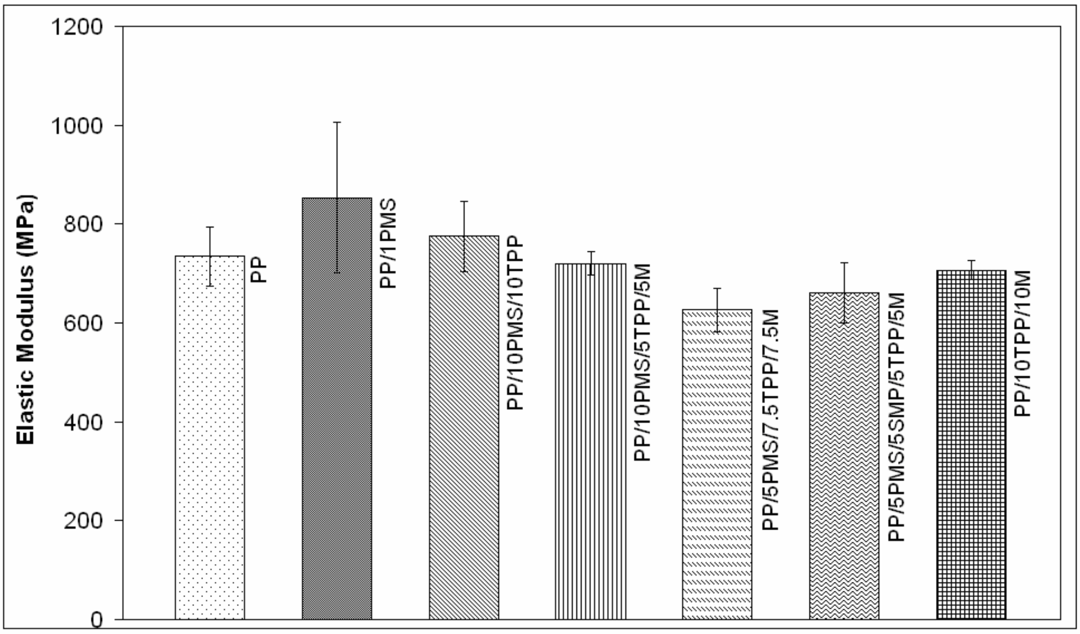

Figure 4.47 Elastic modulus of PP/PMSy blends

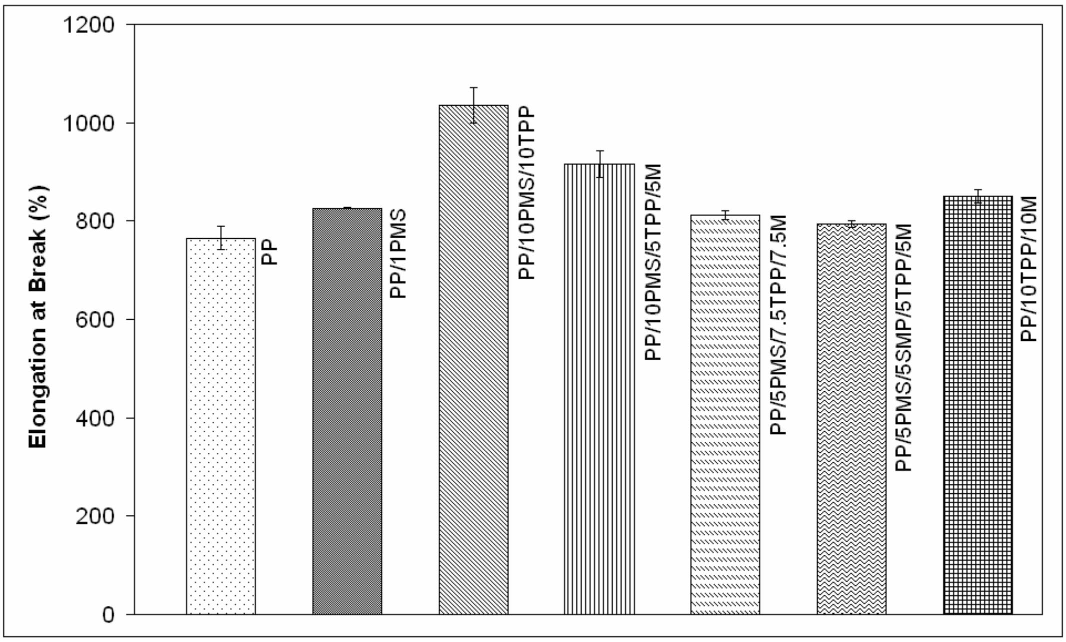

Figure 4.48 Elongation at break values of PP/PMSy blends

From the elongation at break values of PP/PMSy blends that are shown in Figure 4.48, it can be seen that all the results are very close to pure polypropylene except the blends containing 10% PMSy. The elongation at break values of PP/10PMS/10TPP and PP/10PMS/5TPP/5M are significantly higher than the other results due to the plasticizing effect of the components.

As a result of the tensile test, it is seen that when SMP-10 and PMSy are added to polypropylene in low amounts, they result in an increase in the tensile strength and elastic modulus results. Although these increases can not be seen for the blends with 10% or 20% flame retardant additives, increases in elongation at break values are observed for these blends. As a conclusion, it can be observed that although the flame retardant compositions are very high, the high mechanical properties of polypropylene are still maintained.

If the tensile properties of the blends are evaluated based on their morphologies, it can be seen that the highest tensile strength and elastic modulus are obtained in PP/1SMP among all PP/SMP-10 samples. The reason of this result can be explained by the SEM micrograph of PP/1SMP in Figure 4.33b. Since the amount of SMP-10 is very low in this set and it is well dispersed in polypropylene, the tensile properties are higher than the other sets. In addition, the tensile strength and elastic modulus in PP/1SMP – PP/5SMP are increased due to good dispersion in the matrix which can be seen in the SEM results. Tensile strength and elastic modulus start to decrease with 10% SMP-10 addition in PP/10SMP sample due to lower dispersion since the polymer starts to agglomerate in the matrix as seen in Figure 4.33f.

For the samples with SMP-10 and TPP, it can be seen that a whole different morphology is obtained with many different structures. Since the amount of additives is increased in these sets, the continuity of polypropylene phase is decreased therefore significant decreases in the tensile strength and elastic modulus are observed. On the other hand, due to the plasticizing effect of the additives, elongation at break values are increased remarkably. The decrease in tensile strength and elastic modulus values with 10% and 20% flame retardant additive can also be explained by the poor dispersion in the SEM results of the blends in Figure 4.34.

If the tensile properties are discussed for PP/PMSy systems based on their morphologies, it can be seen that the highest tensile strength and elastic modulus are obtained in PP/1PMS blend due to good adhesion and dispersion seen in the morphology. In addition, the similarity of the morphology of PP/10PMS/10TPP with PP provides the highest elastic modulus value of this sample among the blends with 20% flame retardant additive (Figure 4.39c). The mechanical properties of the other samples are also high although they contain 20% additive, this is most probably due to good dispersion of the additives in the matrix (Figures 4.39d, e, f). The increase in the elongation at break values with the addition of the metal complex to the system can be explained by the plasticizing effect and good dispersion of the metal salts in the matrix.

4.2.4.2 Impact Strength

The impact strength of the blends is investigated after tensile properties in order to obtain more information on the mechanical properties of PP/preceramic polymer blends. Figures 4.49 and 4.50 represent the impact strength of the blends with SMP-10 and PMSy, respectively. In both of the figures, the results are compared with pure polypropylene which is ground and extruded as the other blends.

The results show that addition of the flame retardant cause a significant increase in the impact strength of polypropylene. When the polymer blends containing SMP-10 alone (PP/1SMP – PP/10SMP) are investigated, the results are rather unexpected. In these sets, the increase of the impact strength is not proportional with SMP-10 composition. For instance, PP/2SMP and PP/3SMP samples have lower strength than PP/5SMP and PP/10SMP. Another interesting result is that PP/5SMP containing 5% SMP-10 has the highest impact strength among the samples with only SMP-10 as the flame retardant. When the blends containing both SMP-10 and TPP are compared it can be seen that PP/5SMP/5TPP has the highest impact strength among the samples with SMP-10. When PP/5SMP and PP/5SMP/5TPP or PP/10SMP and PP/10SMP/10TPP are compared it can be seen that addition of TPP to PP/SMP-10 blend results in an increase in the impact strength of the blends. Although addition of TPP increases the impact strength of the polymer blends, it can be observed that addition of the metal complex causes a significant decrease. This result is also unexpected since the highest elongation at break value is obtained for this set during tensile testing. In addition, PP/10TPP/10M blend, which is prepared by 10% TPP and 10% metal complex in order to test the effect of TPP and the metal complex without the preceramic polymers in polypropylene, has very high impact strength.

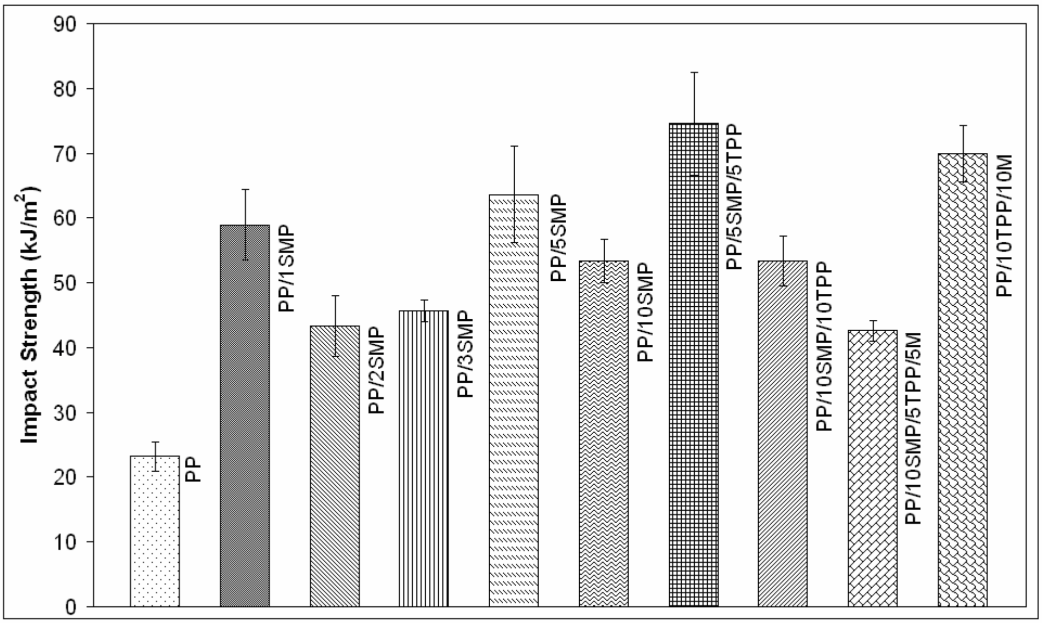

Figure 4.49 Impact strength of PP/SMP-10 blends

As a conclusion, it is seen that the best impact strength values are obtained with SMP-10 compositions of 5% in PP/5SMP and PP/5SMP/5TPP sets. In addition, it is observed that TPP has a positive effect on the impact strengths of the PP/SMP-10 blends.

When the impact strength results are investigated based on the morphologies of the polymer blends, it is observed that the reason why PP/5SMP has the highest impact strength among PP/1SMP – PP/10SMP sets can be explained by the SEM micrographs in Figure 4.33. In PP/1SMP sample, due to good adhesion and well dispersion, there is a significant increase in the impact resistances. When the composition of SMP-10 is 2 or 3% in polypropylene, they are also successfully mixed with the matrix and well dispersed however not effective as PP/1SMP. In PP/5SMP sample, SMP-10 starts to agglomerate and starts to absorb the energy resulting in an increase in the impact strength. The impact strength reduces in the PP/10SMP sample again most probably because the agglomerates become too large as seen in Figure 4.33f.

For the samples containing both SMP-10 and TPP, it is seen that impact properties are higher than the samples containing only SMP-10. This can be explained by the differences in the morphologies. Most probably, the agglomerates of TPP and SMP-10 act as crack stoppers and increase the impact strength of the polymers by absorbing the impact energy. However, the structures seen in PP/10SMP/5TPP/5M set composed of SMP-10, TPP and the metal complex do not show the same effect and cause the impact strength to decrease. As mentioned before, this result is not expected since the highest elongation at break value is obtained for this set.

The impact results of the blends with PMSy can be seen in Figure 4.50. It can be seen that addition of PMSy to polypropylene also provides an increase in the impact strength although these results are not as high as the ones with SMP-10. In the figure, it can be seen that the best impact result is obtained at 1% PMSy composition in PP/1PMS among the blends with PMSy. Another important point is that it can be observed that the samples having 10% PMSy have better impact strength than the samples containing 5% PMSy. It is also seen that the impact results of the samples with PMSy do not follow a trend. For instance, although

PP/10PMS/5TPP/5M sample has a very high impact strength, PP/5PMS/7.5TPP/7.5M sample also containing PMSy, TPP and the metal complex has the lowest strength. Finally, it can be observed that in the last sample containing SMP-10 addition to PMSy, TPP and metal complex, the impact strength is lower than PP/10PMS/5TPP/5M.

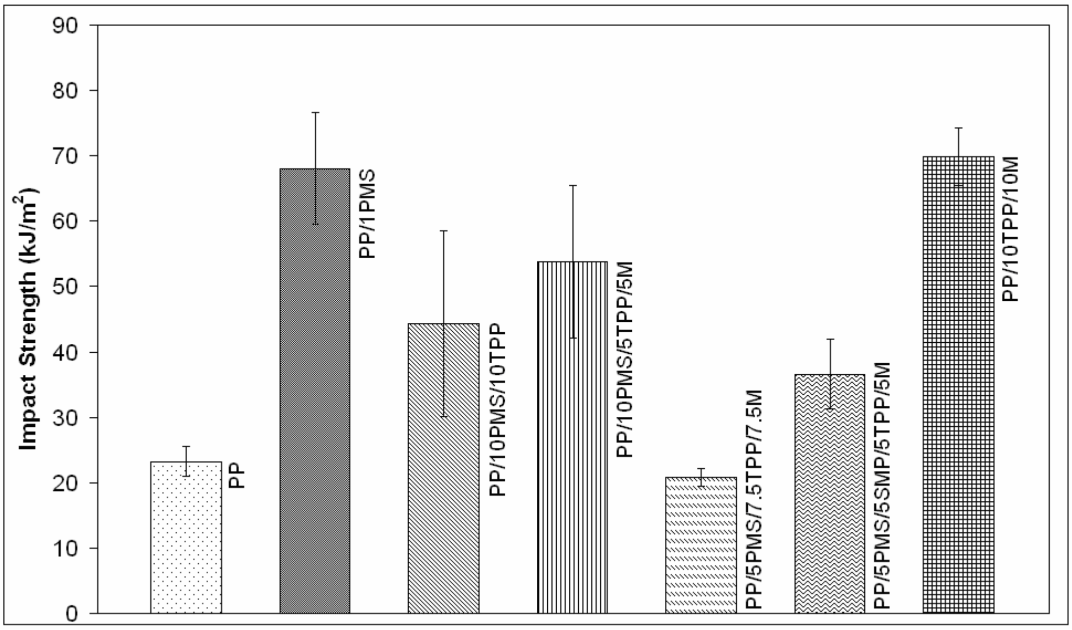

Figure 4.50 Impact strength of PP/PMSy blends

The impact properties can be evaluated based on the morphologies of the samples as follows. Since there is good adhesion and good dispersion of PMSy in polypropylene matrix, the impact resistances of the blends increase significantly. The decrease in the impact strength of PP/5PMS/7.5TPP/7.5M can not be explained by the morphology of the blend since it is very similar to PP/10PMS/5TPP/5M blend which has a significantly higher strength. In addition, blends containing 10% PMSy have higher impact resistances, most probably since PMSy is dispersed better in the matrix in 10% and it starts to absorb the impact energy better.

CHAPTER 5

CONCLUSIONS

In the first part of this dissertation, poly(methylsilyne), which is a silicon-based preceramic polymer for silicon carbide, was synthesized by electrochemical polymerization of methyltrichlorosilane under a constant potential of -6 V both in small and large-scales. In the small-scale, the polymer was synthesized with a simple supporting electrolyte in a shorter reaction time than the ones given in literature. The polymer was then characterized by ^{1}H-NMR, FTIR, UV-Visible Spectroscopy and GPC methods in addition to its distinctive yellow color. In the ^{1}H-NMR spectrum of the polymer, the expected broad Si-CH_3 peak between 0 and 0.5 ppm was observed in addition to the Si-H peak at 4.2 ppm. Besides these two expected peaks, peaks corresponding to the solvents used in purification were also seen. The FTIR spectrum of the polymer was very similar to the results in literature revealing all the expected peaks for poly(methylsilyne). Si-Cl bond was not observed showing that all the remaining bonds were converted into Si-H with the help of $LiAlH_4$. The UV-Visible spectrum of the polymer exhibited a broad UV band tailing down to the visible region around 400 nm. This result also proved the branched structure of the polymer since linear polysilanes have significantly different UV-Visible spectra. As a result of GPC, the molecular weight, M_w, and polydispersity index were determined as 5900 and 1.15, respectively. As a conclusion, the yellow color and ^{1}H-NMR, FTIR, UV-Visible and GPC results indicated that synthesis of poly(methylsilyne) in small-scale was successful.

After the small-scale synthesis and characterization of poly(methylsilyne) were completed, the electrochemical polymerization was scaled-up five times while investigating the effects of the synthesis parameters such as the electrode type, supporting electrolyte type, solvent type, monomer/solvent ratio and reaction time on the electrolysis. For the electrolytic media with acetonitrile, SDS and stainless steel electrodes, it was seen that the products were not successful because of their unwanted physical properties. The only product with successful physical properties was PMS2211 produced with a monomer/solvent ratio of 1:5 and a reaction time of 30 min. Increasing the monomer/solvent ratio and reaction time in this system resulted in unsuccessful products. The differences in the colors of the products were explained by the increase in the impurities coming from the stainless steel electrodes with increasing time. In order to prevent these impurities, copper electrodes were used in the rest of the experiments. In the large-scale synthesis with acetonitrile, SDS and copper electrodes, it was seen that although products with successful physical properties and NMR and FTIR results were obtained, the reproducibility could not be maintained. In order to minimize the effects coming from temperature changes, the rest of the experiments were carried out in a constant temperature bath at 25^0C. In the system with acetonitrile, copper electrodes and temperature control, the effects of reaction time and supporting electrolyte type were investigated. It was seen that increasing the reaction time affected the product in a negative manner, most probably due to the increase in the impurities coming from the deformation of the electrodes with increasing time. The effect of supporting electrolyte type was also examined due to the problems with the low solubility of SDS in acetonitrile. Since it was not very soluble in acetonitrile, the electrolytic media did not have enough ionic conductivity, therefore the current was very low. This was most probably one of the reasons of the problems in the reproducibility of the system with SDS and acetonitrile. Therefore, TBAP, a stronger supporting electrolyte, was used. The current increased nearly 10 times with the use of TBAP in acetonitrile. Peaks due to TBAP were supressing the expected Si-CH_3 peak in the ^{1}H-NMR spectrum since TBAP was significantly present in the product. Therefore, it was seen that purification was required for the samples with TBAP in order to get successful NMR results.

DME was used as the solvent in the rest of the experiments, since it was suspected that another reason of the problems in the reproducibility could be a reaction between acetonitrile and $LiAlH_4$. In the systems with DME and TBAP, the effects of electrode type, monomer/solvent ratio and reaction time were investigated. Each sample was purified with toluene. As a result, it was observed that in the large-scale synthesis with DME and TBAP, successful results were obtained when purified with toluene. In addition, it was seen that the properties of the products were less dependent on the monomer/solvent ratio and reaction time.

In the second part of the dissertation, polypropylene/silicon-based preceramic polymer blends were prepared by twin-screw extruder. Two different preceramic polymers were used in blend preparation: SMP-10, a commercial allylhydridopolycarbosilane, and PMSy, which was synthesized and characterized in the first part of the dissertation. In this part, the effects of these two polymers on the flammability, thermal and mechanical properties and morphologies of polypropylene based composites were investigated.

As a result of the flammability tests, it was seen that SMP-10 and PMSy were not effective flame retardants in small concentrations. In addition, it was observed that SMP-10, TPP and the metal complex provided a synergy and decreased the flammability of polypropylene by char promotion. Furthermore, it was concluded that PMSy was more effective than SMP-10 in polypropylene when it was used alone or with TPP. However, it was also observed that it did not provide a synergy with the metal complex like SMP-10. Therefore, PP/10SMP/5TPP/5M was the best flame retardant blend with a LOI value of 23.5%. The mechanism of flame retardancy of these silicon-based preceramic polymers was explained with the increase in char formation and the thermal stabilities of the composites. As a result, it was also concluded that at least 20 wt% of flame retardant was needed for effective flame retardation of PP.

As a result of the TGA test, it was seen that the addition of SMP-10 and PMSy significantly increased the average decomposition temperature and the char yield of the blends. PP/10SMP/5TPP/5M sample with the lowest flammability had the highest char yield proving the flame retardancy mechanism proposed for the silicon-based preceramic polymers. On the other hand, it was observed that the increase in the char yield with the addition of PMSy was not as high as SMP-10, however the increase in the average decomposition temperatures was very high. Therefore, it was concluded that increasing the thermal stability of the polymer composite is more significant than char promotion in the flame retardancy mechanism of PMSy. As a result of DSC, it was observed that there was no significant change in the melting points of the composites.

For the morphologies of the polymer blends, it was seen that with the addition of SMP-10 or PMSy in low amounts to polypropylene, there was no significant difference in the morphologies of the blends. However, with the addition of 10% SMP-10, the agglomerates of the polymers could be distinctively observed. The most interesting morphological results were obtained for the samples with SMP-10 and TPP showing inorganic crystalline structures. These structures were most probably due to an interaction between the two flame retardants since they were not observed for the blends with PMSy and TPP. As a conclusion, it was seen that the flame retardants were well dispersed in the matrix.

Finally, for the mechanical properties, it was seen that the addition of the silicon-based preceramic polymers in small amounts (1-5%) resulted in an increase in the tensile strength and elastic modulus of the polypropylene based composites. The best tensile results were generally obtained for PP/1SMP and PP/1PMS, most probably due to good dispersion in the polypropylene matrix. For the blends with 20 wt% additive, tensile strength, yield stress and elastic modulus of the composites decreased. For the elongation at break values, it was seen that the blends with 20 wt% flame retardant had higher elongation at break values, most probably due to the plasticizing effect of the additives. As a conclusion, it was observed that the high mechanical properties of polypropylene were kept, although significant amount of flame retardant was added to the polymer. For the impact properties, it was seen that impact resistance of the blends increased to a great extent with the addition of SMP-10, PMSy, TPP and the metal complex.

REFERENCES

[1] Jaschke B., Klingebiel U., Riedel R., Doslik N., Gadow R., “Cyclosilazanes and borazines: polymer precursors to silicon- and boron- containing ceramics”, Appl. Organometal. Chem., 2000, 14, 671-685

[2] Lichtenhan J.D., Gilman J.W., “Preceramic additives as fire retardants for plastics”, US Patent, 2002, US 6,362,279 B2

[3] Pitcher M.W., Joray S.J., Bianconi P.A., “Smooth continuous films of stoichiometric silicon carbide from poly(methylsilyne)”, Adv. Mater., 2004, 16(8), 706-709

[4] Richter R., Roewer G., Bohme U., Busch K., Babonneau F., Martin H.P., Muller E., “Organosilicon polymers – synthesis, architecture, reactivity and applications”, Appl. Organomet. Chem., 1997, 11(2), 71-106

[5] Miller R.D., Michl J., “Polysilane high polymers”, Chem. Rev., 1989, 89, 1359-1410

[6] Bianconi P.A., Weidman T.W., “Poly(n-hexylsilyne): Synthesis and properties of the first alkyl silicon $[RSi]_n$ network polymer”, J. Am. Chem. Soc., 1988, 110, 2342-2344

[7] Vermeulen L.A., Huang K., “Electrosynthesis of new polysilynes: poly(methylsilyne) and poly(cyclohexylsilyne-co-methylsilyne)”, Polymer, 2000, 41(2), 441-444

[8] Vermeulen L.A., Smith K., Wang J., “Electrochemical polymerization of alkyltrichlorosilane monomers to form branched Si backbone polymers”, Electrochimica Acta, 1999, 45, 1007-1014

[9] Watanabe A., Miike H., Tsutsumi Y., Matsuda M., “Photochemical properties of network and branched polysilanes”, Macromolecules, 1993, 26, 2111-2116

[10] Wilson W.L., Weidman T.W., “Excited-state dynamics of one- and two-dimensional σ-conjugated silicon frame polymers: dramatic effects of branching in a series of hexylsilyne-branched poly(hexylmethylsilylene) copolymers”, J. Phys. Chem., 1991, 95, 4568-4572

[11] Furukawa K., Fujino M., Matsumoto N., “Optical properties of silicon network polymers”, Macromolecules, 1990, 23, 3423-3426

[12] Bianconi P.A., Schilling F.C., Weidman T.W., “Ultrasound-mediated reductive condensation synthesis of silicon-silicon bonded network polymers”, Macromolecules, 1989, 22, 1697-1704

[13] Mazali C.A.I., Felisberti M.I.,”Vinyl ester resin modified with silicone-based additives. 2. Flammability properties”, J. Appl. Polym. Sci., 2006, 99, 644-649

[14] Li Q., Jiang P., Wei P., “Studies on the properties of polypropylene with a new silicon-containing intumescent flame retardant”, J. Polym. Sci.: Part B: Polym. Phys., 2005, 43, 2548-2556

[15] Zhang S., Horrocks R.A., “A review of flame retardant polypropylene fibres”, Prog. Polym. Sci., 2003, 28, 1517-1538

[16] Hshieh F., “Shielding effects of silica-ash layer on the combustion of silicones and their possible applications on the fire retardancy of organic polymers”, Fire Mater., 1998, 22, 69-76

[17] Lu S., Hamerton I., “Recent developments in the chemistry of halogen-free flame retardant polymers”, Prog. Polym. Sci., 2002, 27, 1661-1712

[18] Zaikov G.E., Lomakin S.M., “Ecological issue of polymer flame retardancy”, J. Appl. Polym. Sci., 2002, 86, 2449-2462

[19] Zaikov G.E., Lomakin S.M., “Polymer flame retardancy: a new approach”, J. Appl. Polym. Sci., 1998, 68, 715-725

[20] Marosi G., Marton A., Anna P., Bertalan G., Marosfoi B., Szep A., “Ceramic precursor in flame retardant systems”, Polym. Degrad. Stab., 2002, 77(2), 259-265

[21] Marosi G., Anna P., Marton A., Bertalan G., Bota A., Toth A., Mohai M., Racz I., “Flame-retarded polyolefin systems of controlled interphase”, Polym. Adv. Technol., 2002, 13, 1103-1111

[22] Marosi G., Bertalan G., Balogh I., Tohi A., “Silicone-containing intumescent flame retardant systems for polyolefins”, In: Flame retardants 96, London: Interscience Communications; 1996, 115-132

[23] Bolf A.G., Lichtenhan J.D., Am Chem Soc Polym Prepr, 1994, 35, 527-528

[24] Yajima S., Hayashi J., Omori M., “Continuous silicon carbide fiber of high tensile strength”, Chemistry Letters, 1975, 4(9), 931-934

[25] Yajima S., Okamura K., Hayashi J., “Structural analysis in continuous silicon carbide fiber of high tensile strength”, Chemistry Letters, 1975, 4(12), 1209-1212

[26] Yajima S., Okamura K., Hayashi J., Omori M., “Synthesis of continuous SiC fibers with high tensile strength”, J. Am. Ceram. Soc., 1976, 59(7-8), 324-327

[27] Pitcher M.W., “Advanced materials: the fabrication, characterization and study of novel ceramics and composites”, Ph.D. Thesis in Chemistry, University of Massachusetts Amherst, 2001

[28] Sandler S.R., Karo W., Bonesteel J., Pearce E.M., “Polymer synthesis and characterization – a laboratory manual”, Academic Press, San Diego, 1998

[29] “Nuclear magnetic resonance - Wikipedia, the free encyclopedia” (Internet, www) Address: http://en.wikipedia.org/wiki/NMR (Accessed: 15 June 2008)

[30] “Proton NMR - Wikipedia, the free encyclopedia” (Internet, www) Address: http://en.wikipedia.org/wiki/Proton_NMR (Accessed: 15 June 2008)

[31] “Fourier transform spectroscopy - Wikipedia, the free encyclopedia” (Internet, www)

Address: http://en.wikipedia.org/wiki/Fourier_transform_spectroscopy (Accessed: 15 June 2008)

[32] “Ultraviolet-visible spectroscopy - Wikipedia, the free encyclopedia” (Internet, www) Adress: http://en.wikipedia.org/wiki/Ultraviolet-visible_spectroscopy (Accessed: 10 June 2008)

[33] “Size exclusion chromatography - Wikipedia, the free encyclopedia” (Internet, www)
Adress: http://en.wikipedia.org/wiki/Gel_permeation_chromatography (Accessed: 10 June 2008)

[34] Brydson J.A., “Plastics materials”, 7th ed., Butterworth-Heinemann, Boston, 1999

[35] “Polypropylene - Wikipedia, the free encyclopedia” (Internet, www) Address: http://en.wikipedia.org/wiki/Polypropylene (Accessed: 15 June 2008)

[36] Wishman M., Hagler G.E., “Handbook of fire science and technology”, Fibre Chemistry, Vol. 5, Marcel Dekker Inc., New York, 1985

[37] Zhang H., “Fire safe polymers and polymer composites”, 2004, Final Report, DOT-FAA-AR-04-11

[38] Cullis C.F., Hirschler M., “The Combustion of Organic Polymers”, Clarendon Press, Oxford, 1981

[39] Lyon R.E., In International SAMPE Symposium and Exhibition (Proceedings), 1997, 42, 1325-1334.

[40] Green J., “Mechanisms for flame retardancy and smoke suppression – a review”, Journal of Fire Sciences, 1996, 14, 426-442

[41] Atkinson P.A., Haines P.J. and Skinner G.A., “Inorganic tin compounds as flame retardants and smoke suppressants for polyester thermosets”, Thermochim. Acta., 2000, 360, 29-44

[42] Hilado C.J., Flammability Handbook for Plastics, 3rd ed., Technomic Publication, Westport, CT, 1982

[43] Kashiwagi T., Gilman J.W., "Silicon-based flame retardants", Fire Retardancy of Polymeric Materials, Chapter 10, Marcel Dekker, Inc., New York, 2000, Edited by Grand A.F. and Wilkie C.A., pp. 353-389

[44] Jha N.K., Misra A.C., Bajai P., "Flame-retardant additives for polypropylene", J. Macromol. Sci. Chem., 1984, 24(1), 69–116

[45] Delobel R., Le Bras M., Ouassou N., Alistiqsa F., "Thermal behaviour of ammonium polyphosphate–pentaerythritol and ammonium pyrophosphate–pentaerythritol intumescent additives in polypropylene formulations", J. Fire Sci., 1990, 8, 85–108

[46] Delobel R., Ouassou N., Le Bras M. and Leroy J-M., "Fire retardance of polypropylene: action of diammonium pyrophosphate–pentaerythritol intumescent mixture", Polym. Degrad. Stab., 1989, 23, 349–357

[47] Brad D.G., Moberly C.W., Norell J.R., Walters H.C., "Intumescents: a novel effective approach to flame retarding polypropylene", J. Fire Retard. Chem., 1977, 4, 150–164

[48] Anna P., Marosi G.Y., Bourbigot S., Le Bras M., Delobel R., "Intumescent flame retardant systems of modified rheology", Polym. Degrad. Stab., 2002, 77(2), 243–247

[49] Mazali C.A.I, Felisberti M.I., "Vinyl ester resin modified with silicone-based additives. 1. Mechanical properties", J. Appl. Polym. Sci., 2006, 99, 2279-2287

[50] Ryan K.J, Lupton K.E., Pape P.G., John V.B., "Ultra-high-molecular-weight functional siloxane additives in polymers. Effects on processing and properties", Journal of Vinyl and Additive Technology, 2000, 6, 7-19

[51] Jayakody C., Nelson G.L., Sorathia U., Lewandowski S., "A Cone Calorimetric Study of Flame Retardant Elastomeric Polyurethanes Modified with Siloxanes and Commercial Flame Retardant Additives", 1998, J. Fire Sci., 16, 351–383

[52] Work W.J, Horie K., Hess M., Stepto R.F.T., “Definitions of terms related to polymer blends, composites and multiphase polymeric materials (IUPAC recommendations 2004)”, Pure Appl. Chem., 2004, 76(11), 1985-2007

[53] Rosen S.L., “Fundamental principles of polymeric materials”, 2nd ed., John Wiley & Sons, Inc., New York, 1993

[54] Simon G. P., “Polymer Characterization Techniques and Their Applications to Blends”, Oxford University Press, 2003

[55] Shackelford J.F., “Introduction to materials science for engineers”, 6th ed., Pearson Education, Inc., New Jersey, 2005

[56] “Charpy impact test - Wikipedia, the free encyclopedia” (Internet, www) Adress: http://en.wikipedia.org/wiki/Charpy_impact_test (Accessed: 15 June 2008)

[57] “Scanning electron microscope - Wikipedia, the free encyclopedia” (Internet, www)
Adress: http://en.wikipedia.org/wiki/Scanning_Electron_Microscope
(Accessed: 15 June 2008)

[58] “Limiting Oxygen Index ASTM D2863 – IDES The Plastics Web” (Internet, www)
Adress: http://www.ides.com/property_descriptions/ASTMD2863.asp
(Accessed: 20 June 2008)

[59]“Overview of Underwriter’s Laboratory UL94 Test for Flammability – Boedeker Plastics, Inc.” (Internet www)
Adress: http://www.boedeker.com/bpi-ul94.htm (Accessed: 20 June 2008)

[60] Hsiue G.H., Liu Y.L., Tsiao J., “Phosphorus-containing epoxy resins for flame retardancy V: synergistic effect of phosphorus-silicon on flame retardancy”, J. Appl. Polym. Sci., 1999, 78, 1-7

[61] Jang J., Kim J., Bae J.Y., “Synergistic effect of ferric chloride and silicon mixtures on the thermal stabilization enhancement of ABS”, Polymer Degradation and Stability, 2005, 90, 508-514

APPENDIX A

FTIR & ^{1}H-NMR RESULTS OF ALL LARGE-SCALE SYNTHESIS

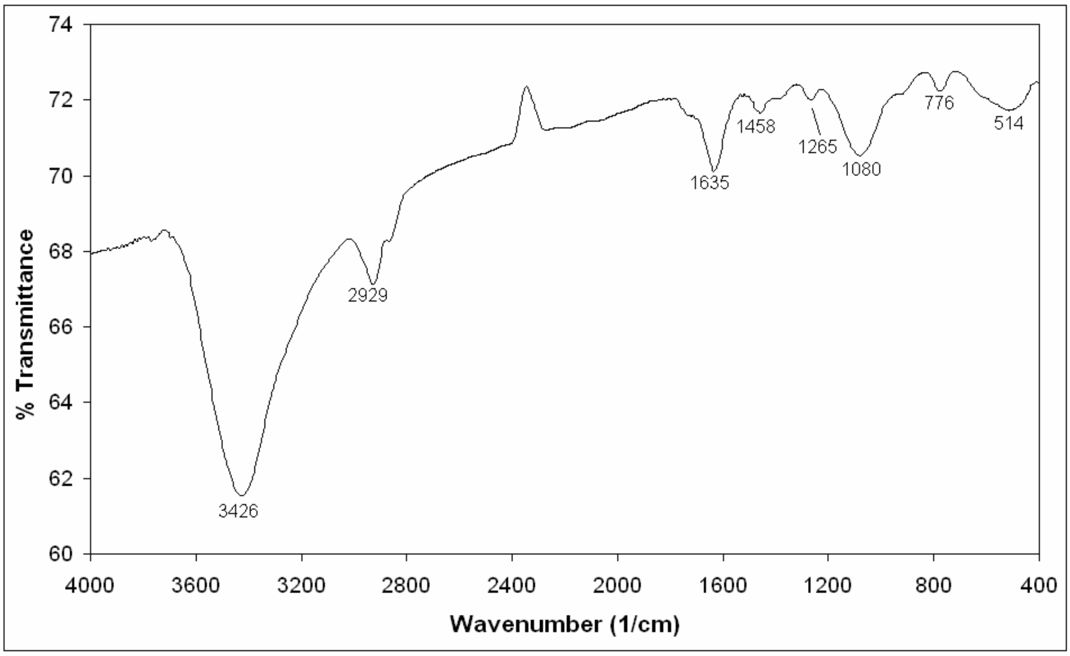

Figure A.1 FTIR spectrum of PMS2211 (THF solution on KBr film, cm^{-1}): 2929 (C-H, Si-CH_3); 1458, 1265 (C-H, Si-CH_3); 1080 (Si-O-Si); 776 (Si-C); 514 (Si-Cl)

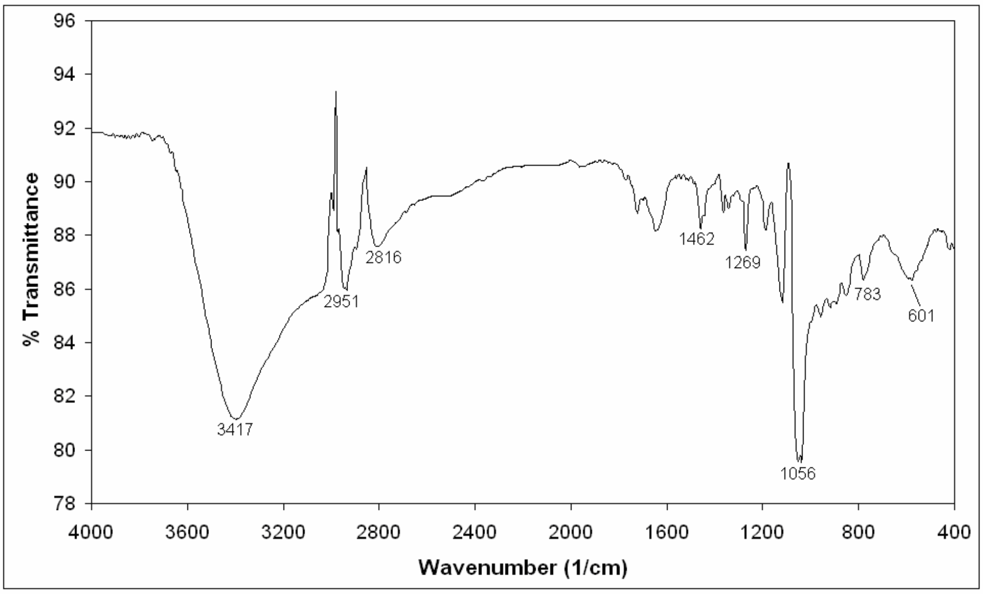

Figure A.2 FTIR spectrum of PMS2311 (THF solution on KBr film, cm^{-1}): 2951, 2816 (C-H, Si-CH_3); 1462, 1269 (C-H, Si-CH_3); 1056 (Si-O-Si); 783 (Si-C); 601 (Si-Cl)

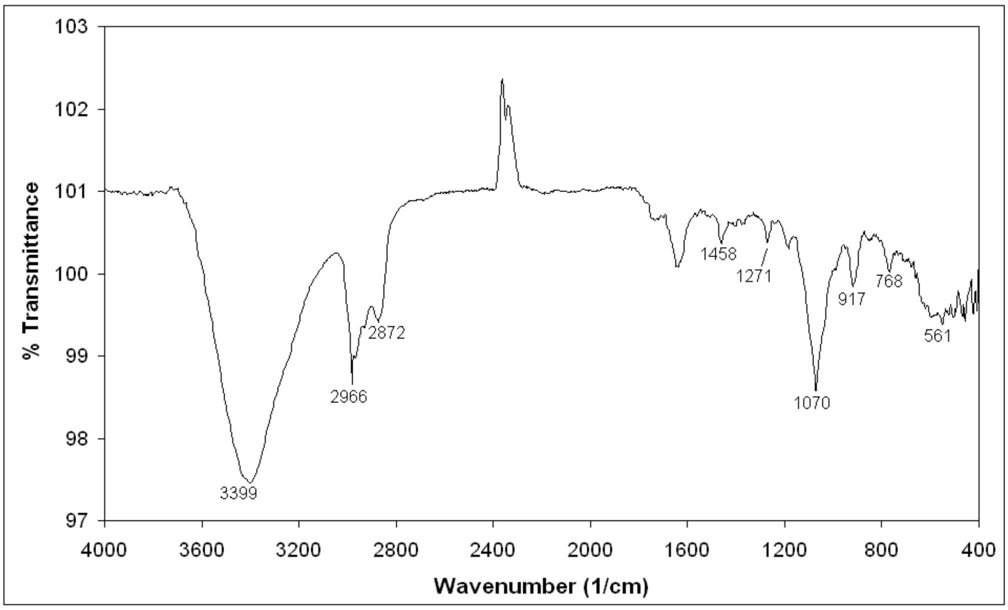

Figure A.3 FTIR spectrum of PMS2411 (THF solution on KBr film, cm^{-1}): 2966, 2872 (C-H, Si-CH_3); 1458, 1271 (C-H, Si-CH_3); 1070 (Si-O-Si); 917 (SiH_2); 768 (Si-C); 561 (Si-Cl)

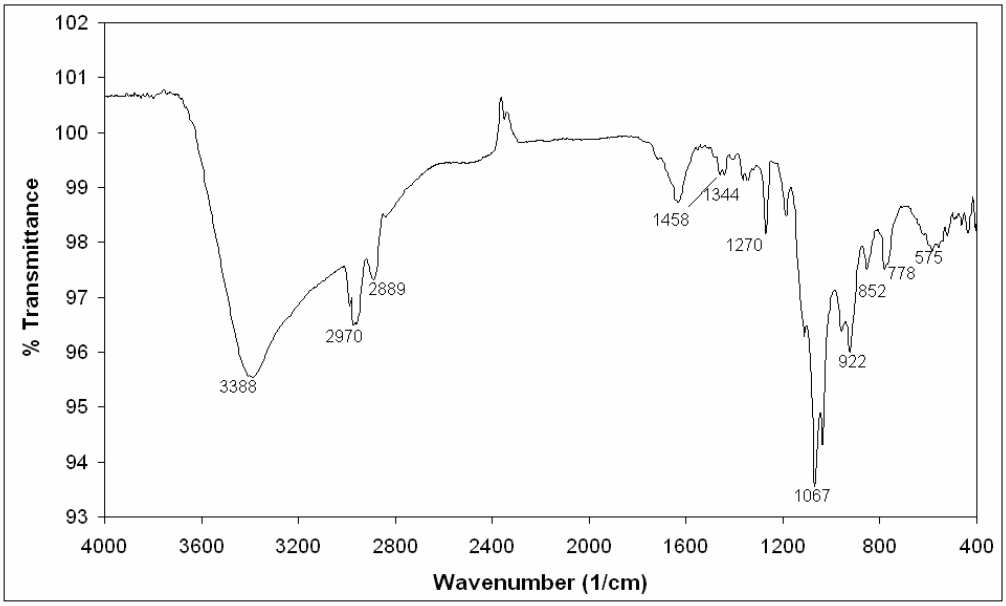

Figure A.4 FTIR spectrum of PMS2611 (THF solution on KBr film, cm^{-1}): 2970, 2889 (C-H, Si-CH_3); 1458, 1344, 1270 (C-H, Si-CH_3); 1067 (Si-O-Si); 922 (SiH_2); 852 (-CH_3); 778 (Si-C); 575 (Si-Cl)

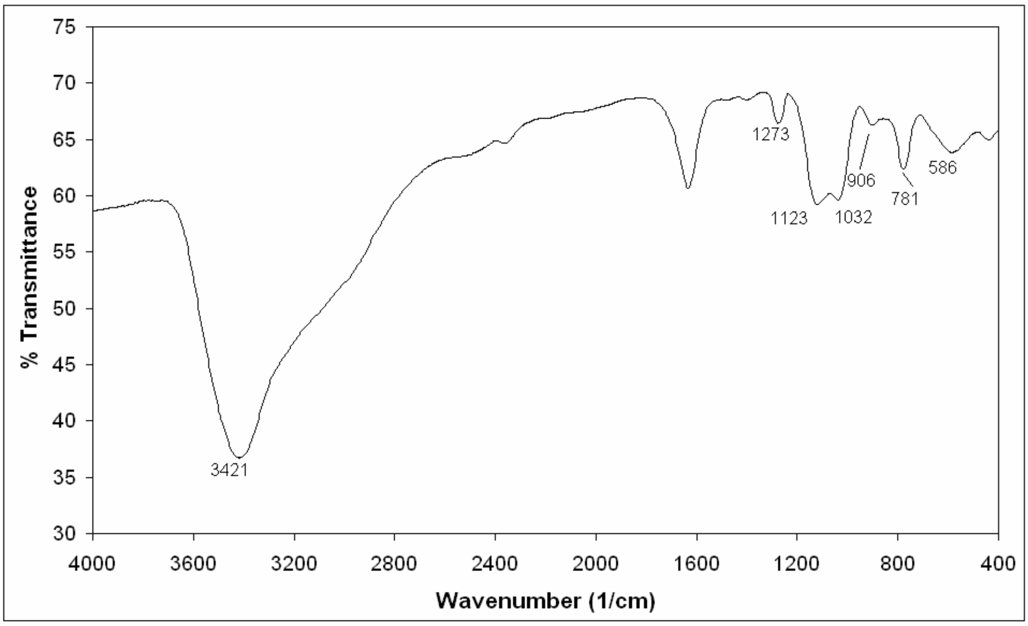

Figure A.5 FTIR spectrum of PMS2711 (THF solution on KBr film, cm^{-1}): 1273 (C-H, Si-CH_3); 1032 (Si-O-Si); 906 (SiH_2); 781 (Si-C); 586 (Si-Cl)

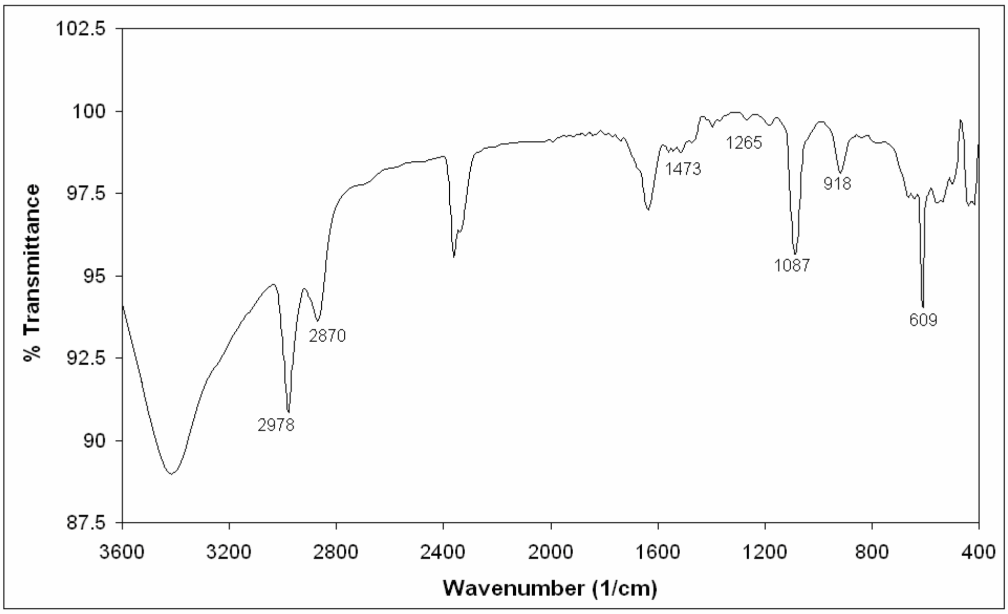

Figure A.6 FTIR spectrum of PMS0512 (THF solution on KBr film, cm^{-1}): 2978, 2870 (C-H, Si-CH_3); 1473, 1265 (C-H, Si-CH_3); 1087 (Si-O-Si); 918 (SiH_2); 609 (Si-Cl)

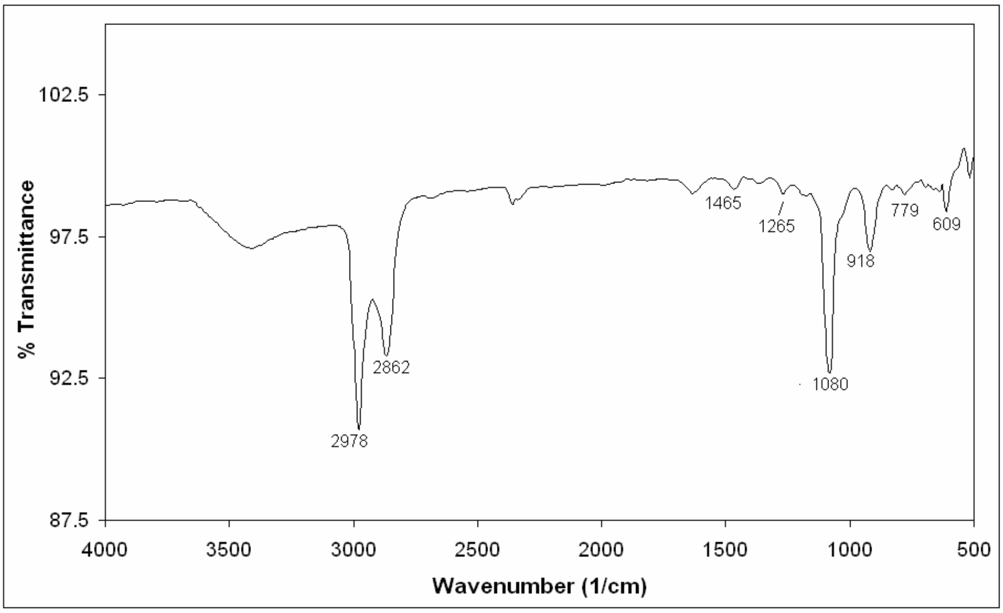

Figure A.7 FTIR spectrum of PMS0712 (THF solution on KBr film, cm^{-1}): 2978, 2862 (C-H, Si-CH_3); 1465, 1265 (C-H, Si-CH_3); 1080 (Si-O-Si); 918 (SiH_2); 779 (Si-C); 609 (Si-Cl)

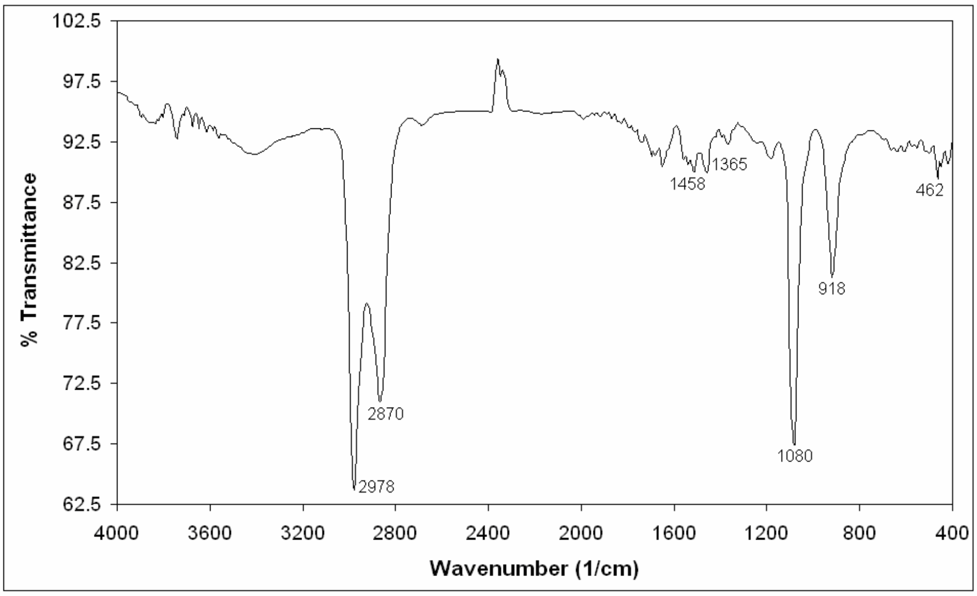

Figure A.8 FTIR spectrum of PMS1112 (THF solution on KBr film, cm^{-1}): 2978, 2870 (C-H, Si-CH_3); 1458, 1365 (C-H, Si-CH_3); 1080 (Si-O-Si); 918 (SiH_2); 462 (Si-Cl)

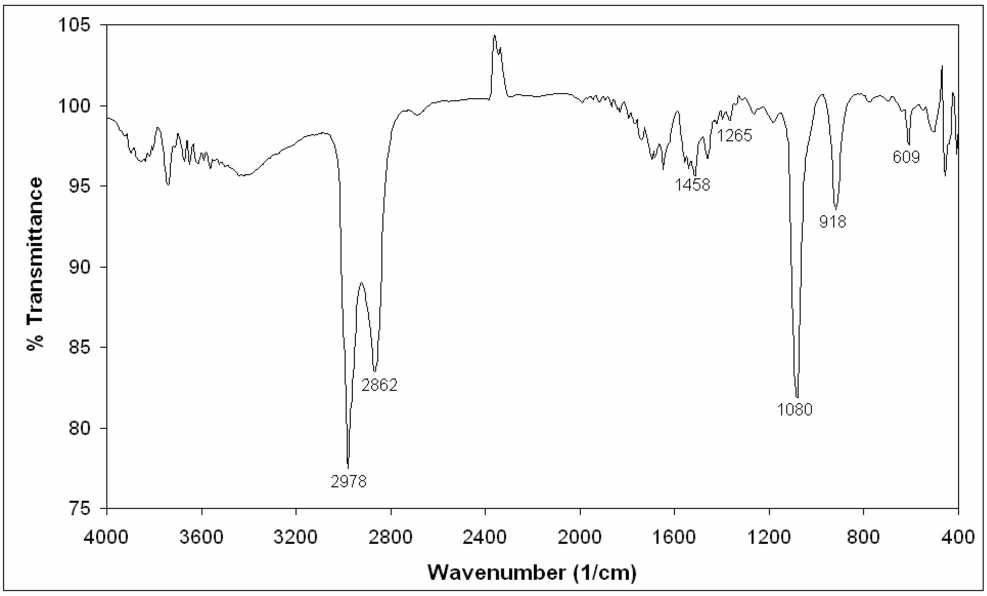

Figure A.9 FTIR spectrum of PMS1312 (THF solution on KBr film, cm^{-1}): 2978, 2862 (C-H, Si-CH_3); 1458, 1265 (C-H, Si-CH_3); 1080 (Si-O-Si); 918 (SiH_2); 609 (Si-Cl)

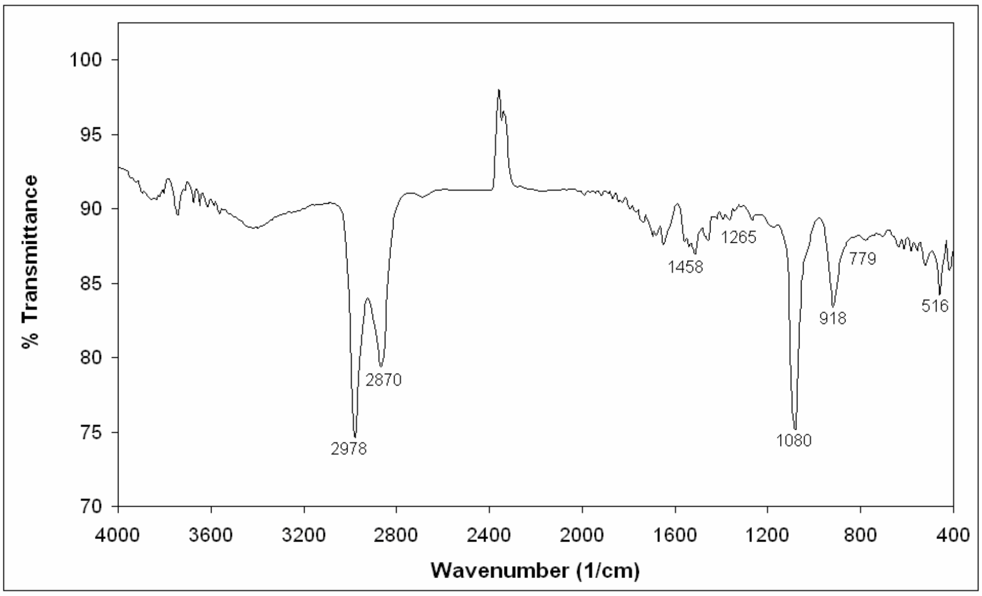

Figure A.10 FTIR spectrum of PMS1712 (THF solution on KBr film, cm^{-1}): 2978, 2870 (C-H, $Si-CH_3$); 1458, 1265 (C-H, $Si-CH_3$); 1080 (Si-O-Si); 918 (SiH_2); 779 (Si-C); 516 (Si-Cl)

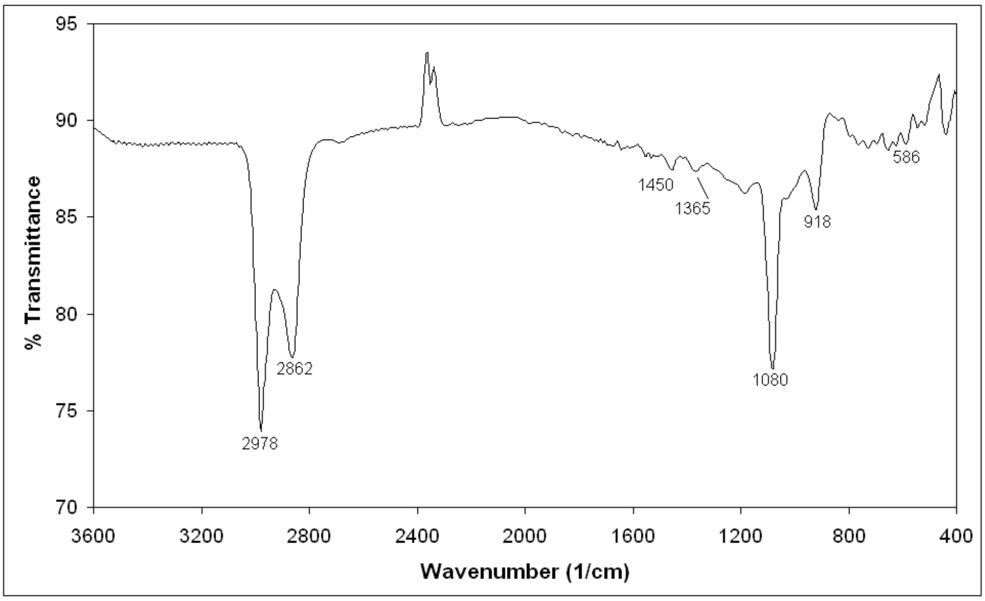

Figure A.11 FTIR spectrum of PMS1601 (THF solution on KBr film, cm^{-1}): 2978, 2862 (C-H, $Si-CH_3$); 1450, 1365 (C-H, $Si-CH_3$); 1080 (Si-O-Si); 918 (SiH_2); 586 (Si-Cl)

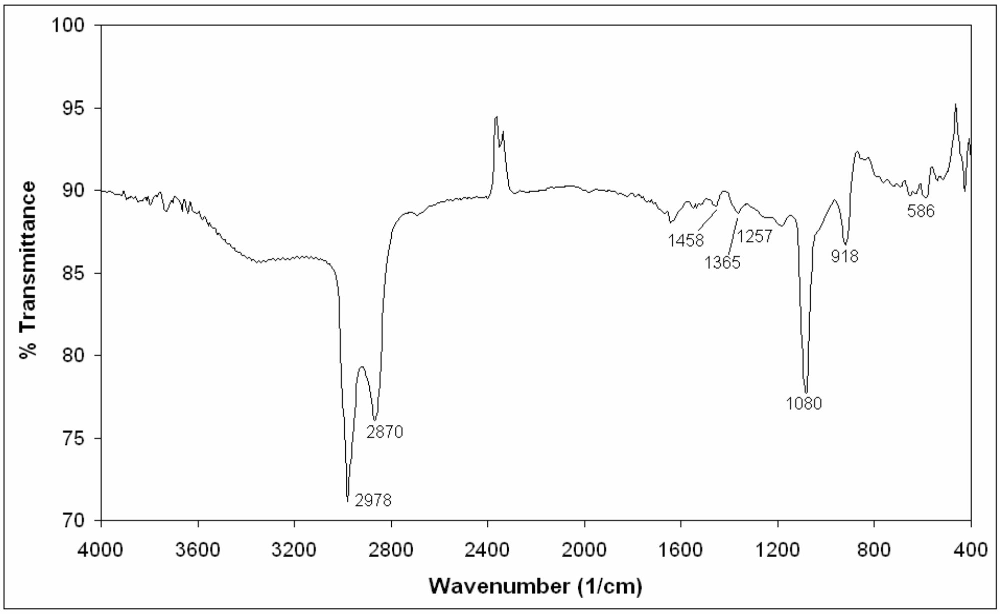

Figure A.12 FTIR spectrum of PMS1701 (THF solution on KBr film, cm^{-1}): 2978, 2870 (C-H, Si-CH_3); 1458, 1365, 1257 (C-H, Si-CH_3); 1080 (Si-O-Si); 918 (SiH_2); 586 (Si-Cl)

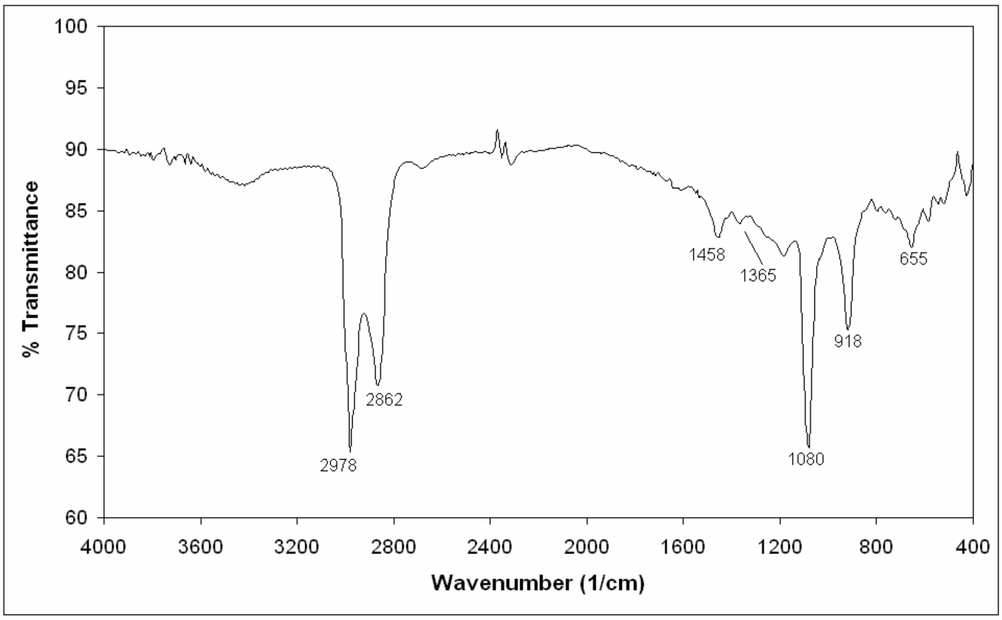

Figure A.13 FTIR spectrum of PMS2101 (THF solution on KBr film, cm^{-1}): 2978, 2862 (C-H, Si-CH_3); 1458, 1365 (C-H, Si-CH_3); 1080 (Si-O-Si); 918 (SiH_2); 655 (Si-C)

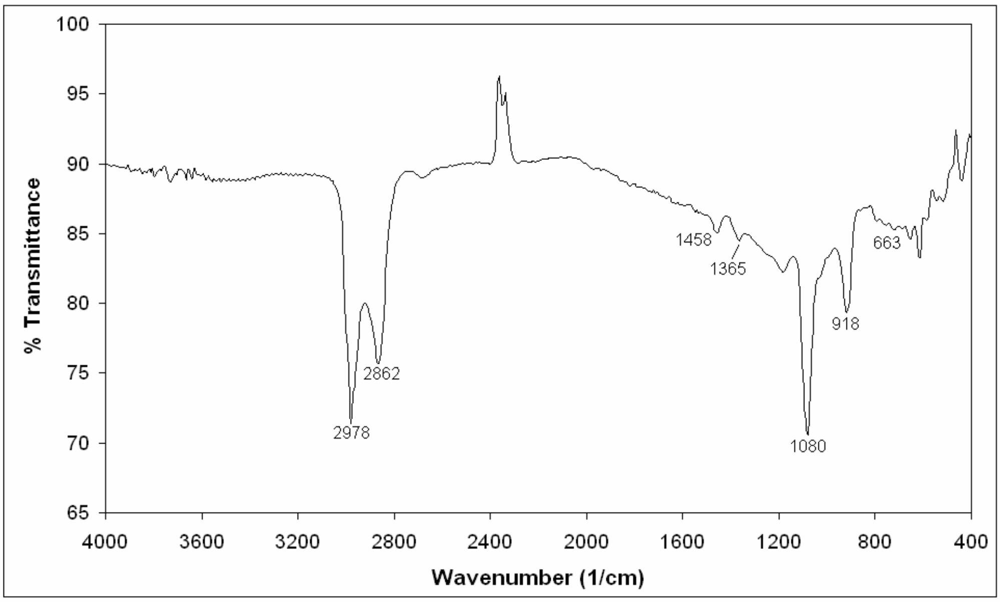

Figure A.14 FTIR spectrum of PMS2501 (THF solution on KBr film, cm^{-1}): 2978, 2862 (C-H, Si-CH_3); 1458, 1365 (C-H, Si-CH_3); 1080 (Si-O-Si); 918 (SiH_2); 663 (Si-C)

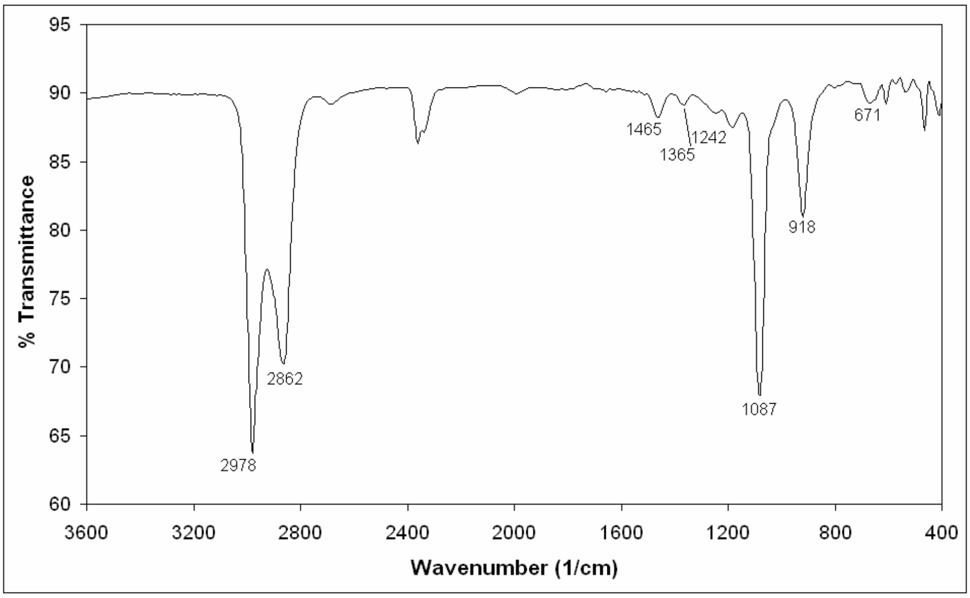

Figure A.15 FTIR spectrum of PMS0204TS (THF solution on KBr film, cm^{-1}): 2978, 2862 (C-H, Si-CH_3); 1465, 1365, 1242 (C-H, Si-CH_3); 1087 (Si-O-Si); 918 (SiH_2); 671 (Si-C)

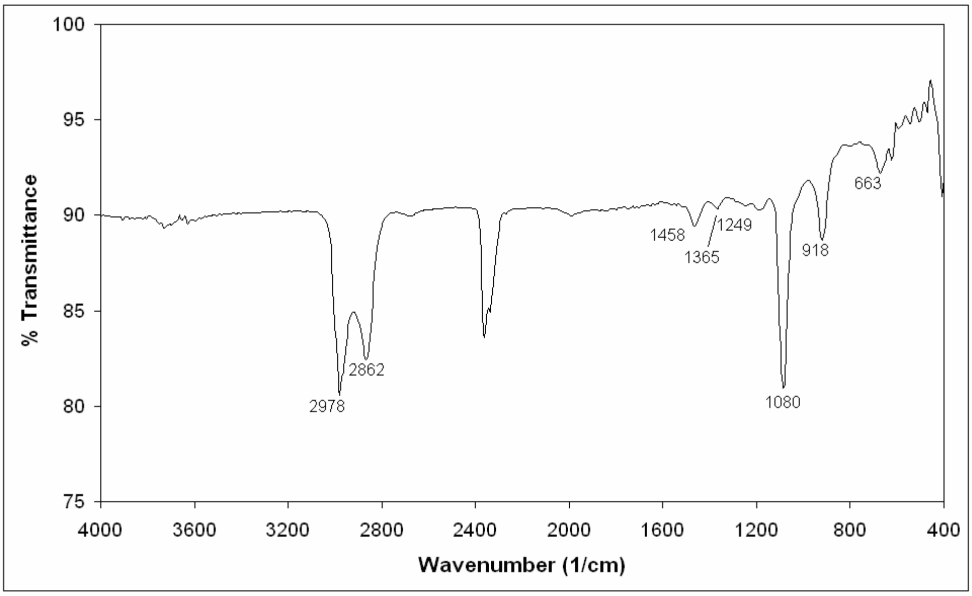

Figure A.16 FTIR spectrum of PMS0204TW (THF solution on KBr film, cm^{-1}): 2978, 2862 (C-H, $Si-CH_3$); 1458, 1365, 1249 (C-H, $Si-CH_3$); 1080 (Si-O-Si); 918 (SiH_2); 663 (Si-C)

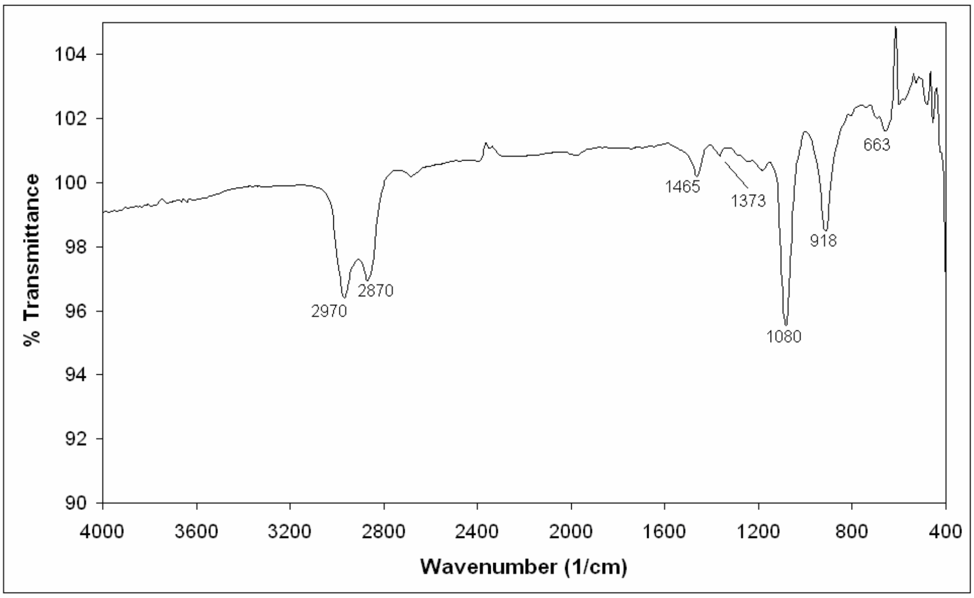

Figure A.17 FTIR spectrum of PMS1104TS (THF solution on KBr film, cm^{-1}): 2970, 2870 (C-H, $Si-CH_3$); 1465, 1373 (C-H, $Si-CH_3$); 1080 (Si-O-Si); 918 (SiH_2); 663 (Si-C)

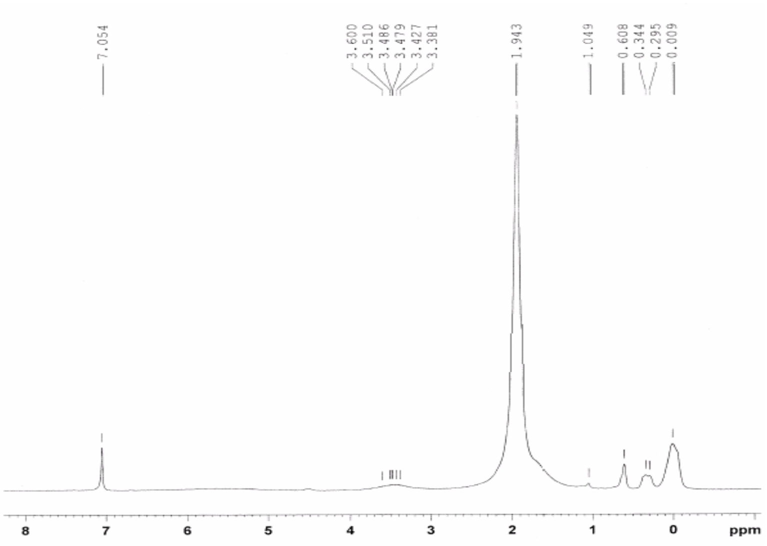

Figure A.18 ^{1}H-NMR result of PMS2211 ($CDCl_3$, δ ppm): 0.009 ppm ($Si\text{-}CH_3$); 1.943 ppm (Acetonitrile); 3.48 ppm (Si-H, $Si\text{-}H_2$); 7.054 (Chloroform)

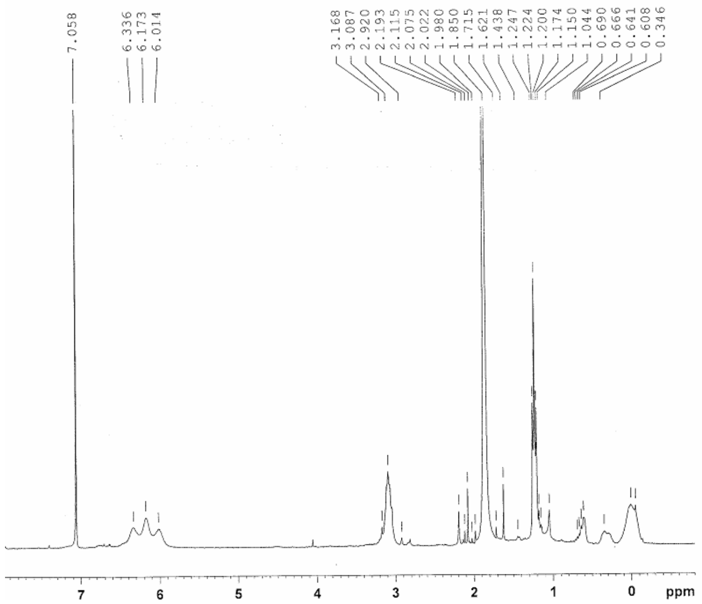

Figure A.19 ^{1}H-NMR result of PMS0512 ($CDCl_3$, δ ppm): 0.01 ppm ($Si\text{-}CH_3$); 1.980 ppm (Acetonitrile); 3.17 ppm (Si-H, $Si\text{-}H_2$); 7.058 (Chloroform)

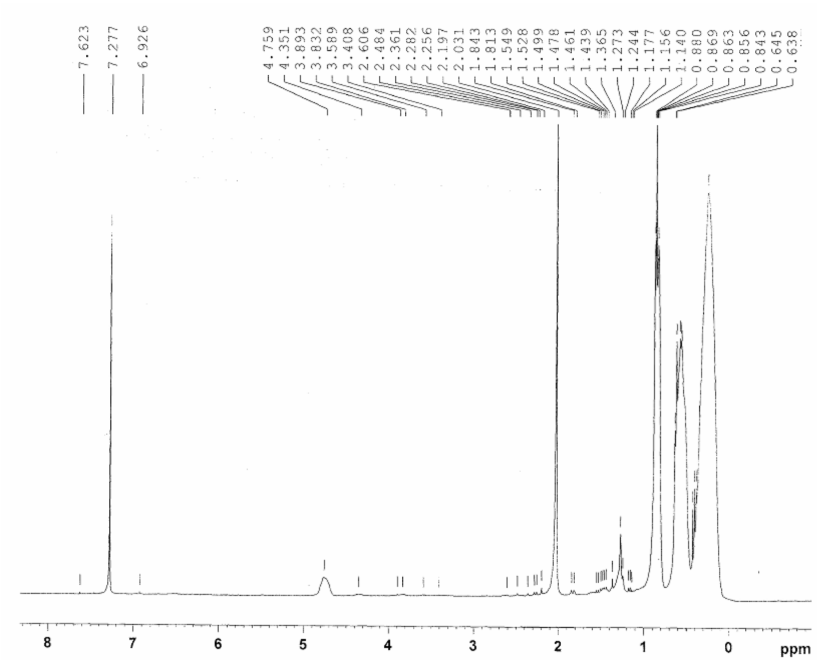

Figure A.20 ^{1}H-NMR result of PMS0712 ($CDCl_3$, δ ppm): 0-0.5 ppm (Si-CH_3); 2.03 ppm (Acetonitrile); 4.76 ppm (Si-H); 7.27 (Chloroform)

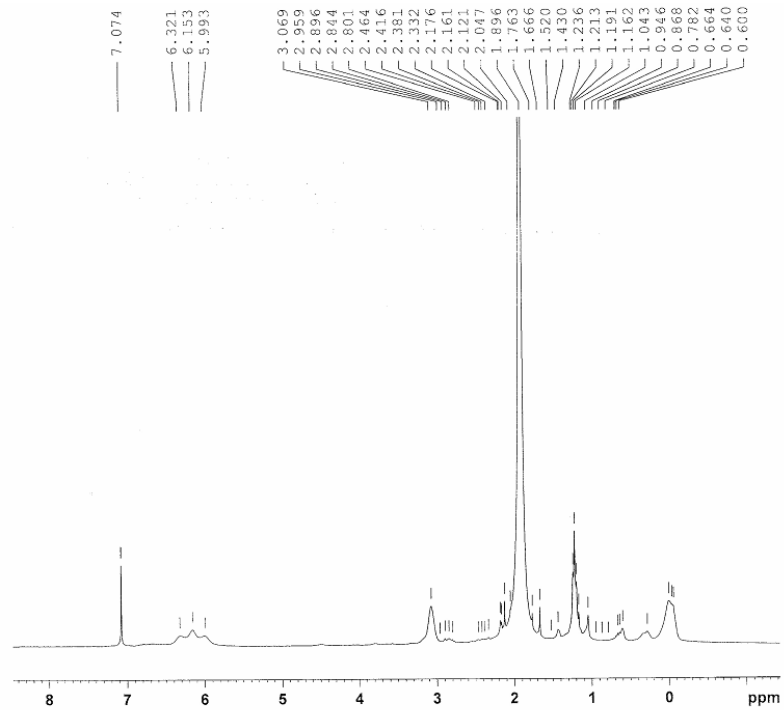

Figure A.21 ^{1}H-NMR result of PMS1112 ($CDCl_3$, δ ppm): 0.1 ppm (Si-CH_3); 1.896 ppm (Acetonitrile); 3.069 ppm (Si-H, Si-H_2); 7.074 (Chloroform)

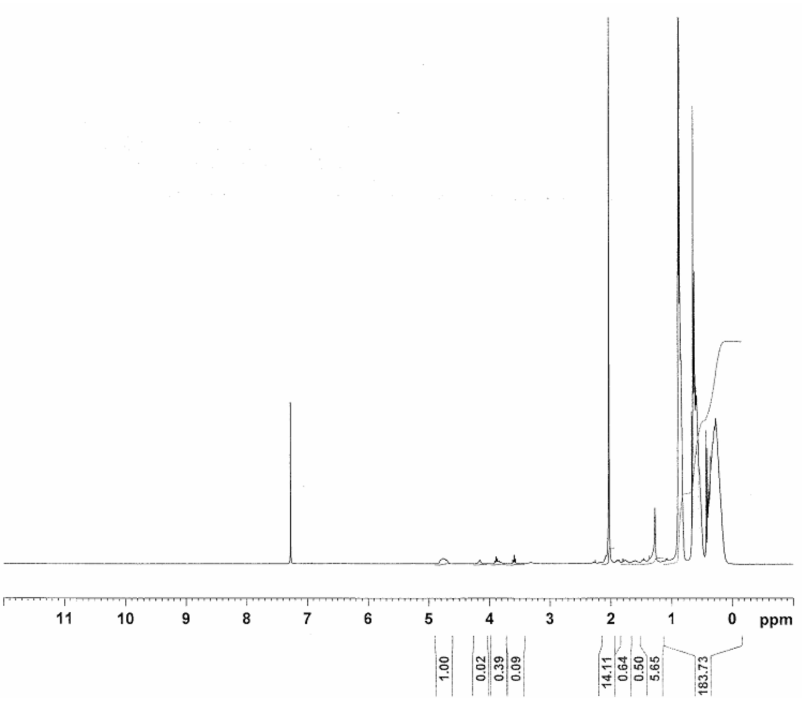

Figure A.22 ^{1}H-NMR result of PMS1312 ($CDCl_3$, δ ppm): 0-0.5 ppm (Si-CH_3); 2.031 ppm (Acetonitrile); 3.57 ppm (Si-H, Si-H_2); 7.278 (Chloroform)

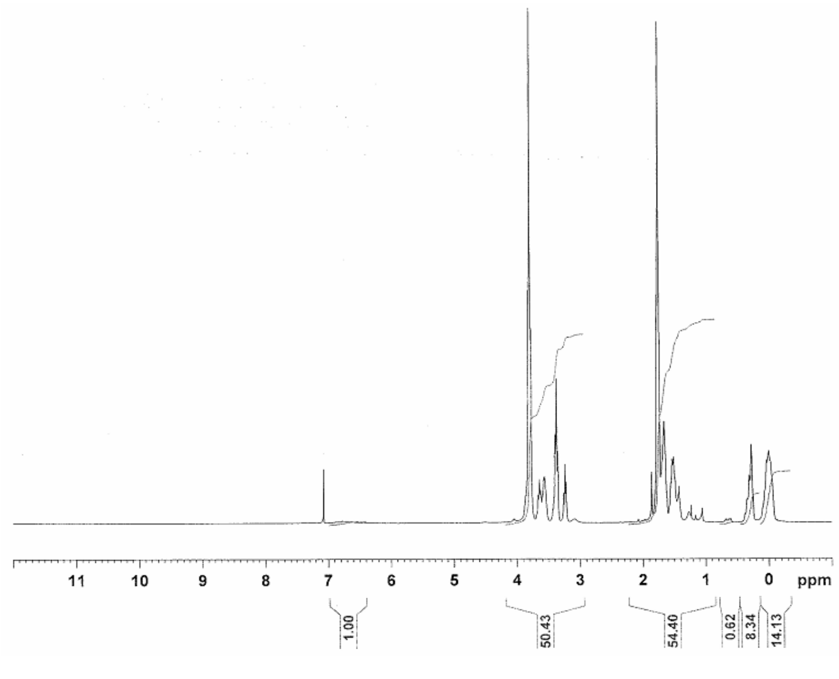

Figure A.23 ^{1}H-NMR result of PMS1712 ($CDCl_3$, δ ppm): 0.1 ppm (Si-CH_3); 1.80 ppm (Acetonitrile); 3.57 ppm (Si-H, Si-H_2); 7.1 (Chloroform)

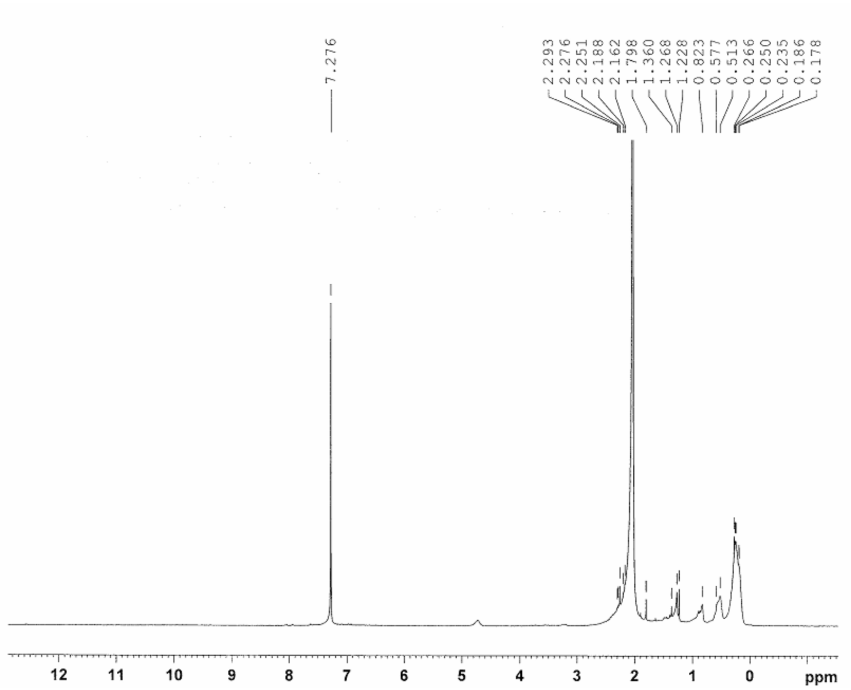

Figure A.24 ^{1}H-NMR result of PMS1601 ($CDCl_3$, δ ppm): 0.178 ppm (Si-CH_3); 2.00 ppm (Acetonitrile); 7.276 ppm (Chloroform)

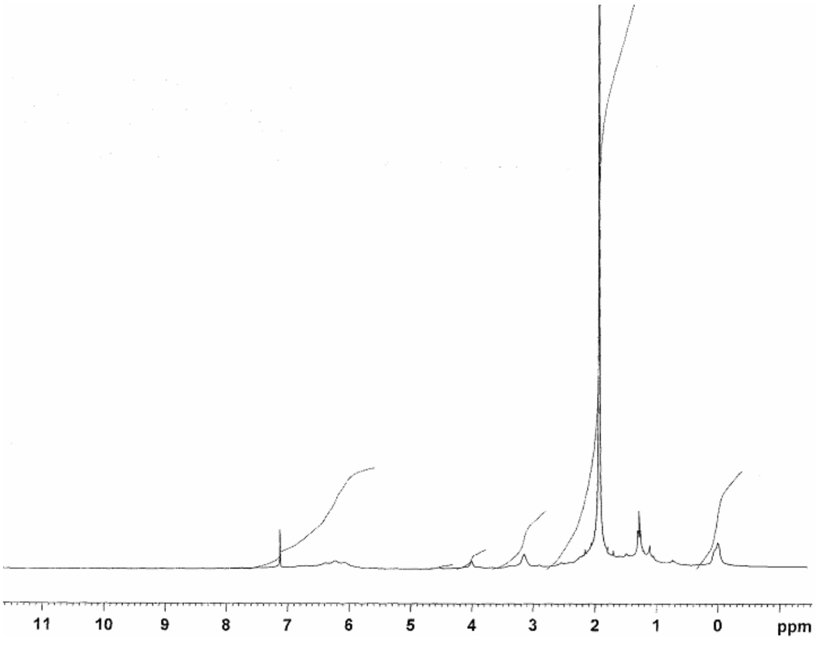

Figure A.25 ^{1}H-NMR result of PMS1701 ($CDCl_3$, δ ppm): 0.1 ppm (Si-CH_3); 1.93 ppm (Acetonitrile);3.2 ppm (Si-H, Si-H_2); 4.1 ppm (Si-H); 7.2 ppm (Chloroform)

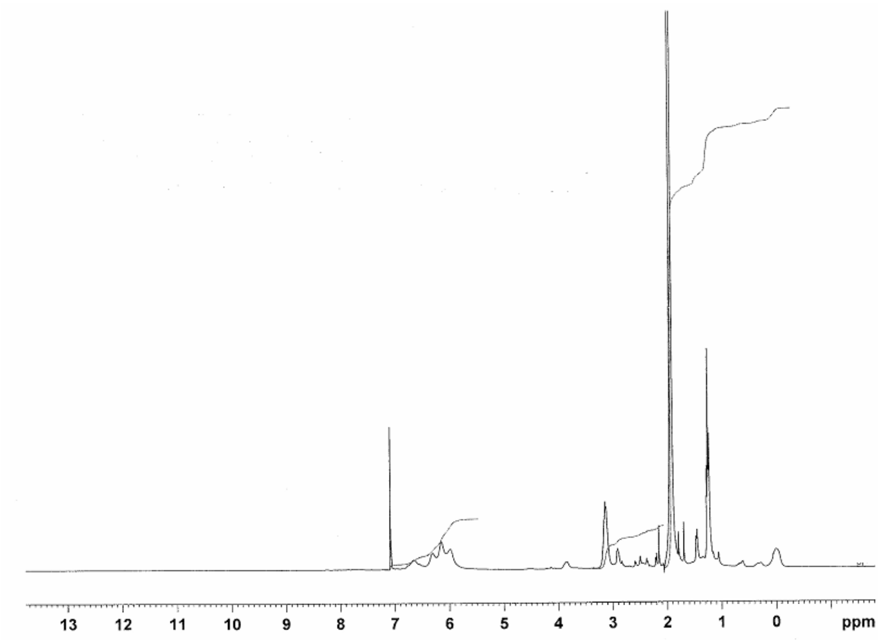

Figure A.26 ^{1}H-NMR result of PMS2101 ($CDCl_3$, δ ppm): 0.054 ppm ($Si-CH_3$); 1.995 ppm (Acetonitrile); 3.2 ppm (Si-H, $Si-H_2$); 7.075 ppm (Chloroform)

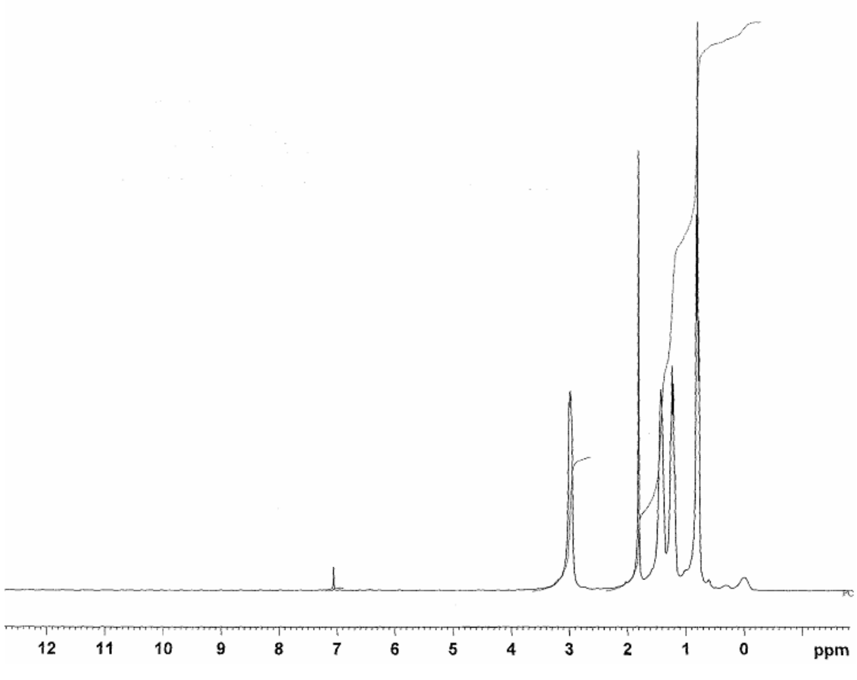

Figure A.27 ^{1}H-NMR result of PMS2501 ($CDCl_3$, δ ppm): 0.0 ppm ($Si-CH_3$); 0.5-1.6 ppm (TBAP); 1.804 ppm (Acetonitrile); 3.1 ppm (Si-H, $Si-H_2$); 7.058 ppm (Chloroform)

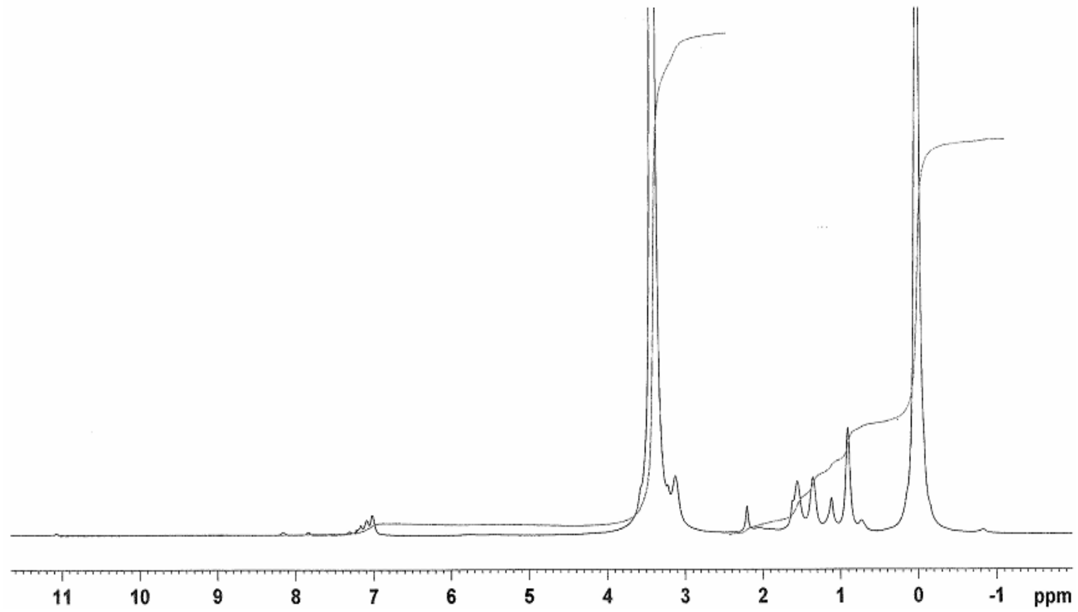

Figure A.28 ^{1}H-NMR result of PMS0204TS ($CDCl_3$, δ ppm): 0.1 ppm (Si-CH_3); 0.6-1.6 ppm (TBAP); 3.5 ppm (Si-OCH_3)

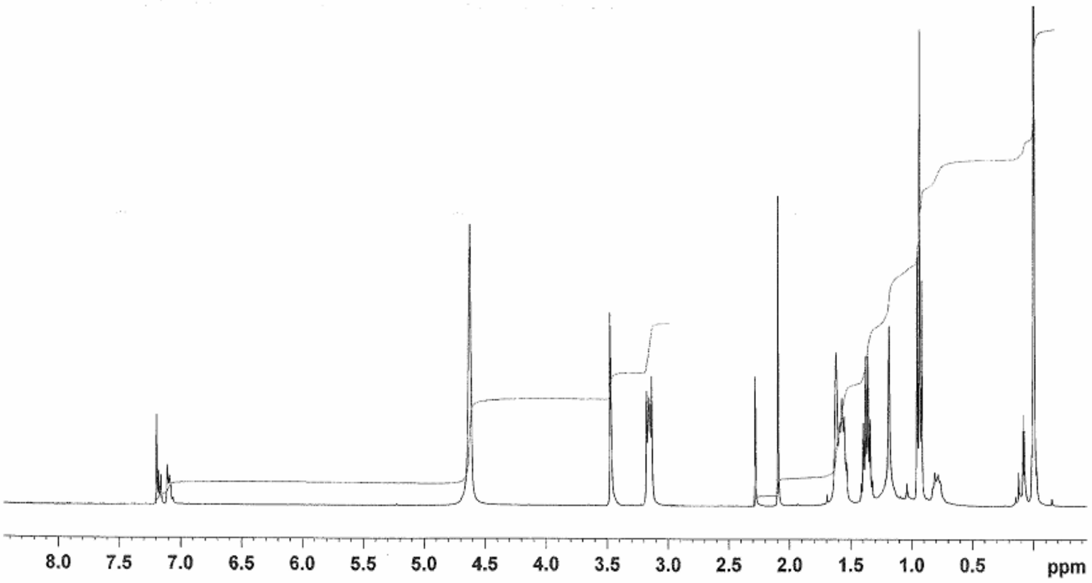

Figure A.29 ^{1}H-NMR result of PMS0204TW ($CDCl_3$, δ ppm): 0.5-1.6 ppm (TBAP); 3.2 ppm (Si-H, Si-H_2); 7.1 ppm (Toluene); 7.2 ppm (Chloroform)

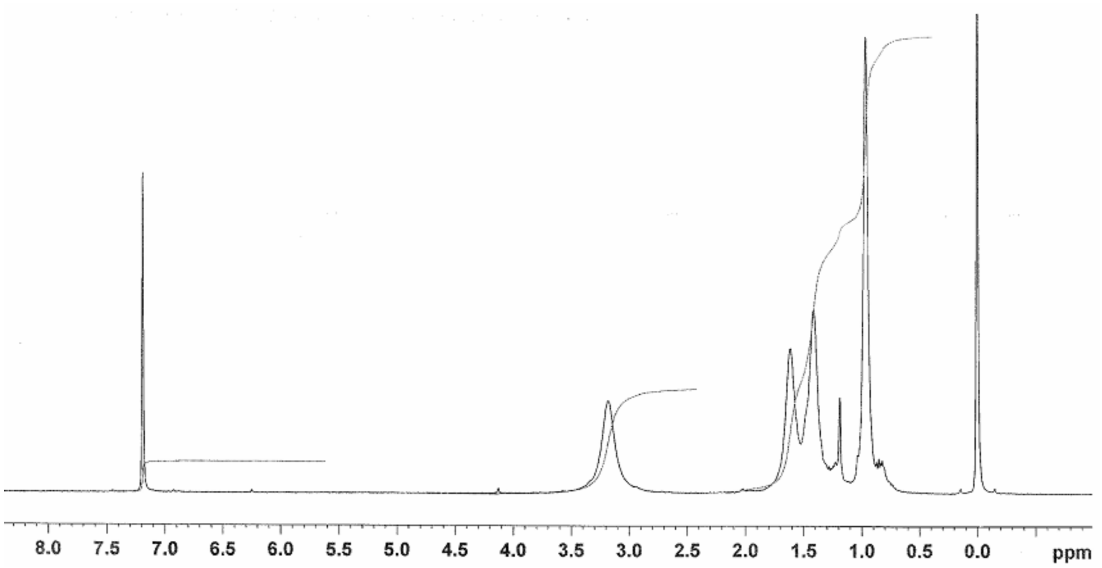

Figure A.30 ^{1}H-NMR result of PMS1104TS ($CDCl_3$, δ ppm): 0.5-1.6 ppm (TBAP); 3.3 ppm (Si-H, Si-H_2);;7.2 ppm (Chloroform)

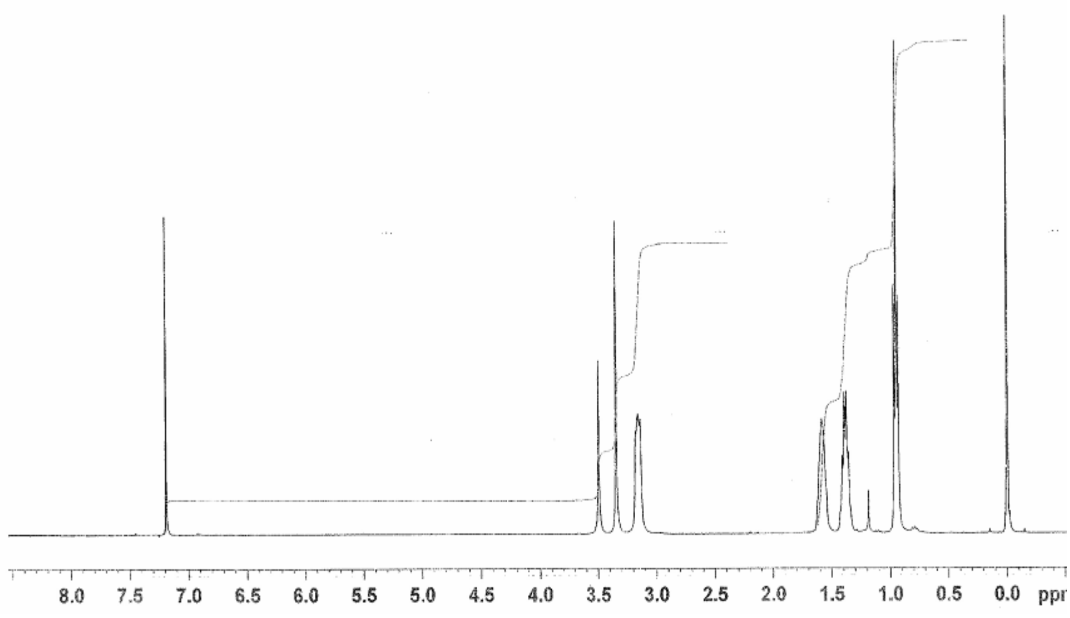

Figure A.31 ^{1}H-NMR result of PMS1405 ($CDCl_3$, δ ppm): 0.7-1.6 ppm (TBAP); 3.2 ppm (Si-H, Si-H_2); 3.4-3.5 ppm (DME); 7.2 ppm (Chloroform)

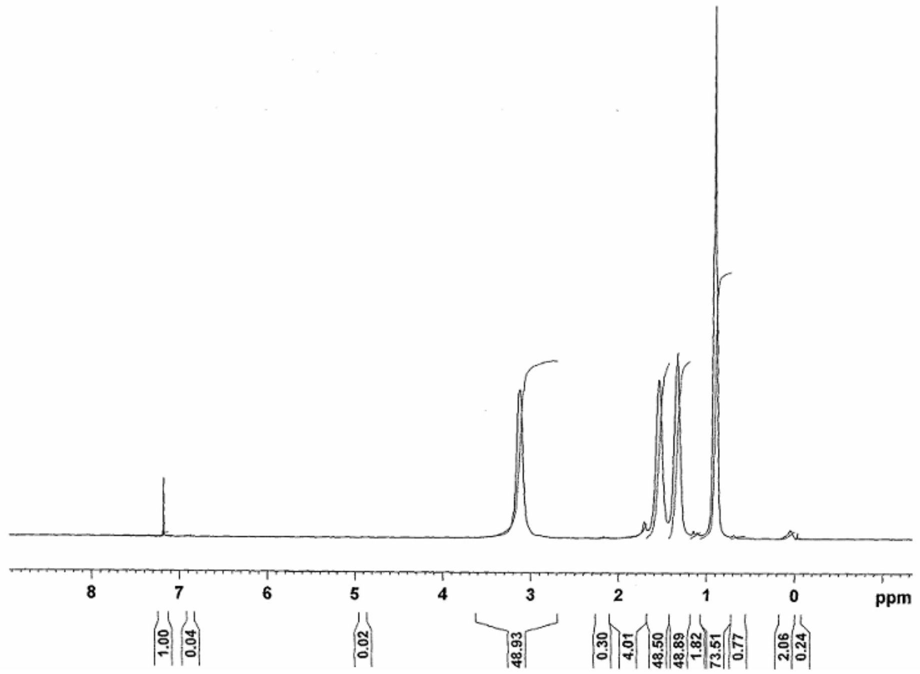

Figure A.32 ^{1}H-NMR result of PMS1405THF ($CDCl_3$, δ ppm): 0.9-1.7 ppm (TBAP); 3.1 ppm (Si-H, $Si-H_2$); 7.2 ppm (Chloroform)

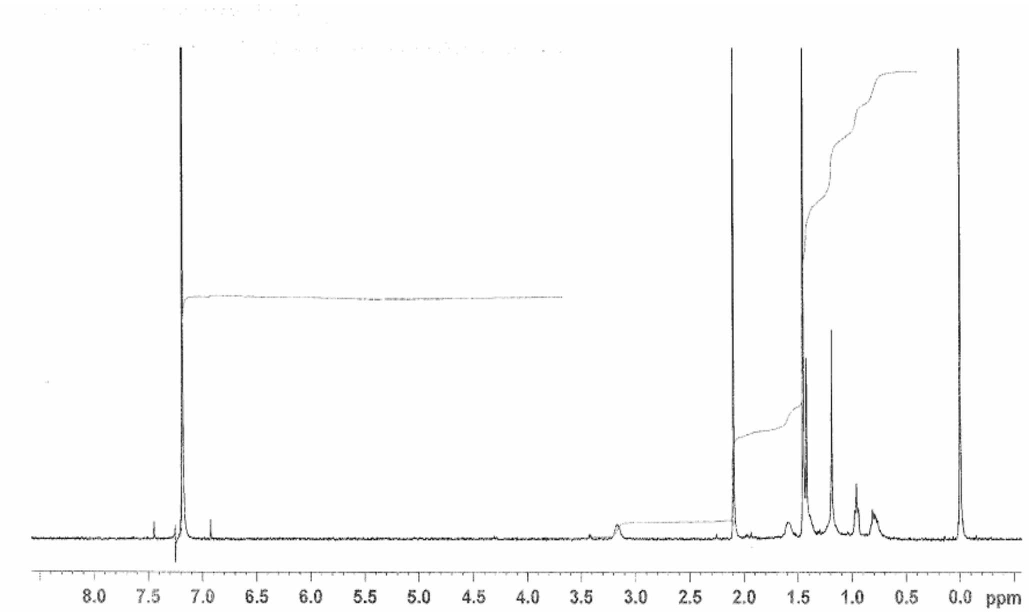

Figure A.33 ^{1}H-NMR result of PMS1405M ($CDCl_3$, δ ppm): 0.7-1.6 ppm (TBAP); 3.1 ppm (Si-H, $Si-H_2$); 7.2 ppm (Chloroform)

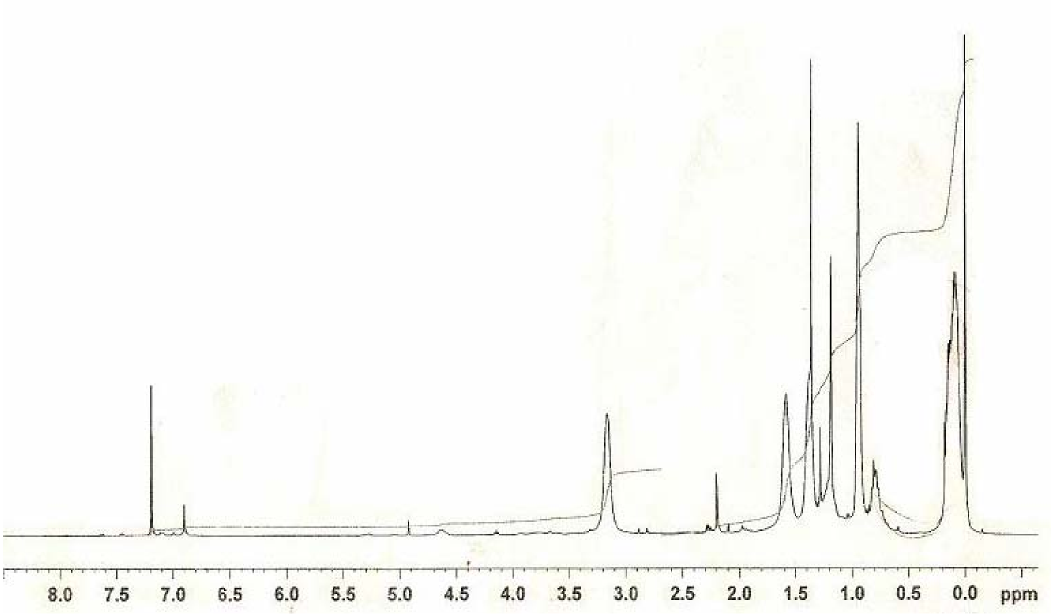

Figure A.34 ^{1}H-NMR result of PMS1405TS ($CDCl_3$, δ ppm): 0-0.3 ppm (Si-CH_3); 0.6-1.6 ppm (TBAP); 3.2 ppm (Si-H, Si-H_2); 4.65 ppm (Si-H); 7.2 ppm (Chloroform)

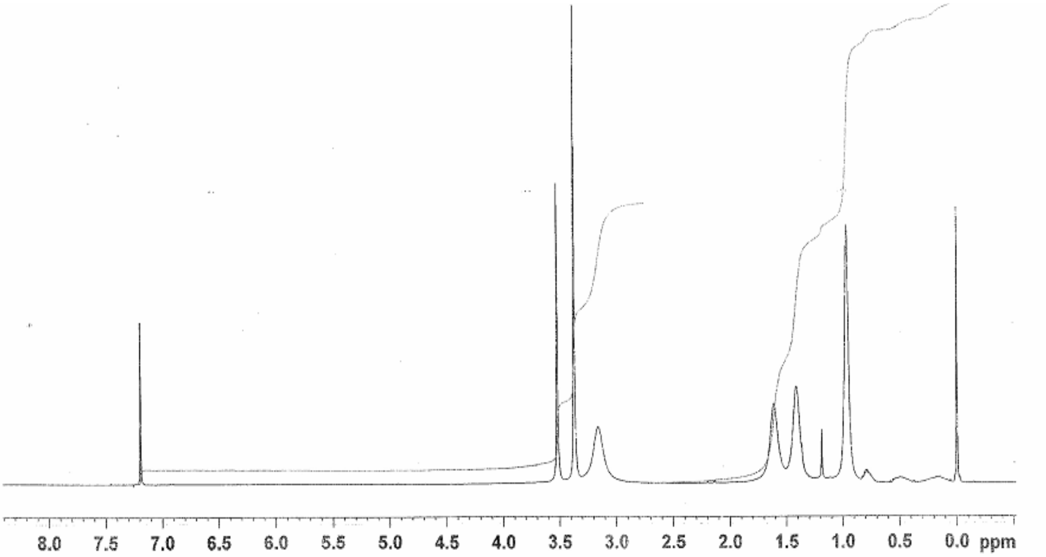

Figure A.35 ^{1}H-NMR result of PMS1505 ($CDCl_3$, δ ppm): 0.5-1.6 ppm (TBAP); 3.4-3.5 ppm (DME); 7.2 ppm (Chloroform)

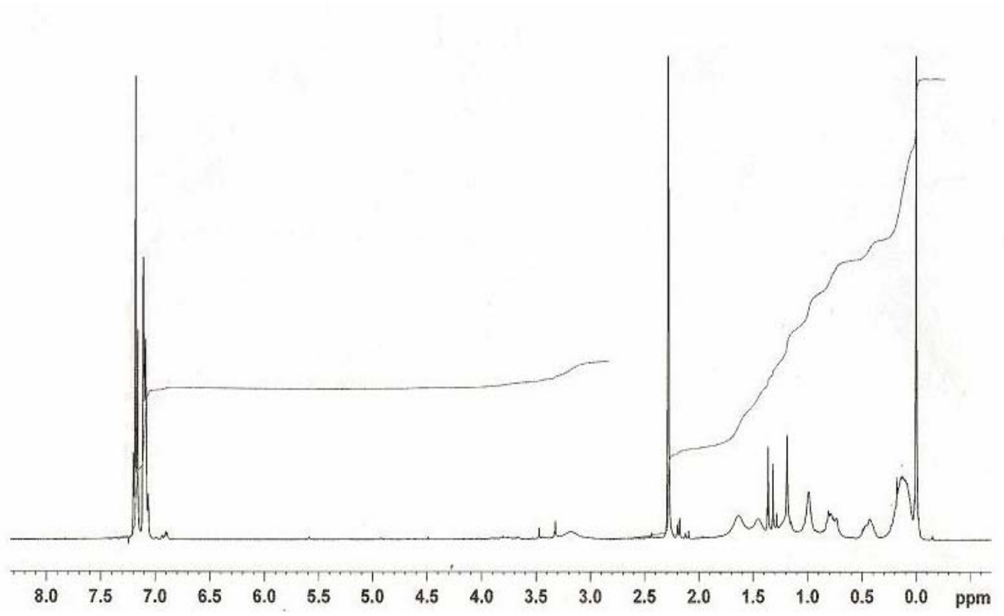

Figure A.36 ^{1}H-NMR result of PMS1505TS ($CDCl_3$, δ ppm): 0-0.3 ppm ($Si-CH_3$); 0.5-1.6 ppm (TBAP); 3.2 ppm (Si-H, $Si-H_2$); 7.1 ppm (Toluene); 7.2 ppm (Chloroform)

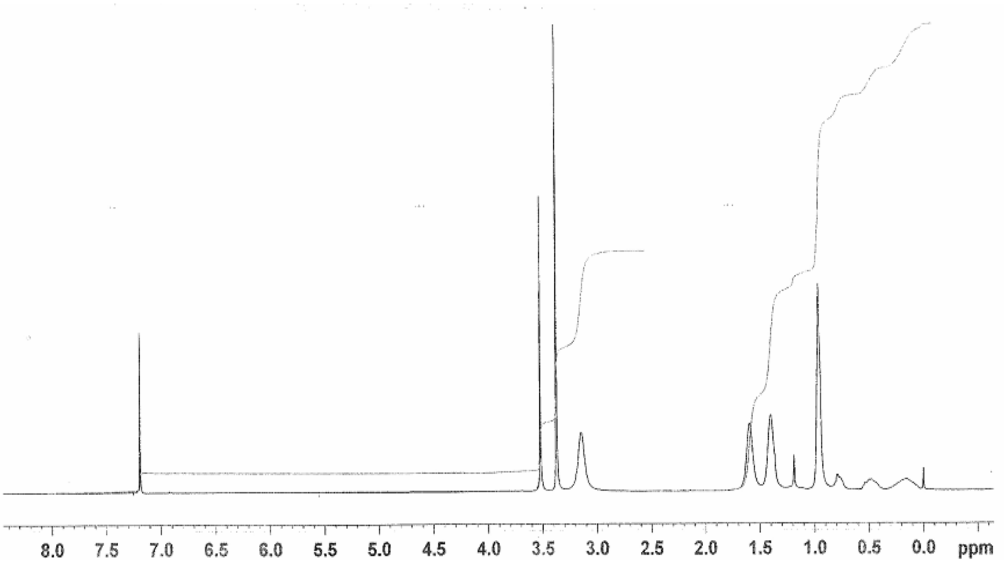

Figure A.37 ^{1}H-NMR result of PMS1605 ($CDCl_3$, δ ppm): 0-0.3 ppm ($Si-CH_3$); 0.5-1.6 ppm (TBAP); 3.2 ppm (Si-H, $Si-H_2$); 3.4-3.5 ppm (DME); 7.2 ppm (Chloroform)

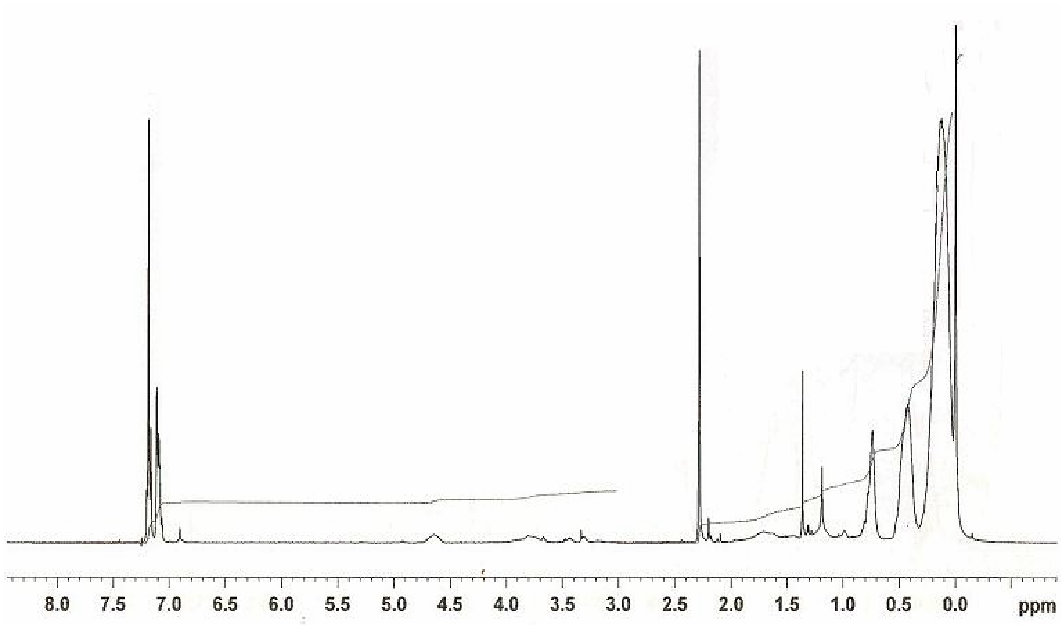

Figure A.38 ^{1}H-NMR result of PMS1605TS ($CDCl_3$, δ ppm): 0-0.4 ppm (Si-CH_3); 0.5-1.6 ppm (TBAP); 7.1 ppm (Toluene); 7.2 ppm (Chloroform)

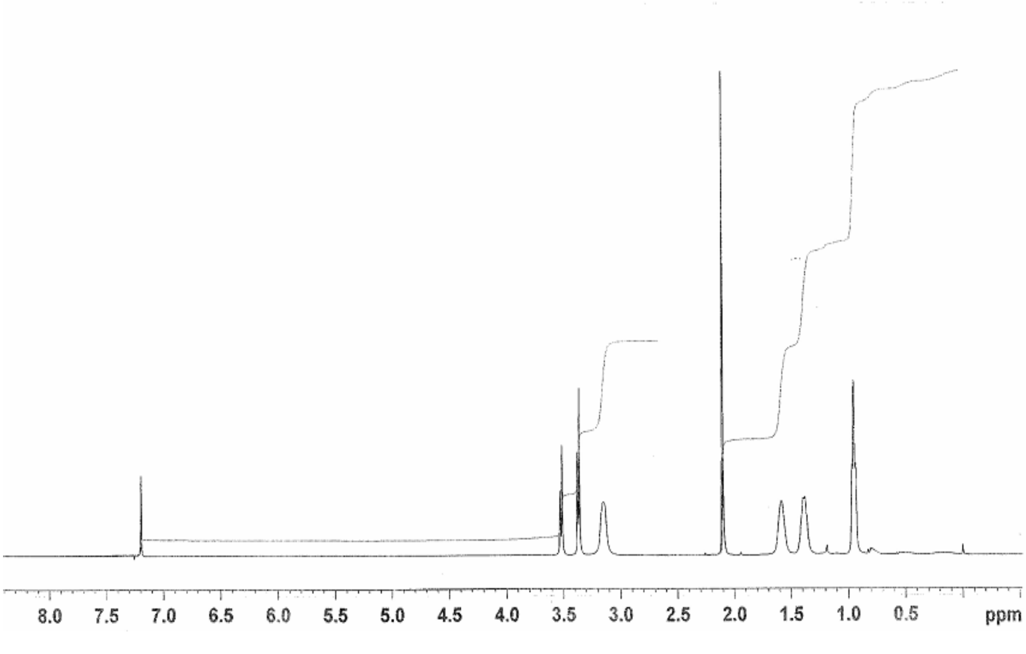

Figure A.39 ^{1}H-NMR result of PMS1905 ($CDCl_3$, δ ppm): 0.7-1.6 ppm (TBAP); 3.2 ppm (Si-H, Si-H_2); 3.4-3.5 ppm (DME); 7.2 ppm (Chloroform)

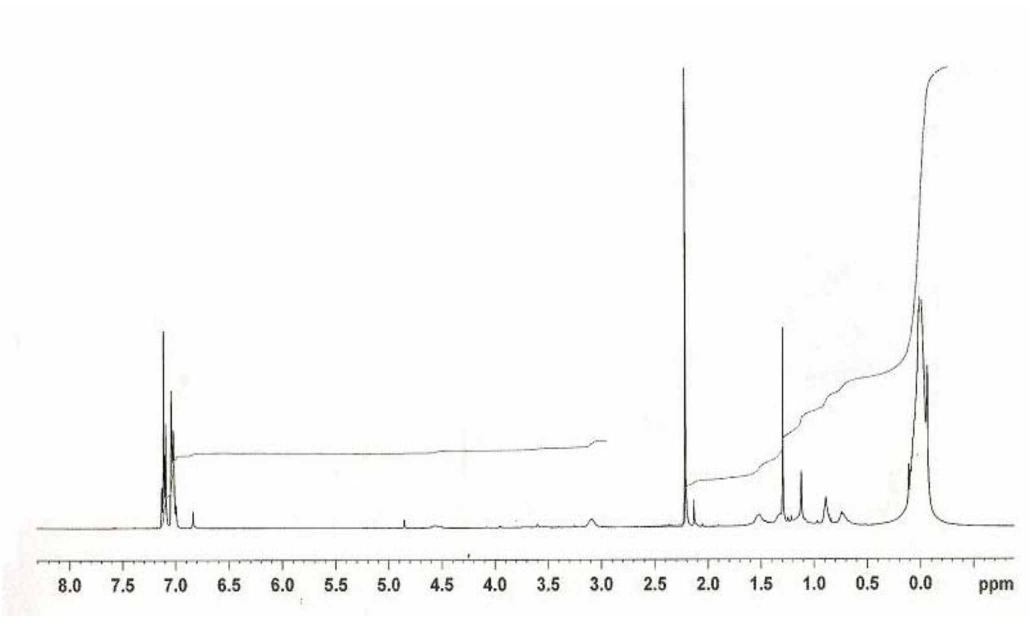

Figure A.40 ^{1}H-NMR result of PMS1905TS ($CDCl_3$, δ ppm): 0-0.3 ppm (Si-CH_3); 0.6-1.6 ppm (TBAP); 3.2 ppm (Si-H, Si-H_2); 7.1 ppm (Toluene); 7.2 ppm (Chloroform)

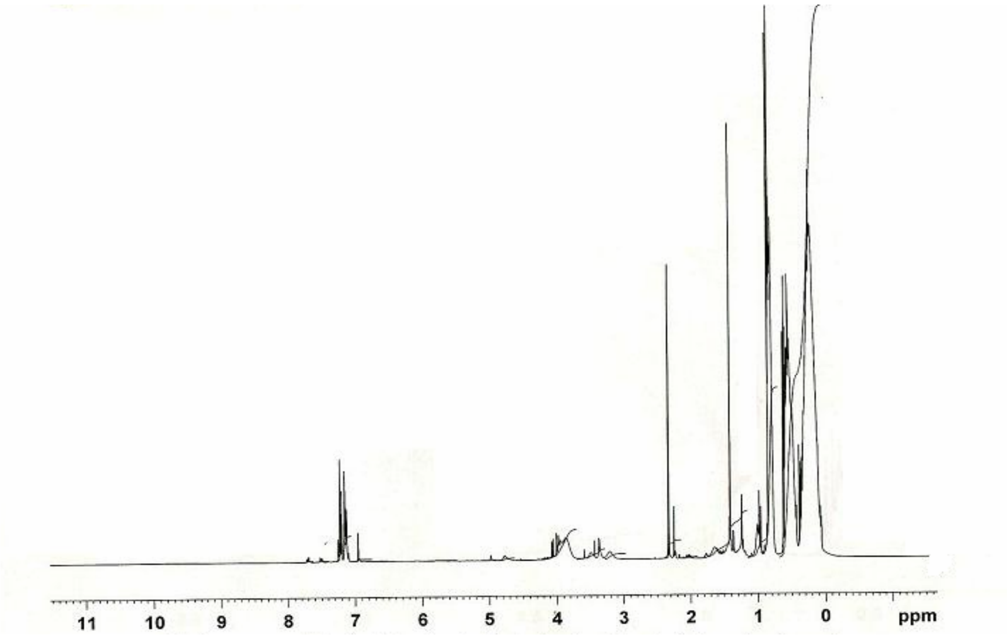

Figure A.41 ^{1}H-NMR result of PMS0506TS ($CDCl_3$, δ ppm): 0-0.4 ppm (Si-CH_3); 0.6-1.7 ppm (TBAP); 7.1 ppm (Toluene); 7.2 ppm (Chloroform)

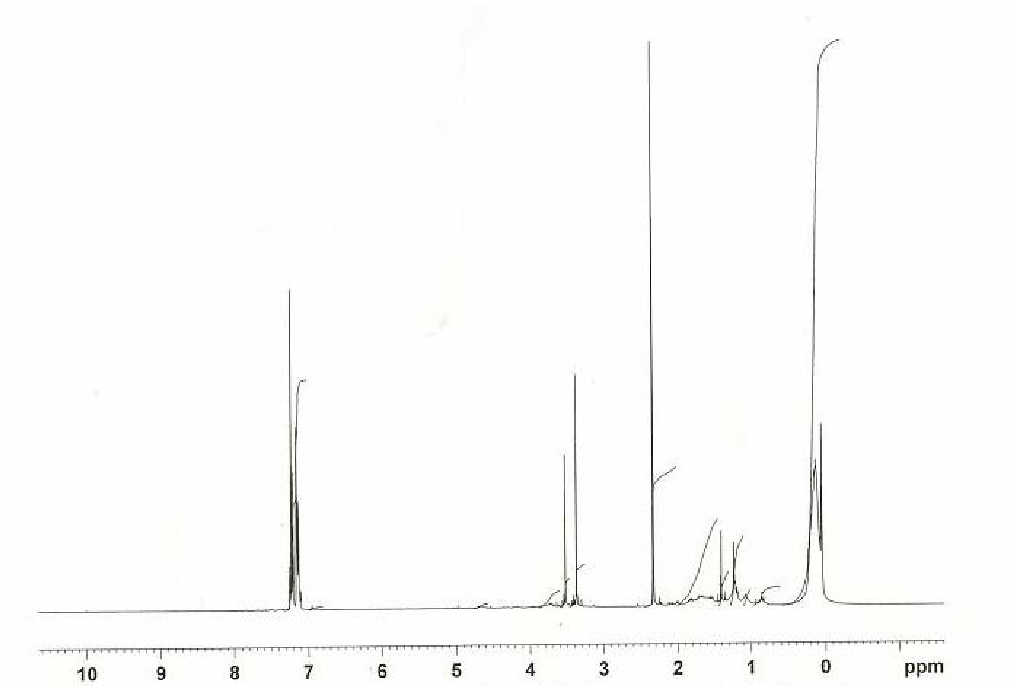

Figure A.42 ^{1}H-NMR result of PMS0606TS ($CDCl_3$, δ ppm): 0-0.3 ppm ($Si-CH_3$); 0.8-1.7 ppm (TBAP);3.4-3.5 ppm (DME); 7.1 ppm (Toluene); 7.2 ppm (Chloroform)

APPENDIX B

TGA & DSC CURVES OF PP/SMP-10 AND PP/PMSy BLENDS

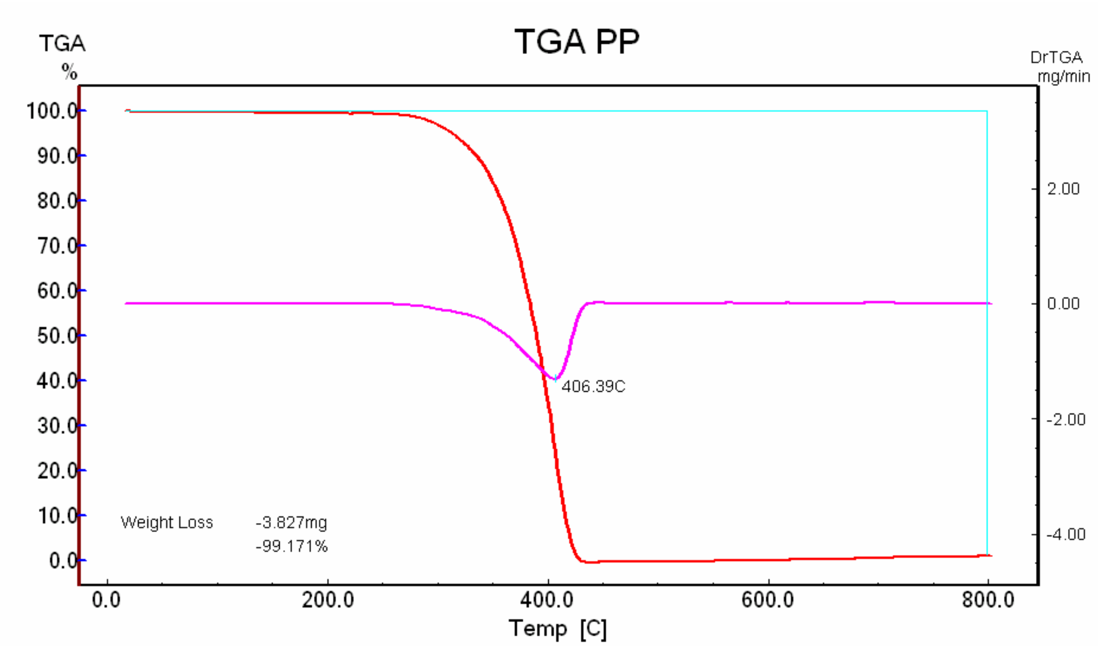

Figure B.1 TGA curve of pure PP (N_2 atm., 20^0C heating rate)

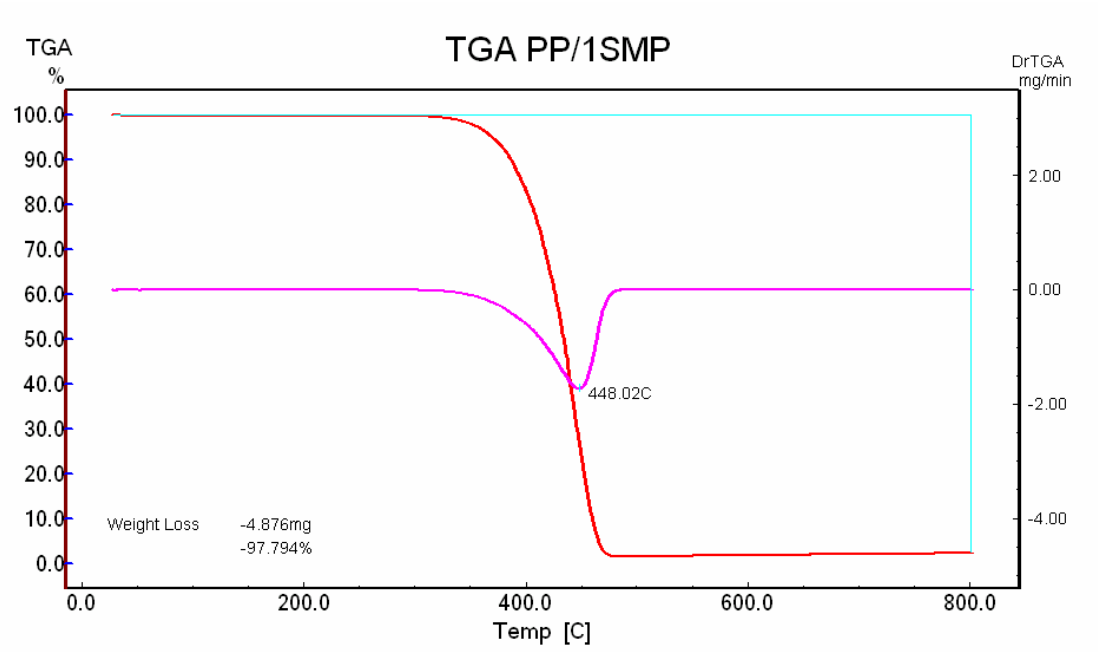

Figure B.2 TGA curve of PP/1SMP (N_2 atm., 20^0C heating rate)

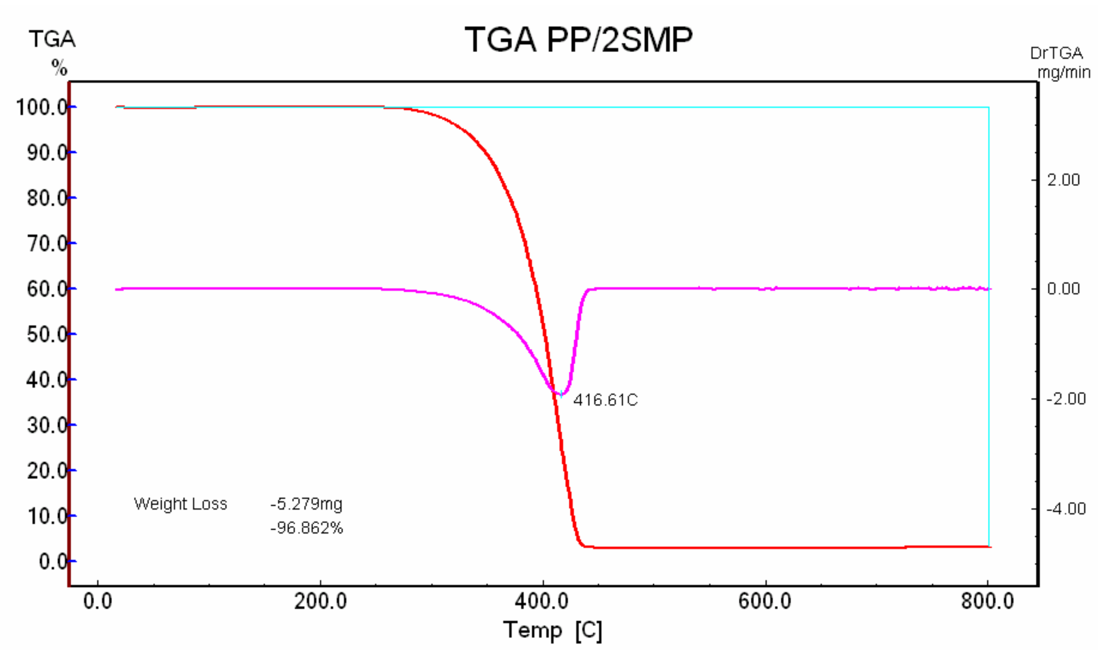

Figure B.3 TGA curve of PP/2SMP (N_2 atm., 20^0C heating rate)

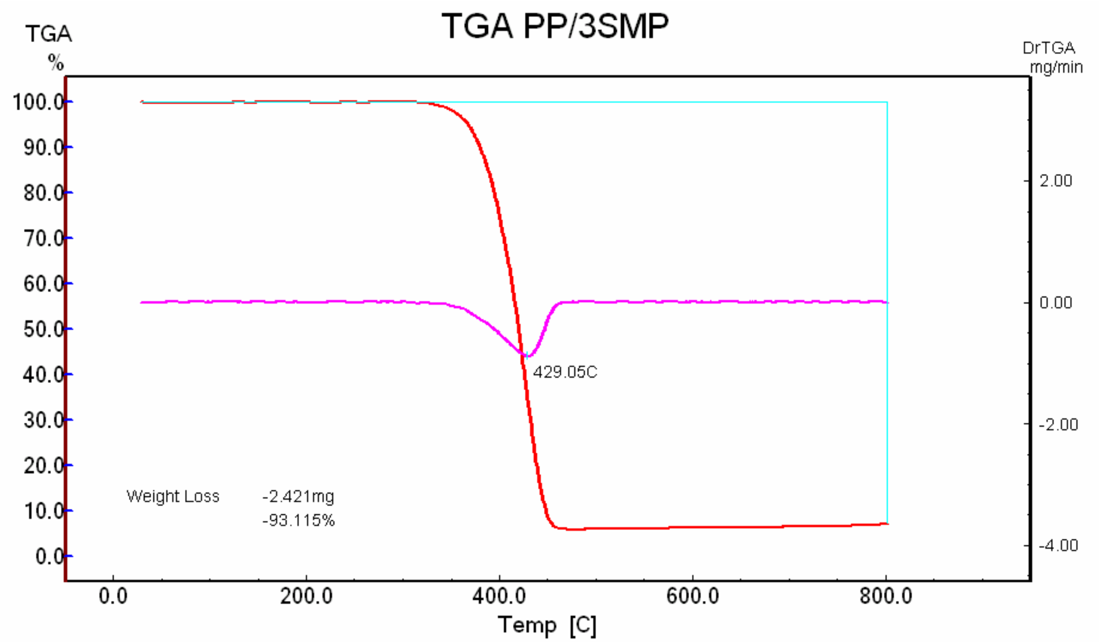

Figure B.4 TGA curve of PP/3SMP (N_2 atm., 20^0C heating rate)

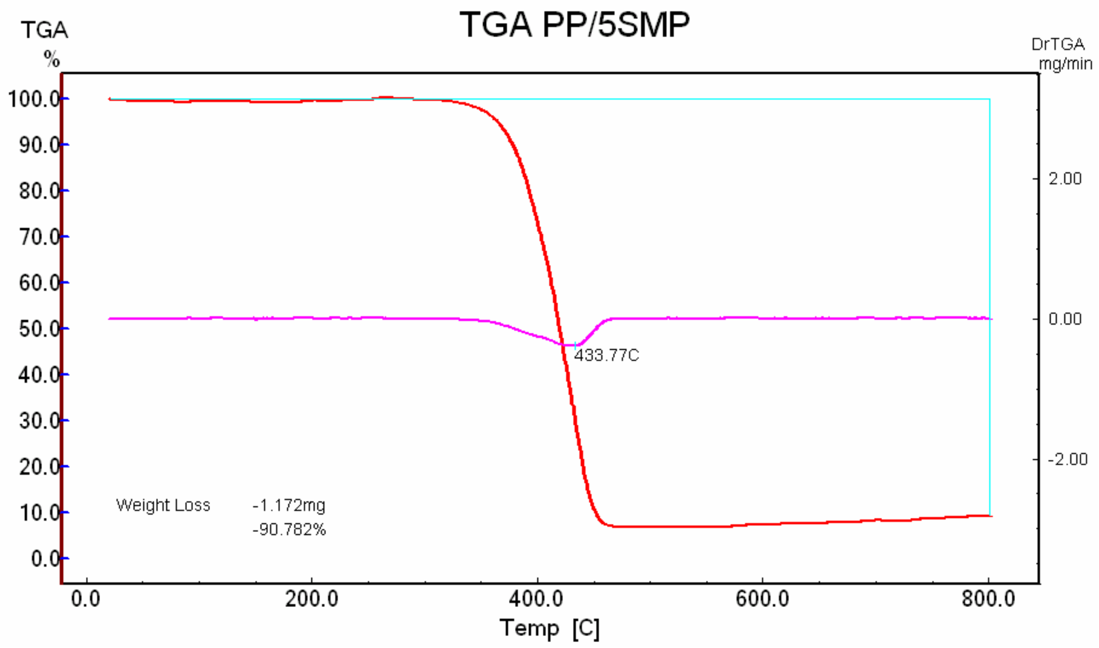

Figure B.5 TGA curve of PP/5SMP (N_2 atm., 20^0C heating rate)

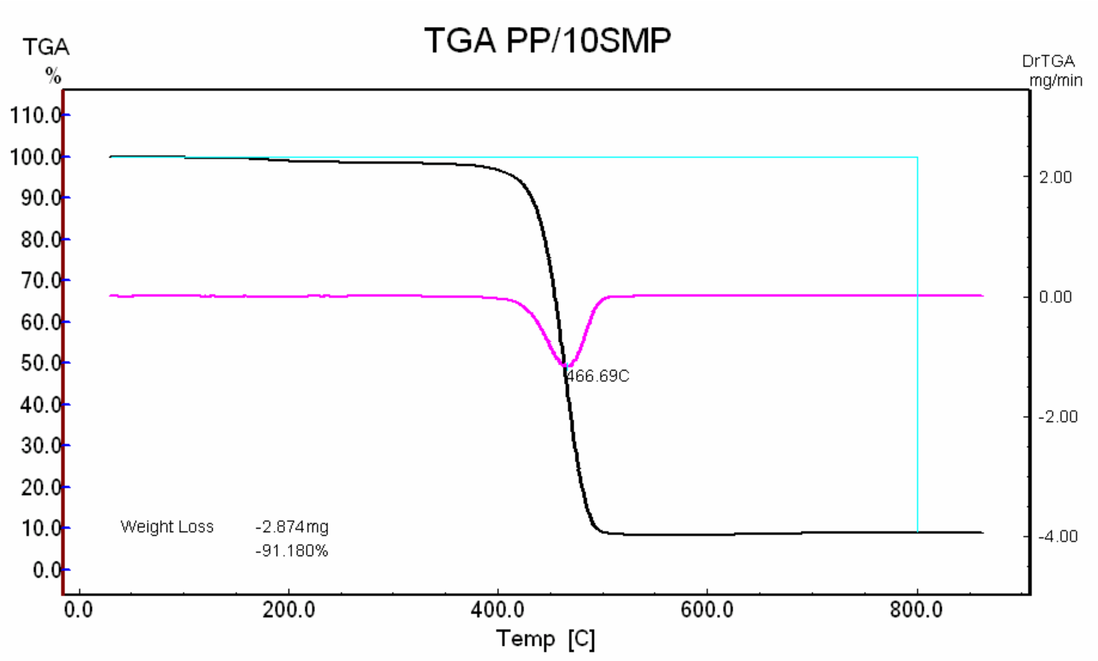

Figure B.6 TGA curve of PP/10SMP (N_2 atm., 20^0C heating rate)

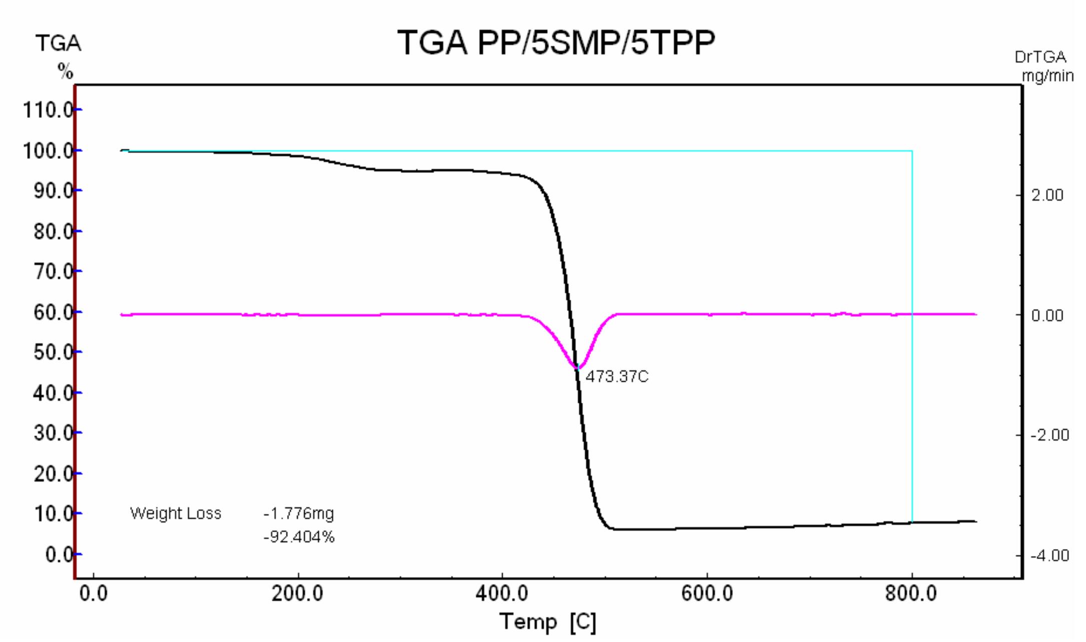

Figure B.7 TGA curve of PP/5SMP/5TPP (N_2 atm., 20^0C heating rate)

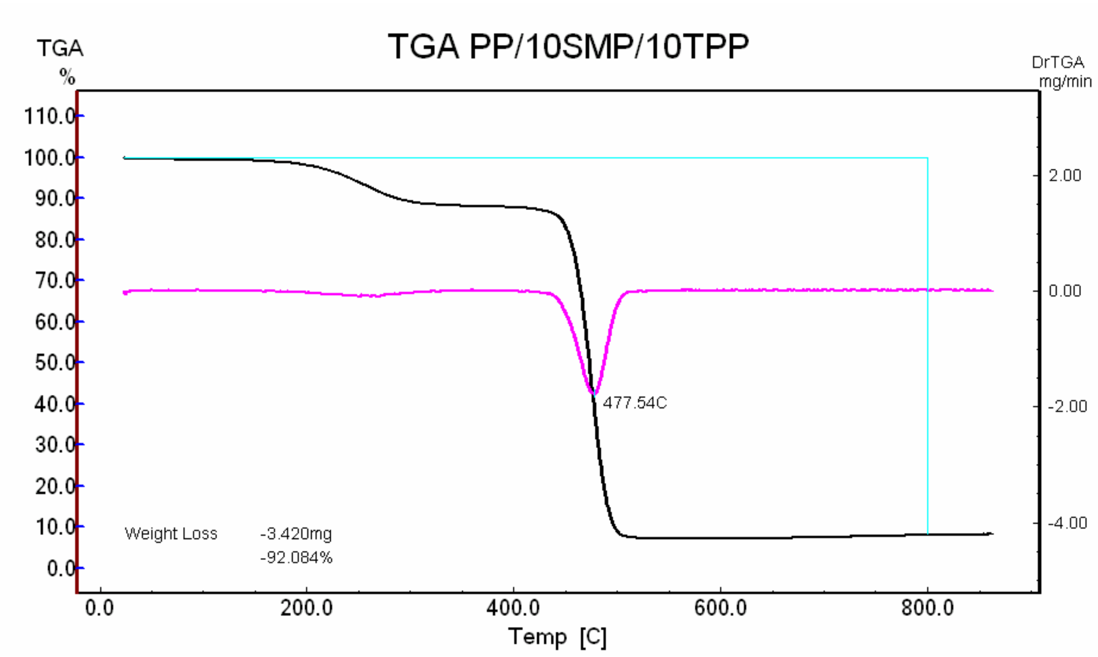

Figure B.8 TGA curve of PP/10SMP/10TPP (N_2 atm., 20^0C heating rate)

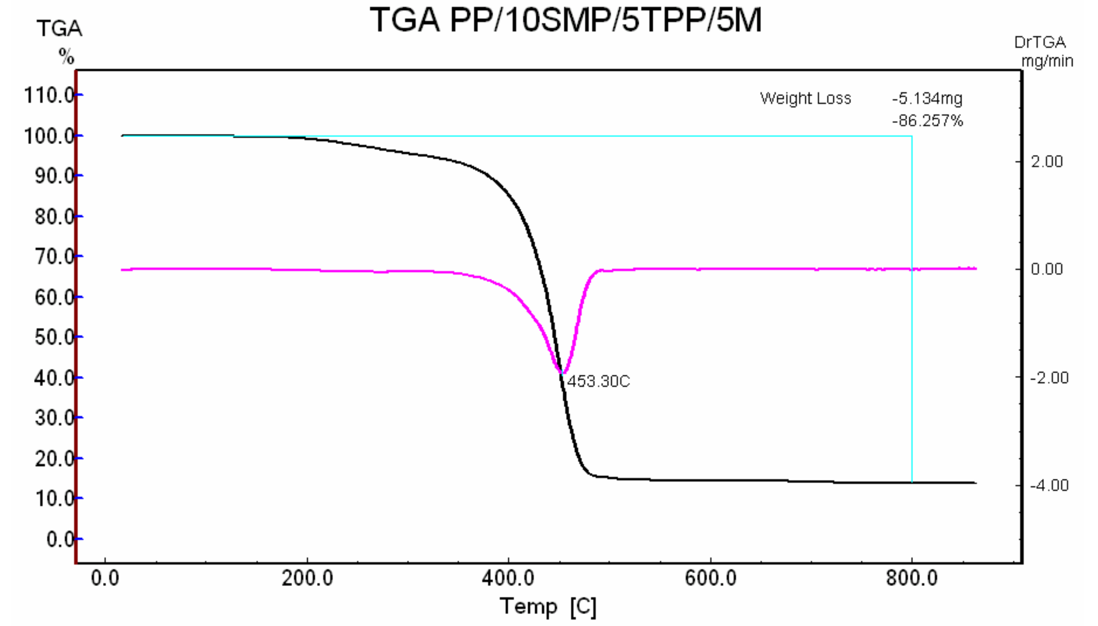

Figure B.9 TGA curve of PP/10SMP/5TPP/5M (N_2 atm., 20^0C heating rate)

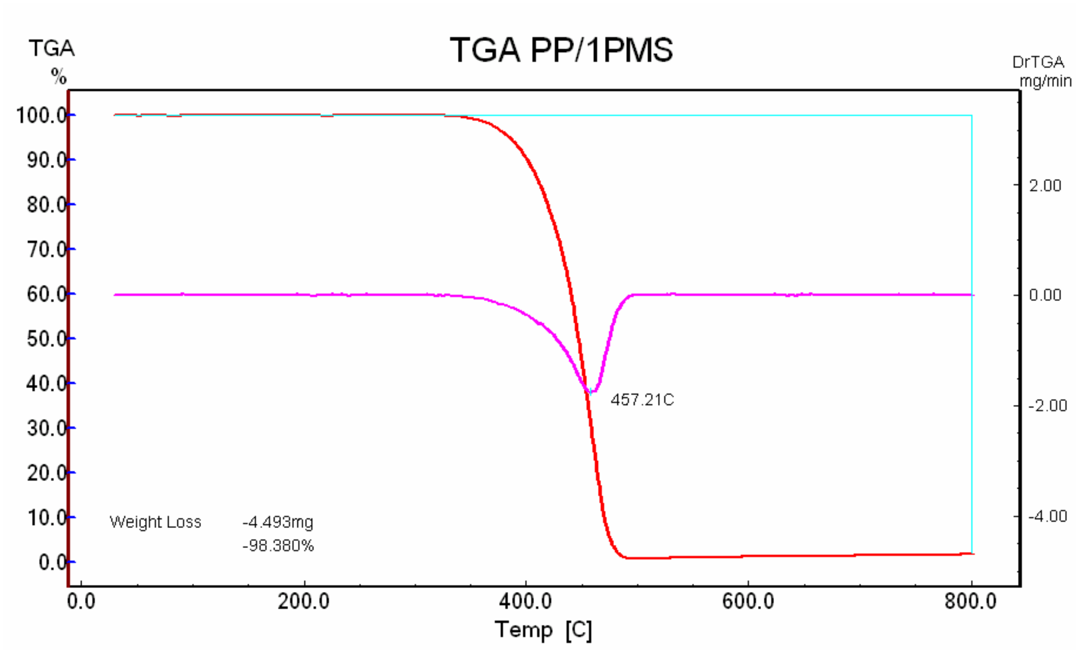

Figure B.10 TGA curve of PP/1PMS (N_2 atm., 20^0C heating rate)

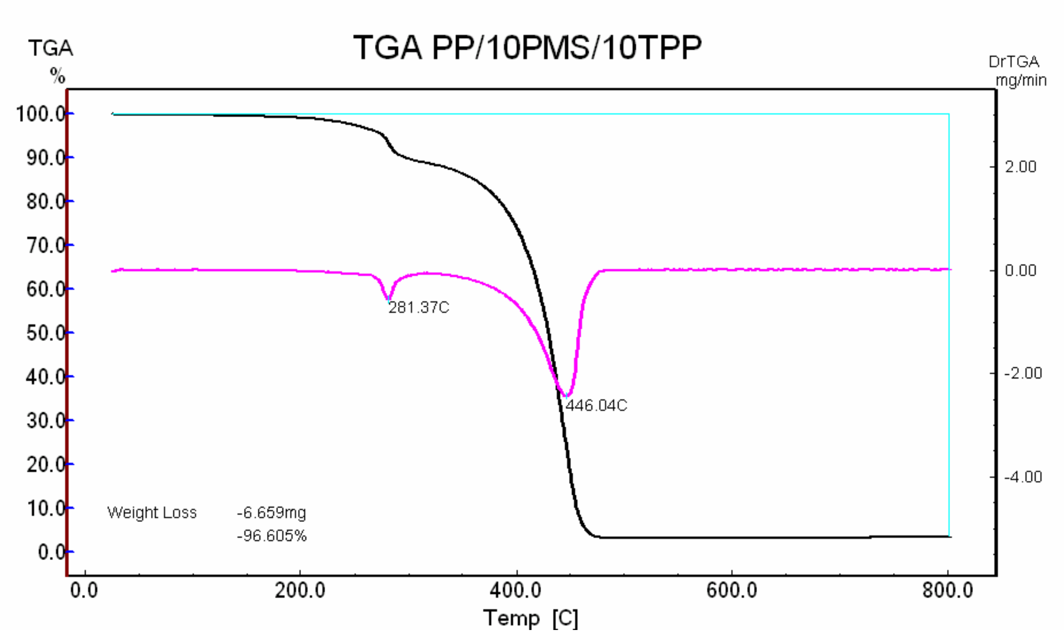

Figure B.11 TGA curve of PP/10PMS/10TPP (N_2 atm., 20^0C heating rate)

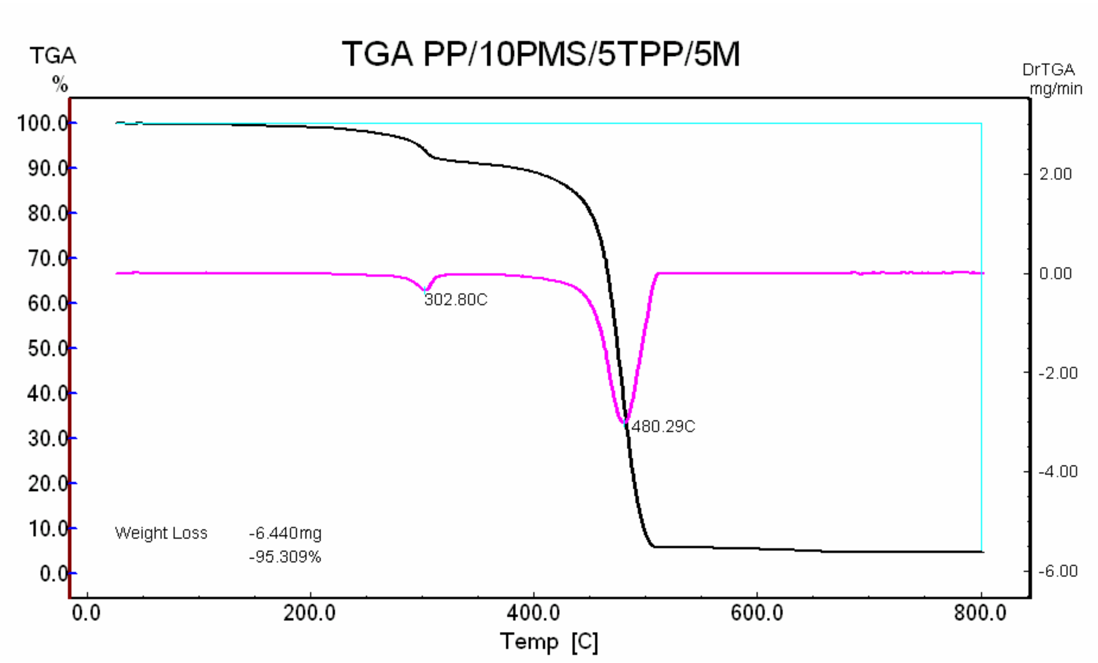

Figure B.12 TGA curve of PP/10PMS/5TPP/5M (N_2 atm., 20^0C heating rate)

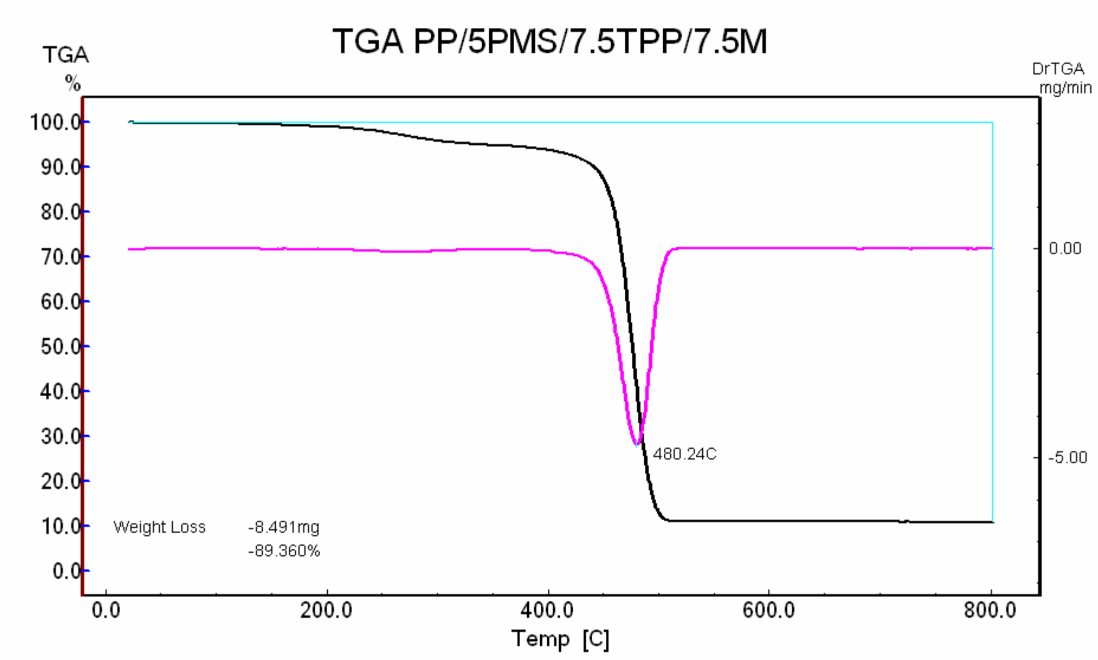

Figure B.13 TGA curve of PP/5PMS/7.5TPP/7.5M (N_2 atm., 20^0C heating rate)

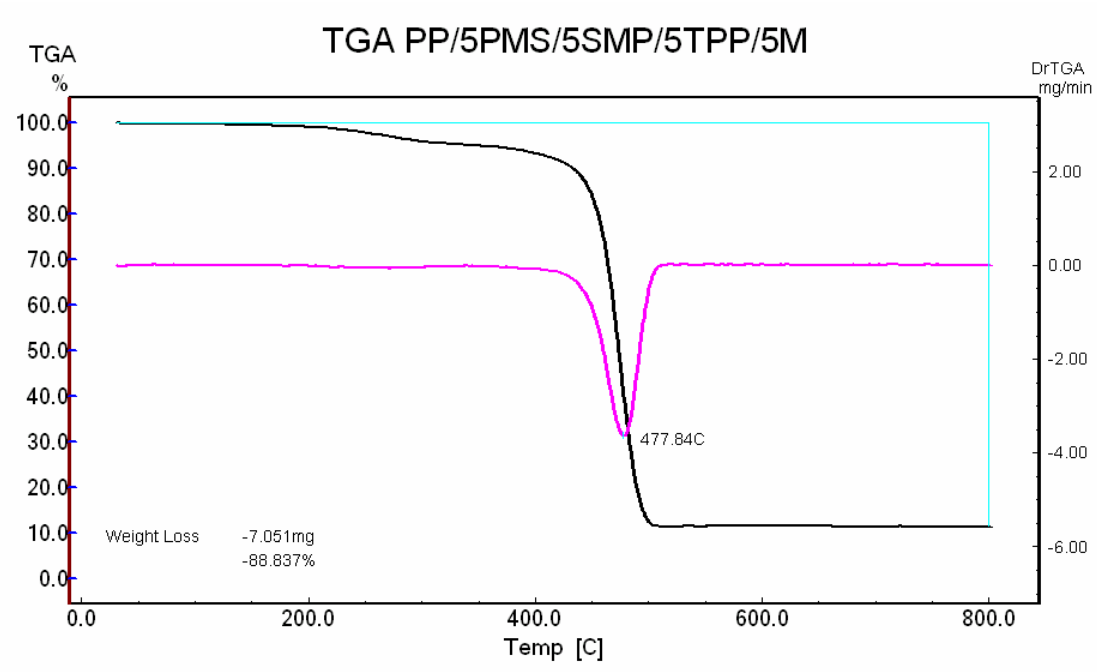

Figure B.14 TGA curve of PP/5PMS/5SMP/5TPP/5M (N_2 atm., 20^0C heating rate)

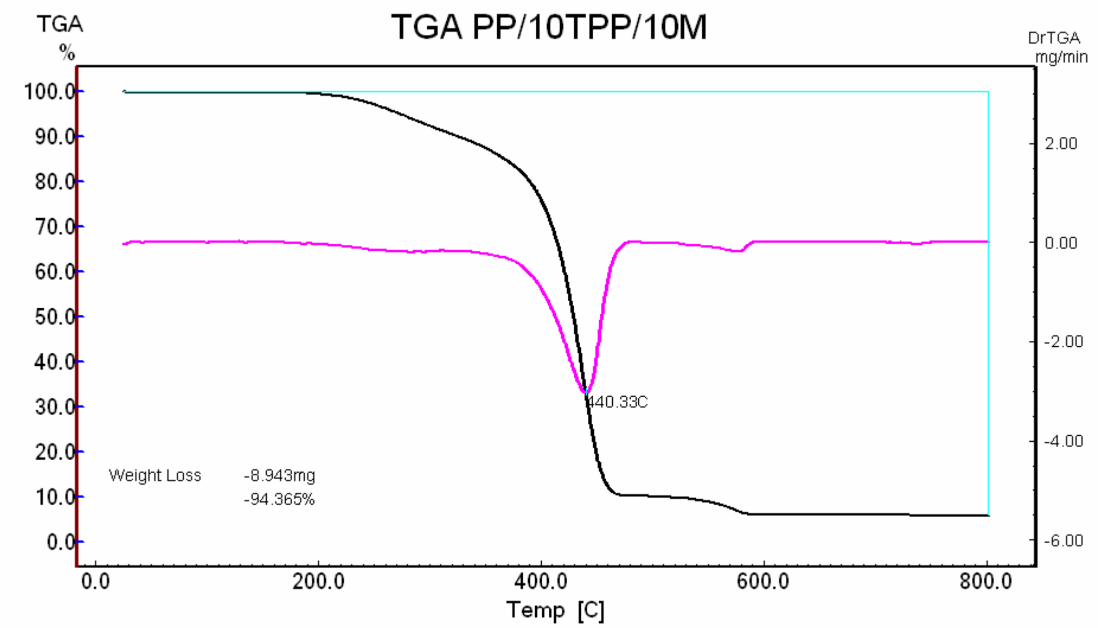

Figure B.15 TGA curve of PP/10TPP/10M (N_2 atm., 20^0C heating rate)

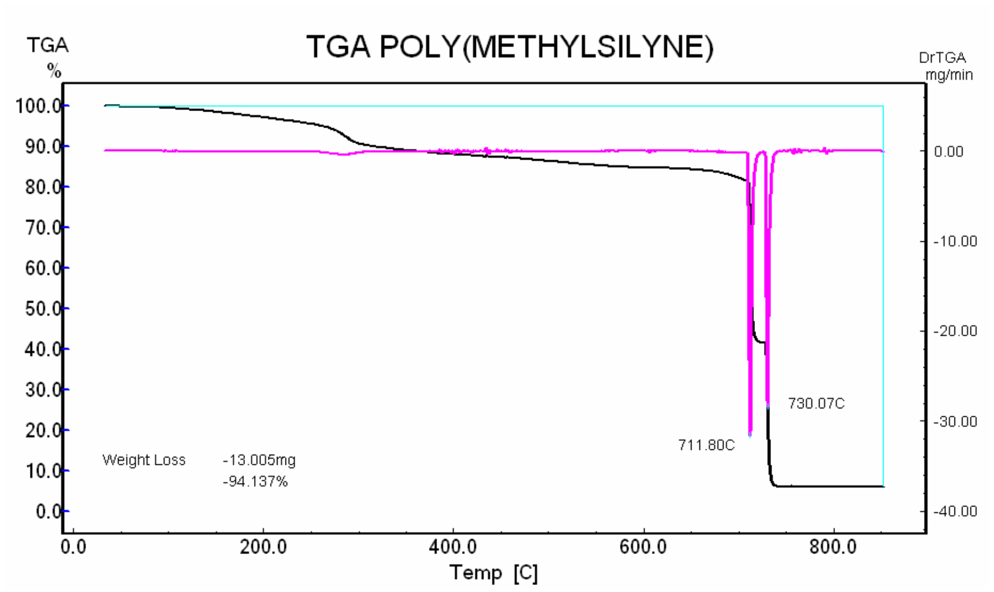

Figure B.16 TGA curve of PMSy (N_2 atm., 20^0C heating rate)

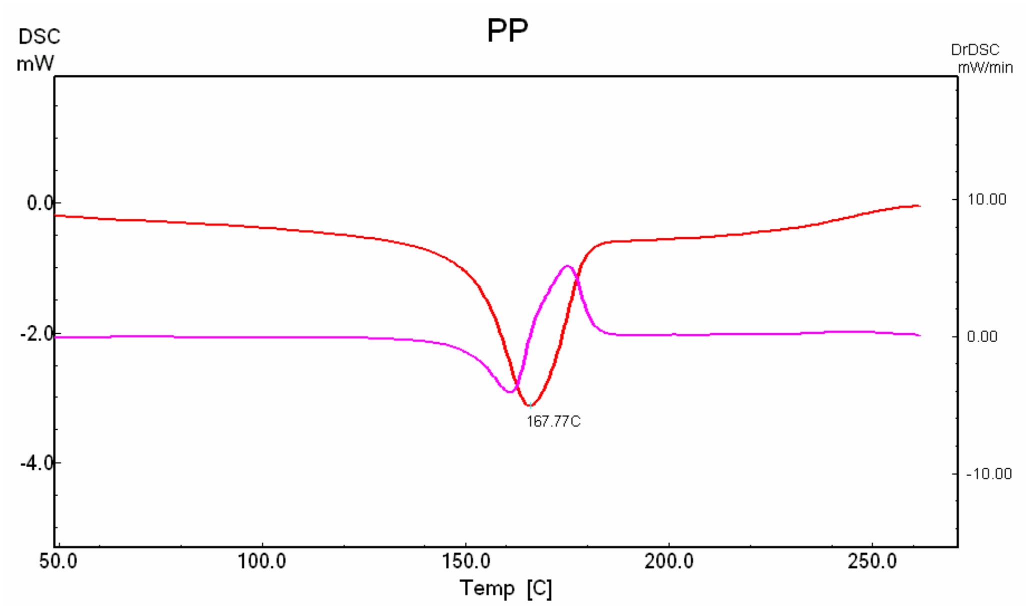

Figure B.17 DSC curve of pure polypropylene (20^0C heating rate)

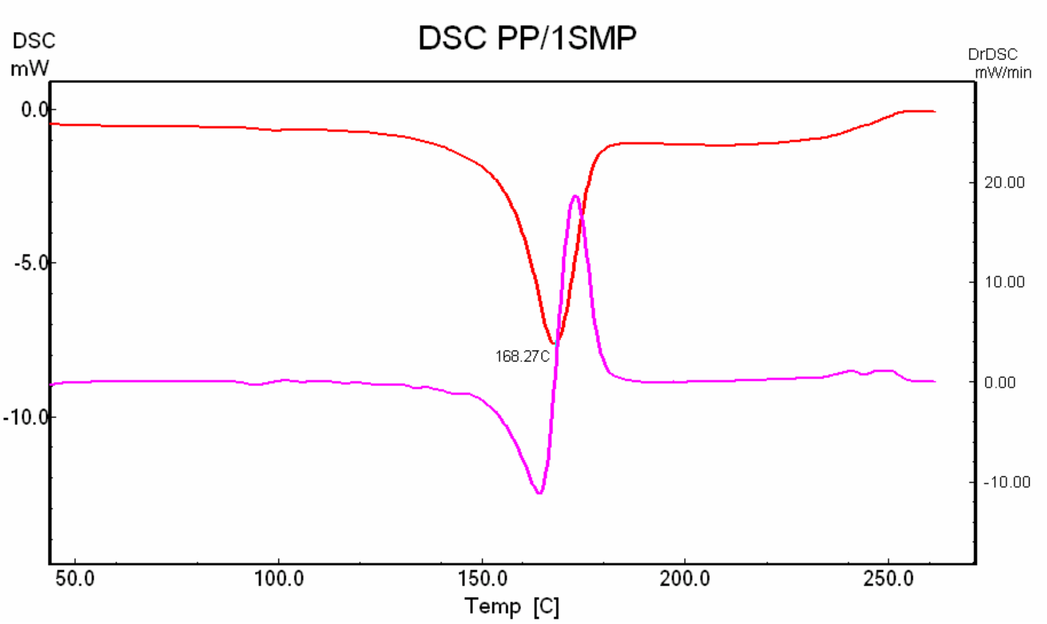

Figure B.18 DSC curve of PP/1SMP (20^{0}C heating rate)

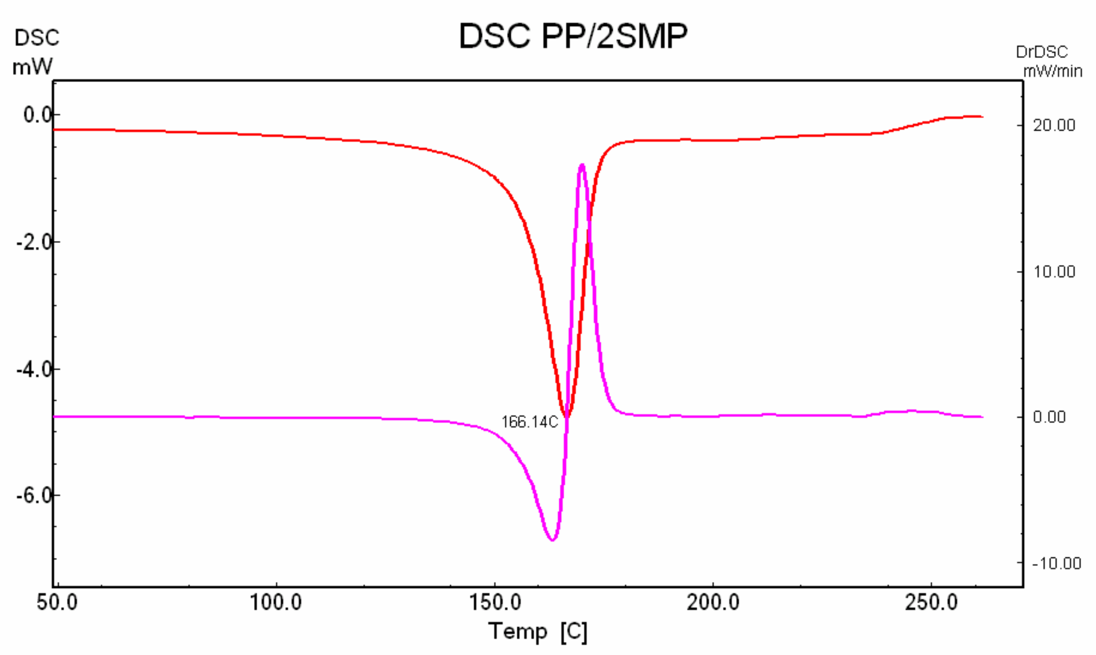

Figure B.19 DSC curve of PP/2SMP (20^{0}C heating rate)

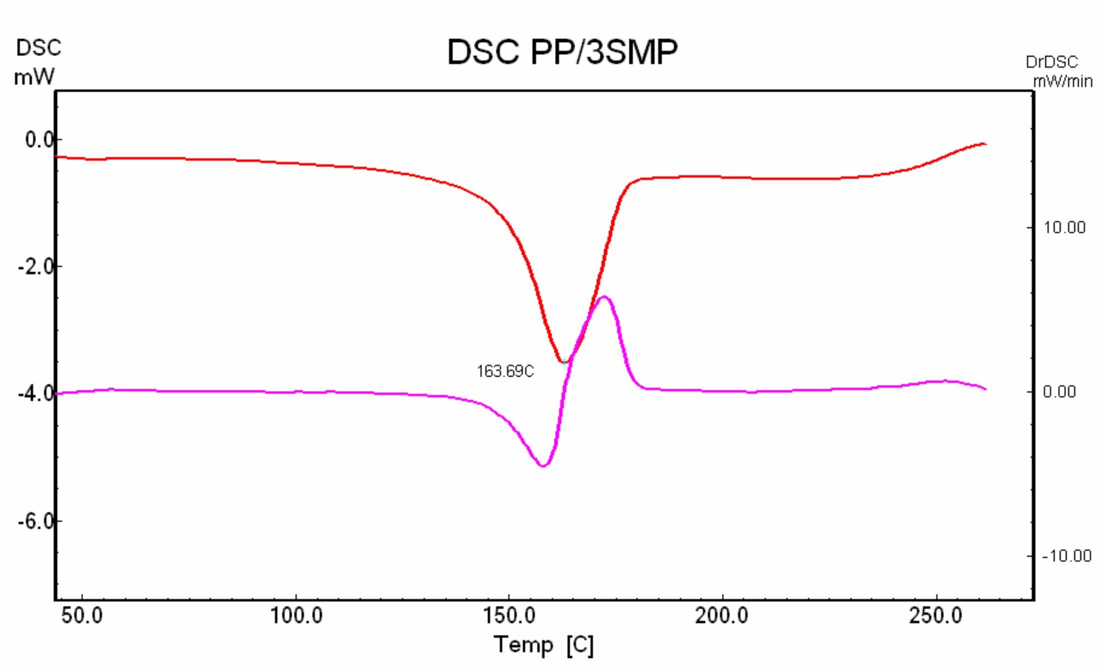

Figure B.20 DSC curve of PP/3SMP (20^{0}C heating rate)

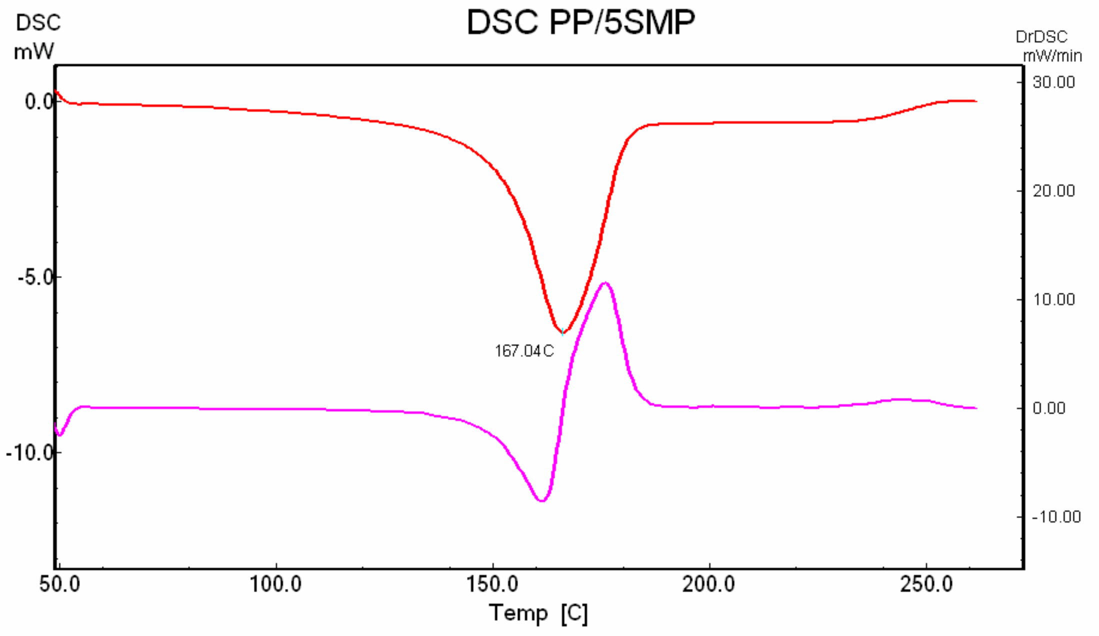

Figure B.21 DSC curve of PP/5SMP (20^{0}C heating rate)

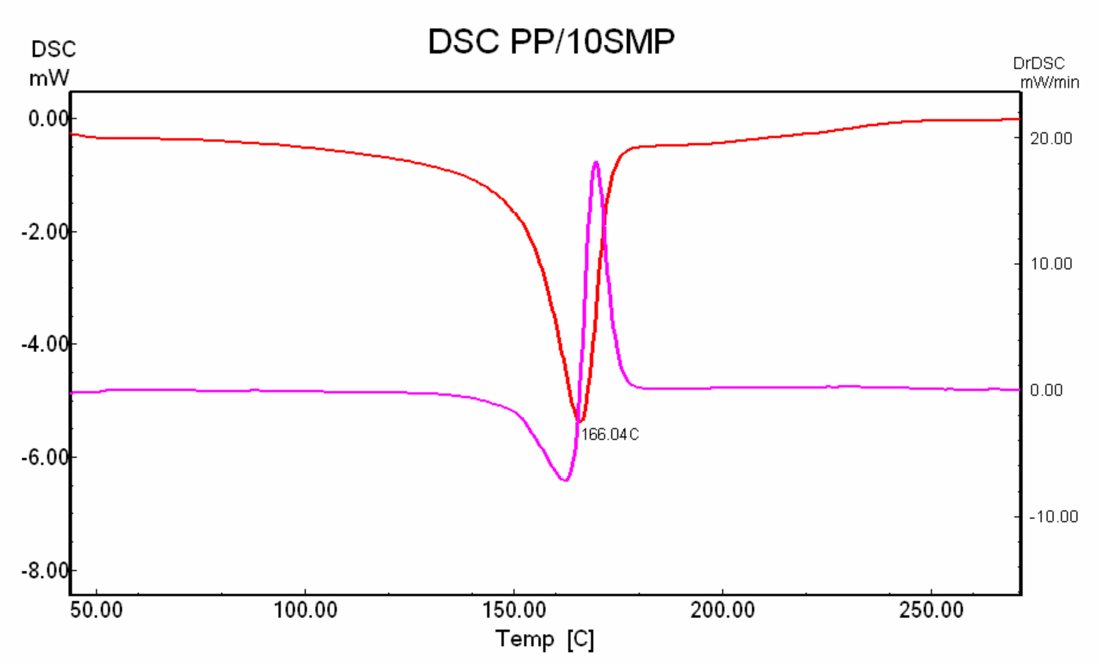

Figure B.22 DSC curve of PP/10SMP (20^{0}C heating rate)

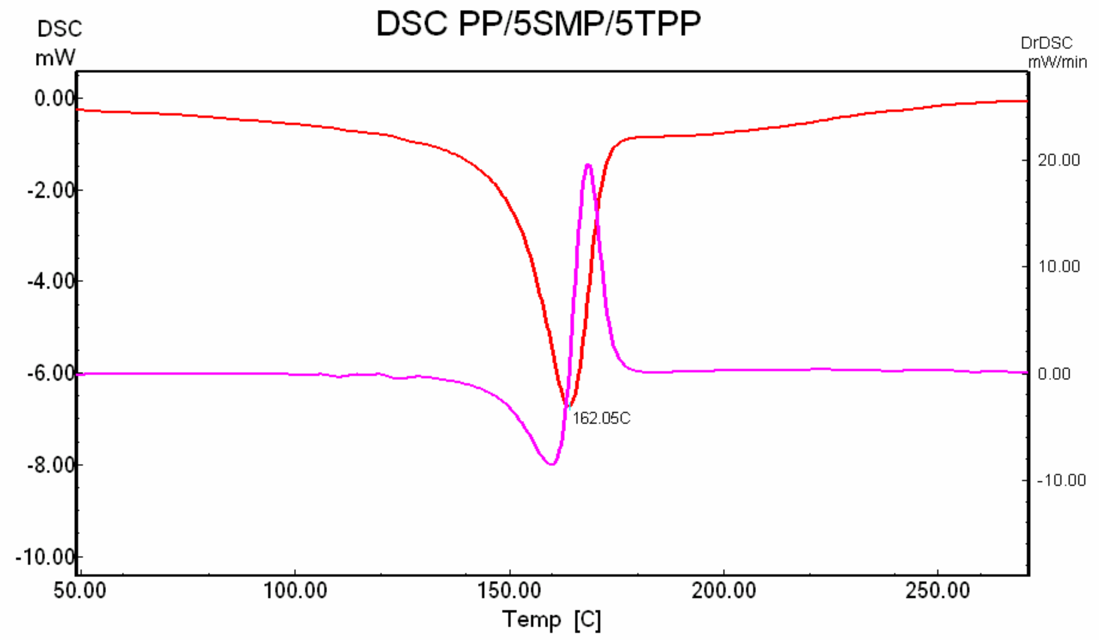

Figure B.23 DSC curve of PP/5SMP/5TPP (20^{0}C heating rate)

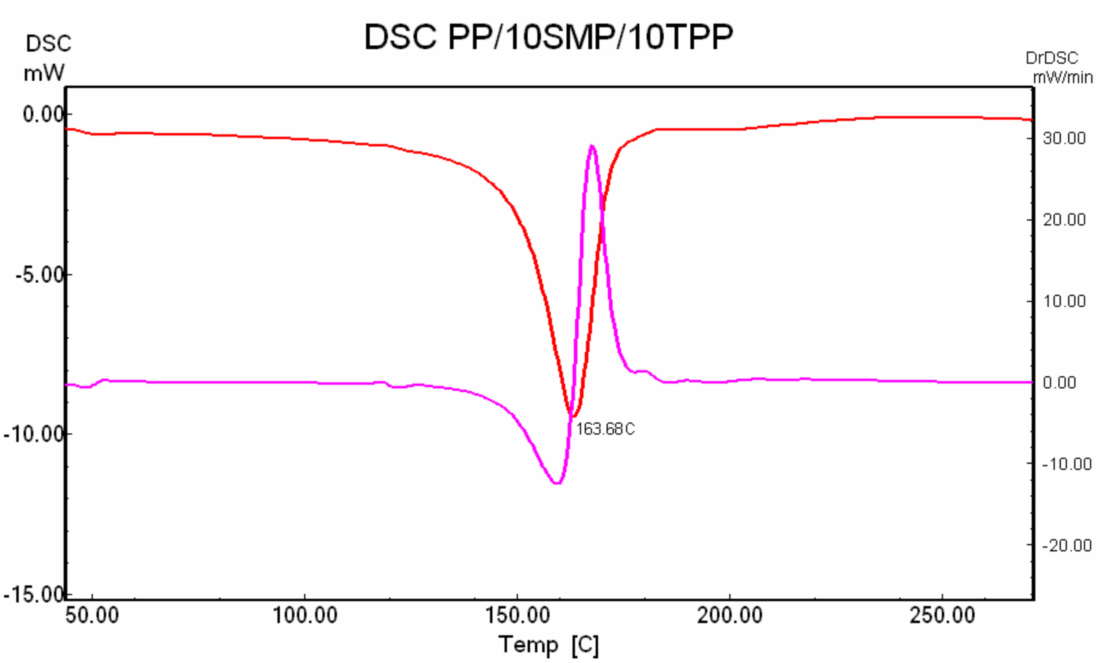

Figure B.24 DSC curve of PP/10SMP/10TPP (20^{0}C heating rate)

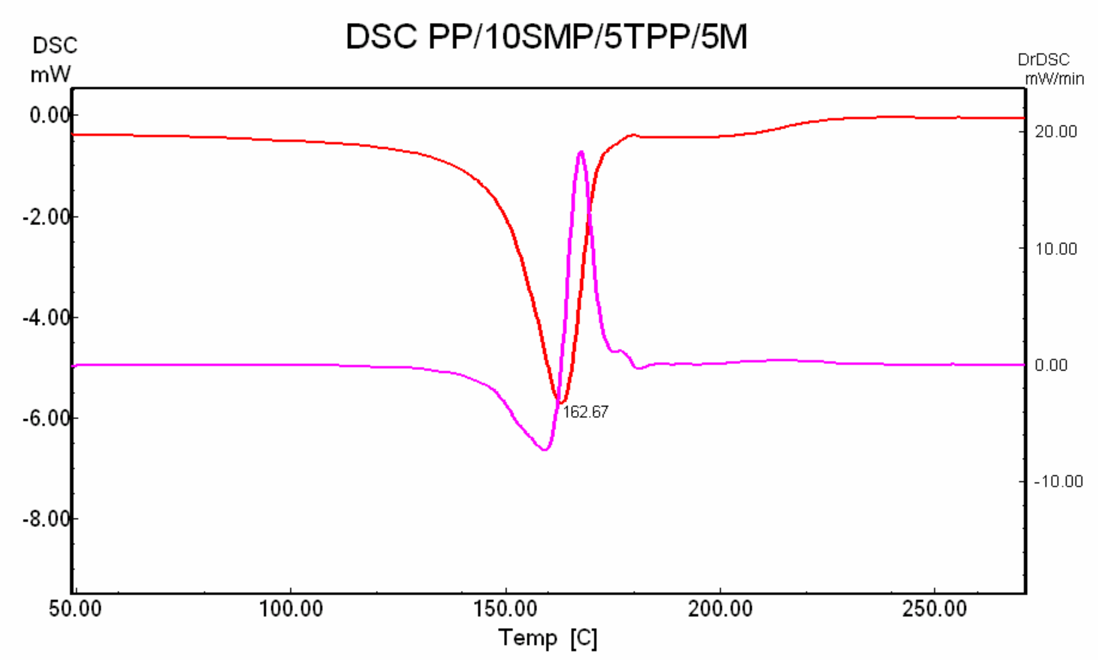

Figure B.25 DSC curve of PP/10SMP/5TPP/5M (20^{0}C heating rate)

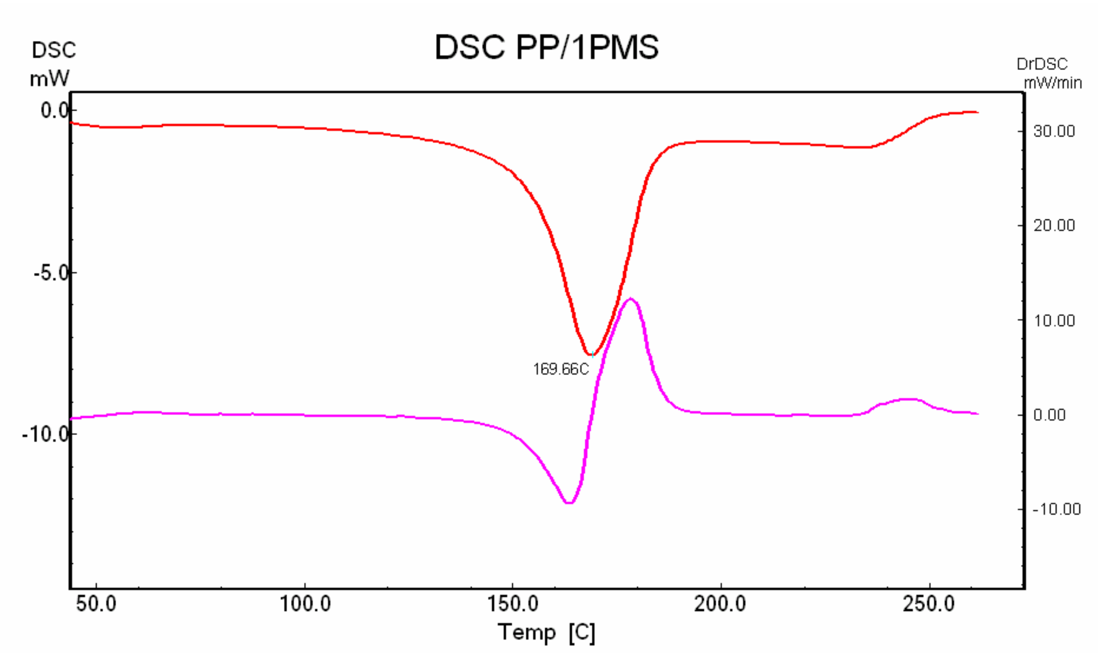

Figure B.26 DSC curve of pure polypropylene (20^{0}C heating rate)

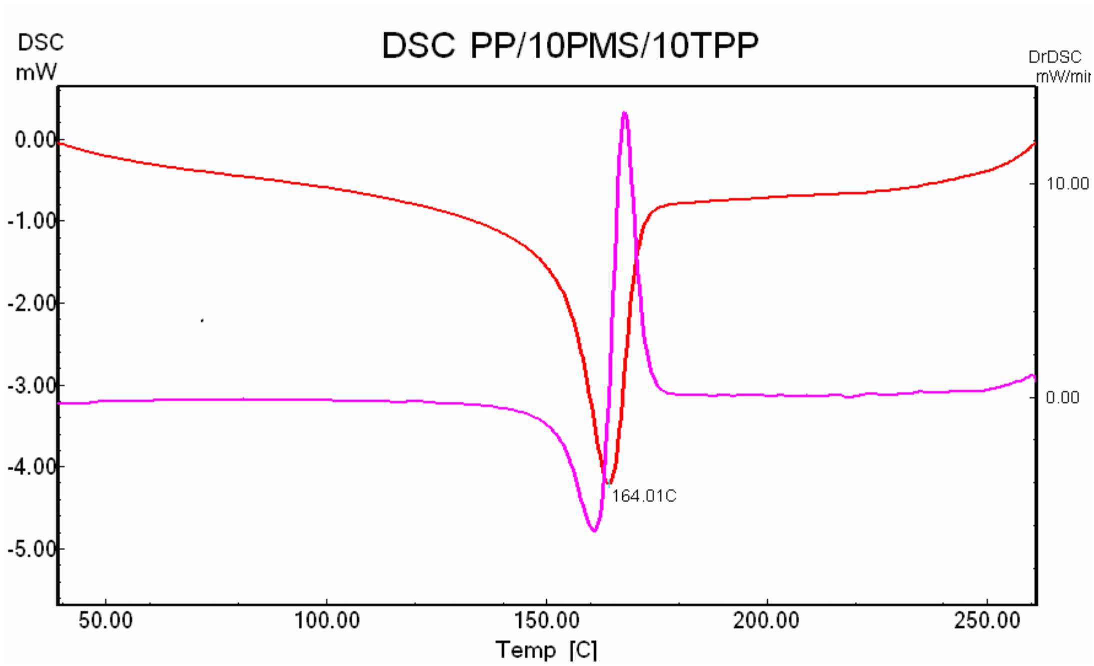

Figure B.27 DSC curve of PP/10PMS/10TPP (20^{0}C heating rate)

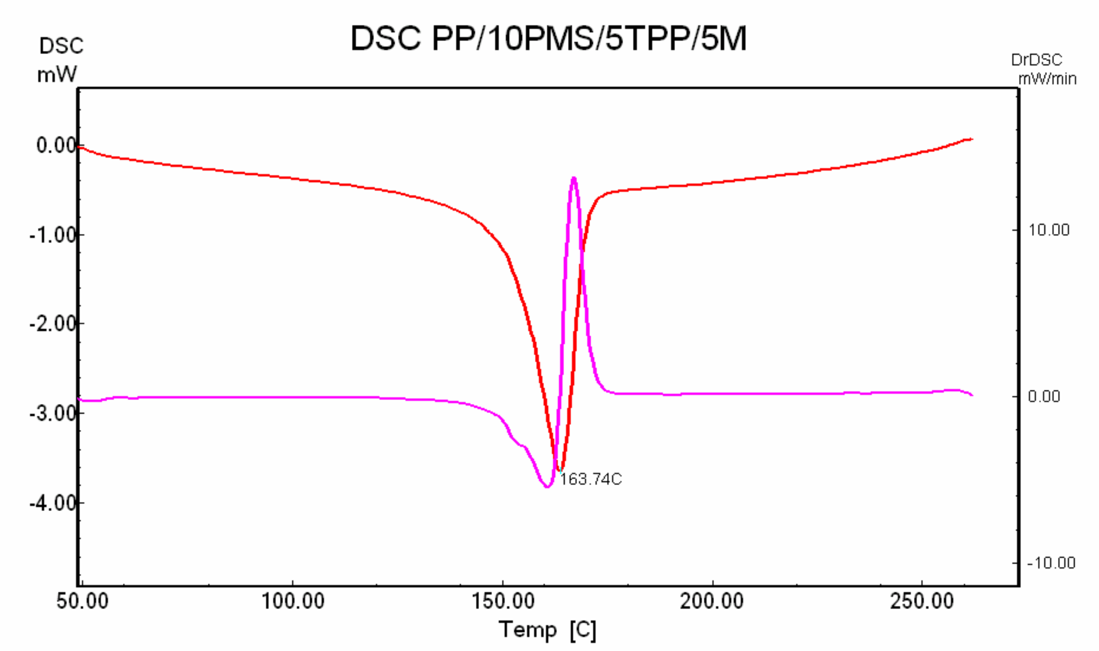

Figure B.28 DSC curve of PP/10PMS/5TPP/5M (20^{0}C heating rate)

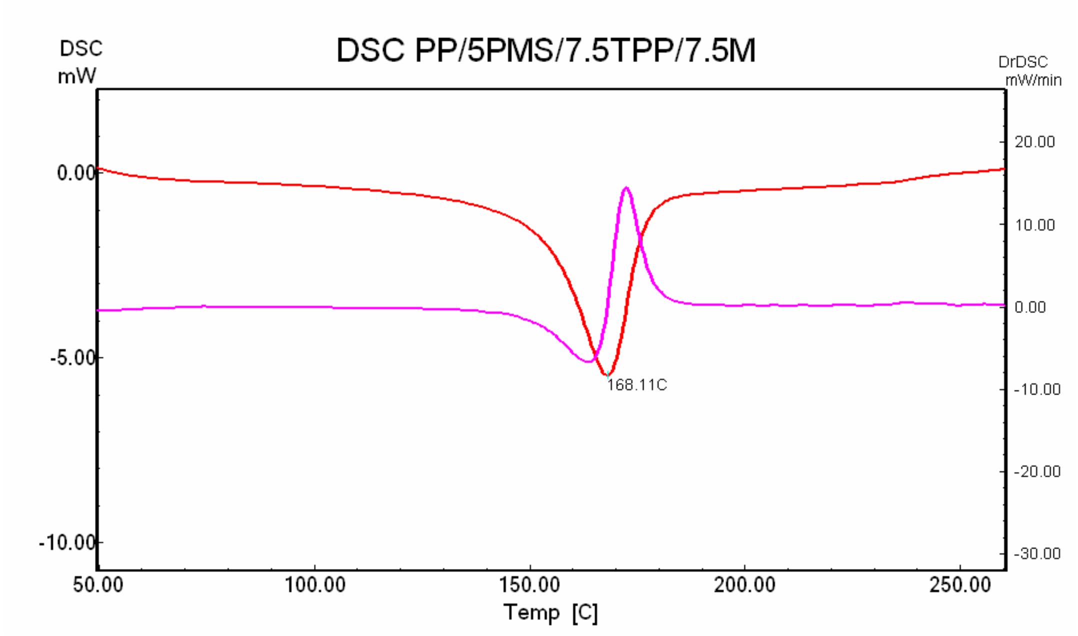

Figure B.29 DSC curve of PP/5PMS/7.5TPP/7.5M (20^{0}C heating rate)

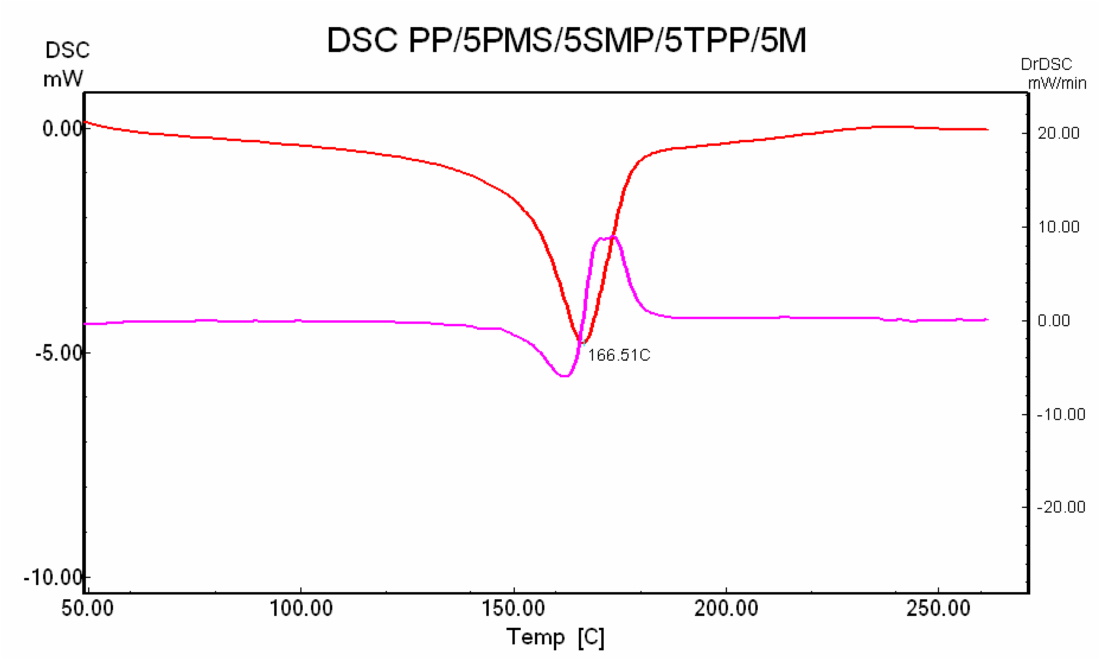

Figure B.30 DSC curve of PP/5PMS/5SMP/5TPP/5M (20^{0}C heating rate)

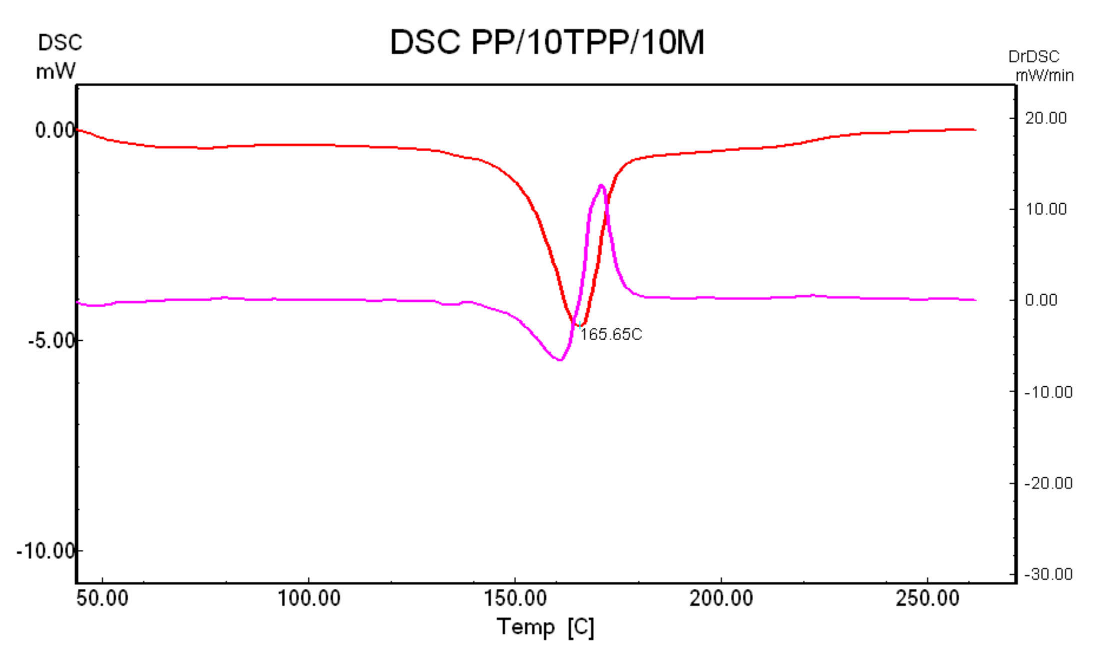

Figure B.31 DSC curve of PP/10TPP/10M (20^{0}C heating rate)

APPENDIX C

SEM RESULTS

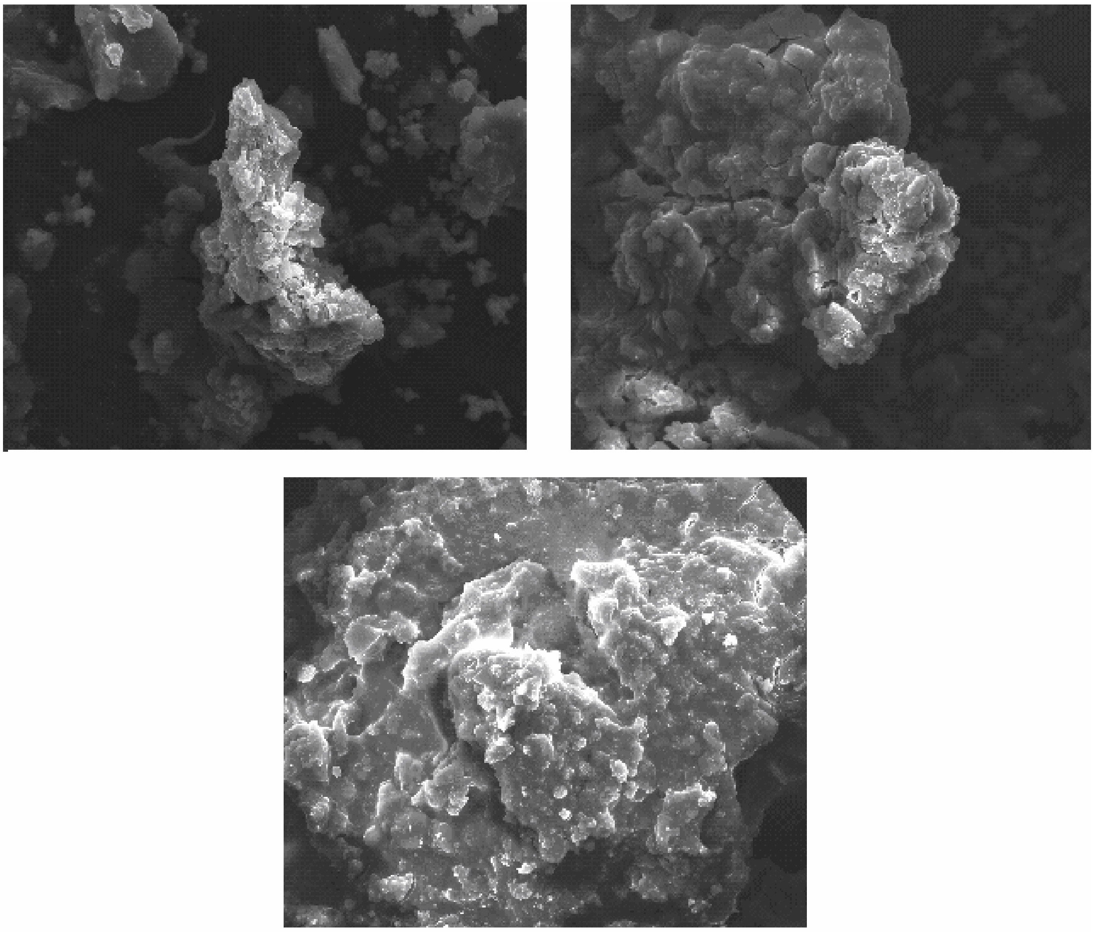

Figure C.1 SEM of poly(methylsilyne) at x1000 magnification

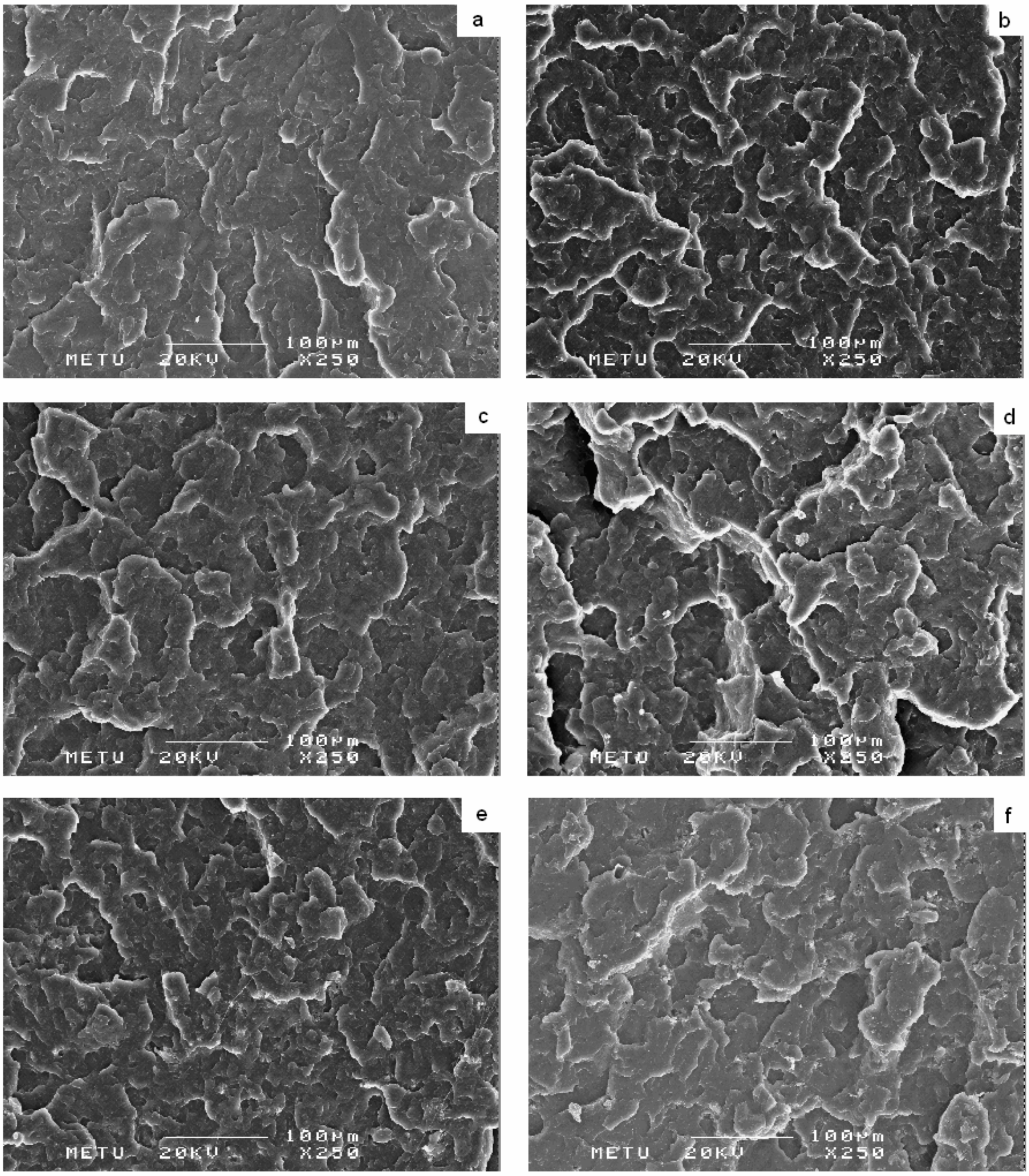

Figure C.2 SEM pictures of (a) PP (b) PP/1SMP (c) PP/2SMP (d) PP/3SMP (e) PP/5SMP (f) PP/10SMP sets at x250 magnification

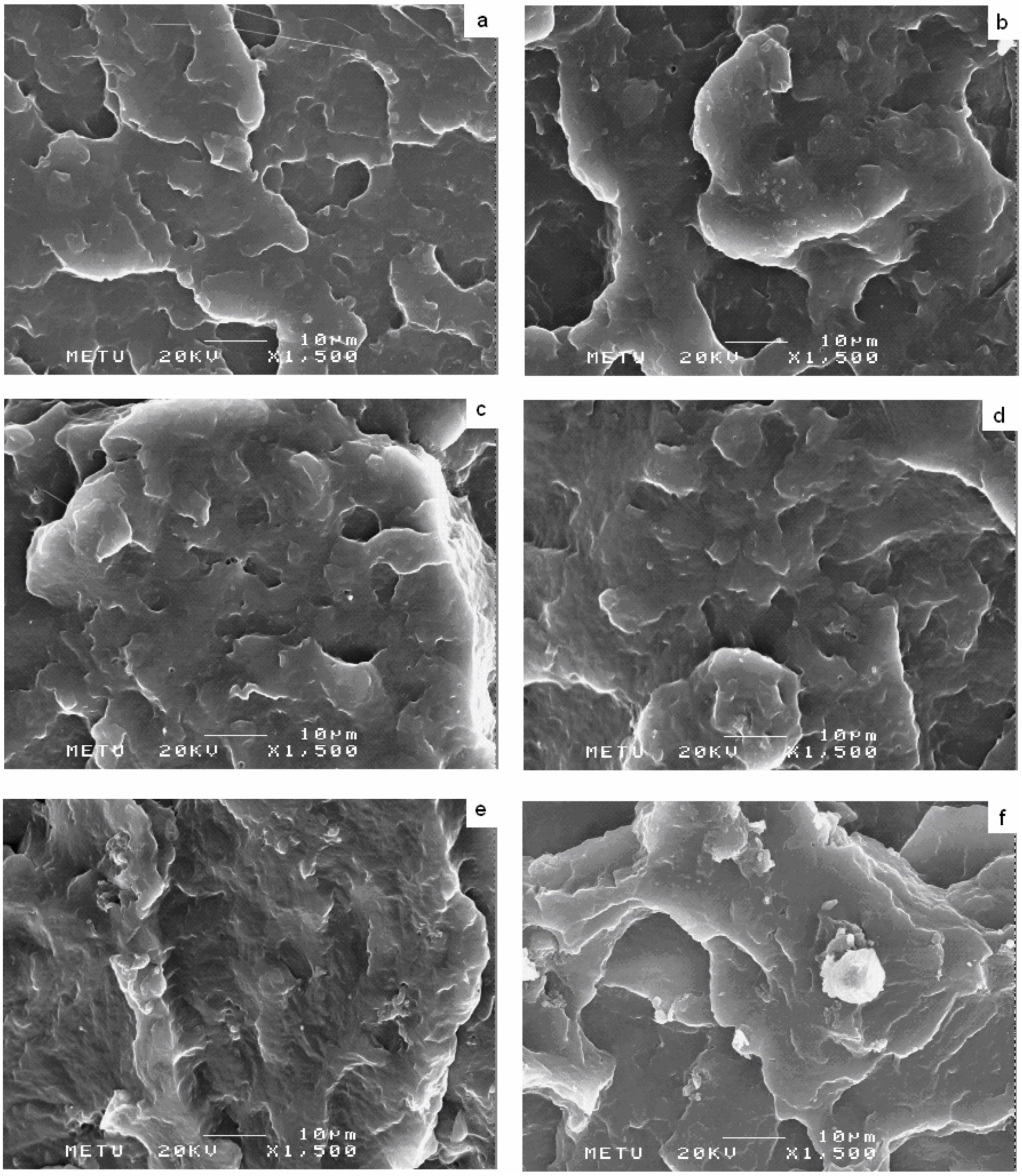

Figure C.3 SEM pictures of (a) PP (b) PP/1SMP (c) PP/2SMP (d) PP/3SMP (e) PP/5SMP (f) PP/10SMP sets at x1500 magnification

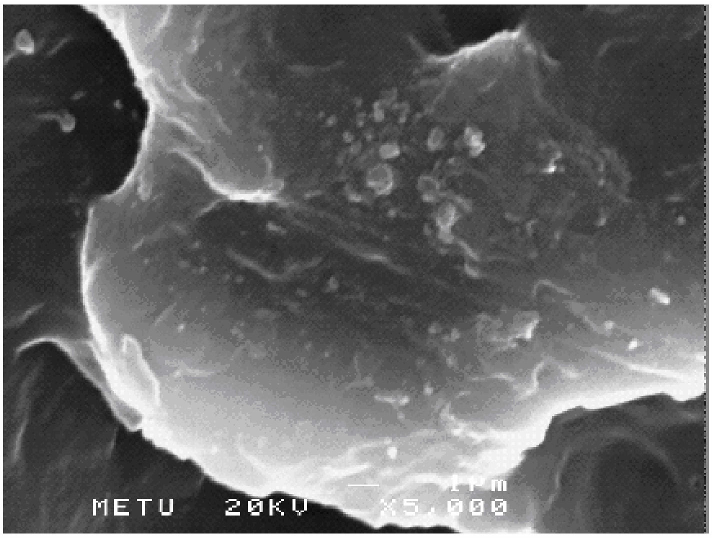

Figure C.4 SEM picture of PP/1SMP at x5000 magnification

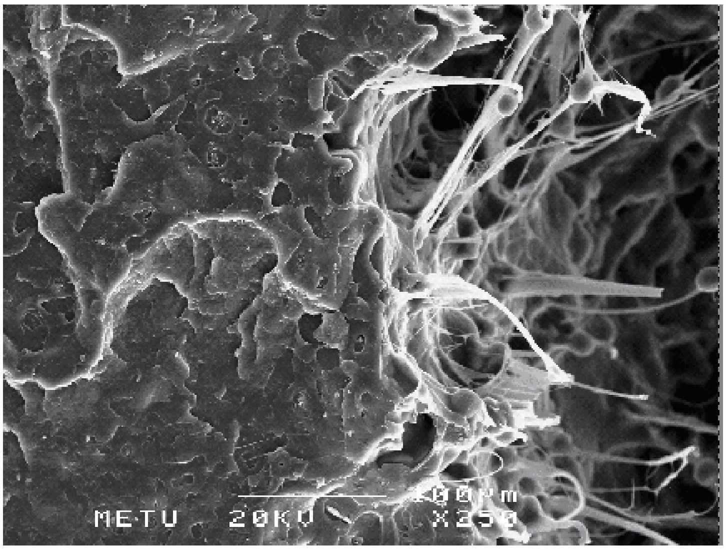

Figure C.5 SEM picture of PP/2SMP at x250 magnification

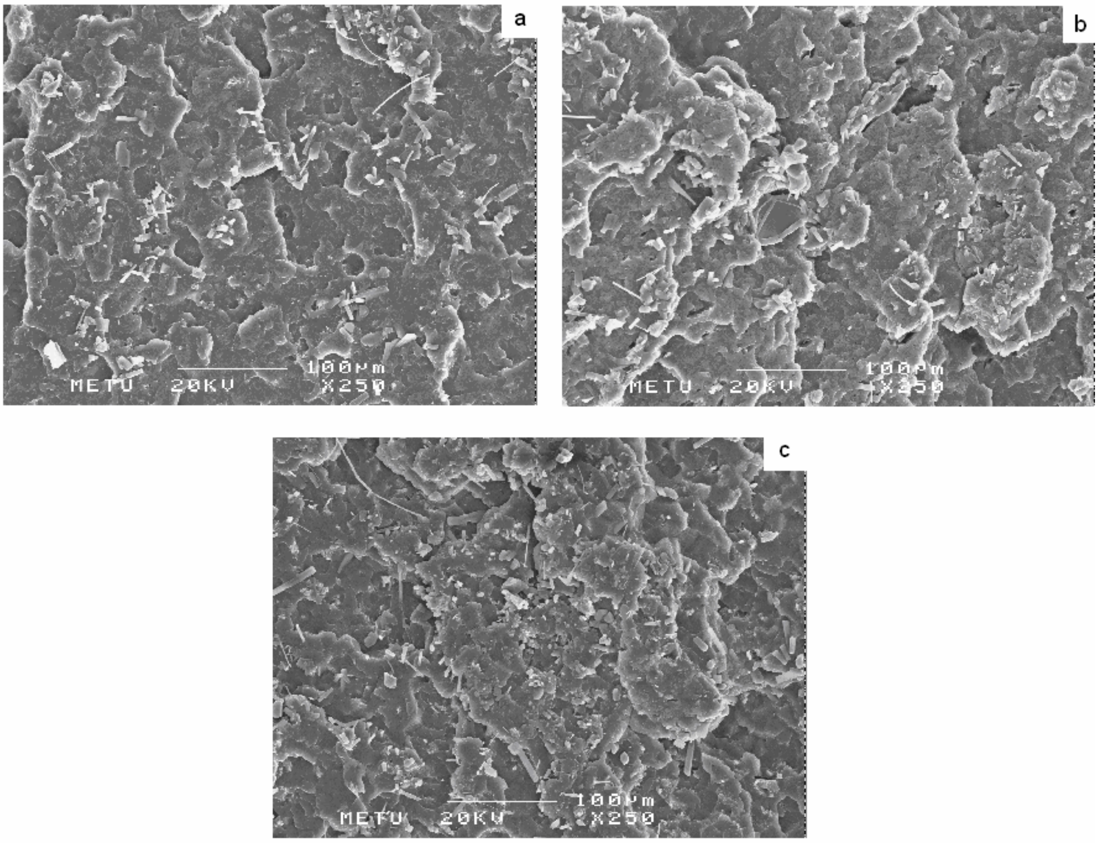

Figure C.6 SEM pictures of (a) PP/5SMP/5TPP (b) PP/10SMP/10TPP (c) PP/10SMP/5TPP/5M sets at x250 magnification

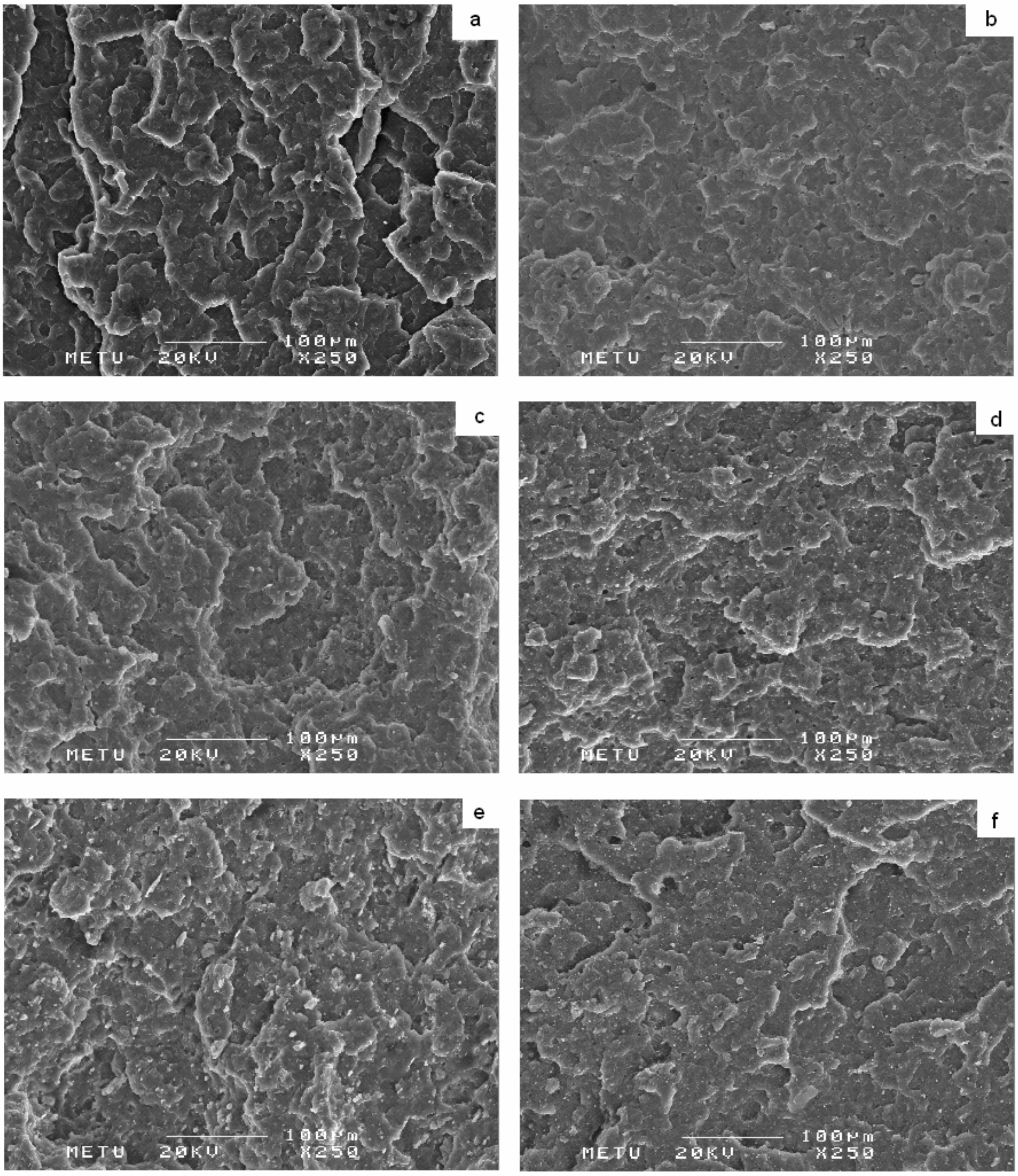

Figure C.7 SEM pictures of (a) PP/1PMS (b) PP/10PMS/10TPP (c) PP/10PMS/5TPP/5M (d) PP/5PMS/7.5TPP/7.5M (e) PP/5PMS/5SMP/5TPP/5M and (f) PP/10TPP/10M sets at x 250 magnification

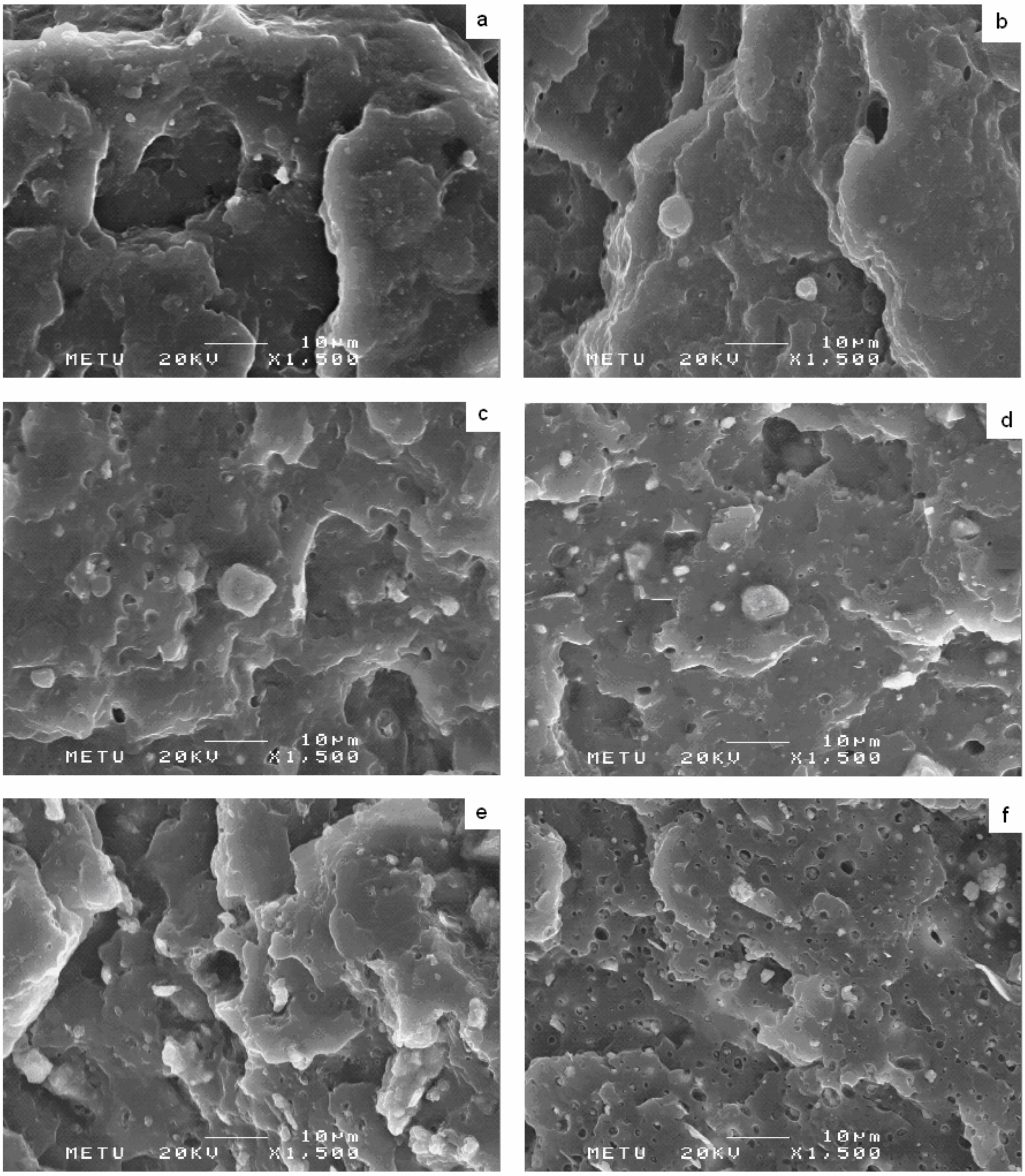

Figure C.8 SEM pictures of (a) PP/1PMS (b) PP/10PMS/10TPP (c) PP/10PMS/5TPP/5M (d) PP/5PMS/7.5TPP/7.5M (e) PP/5PMS/5SMP/5TPP/5M and (f) PP/10TPP/10M sets at x 1500 magnification

APPENDIX D

EDX ANALYSIS OF PP/SMP-10 AND PP/PMSy BLENDS

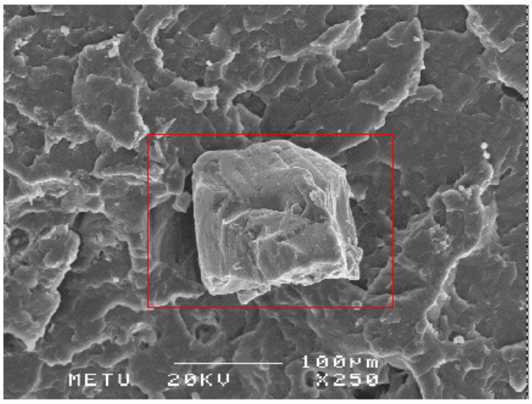

Figure D.1 SEM picture of PP/10SMP blend at x250 magnification

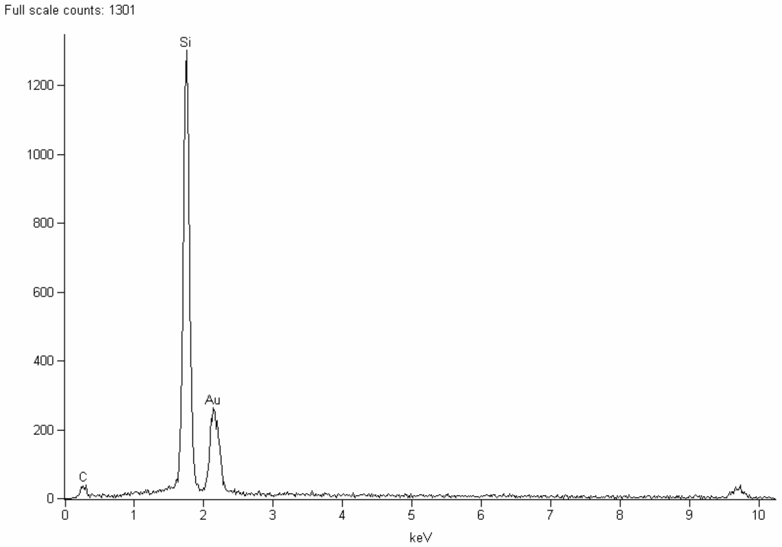

Figure D.2 EDX analysis of the cubical structure in Figure D.1

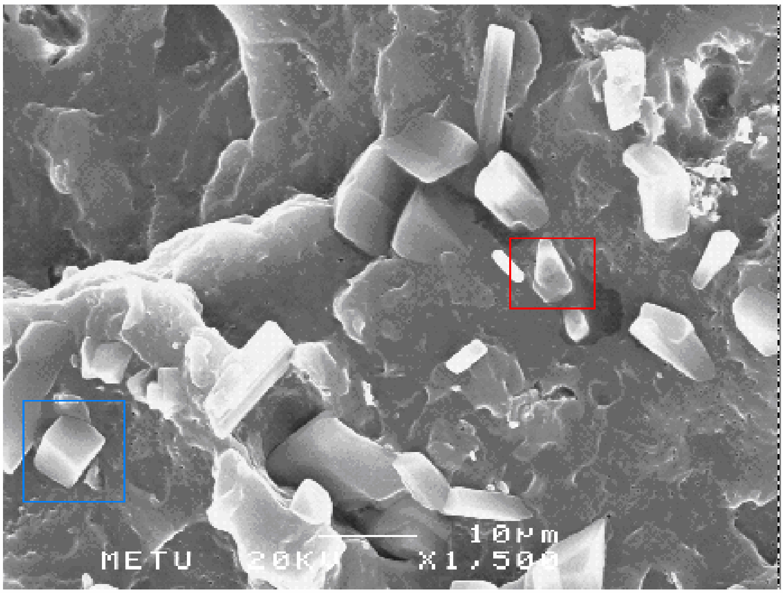

Figure D.3 SEM picture of PP/5SMP/5TPP blend at x1500 magnification

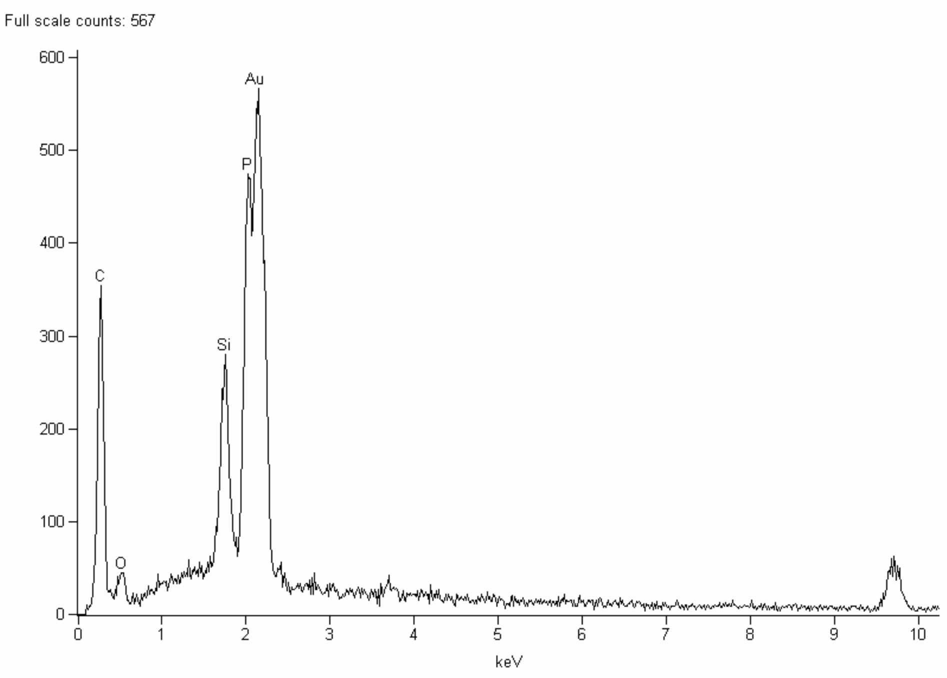

Figure D.4 EDX analysis of the structure in Figure D.3 marked with red

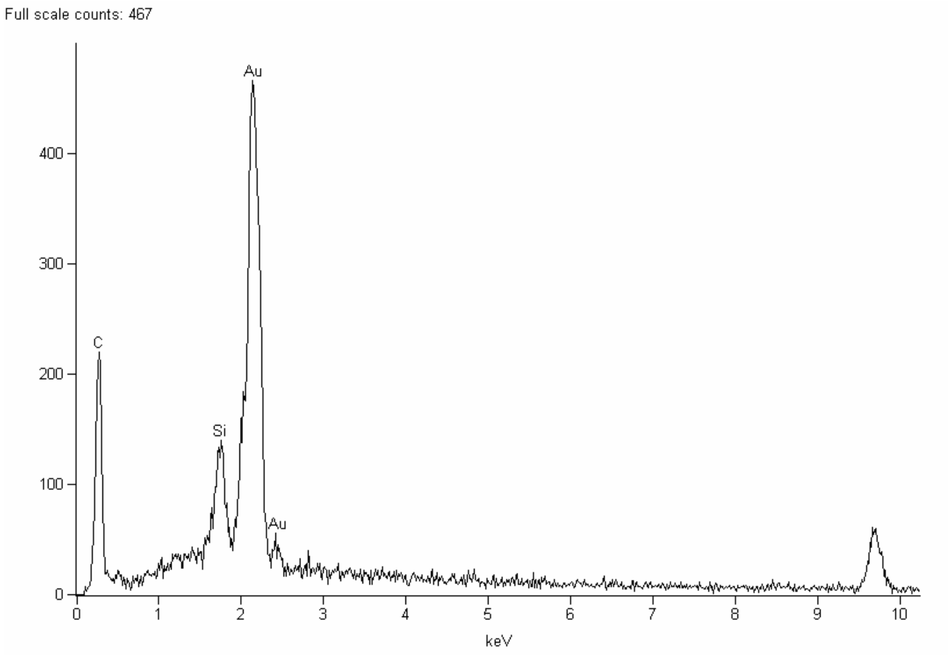

Figure D.5 EDX analysis of the cubical structure in Figure D.3 marked with blue

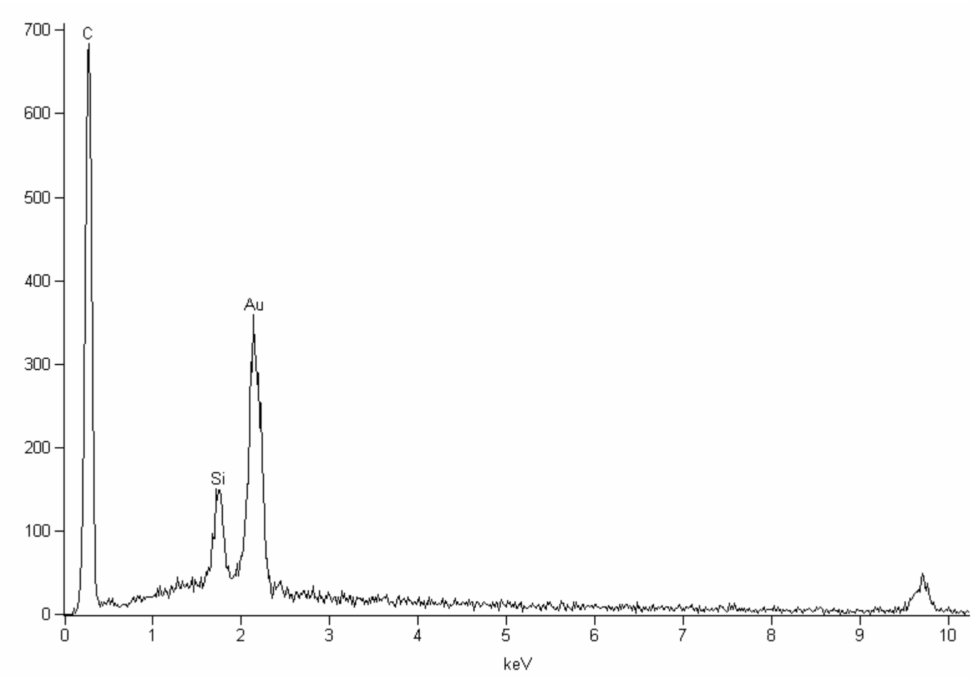

Figure D.6 EDX analysis of the matrix in Figure D.3

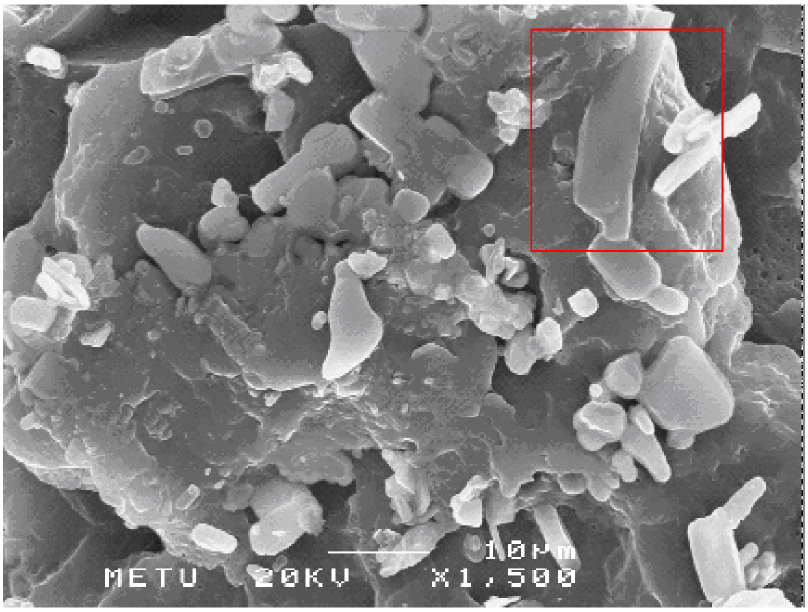

Figure D.7 SEM picture of PP/10SMP/5TPP/5M blend at x1500 magnification

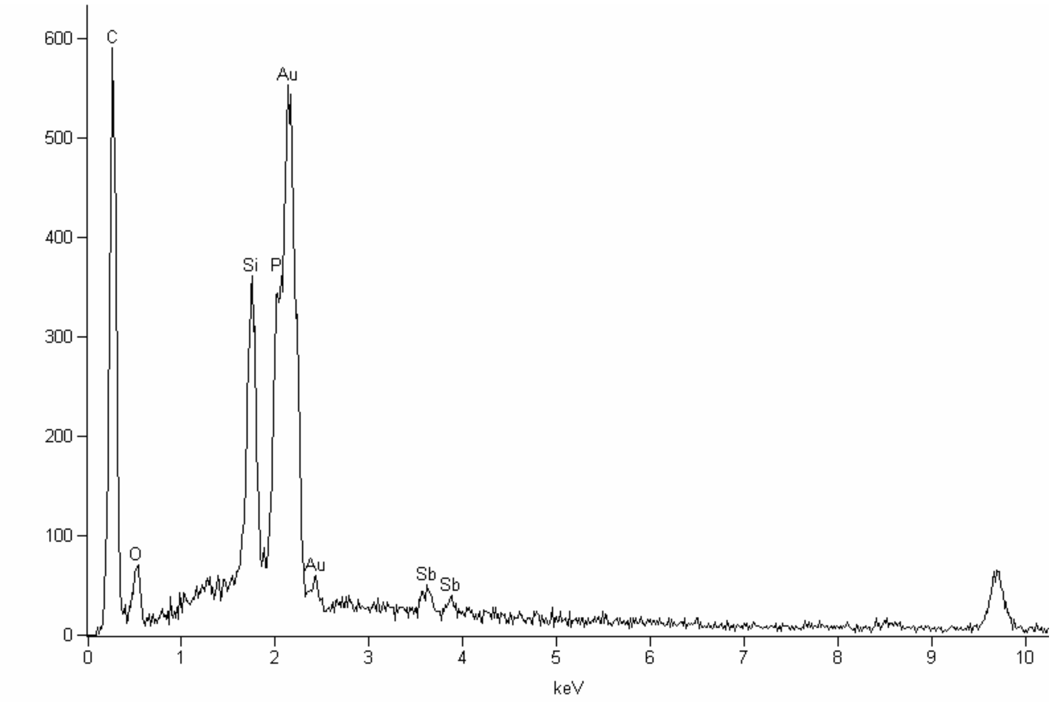

Figure D.8 EDX analysis of the structure in Figure D.7 marked with red

APPENDIX E

MECHANICAL TEST RESULTS

Table E.1 Tensile stress data for PP/SMP-10 blends at break and at yield

	Tensile Strength at Break (MPa)	Tensile Stress at Yield (MPa)
PP	50.3 +/- 0.1	40.5 +/- 0.4
PP/1SMP	54.9 +/- 1.2	42.5 +/- 0.7
PP/2SMP	51.3 +/- 1.0	41.7 +/- 1.6
PP/3SMP	51.6 +/- 1.1	41.9 +/- 0.3
PP/5SMP	51.3 +/- 0.9	40.5 +/- 0.4
PP/10SMP	47.5 +/- 0.3	36.9 +/- 0.3
PP/5SMP/5TPP	48.4 +/- 0.9	37.7 +/- 0.3
PP/10SMP/10TPP	40.8 +/- 0.5	32.0 +/- 0.4
PP/10SMP/5TPP/5M	41.3 +/- 1.2	31.3 +/- 0.2
PP/10TPP/10M	42.4 +/- 0.8	33.9 +/- 0.3

Table E.2 Tensile stress data for PP/PMSy blends at break and at yield

	Tensile Strength at Break (MPa)	Tensile Stress at Yield (MPa)
PP	50.3 +/- 0.1	40.5 +/- 0.4
PP/1PMS	51.6 +/- 0.1	39.5 +/- 0.1
PP/10PMS/10TPP	44.1 +/- 0.7	34.1 +/- 0.6
PP/10PMS/5TPP/5M	44.3 +/- 0.5	35.0 +/- 0.2
PP/5PMS/7.5TPP/7.5M	43.5 +/- 0.7	36.1 +/- 0.6
PP/5PMS/5SMP/5TPP/5M	41.3 +/- 1.5	35.9 +/- 0.7
PP/10TPP/10M	42.4 +/- 0.8	33.9 +/- 0.3

Table E.3 Elastic modulus data for PP/SMP-10 blends

	Elastic Modulus (MPa)
PP	734.5 +/- 59.8
PP/1SMP	920.0 +/- 18.7
PP/2SMP	855.0 +/- 53.8
PP/3SMP	865.5 +/- 21.0
PP/5SMP	815.9 +/- 18.6
PP/10SMP	671.5 +/- 8.6
PP/5SMP/5TPP	679.3 +/- 22.3
PP/10SMP/10TPP	639.2 +/- 33.2
PP/10SMP/5TPP/5M	548.7 +/- 23.5
PP/10TPP/10M	707.1 +/-19.8

Table E.4 Elastic modulus data for PP/PMSy blends

	Elastic Modulus (MPa)
PP	734.5 +/- 59.8
PP/1PMS	853.5 +/- 151.9
PP/10PMS/10TPP	774.9 +/- 71.8
PP/10PMS/5TPP/5M	720.0 +/- 23.5
PP/5PMS/7.5TPP/7.5M	626.1 +/- 44.8
PP/5PMS/5SMP/5TPP/5M	660.9 +/- 60.0
PP/10TPP/10M	707.1 +/- 19.8

Table E.5 Elongation at break data for PP/SMP-10 blends

	Elongation at Break (%)
PP	765.4 +/- 24.3
PP/1SMP	728.7 +/- 18.2
PP/2SMP	688.6 +/- 14.5
PP/3SMP	701.1 +/- 17.9
PP/5SMP	716.0 +/- 5.9
PP/10SMP	775.0 +/- 19.9
PP/5SMP/5TPP	816.5 +/- 8.3
PP/10SMP/10TPP	799.5 +/- 7.6
PP/10SMP/5TPP/5M	926.8 +/- 6.3
PP/10TPP/10M	849.7 +/- 13.8

Table E.6 Elongation at break data for PP/PMSy blends

	Elongation at Break (%)
PP	765.4 +/- 24.3
PP/1PMS	826.0 +/- 1.4
PP/10PMS/10TPP	1034.9 +/- 36.4
PP/10PMS/5TPP/5M	916.6 +/- 26.9
PP/5PMS/7.5TPP/7.5M	812.3 +/- 9.0
PP/5PMS/5SMP/5TPP/5M	794.9 +/- 6.8
PP/10TPP/10M	849.7 +/- 13.8

Table E.7 Impact strength data for PP/SMP-10 blends

	Impact Strength (kJ/m^2)
PP	23.2 +/- 2.2
PP/1SMP	58.9 +/- 5.5
PP/2SMP	43.3 +/- 4.7
PP/3SMP	45.7 +/- 1.7
PP/5SMP	63.6 +/- 7.5
PP/10SMP	51.8 +/- 1.8
PP/5SMP/5TPP	74.6 +/- 7.9
PP/10SMP/10TPP	55.3 +/- 1.0
PP/10SMP/5TPP/5M	42.6 +/- 1.6
PP/10TPP/10M	69.9 +/- 4.3

Table E.8 Impact strength data for PP/PMSy blends

	Impact Strength (kJ/m^2)
PP	23.2 +/- 2.2
PP/1PMS	68.1 +/- 8.5
PP/10PMS/10TPP	44.3 +/- 14.2
PP/10PMS/5TPP/5M	53.8 +/- 11.6
PP/5PMS/7.5TPP/7.5M	20.8 +/- 1.4
PP/5PMS/5SMP/5TPP/5M	36.6 +/- 5.3
PP/10TPP/10M	69.9 +/- 4.3